

UC Santa Barbara

UC Santa Barbara Electronic Theses and Dissertations

Title

Characterization of biologically relevant interactions and mutations in the human DNA methyltransferase 3A (DNMT3A)

Permalink

<https://escholarship.org/uc/item/3qk6659h>

Author

Sandoval, Jonathan Enrique

Publication Date

2021

Peer reviewed|Thesis/dissertation

UNIVERSITY OF CALIFORNIA

Santa Barbara

Characterization of biologically relevant interactions and mutations in the human DNA
methyltransferase 3A (DNMT3A)

A dissertation submitted in partial satisfaction of the
requirements for the degree Doctor of Philosophy
in Molecular, Cellular and Developmental Biology

by

Jonathan E. Sandoval

Committee in charge:

Professor Norbert Reich, Co-Chair

Professor Anthony De Tomaso, Co-Chair

Professor Joel Rothman

Professor David Low

December 2021

The dissertation of Jonathan E. Sandoval is approved.

Joel Rothman

David Low

Anthony De Tomaso, Co-Committee Chair

Norbert Reich, Co-Committee Chair

December 2021

Characterization of biologically relevant interactions and mutations in the human DNA

methyltransferase 3A (DNMT3A)

Copyright © 2021

by

Jonathan E. Sandoval

ACKNOWLEDGEMENTS

I am forever grateful to my family for the support and continued encouragement during my PhD. I am thankful to my graduate advisor, Norbert Reich, for providing an environment to do interesting science, providing me guidance, and motivating me to publish. I would also like to thank my committee members Joel Rothman, David Low, Charles Samuel, and Anthony De Tomaso for their advice and productive conversations.

VITA OF Jonathan E. Sandoval
December 2021

EDUCATION

Bachelor of Science in Biology, James Madison University, May 2013
Master of Science in Biology, James Madison University, May 2015
Master of Art in Molecular, Cellular and Developmental Biology, University of California, Santa Barbara, June 2019
Doctor of Philosophy in Molecular, Cellular and Developmental Biology, University of California, Santa Barbara, December 2021

PROFESSIONAL EMPLOYMENT

2013-15: Teaching Assistant, Department of Biology, James Madison University
2015-2021: Teaching Assistant, Department of Molecular, Cellular and Developmental Biology, University of California, Santa Barbara
2015-2021: Graduate Researcher, Department of Chemistry and Biochemistry, University of California, Santa Barbara

PUBLICATIONS

Huang, S., Stillson, N.J., Sandoval, J.E., Yung, C. and Reich, N.O., 2021. A novel class of selective non-nucleoside inhibitors of human DNA methyltransferase 3A. *Bioorganic & Medicinal Chemistry Letters*, 40, p.127908.

Sandoval, J.E. and Reich, N.O., 2021. p53 and TDG are dominant in regulating the activity of the human de novo DNA methyltransferase DNMT3A on nucleosomes. *Journal of Biological Chemistry*, 296, p.100058.

Sandoval, J.E. and Reich, N.O., 2019. The R882H substitution in the human de novo DNA methyltransferase DNMT3A disrupts allosteric regulation by the tumor suppressor p53. *Journal of Biological Chemistry*, 294(48), pp.18207-18219.

Sandoval, J.E., Huang, Y.H., Muise, A., Goodell, M.A. and Reich, N.O., 2019. Mutations in the DNMT3A DNA methyltransferase in acute myeloid leukemia patients cause both loss and gain of function and differential regulation by protein partners. *Journal of Biological Chemistry*, 294(13), pp.4898-4910.

AWARDS

Underrepresented Trainee Scholarship, Keystone Symposia in Epigenetics and Human Disease, Banff, Alberta, Canada, 2019

Graduate student mentor, Department of Chemistry and Biochemistry, University of California, Santa Barbara, 2019

FIELDS OF STUDY

Major Field: Enzymology of DNMT3A-mediated DNA methylation

Characterize the effect of patient-derived mutations on the enzymatic activity and the allosteric modulation of DNMT3A

Explore the relative roles of histone tails, regulatory proteins, and non-coding RNAs in the simultaneous modulation of DNMT3A activity

Discovery of allosteric small molecule modulators of DNMT3A activity

ABSTRACT

Characterization of biologically relevant interactions and mutations in the human DNA methyltransferase 3A (DNMT3A)

by

Jonathan E. Sandoval

De novo DNA methylation by DNMT3A is a fundamental epigenetic modification for transcriptional regulation during cellular development and differentiation. The establishment of appropriate DNA methylation patterns in the human genome involves a crosstalk between DNMT3A, histone tails, regulatory proteins and RNAs. Mutations in DNMT3A and disruptions to this crosstalk of DNMT3A have been reported in several diseases, including Acute Myeloid Leukemia (AML). We sought to model how previously uncharacterized mutations in DNMT3A contribute to the aberrant DNA methylation observed in AML. We then sought to better understand the relative roles of histone tails, regulatory proteins and RNAs in the simultaneous modulation of DNMT3A activity and identified two molecules that inhibit protein interactions with DNMT3A.

Although 22% of all AML patients exhibit mutations throughout the DNMT3A gene, the effect of many mutations on DNMT3A activity remain uncharacterized. Moreover, little is known of the interactions between DNMT3A mutants and regulatory proteins, or conversely, mutant regulatory proteins and wild type DNMT3A. We show that previously unexplored DNMT3A mutations dramatically alter the enzyme's ability to perform CpG and

non-CpG methylation as well as the ability of partner proteins to modulate enzymatic activity. Additionally, cell-based studies of one of these DNMT3A mutations (S714C) replicated our findings *in vitro* showing a dramatic loss of genome-wide methylation. We found that p53 decreases DNMT3A activity by forming a heterotetramer complex with DNMT3A, and while p53 binds DNMT3A R882H, repression of DNMT3A activity is blocked by this substitution. Using p53 as an example, we also show that cancer-related substitutions to p53 are unable to disrupt DNMT3A heterotetramers, unlike that observed for WT p53.

To provide insights into the crosstalk between DNMT3A and distinct epigenetic mechanisms we initially assessed the relative role of regulatory proteins and histone tails in the simultaneous modulation of DNMT3A activity. Using radiochemical and binding assays under distinct conditions and with biologically relevant substrates, we found that regulatory proteins play dominant roles in the modulation of DNMT3A activity. Furthermore, we provide evidence that the activity of DNMT3A is not limited to DNA that is part of the initial DNMT3A–nucleosome complex. We then expanded on these findings by carrying out similar studies that included non-coding RNAs. We show regulatory RNAs play a dominant role over additional epigenetic mechanisms in the simultaneous modulation of DNMT3A. Additionally, we present evidence that is inconsistent with a model for RNA regulation of DNMT3A that relies on the formation of localized RNA/DNA structures. Lastly, a screen of a diverse small molecule library identified two compounds that act as inhibitors of protein-protein interactions (PPIs) with DNMT3A. Thus, presenting a basis for manipulating the allosteric regulation of DNMT3A.

TABLE OF CONTENTS

Chapter I. Introduction..... Error! Bookmark not defined.

Epigenetic mechanisms in transcriptional regulation	1
Mammalian DNA methyltransferases	2
<i>de novo</i> DNA methyltransferase 3A (DNMT3A)	6
DNMT3A mutations in AML.....	9
Allosteric modulation of DNMT3A	11
Small molecule inhibitors of DNMT3A	14

Chapter II. Mutations in the DNMT3A DNA methyltransferase in acute myeloid leukemia patients cause both loss and gain of function and differential regulation by protein partners

Abstract.....	22
Introduction.....	23
Results.....	26
Discussion.....	46
Methods	51
Supplementary material.....	57

Chapter III. The R882H substitution in the human *de novo* DNA methyltransferase DNMT3A disrupts allosteric regulation by the tumor suppressor p53

Abstract.....	60
Introduction.....	61
Results.....	63

Discussion.....	78
Methods	83
Supplementary material.....	88
Chapter IV. p53 and TDG are dominant in regulating the activity of the human de novo DNA methyltransferase DNMT3A on nucleosome	92
Abstract.....	92
Introduction.....	92
Results.....	97
Discussion.....	109
Methods	115
Supplementary material.....	119
Chapter V. Mechanism of non-coding RNA regulation of DNMT3A and its relation to histones, regulatory proteins, and clinically relevant mutations.....	126
Abstract.....	126
Introduction.....	127
Results.....	130
Discussion.....	148
Methods	152
Supplementary material.....	158
Chapter VI. A novel class of selective non-nucleoside inhibitors of human DNA methyltransferase 3A.....	165
Abstract.....	165
Introduction.....	165
Results and Discussion	168

Methods	175
Supplementary material	177
Chapter VII. Small molecule inhibition of DNMT3A regulation	
by partner proteins	179
Abstract.....	179
Introduction.....	179
Results.....	182
Discussion.....	195
Methods	197
Supplementary material.....	201
References.....	205

LIST OF FIGURES

Chapter I

Figure 1. Epigenetic mechanisms in transcriptional regulation and disease	17
Figure 2. Crosstalk between components of the epigenetic machinery.....	18
Figure 3. Human DNMT family of proteins and types of DNA methylation	19
Figure 4. Mechanism of 5-methylcytosine methylation by DNMT and exploitation of this mechanism by nucleoside inhibitors.....	20
Figure 5. DNMT3A mutations in AML patients.....	21

Chapter II

Figure 1. Mutations from AML patients in a DNMT3A homotetramer model.....	25
Figure 2. A subset of mutations display little change or enhanced activity for <i>p15</i> -pCpG ^L relative to the multiple CpG site substrate poly(dI-dC).	29
Figure 3. Substrate diagram and characteristics	30
Figure 4. Some mutations result in enhanced activity at non-CpG sites.....	31
Figure 5. AML mutants display unique alterations to processive catalysis on the poly(dI-dC) substrate	37
Figure 6. AML mutations display loss of processive catalysis on the <i>p15</i> -pCpG ^L human promoter substrate.....	38
Figure 7. DNMT3L has a higher affinity for binding DNMT3A compared with TDG	41
Figure 8. DNMT3L or TDG binding on DNMT3A tetramer interface are not mutually exclusive.....	42

Figure 9. TDG does not compete with DNMT3L for binding to DNMT3A.....	43
Figure 10. S714C reduces DNA methylation in mESCs.....	45
Figure S1. Equal concertation of TDG to active DNMT3A tetramer maximally inhibits methylation by DNMT3A.....	58
Figure S2. Cell sorting by flow cytometry following a two-week doxycycline induction.....	59

Chapter III

Figure 1. p53 ^{WT} -dependent inhibition of DNA methylation is specific to DNMT3A	65
Figure 2. DNMT3A ^{WT} tetramer interface mutants show highly variable response to p53 ^{WT} inhibition.....	67
Figure 3. DNMT3A ^{WT} and DNMT3AR882H are differentially responsive to modulation by p53 ^{WT}	71
Figure 4. p53 ^{R248W} and p53 ^{R273H} fail to disrupt stimulation of DNMT3A ^{WT} by DNMT3L	74
Figure 5. p53 heterodimerizes with WT and R882H DNMT3A	77
Figure 6. Mutations in DNMT3A lead to diverse interactions with p53.....	82
Figure S1. p53 ^{WT} and p53 ^{R248W} display stronger affinity for DNMT3AWT binding than DNMT3L	89
Figure S2. Models to identify p53 binding surface on DNMT3A.....	90
Figure S3. Depiction of p53 ^{WT} mutations and region on p53 ^{WT} for binding by DNMT3A.....	91

Chapter IV

Figure 1. DNMT3L and H3 tails bind distinct surfaces on DNMT3A for modulation

of enzymatic activity.....	96
Figure 2. Modulation of DNMT3A activity by regulatory proteins is dominant in the presence of H3K4me0 or H3K4me3 peptides	100
Figure 3. DNMT3A remains bound to histone tails in mononucleosomes when acting on free DNA.....	104
Figure 4. Modulation of DNMT3A activity by p53 or TDG using human mono- or polynucleosomes.....	108
Figure S1. Interactions between the N-terminus of DNMT3A and nucleosomes increase catalytic activity on nucleosomal DNA.....	120
Figure S2. Binding curve of DNMT3A with mono- or poly-nucleosomal DNA as a substrate	121
Figure S3. Distances in DNMT3A-Nucleosome interactions	122
Figure S4. 10% SDS-PAGE gel of the purified proteins.....	123
Figure S5. Binding curve DNMT3A to FAM-labeled H3K4me0 peptides.....	124
Figure S6. p53 and TDG specifically inhibit the DNA methylation activity of DNMT3A	125
Chapter V	
Figure 1. Cellular localization of <i>Fos</i> ecRNA and mRNA.....	132
Figure 2. Mutations at the DNMT3A_CD tetramer interface disrupt RNA-mediated inhibition.....	137
Figure 3. The oligomeric state of DNMT3A_CD affects modulation of enzymatic activity by <i>Fos-1</i> RNA.....	139
Figure 4. Formation of DNMT3A_CD ^{R771A} heterotetramers with DNMT3L restores inhibition of enzymatic activity by <i>Fos-1</i> ecRNA	142

Figure 5. Modulation of DNMT3A enzymatic activity by RNA is dominant in DNMT3A_FL ^{WT} - DNMT3L- H3 tail- RNA complexes	146
Figure 6. Models for ecRNA modulation of DNMT3A and interactions with additional components of the epigenetic machinery	147
Figure S1. Functional characterization of RNA-mediated inhibition of DNMT3A_CD ^{WT} activity and selectivity of <i>Fos-1</i> ecRNA for human DNMTs.....	159
Figure S2. Computational models predict <i>Fos-1</i> ecRNA binds at the tetramer interface of DNMT3A	160
Figure S3. Modulation of DNMT3A_CD ^{WT} enzymatic activity by <i>Fos-1</i> ecRNA is dominant in the presence of DNMT3L	161
Figure S4. Binding of Full-length DNMT3A ^{WT} to FAM-labeled H3K4me0 peptides	162
Figure S5. Excess <i>Fos-1</i> and <i>CHD</i> RNAs inhibit Full-length DNMT3A ^{WT} activity with polynucleosomes as substrates	163
Figure S6. Summary gel of proteins used in this study	164
Chapter VI	
Figure 1. Comparison of the primary structures of human DNMTs	171
Figure 2. Crystal structure of DNMT3A-3L heterotetrameric complex.....	172
Figure 3. Best fit plots of the inhibition with respect to both substrates, poly dI-dC (A, B) and AdoMet (C, D).....	173
Figure 4. Inhibitors 1 (A) and 2 (B) modulate the activity of human de novo DNMT3A_CD, DNMT3A_FL and maintenance DNMT1 DNA methyltransferases but not of the bacterial DNA methyltransferase M.SssI.....	174
Figure S1. Results from the secondary screen. Compounds that exhibited more than	

90% inhibition in the primary screen of the Pathogen Box library were subjected to duplicate (n=2) repetition of the inhibition. Activity assays were performed as described in the Methods. The compounds are designated by their location in the library and reference structures are provided below. Compound 1 is designated AC05 while compound 2 is BC02 178

Chapter VII

Figure 1. Surfaces involved with allosteric modulation of DNMT3A and models for disruption of modulation by compounds 1 and 2..... 182

Figure 2. Compounds do not inhibit the activation of DNMT3A_WT by H3 peptides but disrupt DNMT3A-DNMT3L interactions at the DNMT3A tetramer interface 186

Figure 3. Compounds disrupt to DNA-bound DNMT3A_WT in complex with distinct partner proteins 187

Figure 4. Compound 2 inhibits DNMT3A_ R771A-DNMT3L heterotetramers but not DNMT3A_ R771A homodimers..... 190

Figure 5. Compounds 1 and 2 inhibit the activation of DNMT3A_R882H by DNMT3L 193

Figure 6. Compounds disrupt DNA-bound DNMT3A_R882H heterotetramers with distinct partner proteins 194

Figure S1. Structure of Compounds 1 or 2 as well as DNMT3A mutants explored in this study..... 202

Figure S2. Compounds 1 and 2 do not inhibit the activity of the H3K4 histone demethylase KDM5A..... 203

Figure S3. Inspection of the binding pose of BC02 on the tetramer interface 204

LIST OF TABLES

Chapter I

Table 1. k_{cat} values for wildtype and AML patient-derived DNMT3A mutants using poly(dI-dC) and <i>p15</i> -pCpG ^L DNA substrates.....	28
Table 2. Fold inhibition by TDG for wildtype and AML patient-derived DNMT3A mutants using poly(dI-dC) and <i>p15</i> -pCpG ^L DNA substrates	33
Table 3. Fold stimulation by DNMT3L for wildtype and AML patient-derived DNMT3A mutants using poly(dI-dC) and <i>p15</i> -pCpG ^L DNA substrates	35

Chapter VI

Table 1. Values for the various fits of inhibitors with respect to both substrates	174
Table S1. R^2 values for the non-linear fits of the available inhibition data with respect to three generalized inhibition mechanisms: competitive, uncompetitive and noncompetitive (mixed type)	177

Chapter I: Introduction

Epigenetic mechanisms in transcriptional regulation

Although all the cells within multicellular organisms contain the same DNA, these organisms are composed of distinct cells that differentiate into specific types during development in a spatiotemporally regulated manner. The control of gene expression is a central component for this cellular specialization, which is largely driven by the cumulative effects of epigenetic processes, such as DNA methylation, histone modification regulatory proteins and non-coding RNAs (1). The appropriate propagation of these epigenetic marks through successive cycles of cell division contributes to the establishment of cellular memory and maintenance of cellular identity (2). Furthermore, studies show the interactions of DNA methyltransferases (DNMTs) with regulatory proteins, non-coding RNAs or histone tails containing specific modifications are associated with fundamental biological functions, like parental imprinting, memory formation and stem-cell differentiation (Fig. 1 A.) (3-5). Given the importance of epigenetic mechanisms in transcriptional regulation and key biological processes, it is not surprising that epigenetic aberrations have been documented in human diseases, particularly cancer (Fig. 1 B.) (6).

Eukaryotic DNA is wrapped around histone octamers to generate higher order chromatin structures (7). It has been proposed that epigenetic mechanisms contribute to transcriptional regulation by influencing the accessibility of DNA to the transcriptional machinery. That is, eukaryotic chromatin is malleable and undergoes structural changes in response to specific epigenetic marks or ATP-dependent chromatin remodeling complexes (8). In fact, the establishment of a histone code, through the catalysis of specific covalent modifications to histone tails, correlates with alterations to chromatin structure, and in some cases, with DNA methylation (9). For instance, H3K36me2/3, H3K9me3, and

H3K4me0 correlates with DNA methylation and transcriptional silencing (10-12). The apparent interplay between DNA methylation and specific histone modifications may stem from DNA methylation inhibiting the binding of histone modifying enzymes to specific targets. This is observed for Lysine Demethylase 2A (KDM2A), which only binds nucleosomes harboring H3K9me3 and unmethylated DNA (13). While there is a clear association between specific histone modifications and DNA methylation, much less is known about the relationship between non-coding RNAs and the establishment of DNA methylation patterns due to the ongoing discovery of novel non-coding RNAs. However, there is compelling evidence showing non-coding RNAs regulate DNMTs, histone modifying enzymes, and transcription factors (14-18). These observations support a model in which the crosstalk between distinct components of the epigenetic machinery is essential for transcriptional regulation, although how this crosstalk works remains unclear (Fig. 2).

Human DNA methyltransferases

The human DNMT family of proteins, which is responsible for catalyzing DNA methylation, consists of three enzymes DNMT1, DNMT3A and DNMT3B as well as an inactive homolog DNMT3L (19-21). Although DNMTs have a similar domain arrangement, with each protein consisting of a regulatory N-terminal domain and a C-terminal catalytic domain (Fig. 3 A.), DNMT1 and the two DNMT3s have distinct roles in the process of genomic DNA methylation (Fig. 3 B.) (22-24). For instance, DNMT3A and DNMT3B establish *de novo* DNA methylation patterns in unmethylated DNA substrates, which in some cases is modulated by DNMT3L (Fig. 3 B.) (20), (23). Once cellular DNA methylation patterns are established, DNMT1 maintains these patterns in the next generation by preferentially methylating hemimethylated DNA substrates (Fig. 3 B.) (24).

Interestingly, the structural differences between DNMT1 and DNMT3 provide insights into how these enzymes carry out different forms of DNA methylation.

While the catalytic methyltransferase domain, consisting of motifs I-X, is highly conserved across the three enzymes, the N-terminal domain of DNMT1 and DNMT3 is highly variable (Fig. 3 A.) (22). The larger DNMT1 N-terminal domain harbors a DNA methyltransferase associated protein 1 interacting domain (DMAPD), a PCNA binding domain (PBD), a replication foci-targeting sequence (RFTS), a zinc-finger-like (CXXC) motif and two bromo adjacent homology (BAH1 and BAH2) domains (Fig. 3 A.) (22); all of which contribute to the localization and stabilization of DNMT1 on DNA substrates after replication (22), (24). The DNMT3 N-terminal domain contains a PWWP and ADD (Atrx-Dnmt3-Dnmt3l) domain. Whereas both domains associate with various proteins, including histone tails, the PWWP domain only interacts with DNA and RNA (14) (25-29). While there is an evident structural homology between DNMT3L, DNMT3A and DNMT3B, the absence of key residues for DNA methylation (target recognition domain between motifs VIII-IX, motifs IX-X and the inability to bind the cofactor AdoMet) render DNMT3L catalytically inactive (30). Even though DNMT3L is catalytically inactive, studies show DNMT3L associates with DNMT3A and DNMT3B and is a key modulator of *de novo* DNA methylation (21), (31). This modulatory role of DNMT3L is particularly observed during parental imprinting in mammals; a stage of embryonic development when *de novo* DNA methylation is essential (21), (32).

Studies aiming to investigate the role of DNMT3s during parental imprinting *in vivo* show that although DNMT3A and DNMT3B share certain targets, the differences in methylation of specific targets of DNMT3A or DNMT3B produces markedly distinct phenotypes upon the removal of DNMT3A, DNMT3B or both (23), (32-34). In the context

of imprinted genes, DNMT3A targets dispersed repeats whereas DNMT3B acts on pericentric satellite repeats (23), (33), (34). *DNMT3A* and *DNMT3B* knockout mice (*DNMT3A*^{-/-}/*DNMT3B*^{-/-}) are hypomethylated and die mid-gestation (34). However, the conditional knockout of *DNMT3B* (*DNMT3A*^{+/+}/*DNMT3B*^{-/-}) produces no evident phenotype while the effect by the conditional knockout *DNMT3A* (*DNMT3A*^{-/-}/*DNMT3B*^{+/+}) differs between male or female mice (32). Interestingly, the phenotype of the DNMT3L conditional knockout mutants (*DNMT3A*^{+/+}/*DNMT3B*^{+/+}) is indistinguishable from that of DNMT3A (32). Compared to males, which display stunted spermatogenesis and hypomethylation of paternally imprinted genes in these cells, disruption of *DNMT3A* (*DNMT3A*^{-/-}/*DNMT3B*^{+/+}) in female germ cells produces offspring that die at embryonic stages and lack methylation of maternally imprinted genes (32). Although the role of DNMT3s in parental imprinting is the most well characterized, the activity of DNMT3s has been associated with additional biological processes such as X chromosome inactivation, hematopoietic stem cell (HSC) differentiation, aging and DNA damage repair (6) (23), (32-34) (35-37). It is unclear what drives this biological diversity of DNMT3 activity. However, given the spatiotemporal regulation and tissue specificity of DNMT3 activity in normal biological function, it is likely that interactions with modulators, such as specific histone modifications, regulatory proteins and RNAs, contribute to this wide range of biological functions (discussed in more detail in chapters IV and V).

A common feature of genomic regions that are targeted for DNA methylation, despite the function associated with this epigenetic modification, is the overrepresentation of CpG dinucleotides in gene regulatory elements (38). In humans, DNA methylation occurs exclusively at cytosines and CpG dinucleotides are distributed throughout the entire genome within variable surrounding sequences. However, DNA methylation is not restricted to CpG

islands and is also observed in non-CpG sites (CpA, CpT, and CpC), albeit to a much lesser extent (39). In fact, 70–80% of cytosines at CpG sites in somatic cells are methylated while non-CpG methylation accounts for approximately 0.02% of total methyl-cytosines in these cells (39). While CpG and non-CpG cytosine methylation are observed throughout the genome, including protein coding regions, regulatory elements (enhancers and promoters) and repetitive elements, CpG is more ubiquitous and non-CpG methylation is primarily found in specific cell types, like stem cells, oocytes, and neurons (39). The inverse relationship between DNA methylation and inhibition of gene expression was initially identified in the study of CpG islands in promoter regions, which are highly methylated in inactive genes relative to those with active transcription (40). The current model for how CpG methylation contributes to transcriptional silencing entails that, in addition to methylated regions becoming heterochromatic, cytosine methylation directly interferes with the binding of transcription activators or disrupts the binding affinity of these activators to DNA (41-43). Interestingly, additional studies have shown that while hypermethylation at regulatory elements (promoters and enhancers) is associated with transcriptional silencing, hypermethylation of CpG sites in gene bodies increases expression (44). Mechanistically, cytosine methylation involves DNMT binding to DNA and inserting the target recognition domain (region between motifs VIII-IX, Fig. 3 A.) into the DNA, which flips the target cytosine out of the double helix. A nucleophilic attack to the C6 of the target cytosine is then carried out by the thiol side chain of a highly conserved cysteine (C710 in DNMT3A, C651 in DNMT3B and C1225 in DNMT1) (Fig. 4 A.). The activation of the C5 position of the target cytosine facilitates the transfer of a methyl group from the AdoMet cofactor, and after the formation of a 5-methylcytosine, DNMT is released by β elimination (Fig. 4 A.).

The enzyme can then either continue to methylate nearby targets or dissociate from DNA (45), (46).

***De novo* DNA methyltransferase 3A (DNMT3A)**

The *DNMT3A* gene encodes two isoforms, the 130 kDa full-length DNMT3A and the shorter DNMT3A2 which lacks the N-terminal 223 residues of full-length DNMT3A (47). DNMT3A is highly expressed during the early stages of mammalian embryonic development, including primordial germ cells. As cellular differentiation progresses, the expression of DNMT3A reduces, but DNMT3A remains ubiquitously expressed and is detected in most tissues. In contrast, DNMT3A2 expression is restricted to embryonic stem cells and germ cells (47), (48). Despite the differences between DNMT3A and DNMT3A2, recombinant DNMT3A and DNMT3A2 display similar levels of enzymatic activity on a multiple site CpG substrate (k_{cat} of 4-6 h⁻¹) (49), (50). Although this level of activity is comparable to that reported for DNMT3B under similar conditions (k_{cat} of up to 2 h⁻¹), it is much lower than that observed for DNMT1 (k_{cat} of up to 200 h⁻¹) (51), (52). Interestingly, human DNA methyltransferases display much lower levels of enzymatic activity compared to prokaryotic DNA methyltransferases (M. HhaI $k_{cat} = 2 \text{ min}^{-1}$, M.SssI $k_{cat} = < 1 \text{ min}^{-1}$) (53), (54). Another notable difference between human and prokaryotic DNA methyltransferases is the lack of a cognate sequence that contributes to site selection of human enzymes. Prokaryotic DNA methyltransferases rely on a 4-6 base pair substrate recognition sequence (53), (54). In contrast, DNMT3A, like other human DNA methyltransferases, shows minimal sequence preference *in vitro* (49-52). Some studies suggest the flanking sequence of target CpG sites affects the catalytic activity of DNMT3A (55), (56). However, the nucleotide composition of flanking sequences and distance from CpG targets identified in these studies are at odds (55), (56). While one study found DNMT3A displays higher

activity in AT rich flanking sequences that are +/- 4 base pairs around the central CG site (55), another study found similar results but with TC rich flanking sequences that are +/- 4 base pairs from the CG target site (56). Thus, there is more compelling evidence that substrate CpG density and the oligomerization state directly influence processive *de novo* DNA methylation by DNMT3A.

Oligomeric proteins, consisting of two or more subunits, carry out a wide range of functions and comprise a large fraction of cellular proteins. Interestingly, factors like protein concentration, post-translational modifications or environmental changes allow proteins to exist in more than one oligomeric state with varied cellular activities (57). Therefore, it has been proposed that the ability of proteins to form higher order complexes may have evolved to bring about distinct functions or allosterically modulate enzymatic activity, as appears to be the case in DNMT3A (57). Our understanding of the oligomerization of DNMT3A stems from the crystal structures of DNMT3L in complex with the DNMT3A catalytic domain or DNMT3A catalytic and ADD domains (58), (59). These structures show that the DNMT3A-DNMT3L heterotetramers contains two outer DNMT3A-DNMT3L interfaces (tetramer interface) and one central DNMT3A-DNMT3A interface (dimer interface) where DNA binding occurs (58), (59). The crystal structure of a DNMT3A-DNMT3L heterotetramer in complex with DNA containing two CpG sites separated by 14 base pairs suggests DNMT3A monomers can simultaneously methylate two CpG sites in a single binding event (Chapter III, Fig. 2 A.) (58). While there is additional data in support of this hypothesis, the precise mechanism for how DNMT3A-DNMT3L heterotetramers simultaneously methylate substrates containing two CpG sites is not fully understood (59). To date, the crystal structure of a DNMT3A homotetramers remains unsolved. However, there is compelling evidence that DNMT3A self-oligomerizes in the

absence of DNA and exists as homotetramers in cells (60), (61). In fact, computational modeling and mutational mapping indicate that DNMT3A monomers bind the same surface as DNMT3L to form homotetramers (61). Interestingly, mutations to key residues of the DNMT3A tetramer interface leads to distinct oligomeric states, and although catalytically active, mutant DNMT3A lose the ability to carry out processive DNA methylation (61), (62).

Processive catalysis, defined as the ability of an enzyme to perform multiple rounds of catalysis before dissociating from its substrate, is observed in a wide range of human enzymes, including those involved with DNA synthesis, repair, and modifications (63). It has been proposed that the ability of processive enzymes to remain bound to their substrates enhances the enzyme's efficiency (63). In fact, many processive enzymes display a low K_M and a high V_{MAX} , which in some enzymes, like DNMT3A, is achieved through interactions with partner proteins (61), (63). Initial evidence for DNMT3A being a processive enzyme comes from data showing the methylation rate increases with the number of CpG sites in DNA substrates and is unaffected by the size of these substrates (49). The processivity of DNMT3A has since been shown in several substrates using a chase assay designed for DNMT3A which tests the ability of DNMT3A to stay bound to its substrate after the addition of excess non-CpG DNA (49), (61), (62). Using this assay, we have shown that mutations in DNMT3A, including those identified in AML, mildly affect methylation activity but drastically disrupt processive catalysis. Interestingly, DNMT3L restores the processivity of DNMT3A mutants by decreasing K_M^{DNA} (61). Human DNMTs methylate ~70% of CpG sites in the genome over a short developmental period (64). It has been proposed that the use of processive catalysis allows human DNMTs, which are significantly slower than prokaryotic DNMTs, to carry out this task (49), (50), (53), (54), (62).

Furthermore, our work provides a mechanism for how mutations in DNMT3A identified in AML patients may contribute to the aberrant DNA methylation observed in these patients (65).

DNMT3A mutations in AML

Initial evidence that DNMT3A contributes to the development of AML came from studies showing that DNMT3A is essential for differentiation of HSCs into distinct blood cell lineages (Fig. 5 A.) (5), (65). In these studies, conditional knock out of *DNMT3A* in HSCs was found to favor self-renewal and maintained most HSCs in a pluripotent state rather than differentiating (5). The increased self-renewal of DNMT3A deficient HSCs caused these cells to outcompete their wild type counterparts and resulted in fewer terminally differentiated blood lineage cells (5). Consistent with the observed phenotype, loss of DNMT3A led to global hypomethylation of genes associated with self-renewal in stem cells, such as homeobox A9 (*Hoxa9*), Meis homeobox 1 (*Meis1*), and MDS1-EVI1 complex locus (*Mecom*) (5). Following these initial studies, whole genome sequencing efforts identified that *DNMT3A* is recurrently mutated in AML patients (Fig. 5 B.) (66). These sequencing studies showed *DNMT3A* is mutated in ~22% of all AML patients and is associated with decreased survival (66). Although mutations were identified throughout *DNMT3A*, mutations were more prevalent in the catalytic domain of DNMT3A with substitutions to R882 accounting for >50% of all mutations (Fig. 5 B.) (66). Interestingly, *DNMT3A* mutations in AML patients correlates with mutations to isocitrate dehydrogenase 1 (*IDH1*) and isocitrate dehydrogenase 2 (*IDH2*), Tet oncogene family member 2 (*TET2*) and FMS-like tyrosine kinase 3 (*FLT3*) (66), (67).

Although the aberrant DNA methylation observed in AML patients provides insights into how DNMT3A mutations may contribute to AML, the precise mechanisms remain

unclear. Analysis of DNA methylation in primary cells from AML patients harboring R882 and non-R882 substitutions revealed DNA heterogeneity is a feature of DNMT3A mutations. While both R882 and non-R882 substitutions correlate with global hypomethylation, DNMT3A mutants differed in DNA methylation levels at specific genomic regions such as CpG islands, shores, promoters and non-CpG targets, with R882 mutants even displaying some promoter hypermethylation (60). Biochemical studies have largely focused on the R882 substitution to DNMT3A and are limited to the impact of mutations on the inherent enzymatic activity. Given that non-R882 substitutions remain largely uncharacterized, I sought to explore how these substitutions, which are mapped to distinct functional domains of DNMT3A, may contribute to the heterogeneity in DNA methylation observed in clinical isolates. Based on this heterogeneity and the differences in DNA methylation at specific genomic regions, I proposed that DNMT3A mutations disrupt interactions with partner proteins, which modulate localization and enzymatic activity, and contribute to these differences. As shown in chapter II, we found that DNMT3A mutations resulted in hypo- and hypermethylation as well as disruptions to interactions with partner proteins. The latter motivated my research to explore how mutations in regulatory proteins may affect interactions with DNMT3A. For this approach we relied on p53, which is mutated in a wide range of cancers and has been shown to interact with DNMT3A.

While tumor suppressor p53 (*p53*) is mutated in over 50% of all human cancers, there are some cancers, like AML, that exhibit lower frequencies of p53 mutations and the activity of wild type p53 is altered via distinct mechanisms such as disruptions to protein-protein interactions (PPIs) (68), (69). Altered p53 activity has been associated with chemoresistance, increased risk of cancer relapse and decreased survival in AML patients carrying wild type or mutant *p53* alleles (70). However, p53 mutations are associated with

worst outcomes of AML patients compared to AML patients carrying wild type *p53* alleles (70). Substitutions to *p53* R248 and R273, which have been identified in AML, are characterized as gain of function mutants due to the acquired ability to inappropriately interact with partner proteins of *p53* as well as exerting a dominant-negative effect over wild type *p53* (71), (72). The cellular impacts of these gain of function mutants include genomic destabilization, suppression of apoptosis and loss of cell cycle regulation (70). DNMT3A was previously shown to directly interact with *p53* and inhibit *p53*-mediated transcription (73). However, the surface on DNMT3A bound by *p53*, the effect of *p53* on the enzymatic activity of DNMT3A or the impact of *p53* mutations on DNMT3A-*p53* interactions remained unexplored. As shown in chapter III, we show that *p53* binds the tetramer interface of wild type and R882H DNMT3A but only allosterically inhibits the enzymatic activity of wild type DNMT3A. Furthermore, *p53* mutations (R248W and 273H) were unable to inhibit DNMT3A in DNMT3A-DNMT3L heterotetramers, unlike wild type *p53*. After exploring PPIs with DNMT3A in the context of medically relevant mutations, I turned my efforts to the relationship between partner proteins, histone tails and regulatory RNAs in the simultaneous modulation of DNMT3A.

Allosteric modulation of DNMT3A

The crystal structure of DNMT3A in complex with histone H3 tail and DNMT3L shows DNMT3A is simultaneously bound at distinct surfaces for modulation of enzymatic activity (59). Insights into the combinatorial effect of regulatory proteins and histone H3 tails in the modulation of DNMT3A activity have focused solely on DNMT3L, which is complicated by the fact that both DNMT3L and H3 tails activate DNMT3A activity (59), (74), (75). Much less is known about the interactions between DNMT3A, H3 tails, non-coding RNA and additional partner proteins even though there are several lines of evidence

for a crosstalk between these components of the epigenetic machinery (76-78). Therefore, I sought to better model the cellular interactions of these epigenetic mechanisms and explore the relative roles of H3 tails, regulatory proteins and RNAs in the simultaneous modulation of DNMT3A activity (Fig. 2).

DNMT3A is predicted to interact with many proteins, which are associated with distinct biological functions such as cell cycle regulation, transcription factors, DNA repair, chromatin modifying and remodeling enzymes (27), (73), (79), (80). However, many of these potential interactions have been identified through methods that are unable to discriminate between direct or indirect PPIs, such as co-immunoprecipitation. To date, only DNMT3L, Thymine DNA glycosylase (TDG) and p53 (identified in chapter III) have been shown to directly modulate the enzymatic activity of DNMT3A (79), (81), (82). In addition to the fact that both DNMT3L and H3 tails activate DNMT3A activity, studies involving these two modulators of DNMT3A are further complicated due to the ability of both DNMT3A and DNMT3L to bind H3 tails (75). Therefore, I relied on p53 and TDG, which do not directly interact with H3 tails, to assess the relative roles of regulatory proteins and H3 tails in the simultaneous regulation of DNMT3A activity. This key difference between partner proteins of DNMT3A led me to propose a model that considers the relationship between DNMT3A heterotetramers and nucleosome substrates (Chapter IV). That is, (I) DNMT3A may act as a reader of histone marks with histone tails modulating enzymatic activity or with histone tails primarily recruiting DNMT3A and partner proteins modulating enzymatic activity. Alternatively, (II) regulatory proteins in DNMT3A heterotetramers may serve as readers of histone marks and the enzymatic activity of DNMT3A is modulated by regulatory proteins or a combination of regulatory protein–histone tail interactions.

Focusing on DNMT3A as reader of histone marks (I) and using p53 and TDG as examples of partner proteins whose interactions and perturbations of DNMT3A are characterized, I found that the modulation of DNMT3A activity by regulatory proteins is dominant over H3 tails (H3K4me0 or H3K4me3). Furthermore, we found that DNMT3A acts on DNA within a single nucleosome (intranucleosomal DNA methylation) as well as DNA not associated with the DNMT3A–nucleosome complex (internucleosomal DNA methylation). Our findings have direct bearing on the contributions of regulatory proteins and the histone code to the modulation of DNA methylation and how the crosstalk between these epigenetic mechanisms may contribute to transcriptional regulation. These findings led me to consider the role of non-coding RNA in the mechanisms of epigenetic crosstalk (Fig. 2).

Non-coding RNAs (ncRNAs) are divided into two categories based on size: long non-coding RNAs (lncRNA; >200 nucleotides and short non-coding RNAs (sncRNA; <200 nucleotides) (78). Short non-coding RNAs are further classified based on genomic origin and mechanism of action, which include extra coding RNAs (ecRNA), small interfering RNA (siRNA), microRNAs (miRNAs) and Piwi-interacting RNA (piRNA) (78). While studies show lncRNAs directly and indirectly contribute to epigenetic regulation by acting as signals, decoys, guides, and scaffolds, the role of sncRNAs in epigenetics is less understood (18). However, there is increasing evidence for sncRNAs directly interacting with histone modifying complexes or DNA methyltransferases, thus I turned my efforts to exploring the mechanisms for how sncRNAs engage into the epigenetic regulatory network (Fig. 2). For instance, sncRNAs (~100 nucleotides) transcribed from the 5' end of Polycomb Repressive Complex-2 (PRC2) target-genes directly bind PRC2 and enhance the catalysis of histone H3 lysine-27 trimethylation (H3K27me3) by PRC2, which impacts the differentiation of murine ES cells (83). Additionally, Fos Proto-Oncogene (Fos) extra-

coding RNA (ecRNA), defined as non-polyadenylated RNAs originating from the sense strand of regions outside gene boundaries (transcription start and end sites), directly inhibits DNMT3A activity in neurons and is associated with long-term fear memory formation in adult rats (4). In chapter V I relied on *Fos* ecRNA, DNMT3L and synthetic histone H3 tails or reconstituted polynucleosomes to assess the roles of distinct epigenetic mechanisms in the simultaneous modulation of DNMT3A activity and better model the cellular interactions of the epigenetic regulatory network.

In chapter V I showed that *Fos-1* ecRNA binds the tetramer interface of DNMT3A, which relies on localized production of ecRNAs rather than the formation of ecRNA/DNA structures. I also found that ecRNAs play dominant roles in the modulation of DNMT3A activity in DNMT3A-histone H3 tails-regulatory protein-ecRNA complexes. Although there is a growing interest in understanding the dynamic interplay between distinct epigenetic mechanisms, few studies have characterized how the crosstalk between de novo DNA methylation, histone modifications, regulatory proteins and ncRNAs translates into meaningful biological outcomes (76-78), (84). Our work provides mechanistic insights into how the interactions between distinct components of the epigenetic machinery may target and modulate the activity of DNMT3A at specific genomic regions, which to date remains largely uncharacterized.

Small molecule inhibitors of DNMT3A

The establishment of specific epigenetic modifications is achieved by the action and modulation of writers, such as DNA methyltransferases, histone acetyltransferases and histone methyltransferases (85). Modifications on DNA or histone tails may then recruit proteins containing reader domains, which recognize specific marks, or eraser enzymes that can remove modifications to DNA or histones (85). Given the reversible nature of

epigenetic modifications, there is a growing interest in the development of therapeutics targeting epigenetic enzymes, particularly allosteric modulators (86), (87). While some success has been reported in the identification of allosteric inhibitors targeting histone modifiers, DNMTs have proven challenging in this regard (88-90). In fact, the U.S. Food and Drug Administration (FDA) has only approved two nucleoside inhibitors (Azacitidine and Decitabine) of DNMTs to date (91), (92). Azacitidine and Decitabine function as prodrugs that are incorporated into DNA and inhibit DNMT activity through the formation of a covalent irreversible DNMT-DNA suicide complex (Fig. 4 C.) (91), (92). In addition to these nucleoside inhibitors of DNMTs, small molecules that act as cofactor AdoMet competitors to inhibit DNMT3A have been reported (93-97). However, the use of competitive inhibitors of DNMT3A is not only highly cytotoxic but also presents several disadvantages compared to allosteric inhibitors in terms of specificity within a family of related proteins, non-related proteins with shared cofactor or inability to target surfaces involved with modulation of enzymatic activity (98). Based on these observations I sought to identify (chapter VI) and characterize (chapter VII) novel allosteric modulators of DNMT3A.

Using a DNA methylation-based assay, we screened a library of chemically diverse compounds (Medicines for Malaria Venture Pathogen Box) and identified two structurally related pyrazolone (inhibitor 1) and pyridazine (inhibitor 2) inhibitors of DNMT3A with low micromolar inhibition constants. Furthermore, inhibitors 1 and 2 do not display a competitive mechanism with DNA or AdoMet and are selective for DNMT3A in comparison to DNMT1 and bacterial CpG methyltransferases (chapter VI). Given that our data is consistent with inhibitors 1 and 2 acting as allosteric inhibitors of DNMT3A, I sought to characterize the precise mechanism of action and the surface on DNMT3A bound by

these inhibitors. With the use of mutational mapping, radiochemical and binding assays under various conditions, I found that inhibitors 1 and 2 selectively inhibit DNMT3A activity by disrupting PPIs at the tetramer interface and that this mechanism of inhibition persists even when DNMT3A is in complex with distinct partner proteins. These findings present two novel compounds with the potential use for modulation of epigenetic pathways through disruption of PPIs with DNMT3A (Fig. 2).

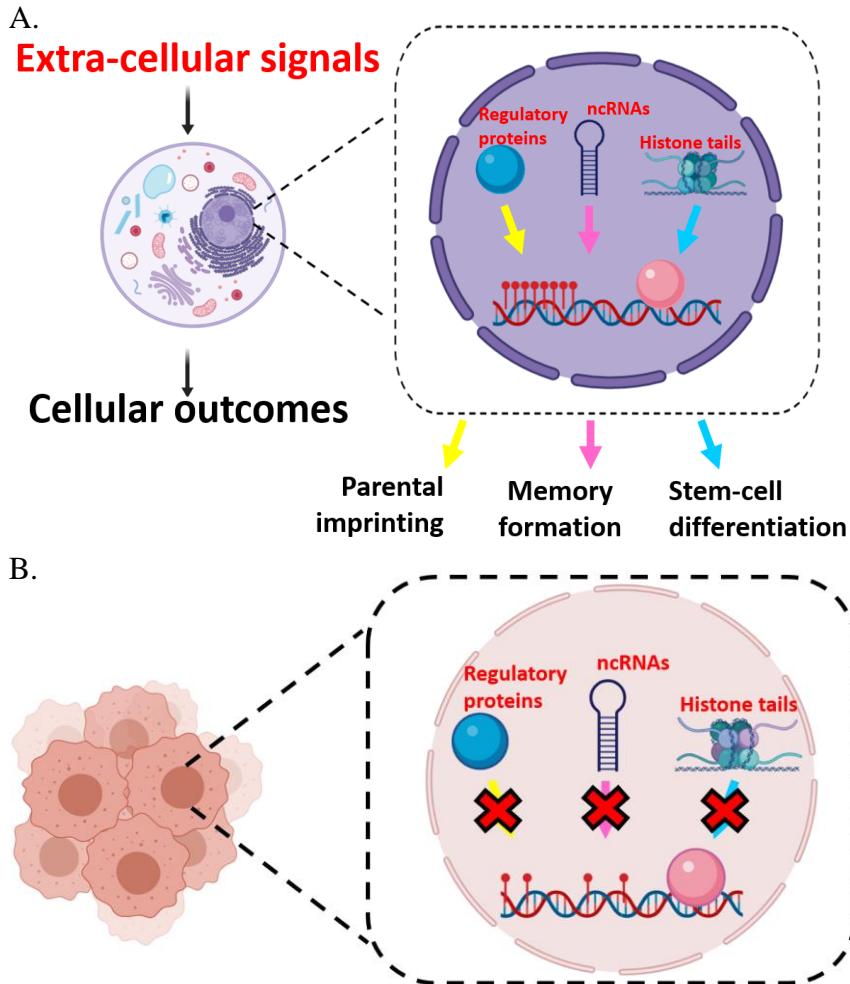


Figure 1. Epigenetic mechanisms in transcriptional regulation and disease. **A.** The combinatorial effects of distinct epigenetic mechanisms on biological responses. **B.** Disruption of the crosstalk between epigenetic mechanisms leads to inappropriate gene expression and is associated with human diseases like cancer.

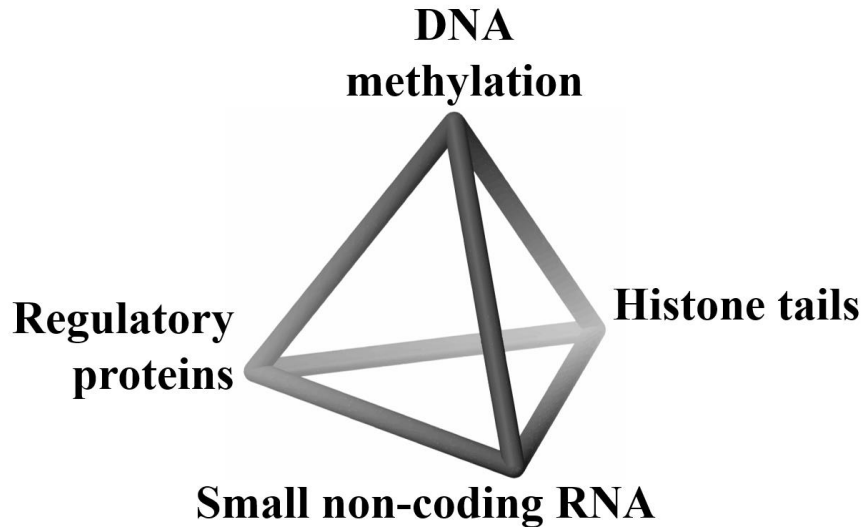


Figure 2. Crosstalk between components of the epigenetic machinery. The combinatorial activity of DNA methyltransferases and histone modifiers, with their modulation by regulatory proteins and non-coding RNAs, contributes to transcriptional regulation.

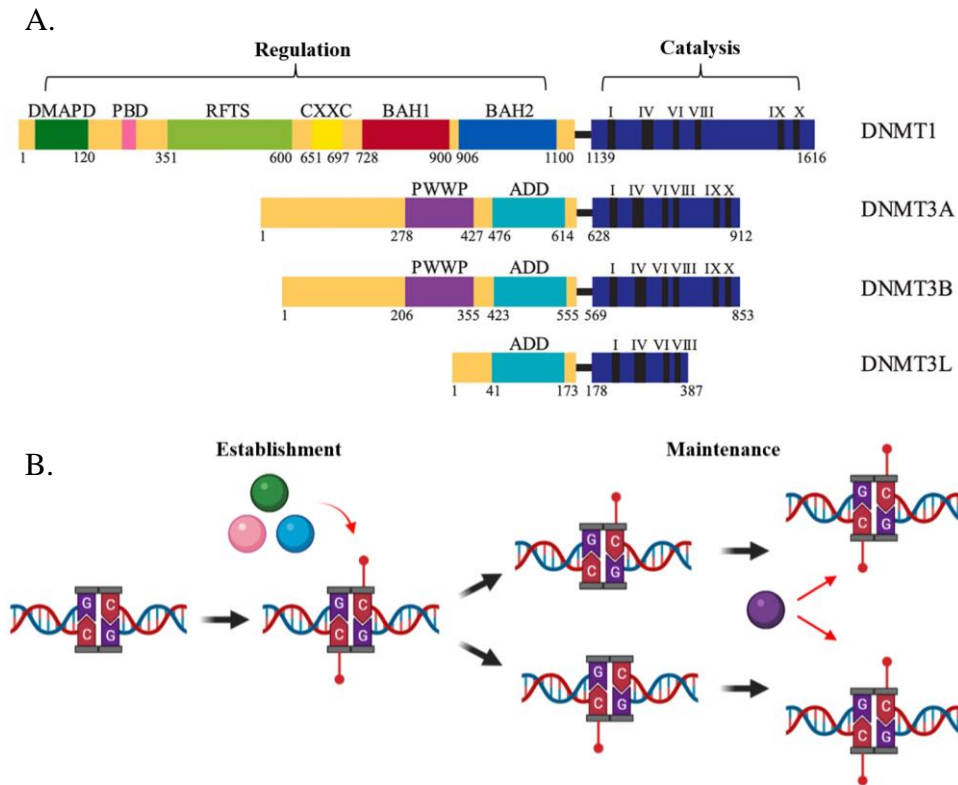


Figure 3. Human DNMT family of proteins and types of DNA methylation. **A.** Apart from the non-catalytic DNMT3L, DNMT catalytic domains consist of conserved motifs (I-X), which are catalytically active in the absence of the regulatory N-terminal domains. **B.** DNMT3A (■), DNMT3B (■) and DNMT3L (■) are associated with the establishment of new DNA methylation patterns in unmethylated cytosine substrates. In contrast, DNMT1 (■) acts on hemimethylated cytosine substrates to propagate these patterns in daughter cells after replication.

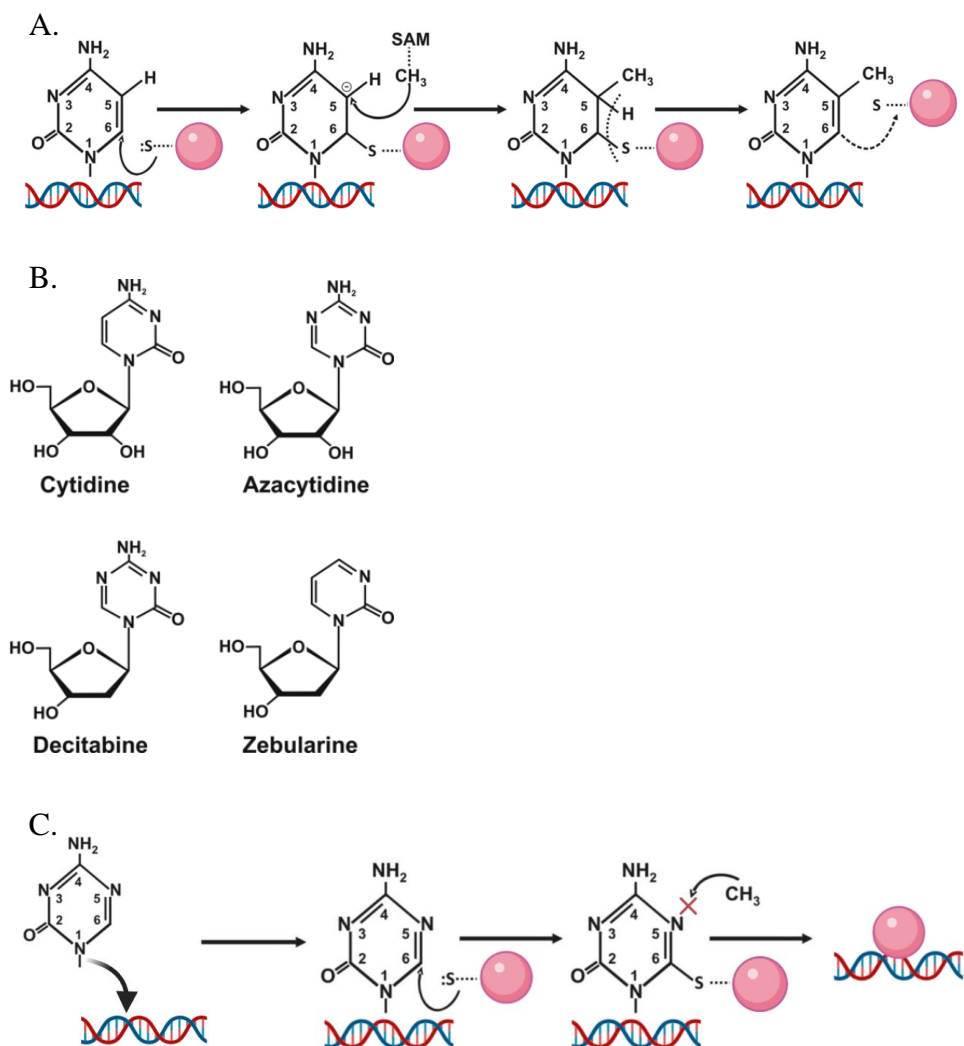


Figure 4. Mechanism of 5-methylcytosine methylation by DNMT and exploitation of this mechanism by nucleoside inhibitors. A. Methylation at the 5-position of a cytosine ring is initiated by the nucleophilic attack of a highly conserved cysteine in the DNMT catalytic domain. The methyl group is then transferred from the S-adenosyl-L methionine (SAM) cofactor, β elimination releases the enzyme and produce 5-methylcytosine. **B.** Structures of nucleoside analog inhibitors of DNMT3A. Azacytidine and Decitabine have been approved by the U.S. Food and Drug Administration (FDA). **C.** Nucleoside analogs (**B.**) act as a pro-drug that is inserted into DNA for inhibition of DNMTs. The presence of a nitrogen atom at the 5-position of these analogs prevents the transfer of a methyl group from the cofactor after the nucleophilic attack by DNMTs. The inability to release the enzyme by β elimination results in a covalent irreversible DNMT-DNA complex.

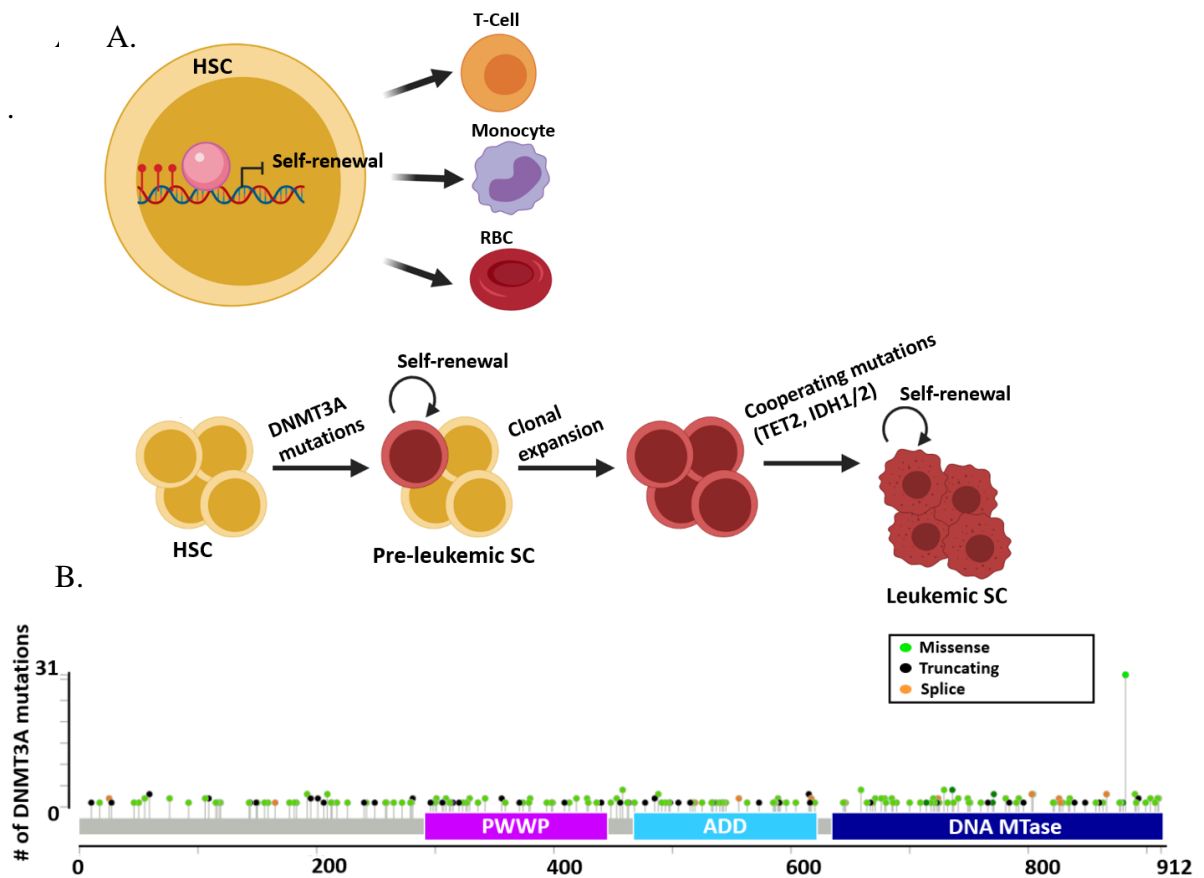


Figure 5. DNMT3A mutations in AML. **A.** (Top) DNMT3A silences genes associated with self-renewal in Hematopoietic stem cells (HSCs), which leads to the differentiation of distinct blood cell lineages. (Bottom) HSCs acquire the ability to self-renew and form pre-leukemic stem cells due to the mutations in *DNMT3A* and loss of DNA methylation activity. Clonal expansion and the presence of cooperating mutations leads to the establishment of leukemic stem cells (65), (66). **B.** Data obtained from The Cancer Genome Atlas (TCGA) of 280 patients with *de novo* AML reveal DNMT3A is recurrently mutated in AML patients.

Chapter II: Mutations in the DNMT3A DNA methyltransferase in acute myeloid leukemia patients cause both loss and gain of function and differential regulation by protein partners

Abstract

Eukaryotic DNA methylation prevents genomic instability by regulating the expression of oncogenes and tumor-suppressor genes. The negative effects of dysregulated DNA methylation are highlighted by a strong correlation between mutations in the *de novo* DNA methyltransferase gene *DNA methyltransferase 3A (DNMT3A)* and poor prognoses among acute myeloid leukemia (AML) patients. We show here that clinically observed *DNMT3A* mutations dramatically alter enzymatic activity, including mutations that lead to 6-fold hypermethylation and 3-fold hypomethylation of the human *cyclin-dependent kinase inhibitor 2B (CDKN2B or p15)* gene promoter. Our results provide insights into the clinically observed heterogeneity of *p15* methylation in AML. Cytogenetically normal AML (CN-AML) constitutes 40–50% of all AML cases and is the most epigenetically diverse AML subtype with pronounced changes in non-CpG DNA methylation. We identified a subset of *DNMT3A* mutations that enhance the enzyme's ability to perform non-CpG methylation by 2–8-fold. Many of these mutations mapped to *DNMT3A* regions known to interact with proteins that themselves contribute to AML, such as thymine DNA glycosylase (TDG). Using functional mapping of TDG–*DNMT3A* interactions, we provide evidence that TDG and DNMT3-like (DNMT3L) bind distinct regions of *DNMT3A*. Furthermore, *DNMT3A* mutations caused diverse changes in the ability of TDG and DNMT3L to affect *DNMT3A* function. Cell-based studies of one of these *DNMT3A* mutations (S714C) replicated the enzymatic studies and revealed that it causes dramatic losses of genome-wide

methylation. In summary, mutations in DNMT3A lead to diverse levels of activity, interactions with epigenetic machinery components and cellular changes.

Introduction

5-Methylcytosine (5-MC) is a naturally occurring epigenetic modification of mammalian DNA associated with essential cellular processes such as transcriptional regulation and cellular differentiation (1, 2). Like many cancers, acute myeloid leukemia (AML) involves changes to gene expression arising from aberrant DNA methylation patterning (3, 4). Yet unlike most cancers, and compared with genetic abnormalities, epigenetic aberrations appear to be more prevalent in AML (5). In fact, AML is marked by recurring mutations in genes of epigenetic modifiers including the de novo DNA methyltransferase, DNMT3A, in which mutations throughout the *DNMT3A* gene are observed in 22% of all AML patients (6, 7). Furthermore, DNA methylation profiles of AML patients reveal that aberrant methylation is heterogenous and can occur as either hyper- or hypomethylation (4). In addition to changes in DNA methylation, specific mutations in DNMT3A sufficiently disrupt interactions with regulatory components, which can be restored pharmacologically (7). The ability to rationally direct such changes will require a fundamental biochemical understanding of mutations in DNMT3A.

DNMT3A forms homo- and heterotetrameric complexes, and prior structure–function studies highlighted the importance of residues in the DNMT3A interfaces for methylation activity, processive catalysis, and oligomerization (8). In addition, some mutations, like R882H, coincided with those observed in AML patients, thereby highlighting the contributions of specific residues to catalysis and regulation through interactions that stabilize the homotetramer as well as complexes involving partner proteins (8). Due to its striking prevalence in AML patients, R882H has been extensively studied

and its biochemical characterization has provided possible mechanisms of how this substitution may manifest itself in AML (8–10). Therefore, establishing a fundamental biochemical understanding of additional AML mutations in DNMT3A may broaden our understanding of the role aberrant DNMT3A activity plays in AML.

AML patients harbor a wide-range of mutations dispersed throughout the *DNMT3A* gene at varying frequencies with distinct predicted consequences to enzymatic function (Fig. 1) (11). Here we combine a detailed functional analysis of DNMT3A with mutations identified in AML patients that remain largely unexplored at the level of activity and regulation through interactions with partner proteins. Some DNMT3A mutants show enhanced activity, whereas others show an attenuated ability to methylate the *p15* promoter, a genomic target that is linked to AML (12–15). The methylation of non-CpG sites is altered in AML subtypes, and we show that this activity is enhanced in some DNMT3A mutants (16, 17). Several mutants show differential regulation by thymine-DNA glycosylase (TDG), a component of the base excision repair (BER) system (18, 19), and DNMT3-like (DNMT3L), another partner protein (20, 21). Overall, we show how clinically relevant DNMT3A mutations may contribute to the aberrant DNA methylation in these patients.

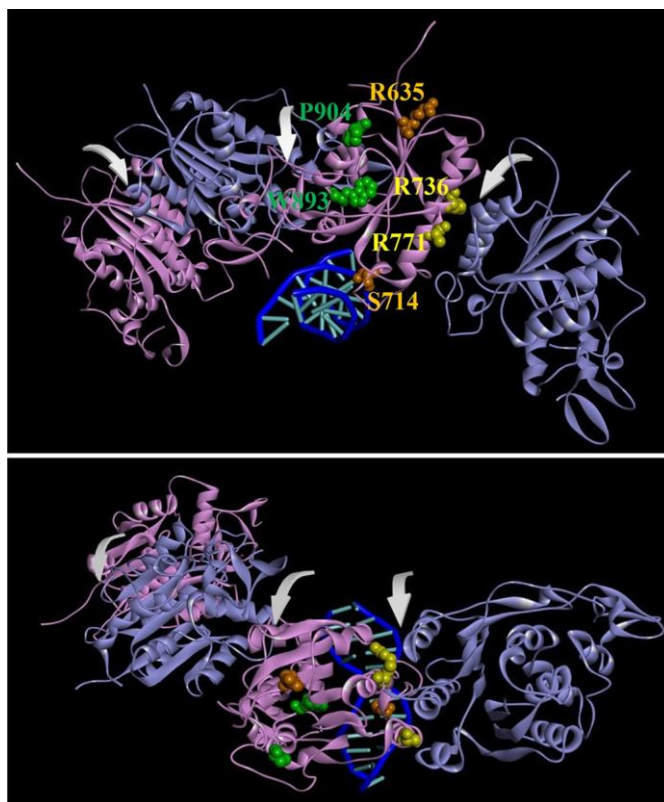


Figure 1. Mutations from AML patients in a DNMT3A homotetramer model. A model of the DNMT3A homotetramer (alternating purple and cyan monomers) bound to DNA was generated by aligning DNMT3A monomers to DNMT3L in a DNMT3A–DNMT3L heterotetramer crystal structure (PDB ID code 2QRV) followed by a subsequent alignment of a DNMT3A monomer to a M.HhaI-dsDNA co-crystal structure (PDB ID code 3EEO). Arrows in front view (A) and top view (B) indicate dimer and tetramer interfaces. Mutated residues are categorized based on location as follows: surface, orange; tetramer inter- face, yellow; and internal, green.

Results

Mutations from AML patients in the DNMT3A catalytic domain lead to varying degrees of DNA methylation

A common feature of AML patients carrying mutations in DNMT3A is the heterogeneity in both patterns and levels of DNA methylation, including the promoter region of the *p15* tumor suppressor gene (12, 13). Furthermore, patients with mutations in DNMT3A display hypermethylation of the *p15* promoter and reduced levels of this tumor suppressor (14, 15). Due to the diverse spatial distribution of the mutations throughout the DNMT3A catalytic domain, we sought to determine whether individual mutations vary to the extent and mechanism of DNMT3A functional changes, thereby contributing to the heterogeneity in DNA methylation observed within the AML population. We studied the ability of the WT and mutant DNMT3A (catalytic domain) to methylate the *p15* promoter by inserting the promoter into a vector lacking any CpG sites (pCpG^L) (21), referred to as *p15*-pCpG^L. Due to the limited number of CpG sites, DNMT3A has reduced activity on the *p15* human promoter (compared with poly(dI-dC) (Table 1) (21). Poly(dI-dC) represents the extreme of a high site-density substrate, whereas the *p15*-pCpG^L represents a low-density substrate, but being derived from a CpG island, is still higher density than is typical of the human genome.

Relative to WT enzyme, R771P, S714C, and R635G, led to a 3-, 2.5-, and 1.5-fold decrease in activity, respectively, on the *p15*-pCpG^L substrate (Table 1). Alternatively, we found that R736H, R771Q, R771G, W893S, and P904L displayed varying levels of *p15*-pCpG^L hypermethylation compared with WT (Table 1). R771Q showed the most robust hypermethylation with a 6-fold increase in activity, followed by R736H and P904L with nearly a 4-fold increase, then R771G and W893S with roughly

a 2-fold increase (Table 1). Our results suggest mutations in DNMT3A identified in AML patients significantly vary in their ability to methylate *p15*-pCpG^L, which agrees with the heterogeneity in both patterns and levels of DNA methylation observed in these patients.

The k_{cat} for WT DNMT3A using poly(dI-dC) is 4.7 h⁻¹ and is comparable with previous findings using similar substrate and enzyme concentrations (Table 1) (21). Like that observed in *p15*- pCpG^L, the impact on enzyme function observed in the various AML mutants varied extensively with poly(dI-dC) as a substrate. However, in contrast to our results using the *p15*- pCpG^L substrate, most AML mutants displayed hypomethylation of poly(dI-dC) relative to WT. Although R635G, W893S, and R771G displayed minimal levels of DNA methylation, S714C, P904L, R771P, and R736H resulted in at least a 2-fold decrease in activity relative to WT (Table 1). Of the mutations studied here, including additional substitutions to the R771 codon, R771Q was the only enzyme that exhibited an elevated rate of poly(dI-dC) methylation with a 2-fold increase relative to WT (Table 1). However, for several mutants we observed enhanced activity on *p15*- pCpG^L showing that the density of sites contributes to how these mutations impact function. Although R771Q, S714C, and R771P displayed a similar trend as WT, P904L, W893S, R771G, and R635G led to enhanced activity on *p15*- pCpG^L (Fig. 2).

In summary, compared with the WT DNMT3A, five of the eight mutants show differential changes when comparing the two substrates (poly(dI-dC) and *p15*- pCpG^L). For example, R635G is significantly worse with the high-density substrate than *p15*- pCpG^L, whereas R771Q shows the opposite trend. Even more surprising, some mutants actually reverse the trends compared with the WT enzyme; thus, W893S shows

dramatically worse activity than the WT enzyme on poly(dI-dC) but shows improved activity with the *p15*-pCpG^L substrate. R736H and R771G show a similar trend. Thus, the mutants may result in highly variable changes in their ability to methylate regions of high- and low-density CpG sites.

Table 1. k_{cat} values for wildtype and AML patient-derived DNMT3A mutants using poly(dI-dC) and *p15*-pCpG^L DNA substrates. Mutations mapped to similar locations within the DNMT3A catalytic domain display different levels of activity, such as mutations at the tetramer interface, which display both loss- and gain-of-function. All enzymes were at 150 nM tetramer, corresponding to 27 nM active tetramer enzyme (24). DNA substrate concentrations were: 5 μ M bp for poly(dI-dC) and 10 μ M bp for *p15*-pCpG^L plasmid. Product formation was measured after 1 h and the data for each substrate were fit to a linear regression and k_{cat} values were obtained by dividing V_{max} by the amount of active enzyme. Data reflect the results from at least 3 independent reactions. Mutations are categorized based on their respective location within the DNMT3A catalytic domain (red denotes hypomethylation and green denotes hypermethylation).

		k_{cat} (hr ⁻¹)	
		<i>p15</i> -pCpG ^L	poly dI-dC
	WT	0.71±0.08	4.7 ±0.09
Surface	R635G	0.45±0.06	0.20 ±0.04
	S714C	0.28±0.06	1.44 ±0.51
Internal	W893S	1.44±0.27	0.59±0.05
	P904L	2.24±0.20	1.69±0.30
Tetramer Interface	R736H	2.56±0.55	2.73±0.40
	R771Q	4.76±0.20	10.97±1.78
	R771P	0.24±0.02	1.33±0.05
	R771G	1.90±0.10	0.57±0.19

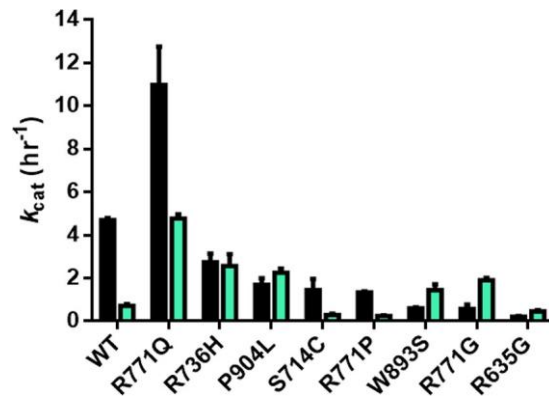


Figure 2. A subset of mutations display little change or enhanced activity for *p15*-pCpG^L relative to the multiple CpG site substrate poly(dI-dC). WT DNMT3A has significantly reduced activity on *p15*-pCpG^L (cyan, 20 μ M bp) relative to poly(dI-dC) (black, 5 μ M bp) due to the limited number of CpG sites on the human promoter substrate (~10-fold less). R736H and P904L display minimal change in activity across DNA substrates, whereas W893S, R771G, and R635G lead to enhanced activity in *p15*-pCpG^L. R771Q maintains significantly higher activity for both DNA substrates. Enzyme concentrations are 150 nM tetramer (27 nM active tetramer) (24) and k_{cat} (h^{-1}) values were determined as described under “Experimental procedures.”

A subset of AML mutations display enhanced ability to perform non-CpG methylation

In healthy cells, DNMT3A-mediated non-CpG methylation is associated with maintaining pluripotency (16, 22). Alternatively, compared with healthy bone marrow cells, non-CpG regions of cytogenetically normal AML (CN-AML) cells show the most pronounced changes in DNA methylation. Mutations in DNMT3A may contribute to this aberrant methylation and disease pathology (17). The pCpG^L vector, lacking any CpG sites and the *p15* insert, provide an opportunity to measure cytosine methylation at non-CpG sites (Fig. 3). Given that WT DNMT3A has minimal activity with pCpG^L (k_{cat} , 0.1– 0.2 h^{-1}) and the rate of product formation increases with the number of

substrate CpG sites, the pattern observed for the rate of product formation by WT DNMT3A is as follows: poly(dI-dC) > *p15*- pCpG^L > pCpG^L L (21). Unlike the WT enzyme, R771G, R635G, and W893S show comparable activity on poly(dI-dC) and pCpG^L and the greatest activity with *p15*- pCpG^L (Fig. 4). Alternatively, R736H displayed virtually equal levels of activity across poly(dI-dC), *p15*- pCpG^L, and pCpG^L. Along with distinct patterns of activity across the substrates tested, R771G, W893S, and R736H displayed a 3-, 4-, and 9-fold increase in non-CpG methylation, respectively, compared with the WT enzyme (Fig. 4).



Substrate	CpG sites	Size (bp)	CpG spacing
poly dI-dC	~500	~1000	
<i>p15</i>	54	749	

Figure 3. Substrate diagram and characteristics. Although poly(dI-dC) contains an extensive number of CpG sites with virtually no space between, *p15*- pCpG^L consists of a limited number of sites available for methylation that are heterogeneously spread. The pCpG^L vector, to which the *p15* human promoter was inserted, is 3,872 bp in size and lacks any CpG sites for methylation

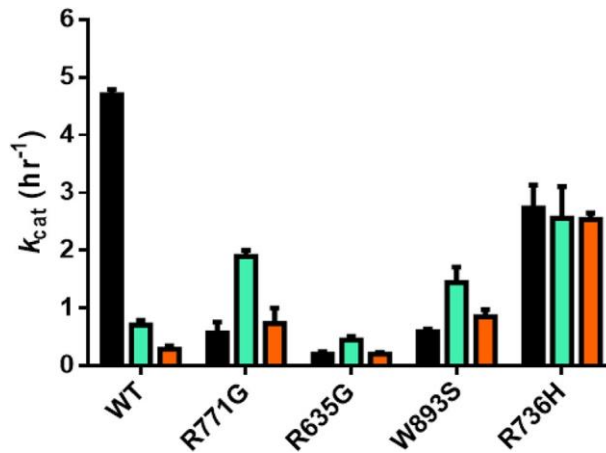


Figure 4. Some mutations result in enhanced activity at non-CpG sites. WT DNMT3A activity is affected by the availability of CpG sites on the DNA substrate as noted by the drastic activity loss from poly(dI-dC) (*black*, 5 μ M bp poly(dI-dC)) to *p15*-pCpG^L (*cyan*, 20 μ M bp) and limited activity on a non-CpG substrate (*orange*, 20 μ M bp pCpG^L). In contrast to the WT enzyme, R771G, R635G, and W893S display a similar pattern of activity across substrates with enhancement on *p15*-pCpG^L (*cyan*, 20 μ M bp) and comparable levels on poly(dI-dC) (*black*, 5 μ M bp poly(dI-dC)) and non-CpG substrate (*orange*, 20 μ M bp pCpG^L). R736H activity on the non-CpG substrate is significantly higher and virtually equal to substrates with multiple CpG sites. Enzyme concentrations are 150 nM tetramer (27 nM active tetramer) (24). Data reflect the results from at least three independent reactions.

Most AML mutations are unresponsive to modulation by TDG

TDG, a component of the BER system, is responsible for removing single T bases in G–T mismatches that arise from spontaneous deamination of 5-methylcytosine (23). Furthermore, there is *in vivo* and *in vitro* evidence suggesting the direct DNMT3A–TDG interaction affects the activity of both enzymes in a reciprocal manner (18). Given that components of the BER system are affected in AML, the regulatory effect of TDG on the activity of AML-derived DNMT3A mutants was assessed (19). Li *et al.* (18) show that TDG inhibits DNMT3A activity in a dose-dependent manner with

2-fold excess TDG to DNMT3A having a greater inhibitory effect than equimolar concentrations of both proteins. In our hands, increasing concentrations of TDG relative to WT DNMT3A (1:1, 1:2, and 1:3, DNMT3A:TDG) did not further augment the 3-fold TDG-mediated inhibition (Fig. S1) (24). Therefore, the inhibitory effect of TDG on the various DNMT3A AML variants was tested at equimolar concentration of both enzymes. Given that DNMT3A and TDG contribute to the normal methylation and de-methylation of the *p15* promoter, *p15*-pCpGL presents a biologically relevant platform to assess the interactions among the two enzymes (25). Co-incubation of TDG with WT DNMT3A and the *p15*-pCpGL human promoter substrate, led to approximately a 2.5-fold decrease in methylation, which we also observed in all mutants except for R771Q and R736H (Table 2). Interestingly, although the WT enzyme shows a similar effect when using the high site-density substrate (poly(dI- dC)), the TDG-mediated inhibition for the R771Q mutant is ~15-fold with this substrate (Table 2).

Table 2. Fold inhibition by TDG for wildtype and AML patient-derived DNMT3A mutants using poly(dI-dC) and *p15*-pCpG^L DNA substrates. Fold inhibition was determined by product formed by DNMT3A alone divided by product formed by DNMT3A with TDG. Except for R771Q, all other surface, tetramer interface, and internal mutations lead to comparable levels of reduced sensitivity to inhibition by TDG. All enzymes were at 150 nM tetramer (27 nM active tetramer for DNMT3A) (24) and DNA substrate concentrations were: 5 μM bp for poly(dI-dC) and 10 μM bp for *p15*-pCpG^L plasmid. Wildtype DNMT3A and mutant variants were preincubated with TDG for 1 h at 37 °C prior to initiating the reaction by the addition of substrate DNA. Mutations are categorized based on their respective location within the DNMT3A catalytic domain (red denotes greater inhibition, while green denotes lower inhibition, relative to wildtype). Data reflect the results from at least three independent DNMT3A-TDG co-incubation reactions.

		TDG fold inhibition	
		<i>p15</i> -pCpG ^L	poly dI-dC
	WT	2.67 ±0.27	2.15 ±0.15
Surface	R635G	1.15±0.06	1.10±0.05
	S714C	1.65±0.24	1.77±0.48
Internal	W893S	1.18±0.02	1.10±0.02
	P904L	1.67±0.18	1.32±0.05
Tetramer Interface	R736H	3.13±0.05	1.60 ±0.24
	R771Q	5.23±0.20	15.41±1.51
	R771P	1.15±0.04	1.38±0.04
	R771G	1.46±0.21	1.07±0.02

AML mutations are variably responsive to stimulation by DNMT3-like (DNMT3L)

Ultimately our interest is to better understand how protein– protein interactions influence DNMT3A function, and how mutations might impact those interactions. Although the number of proteins shown or implicated in interacting with DNMT3A is extensive (26 –28), we know very little about the regions on the DNMT3A surface

involved in these complexes and the functional consequences of these altered interactions. The DNMT3A–DNMT3L co-crystal structure provides compelling insights into such interactions (29). Ley *et al.* (9) showed that although primary tissue samples from AML patients lack expression of the catalytically inactive member of the DNMT family, DNMT3L, spliced variants of DNMT3L transcripts were detected in various patients. Furthermore, DNMT3L provides an example of how an auxiliary protein interacts with and modulates DNMT3A function, and how mutations may impact on that function. A 1-h preincubation of DNMT3L with DNMT3A at a 1:1 ratio activates WT DNMT3A activity by ~5-fold on *p15*-pCpG^L, which we also observed in P904L and R771Q (Table 3). Alternatively, the rest of the mutants assessed in this study appeared to be desensitized to DNMT3L and displayed approximately half the extent of DNMT3L activation (Table 3). Under identical conditions and comparable with previous findings, DNMT3L activation was ~7-fold for WT DNMT3A using poly(dI-dC) as a substrate (Table 3) (20). With the same high site-density substrate (poly(dI- dC)), R736H was the only substitution with comparable levels of DNMT3L stimulation as WT (Table 3). Although R771Q resulted in a 2-fold increase in DNMT3L activation, the remaining mutants assessed in this study displayed reduced modulation of DNA methylation activity by DNMT3L (Table 3). In summary, our results imply that in addition to direct changes in DNMT3A activity, AML patient-derived mutations in DNMT3A additionally disrupt modulation of DNMT3A by partner proteins.

Table 3. Fold stimulation by DNMT3L for wildtype and AML patient-derived DNMT3A mutants using poly(dI-dC) and *p15*-pCpG^L DNA substrates. Fold stimulation was determined by the sum of product formed by DNMT3A with DNMT3L divided by product formed by DNMT3A without DNMT3L. DNMT3L, known to interact at the tetramer interface of DNMT3A, leads to varying levels of responsiveness for tetramer interface and internal mutations, but comparable reduced stimulation in surface mutations. All DNMT3As were at 150 nM tetramer, corresponding to 27 nM active tetramer enzyme (24). DNA substrate concentrations were: 5 μM bp for poly(dI-dC) and 10 μM bp for *p15*-pCpG^L plasmid. Wildtype and DNMT3A mutants were preincubated with DNMT3L (1:1) for 1 h at 37 °C prior to initiating the reaction by the addition of substrate DNA. Mutations are categorized based on their respective location within the DNMT3A catalytic domain (red corresponds to decreased stimulation and green corresponds to increased stimulation, compared to wildtype). Data reflect the results from at least three independent DNMT3A–DNMT3L co-incubation reactions.

		DNMT3L fold stimulation	
		<i>p15</i> -pCpG ^L	poly dI-dC
	WT	5.30±0.61	6.82±0.50
Surface	R635G	2.33±0.20	3.91±0.48
	S714C	2.93±0.60	3.64 ±1.04
Internal	W893S	2.10±0.05	2.06±0.02
	P904L	5.03±0.18	4.52±0.98
Tetramer Interface	R736H	3.95±0.18	5.82±1.61
	R771Q	5.44±0.14	12.92±0.20
	R771P	2.20±0.12	2.23±0.10
	R771G	2.38±0.07	2.32±0.34

P904L and R736H display distinct alterations to processive catalysis that are sensitive to substrate CpG density

WT DNMT3A is highly processive on both biological and synthetic DNA substrates (20, 21). Furthermore, mutational analyses suggest residues at the dimer interface are essential for DNMT3A to perform processive catalysis (8). The ability of WT DNMT3A, and the two mutants P904L and R736H to processively methylate poly(dI-dC) or *p15*-pCpG^L was assessed using the chase processivity assay (21). Comparable with previous findings, WT DNMT3A continually methylates the initially bound substrate for multiple rounds of methylation as noted by the same degree of poly(dI-dC) methylation observed in both the substrate only and chase conditions for 100 min following the addition of chase DNA (pCpG^L, Fig. 5A). Alternatively, addition of chase DNA led to a considerable decrease in the ability of P904L to methylate poly(dI-dC), indicating this mutant rapidly dissociates from the poly(dI-dC) substrate during catalysis (Fig. 5B). As a control, the addition of a mixture of both substrate and chase DNA at the start of the reaction virtually eliminates all methylation activity with the WT enzyme (Fig. 5A). However, R736H appears to treat chase DNA (which lacks CpG sites) as a substrate in the presence of poly(dI-dC) because we observe nearly identical levels of methylation under all conditions tested (Fig. 5C). As in the case of the high site-density substrate (poly(dI-dC)), addition of chase DNA (pCpG^L) to the WT enzyme failed to disrupt processive catalysis in the presence of *p15*-pCpG^L indicating a high degree of processivity. In contrast P904L displayed substantial disruptions of processivity on both substrates (Fig. 6B); the fact that the R736H mutant shows such strikingly different responses to the type of substrate being tested (Fig. 6B) suggests that the mutations have distinctive consequences on the ability of DNMT3A to carry out repeated catalysis on the same DNA molecule.

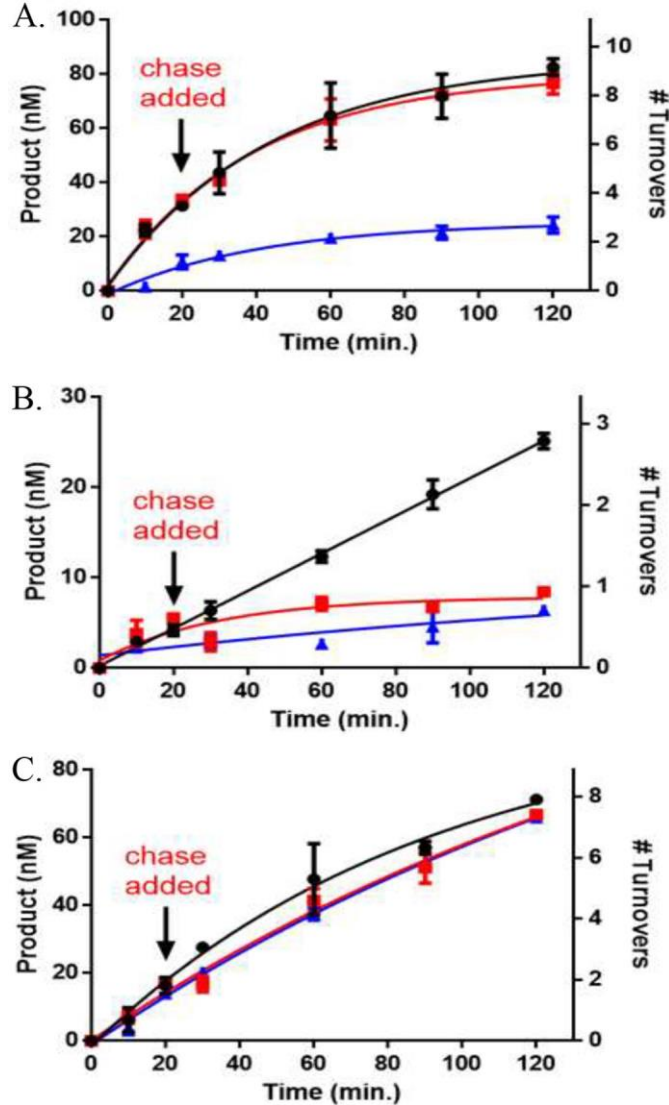


Figure 5. AML mutants display unique alterations to processive catalysis on the poly(dI-dC) substrate. **A.** WT DNMT3A; **B.** P904L; and **C.** R736H at 50 nM tetramer. Substrates were added at time 0 to start the reaction and chase assay conditions were as follows: *black circle*, substrate only (2 μ M bp poly(dI dC)); *red square*, substrate and then 20 min chase (40 μ M bp pCpG^L); *blue triangle*, substrate (2 μ M bp poly(dI-dC)) and chase (40 μ M bp pCpG^L) at the start of the reaction. Data reflect the results from at least three independent experiments.

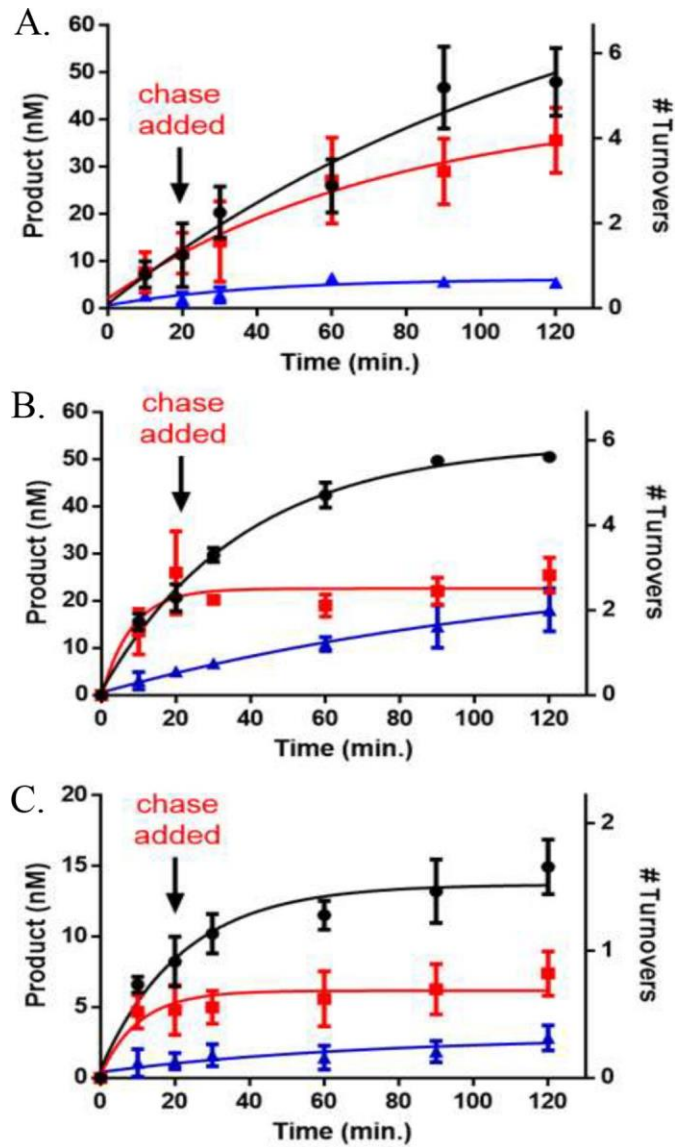


Figure 6. AML mutations display loss of processive catalysis on the *p15*-pCpG^L human promoter substrate. **A.** WT DNMT3A retains the ability to perform processive catalysis when tested with the *p15*-pCpG^L substrate, whereas **B.** R736H and **C.** P904L resulted in a loss of processivity. All enzyme concentrations were 50 nM tetramer. Substrates were added at time 0 to start the reaction and chase assay conditions were as follows: *black circle*, substrate only (10 μ M bp *p15*-pCpG^L); *red square*, substrate and then 20 min chase (200 μ M bp pCpG^L); *blue triangle*, substrate (10 μ M bp *p15*-pCpG^L) and chase (200 μ M bp pCpG^L) at the start of the reaction. Data reflect the results from at least three independent experiments.

TDG does not compete with DNMT3L for binding on the DNMT3A tetramer interface

The DNMT3A–DNMT3L co-crystal structure implicates the DNMT3A tetramer interface as a region for binding by DNMT3L (29). Although DNMT3A interacts with a wide range of partner proteins, the specific region on the DNMT3A surface (*e.g.* tetramer interface or elsewhere) involved in formation of heterotetrameric complexes remains unknown (26–28). Functional assays can be used to define a protein–protein interface; for example, Doherty *et al.* (30) mapped regions on the Werner syndrome helicase important for replication protein A binding. Using a nonfunctional approach (size-exclusion chromatography), Chen *et al.* (31) showed SKI proto-oncogene (SKI) and CREB-binding protein compete for the same binding region on SMAD3. To elucidate the region on DNMT3A for TDG binding, we determined whether TDG and DNMT3L compete for binding to the DNMT3A tetramer interface. We first determined the relative binding affinities of each for DNMT3A. DNMT3A co-incubations with DNMT3L resulted in a $K_{D,app}$ of 80 ± 12 nM (Fig. 7A), whereas a $K_{D,app}$ of 223 ± 74 nM was determined from DNMT3A co-incubations with TDG (Fig. 7B). To assess whether DNMT3L or TDG binding to DNMT3A are mutually exclusive, all three proteins were preincubated for 1 h prior to starting the reaction by the addition of substrate DNA and DNMT3A activity measured at 30, 60, and 90 min. The combined results (Fig. 8, *light grey*) are distinct from the results when DNMT3A is incubated with DNMT3L (Fig. 8, *medium grey*) or TDG (Fig. 8, *dark grey*) alone. Instead, WT DNMT3A, DNMT3L, and TDG preparations (Fig. 8, *light grey*) reflected virtually the same level of activity as WT DNMT3A alone (Fig. 8, *black*). The results obtained from WT DNMT3A–DNMT3L–TDG co-incubations suggest: 1) TDG does not bind the DNMT3A tetramer interface and the activity of a WT DNMT3A–DNMT3L–TDG

complex equals that of WT DNMT3A alone, or 2) co-incubation results in formation of a subset of DNMT3A–DNMT3L and DNMT3A–TDG complexes that yield the same level of activity as WT DNMT3A alone, or 3) DNMT3L and TDG interact with one another leaving WT DNMT3A alone.

To further assess whether DNMT3L or TDG binding to the DNMT3A tetramer interface are mutually exclusive events, active DNMT3A–DNMT3L (or DNMT3A–TDG) heterotetramers were challenged by the addition of TDG (or DNMT3L). In reactions where WT DNMT3A–DNMT3L co-incubations ran for 30 min, the addition of TDG did not disrupt active WT DNMT3A–DNMT3L heterotetramers (Fig. 9A, *green*) and displayed comparable activity as WT DNMT3A–DNMT3L co-incubations (Fig. 9A, *black*). However, the addition of DNMT3L to active WT DNMT3A–TDG heterotetramers (Fig. 9B, *green*) led to a rapid increase in product formation that was greater than WT DNMT3A–TDG co-incubations (Fig. 9B, *black*). Taken together, the results suggest: 1) TDG does not compete with DNMT3L for binding to the DNMT3A tetramer interface, 2) the DNMT3A tetramer interface is accessible for DNMT3L binding in the presence of TDG, and 3) the location for TDG binding on DNMT3A is inaccessible to TDG in the presence of DNMT3L.

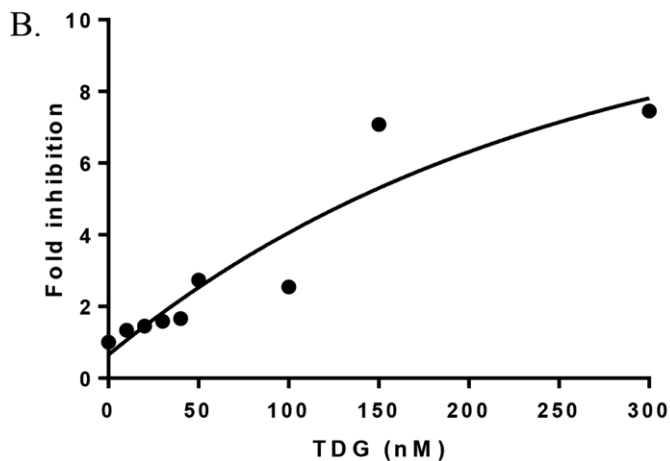
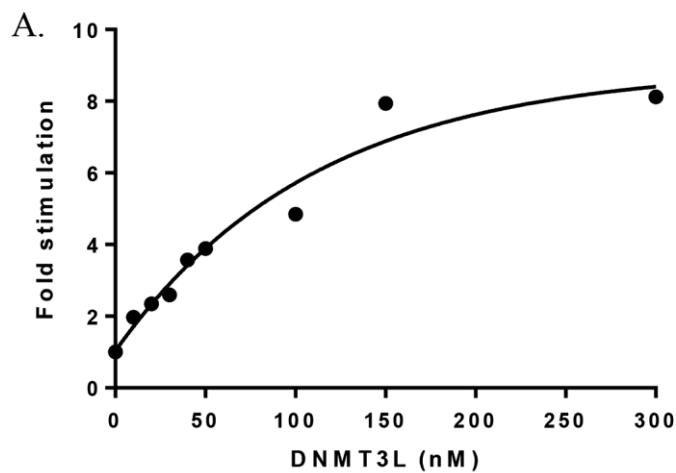


Figure 7. DNMT3L has a higher affinity for binding DNMT3A compared with TDG. In **A.** and **B.**, DNMT3A (10 nM) was preincubated in reaction buffer for 1 h at 37 °C with varying concentrations of TDG or DNMT3L (0–300 nM). Reactions were initiated by the addition of 5 μ M bp poly(dI-dC) and run for 1 h. Fold stimulation was determined by the sum of product formed by DNMT3A with DNMT3L divided by product formed by DNMT3A without DNMT3L **A.** Fold inhibition was determined by product formed by DNMT3A alone divided by product formed by DNMT3A with TDG **B.** Data reflect the results from at least three independent co-incubation reactions.

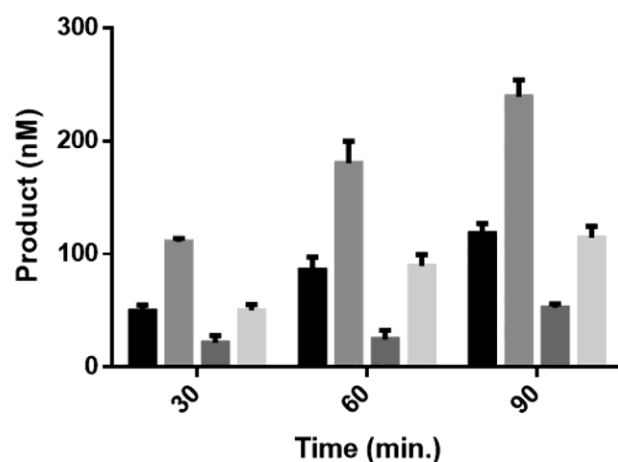


Figure 8. DNMT3L or TDG binding on DNMT3A tetramer interface are not mutually exclusive. WT DNMT3A, DNMT3L, and TDG co-incubations did not reflect the modulatory effect observed when either DNMT3L or TDG are pre-incubated with DNMT3A. Enzyme concentrations for all the reactions performed were 150 nM and at 1:1 for co-incubations. Prior to initiating the reaction by the addition of 5 μ M bp poly(dI-dC); *light grey*, WT DNMT3A, DNMT3L, and TDG were preincubated for 1 h at 37 $^{\circ}$ C. Under similar conditions, the following reactions were performed as controls: *black*, WT DNMT3A; *medium grey*, WT DNMT3A and DNMT3L; *dark grey*, WT DNMT3A and TDG. Data reflect the results from at least three independent competitive co-incubation experiments.

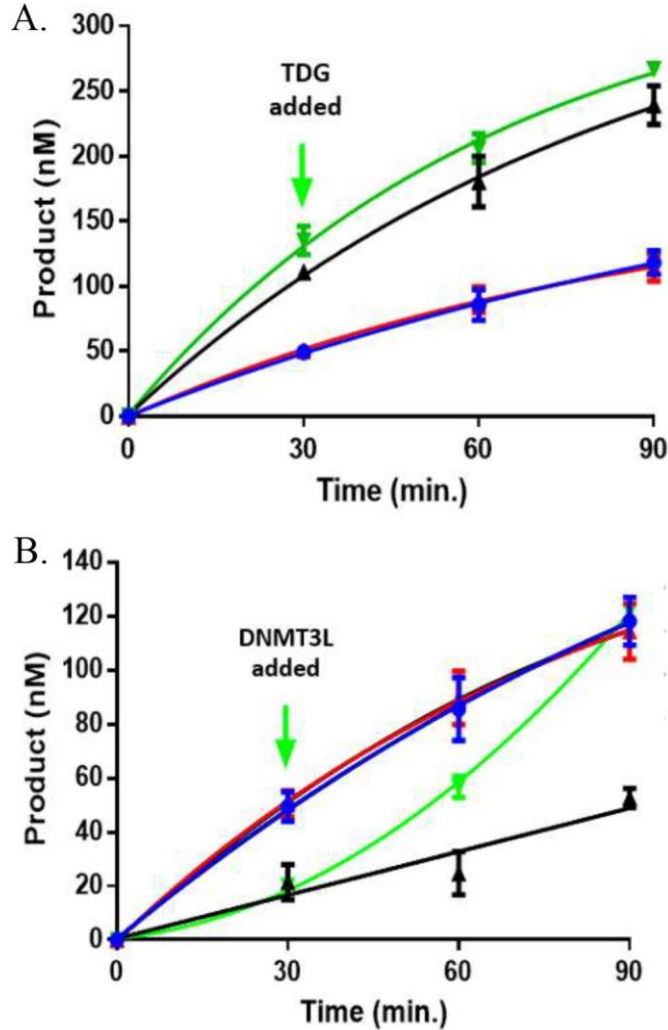


Figure 9. TDG does not compete with DNMT3L for binding to DNMT3A. The addition of TDG does not disrupt the activity of a functional DNMT3A– DNMT3L heterotetramer, but the addition of DNMT3L increases the activity of a functional DNMT3A–TDG heterotetramer. In all experiments performed, enzyme concentrations were 150 nM (1:1 for co-incubations or binding competitions) and reaction were initiated by the addition of 5 μ M bp poly(dI-dC). **A.**, *green*, WT DNMT3A was preincubated with DNMT3L for 1h at 37 $^{\circ}$ C and the reaction run for 30 min prior to the addition of TDG. **B.** *green*, WT DNMT3A was preincubated with TDG for 1h at 37 $^{\circ}$ C and the reaction run for 30 min prior to the addition of DNMT3L. The following reactions were also tested as controls: **A.** *black*, WT DNMT3A and DNMT3L; **B.** *black*, WT DNMT3A and TDG; **A.** and **B.** *blue*, WT DNMT3A; **A.** and **B.** *red*, WT DNMT3A, DNMT3L, and TDG preincubated at the start of the reaction (**A.** and **B.**). Data reflect the results from three independent experiments.

Whereas R771Q leads to a modest decrease in methylation, S714C appears to be catalytically inactive in murine embryonic stem cells

To determine the cell-based activity of the DNMT3A mutants, we utilized a system allowing the induction of full-length doxycycline-inducible DNMT3A–GFP fusion expression in methylation-deficient murine embryonic stem cells (DNMT3A/3B double knock-out mESCs; DKO mESCs). DNMT3A mutant-expressing cells were sorted by flow cytometry after doxycycline induction for 2 weeks (Fig. 2, A–D). The mean fluorescence intensity between mutant and control samples was similar (Fig. S2E), suggesting that protein expression level of DNMT3A^{WT}, DNMT3A^{S714C}, and DNMT3A^{R771Q} was comparable. The methylation level of DKO mESCs was undetectable using a dot-blot assay to measure 5-mC (Fig. 10). Re-expressing DNMT3A^{WT} significantly increases overall DNA methylation. In addition, DNMT3A^{R771Q} showed a slight decrease of DNA methyltransferase activity compared with the cells expressing DNMT3A^{WT}, whereas the DNMT3A^{S714C} mutant seemed to be a catalytic inactive mutation with negligible DNA methylation detectable after introduction into the ES cells (Fig. 10).

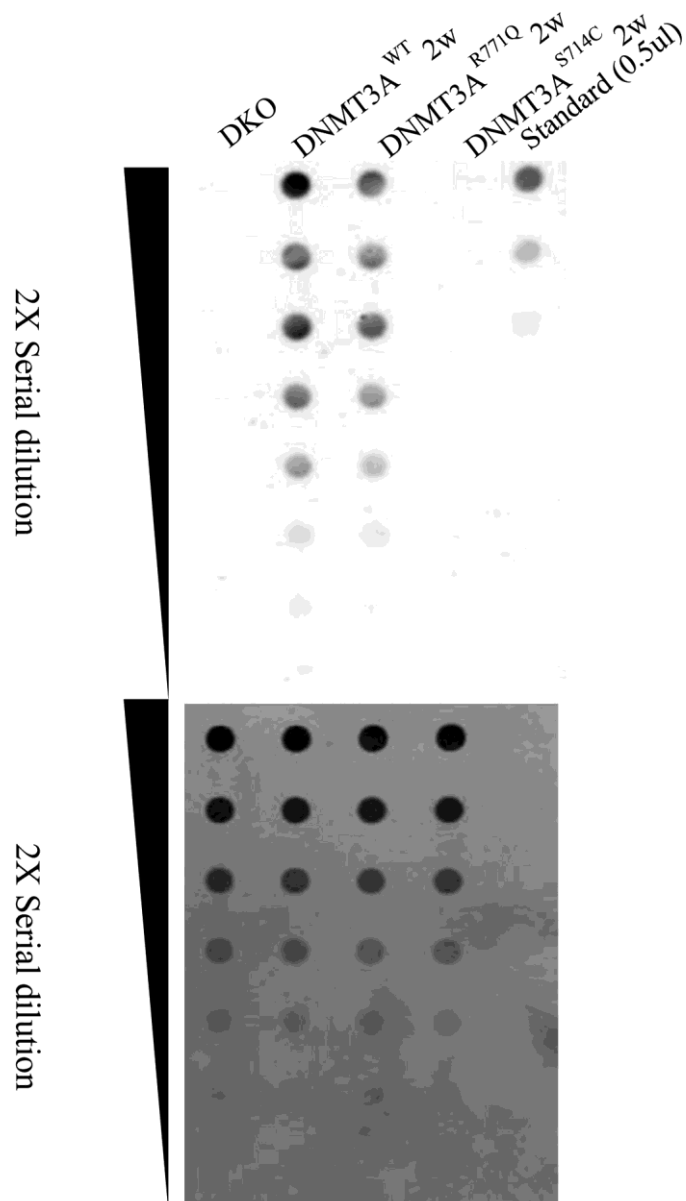


Figure 10. S714C reduces DNA methylation in mESCs. The images show the methylation level as determined by a dot-blot assay in doxycycline-inducible DNMT3A mutant-expressing DKO mESCs after doxycycline induction for 2 weeks. The *upper blot* represents serial dilution of DNA derived from the indicated cells in the dot-blot, probed with an antibody against 5-mC. The *lower blot* represents serial dilution of standard methylated DNA as a control.

Discussion

Our motivation for this study is based on several intertwined observations. Mutations in DNMT3A have emerged as very important drivers of disease in various hematological disorders including AML (9, 32–35). Our prior work suggests that the functional consequences from such mutations involve changes in methylation efficiency, the enzyme's oligomeric state, and ability to carry out processive catalysis (8, 20). Finally, DNMT3A directly and indirectly interacts with a large number of partner proteins; in many cases such interactions are known to directly influence the enzyme's specificity, subcellular localization, and overall activity (26, 27, 36, 37).

Our focus on the subset of clinically relevant DNMT3A mutants (Table 1) was determined by their relative frequency in AML patients, a lack of any previous biochemical characterization, and our prior work demonstrating that mutations at the dimer and tetramer DNMT3A–DNMT3A interfaces disrupt the oligomeric state of the tetramer (8). Multiple regions of DNMT3A form minor mutational hot spots, and the frequency and position of these hot spots vary significantly in a cancer-specific fashion; for example, in AML, Arg-882 is mutated in 58% of patients and mutations to Arg-736 are observed in 2%. The fact that patient-identified mutations appear across the entire DNMT3A protein suggests that they may result in distinctive molecular phenotypes. A working hypothesis is that some of these regions and mutations alter protein–protein interactions between DNMT3A and its partner proteins.

The most striking feature of our study is the range of functional consequences resulting from the different DNMT3A mutations, in some cases involving the same position (*e.g.* R771Q, -P, and -G), or spatially related residues like W893S and P904L. Thus, compared with the WT enzyme, we observe dramatic increases (~7-fold, R771Q

on *p15*-pCpGL) and decreases (24-fold, R635G on poly(dI-dC)) in activity (Table 1). This is also revealed in how the different mutations impact the ability of DNMT3A to act processively in carrying out methylation of spatially proximal sites. For example, P904L is dramatically decreased in this activity, whereas R736H is not impacted at all (Fig. 5). Changes in this activity are anticipated to impact the ability of the enzyme to efficiently methylate regions of the genome undergoing rapid methylation (38). Furthermore, R736H, unlike the WT enzyme, is fully capable of methylating cytosines at non-CpG positions (Figs. 3 and 5). This feature of R736H is not unique, as W893S and R771G both show enhanced non-CpG activity relative to the WT enzyme. Non-CpG methylation, associated with maintaining pluripotency, is accomplished by DNMT3A in mammalian stem cells (16, 28). CN-AML account for 40–50% of all AML cases observed (39). CN-AML cells show pronounced changes in non-CpG methylation when compared with healthy CD34+ bone marrow cells (17). Therefore, mutations in DNMT3A with altered non-CpG methylation activity may have detrimental consequences *in vivo*.

The functional consequences of methylating the *p15*-pCpGL substrate are particularly relevant because a hallmark of AML patients with mutations in DNMT3A is the heterogeneity in both patterns and levels of DNA methylation in the promoter region of the *p15* tumor suppressor gene (12, 13). The range of changes relative to the WT enzyme, 3-fold reduction in R771P to 7-fold enhancement in R771Q (Table 1), suggest that these mutations will profoundly differ in their impact on DNA methylation *in vivo*. Studies have additionally shown that AML patients carrying mutations in DNMT3A display reduced *p15* levels and hypermethylation of the *p15* promoter (14,

15). Our results show that most mutations led to hypermethylation of the *p15*-pCpGL substrate, which is in agreement with that observed in AML patients.

Perhaps surprisingly, the positions of particular changes (*e.g.* Fig. 1, *orange*, surface, *yellow*, tetramer, or *green*, internal) are not uniformly correlated with any particular functional consequence. The four changes at the tetramer interface (three at Arg-771 and R736H) result in decreases (R771P) and increases (R736H, R771Q, and R771G) in activity with *p15*-pCpGL (Table 1). However, the two tetramer interface mutations R771G and R736H both result in dramatic enhancement of non-CpG methylation (Fig. 4). Also, the two internal substitutions (W893S and P904L) both result in decreased activity with *p15*-pCpGL, and the two surface substitutions (R635G and S714C) both show increases in this activity relative to the WT enzyme (Table 1). Although the effect of some mutants may be predicted by their location on DNMT3A, our results highlight the importance of functional characterization given that mutations on the same location on DNMT3A can lead to pronounced changes in activity.

Proteins that direct epigenetic changes in distinct pathways (*e.g.* DNA methylation, histone modification, RNA) are now understood to rely on extensive cross-talk, largely mediated through protein–protein interactions (40, 41). Because many proteins have been identified to interact with DNMT3A, we sought to determine how the mutations studied here impact some of these interactions, and how those interactions alter DNMT3A function. The DNMT3A–DNMT3L co-crystal structure implicates the DNMT3A tetramer interface as a region for binding and regulation of DNMT3A by a partner protein. Therefore, if the DNMT3A tetramer interface region is the only surface occupied by partner proteins, mutations at the tetramer interface would be predicted to have similar responses to TDG and DNMT3L modulation. However, tetramer interface

mutants were differentially responsive to TDG inhibition (Table 2) and DNMT3L stimulation (Table 3), and overall, most mutations were desensitized to modulation by TDG or DNMT3L. Given that the region on DNMT3A for DNMT3L binding is well-defined, we then sought to explore whether TDG competes with DNMT3L for binding on the DNMT3A tetramer interface, or alternatively, TDG binds a different surface on DNMT3A. Our results from DNMT3L/TDG competitions for binding to DNMT3A suggest TDG does not compete with DNMT3L for binding to DNMT3A. Furthermore, the DNMT3A tetramer interface is accessible to DNMT3L in the presence of TDG and the surface for TDG binding on DNMT3A is inaccessible to TDG in the presence of DNMT3L (Figs. 8 and 9). DNMT3A has been shown to directly interact with a wide range of partner proteins that can impact enzymatic activity (25, 27, 28). The functional mapping used in this study by competitive binding using a well-defined regulatory protein, like DNMT3L, provides a rapid approach to explore the location of additional partner proteins of DNMT3A.

Our goal is to understand how mutations in DNMT3A derived from AML patients alter DNMT3A activity, either directly, or through interactions with other cellular components. Prior work has focused largely on R882H, which displays substantial hypomethylation in focal regions of the genome, although global methylation levels are comparable with WT DNMT3A (42, 43). In addition, the changes in methylation patterns observed in R882H appear to be dependent on the cell context and factors therein (42). Both enzyme- and cell-based studies show that R882H disrupts the oligomeric state of the protein and alters its ability to act on DNA (8, 10, 42). Here we show that S714C results in undetectable cellular levels of global methylation, whereas R771Q showed a slight decrease in methylation compared with WT (Fig. 10). For

S714C, the enzyme and cell-based data are in accordance, suggesting that this substitution disrupts intrinsic enzymatic activity, which cannot be restored by additional regulatory components found in cells.

On the other hand, whereas the R771Q displayed increased DNA methylation activity *in vitro*, this hypermethylation activity was not observed in the ES cell-based assay; instead, a moderate decrease in activity was observed. These discordant results with R771Q could be explained by a number of factors. In the enzyme studies, we are using a specific substrate, poly(dI-dC), that is routinely used to measure DNMT3A activity (44), and the plasmid bearing the p15 promoter. In contrast, the cell-based assay measures the aggregate effect of methylation changes over the whole genome, including many different types of targets. Thus, the enhanced activity seen with specific substrates and R771Q may simply result from composition of the DNA substrates, and the enzyme activity across the whole genome is, on aggregate, largely unchanged from the WT DNMT3A.

Another likely possibility is that cellular factors modulate the activity of particular mutants directly or indirectly. Of note, the *ex vivo* methylation assays were performed with the catalytic domain of DNMT3A, whereas the cell-based assays were performed with the full-length version of DNMT3A. The N-terminal regulatory domains (45, 46) of DNMT3A, including the ATX–DNMT3A–DNMT3L (ADD) and PWWP domains, may modulate the enzyme's activities. These and other DNMT3A sequences are known to interact with numerous partner proteins. Thus, cellular factors may regulate the ultimate outcomes of particular DNMT3A mutations. Indirect support for this explanation comes from the observation that a Tatten-Brown-Rahman syndrome patient with the R882H mutation had modest changes in methylation patterns of blood cells

(peripheral blood polymorphonuclear cells, monocytes, and T cells), whereas more substantial changes are observed in R882H expressing primary AML samples (42). Thus, implying cellular factors appear to ultimately dictate the cellular outcomes of a particular DNMT3A mutation throughout AML progression.

In conclusion, mutations in DNMT3A can directly alter DNMT3A function as well as indirectly through changing the enzyme's interaction with partner proteins. Diseases that show evidence of changes in DNA methylation, including cancer and in particular AML, are likely to result from a blend of these direct and indirect mechanisms. Interestingly, for those mutations studied here, the indirect mechanisms involving partner proteins do not restore the enzyme's WT activity. The latter changes may well be approachable therapeutically, because small molecules that interfere with protein–protein interactions, whereas challenging to design, have achieved some success.

Methods

Expression constructs

The catalytic domain of DNMT3A (residues 634–912) was used for all DNMT3A experiments, given the catalytic domain and full-length enzyme have comparable kinetic parameters (k_{cat} , K_m^{DNA} , K_m^{AdoMet} , processivity, and DNMT3L stimulation) (47, 48). The codon-optimized plasmids used for recombinant protein expression include pET28a–hDNMT3A_CD (Δ 1–611) for the DNMT3A catalytic domain (24), pTYB1–3L for full-length DNMT3L (49), and pET28a–hTDG (Δ 1–175) for the TDG construct (50). The catalytic domain mutants in the pET28a–hDNMT3A_CD (Δ 1–611) expression construct were generated using a QuikChange Lightning Site-directed Mutagenesis kit (Agilent).

Protein expression and purification

DNMT3A (WT and mutants), DNMT3L, and TDG were expressed in NiCo21 (DE3) competent *Escherichia coli* cells (New England Biolabs). Cell cultures were grown in LB medium at 37 °C to an $A_{600\text{ nm}}$ of 0.7 (WT and mutant DNMT3A), 0.5 (DNMT3L), and 0.8 (TDG). Expression was induced by the addition of 1 mM isopropyl β -D-thiogalactopyranoside (Gold Biotechnology) at 28 °C. Induction times were 6 h for DNMT3A (WT and mutants), overnight for DNMT3L, and 4 h for TDG. Cells were then collected by centrifugation and stored frozen at $-80\text{ }^{\circ}\text{C}$. All proteins were purified from cells lysed by sonication in 50 mM HEPES, 350 mM NaCl, 50 mM imidazole, 10% glycerol, and 1% phenylmethylsulfonyl fluoride, pH 7.8, which were then clarified by centrifugation. Lysates were loaded onto a AKTA start FPLC system (GE Healthcare) for purification using a nickel-nitrilotriacetic acid column (GE Healthcare). Columns were equilibrated with 50 mM HEPES, 350 mM NaCl, 50 mM imidazole, 10% glycerol, and 1% phenyl- methylsulfonyl fluoride, pH 7.8, and washed with identical buffer but 70 mM imidazole. WT DNMT3A, along with all mutant variants, were eluted with 162.5 mM imidazole, 200 mM imidazole for DNMT3L, and 250 mM imidazole for TDG, and stored at $-80\text{ }^{\circ}\text{C}$ in storage buffer (50 mM $\text{KH}_2\text{PO}_4/\text{K}_2\text{HPO}_4$, 20% glycerol, pH 7.8).

Methylation assays

Assays were carried out to measure total methyl groups transferred from the AdoMet cofactor to substrate DNA by DNMT3A. Reactions took place at 37 °C in a buffer composed of 50 mM $\text{KH}_2\text{PO}_4/\text{K}_2\text{HPO}_4$, 1 mM EDTA, 1 mM DTT, 0.2 mg/ml of BSA, 20 mM NaCl, and 5 μM AdoMet (from a 50 μM stock composed of 45 μM unlabeled and 5 μM 3H-methyl labeled) at pH 7.8. 15- μl Aliquots were taken from a larger reaction and quenched by mixing with 0.1% SDS (1:1). Samples were spotted

onto Hybond-XL membranes (GE Healthcare), washed, and dried as previously established (51).

Catalysis (k_{cat})

WT DNMT3A and AML mutants (150 nM tetramer) correspond to 27 nM active tetramer, as previously determined (24). Reactions were initiated by the addition of substrate DNA (5 μ M bp poly(dI-dC), 10 μ M bp *p15*-pCpGL or 20 μ M) at saturation, run for 1h at 37 °C, and quenched as stated above. Values were determined as described in Holz-Schietinger *et al.* (20). In brief, data were fit to a linear regression and k_{cat} values were obtained by dividing V_{max} by the amount of active enzyme (Prism version 6.01). Data reflect the results from at least three independent reactions.

DNMT3L and TDG assays

DNMT3A was preincubated in reaction buffer with either DNMT3L or TDG for 1h at 37 °C prior to initiating the reaction by the addition of DNA (5 μ M bp poly(dI-dC) or 10 μ M bp *p15*-pCpGL). Reactions were quenched as stated above after 1 h at 37 °C. DNMT3L yields maximum activation of DNMT3A when preincubated at a ratio of 1:1 (21); therefore, equal concentrations of 150 nM of both enzymes were used for all DNMT3L assays. TDG inhibition of DNMT3A was tested at 1:1, 1:2, and 1:3 ratios of DNMT3A to TDG concentration. Given that no significant changes were observed on DNMT3A inhibition with varying TDG concentrations, equal concentrations of 150 nM DNMT3A and TDG were used for TDG assays. DNMT3L stimulation was calculated by the sum of product formed by DNMT3A with DNMT3L divided by product formed by DNMT3A in the absence of DNMT3L as previously described in Holz-Schietinger *et al.* (21). TDG- fold inhibition was calculated by product formed by DNMT3A alone

divided by product formed by DNMT3A with TDG. Data reflect the results from at least three independent co-incubation reactions.

Processivity assays

Processivity assays were performed to assess the fidelity of enzymes to methylate a multiple CG site DNA substrate when presented with an excess concentration of additional DNA lacking CG-methylation sites. Assays were performed as previously established (21) with enzyme concentrations of 50 nM tetramer, and substrate DNA concentrations of 2 μ M bp poly(dI-dC) or 40 μ M bp pCpGL. Following a 3-min preincubation at 37 °C, the reaction was initiated by the addition of 2 μ M bp poly(dI-dC) and the enzyme was allowed to carry out 1–2 turnovers on poly(dI-dC) (20 min). 40 μ M bp pCpGL (20-fold excess) was then added at 20 min to generate the chase condition. A reaction with a mixture of 2 μ M bp poly(dI-dC) and 40 μ M bp pCpGL at the start of the reaction was used as a control. The data were fit to a nonlinear regression (one phase decay) using Prism (version 6.01) as described in Holz-Schietinger *et al.* (8). Data reflect the results from at least three independent experiments.

Functional competitive binding assay

The DNMT3A–DNMT3L co-crystal structure provides a defined region on DNMT3A for DNMT3L binding and formation of a heterotetrameric complex. Although this tetramer interface region is well-defined, the surface on DNMT3A for TDG binding remains unknown. Therefore, a functional methylation assay was employed to assess whether TDG and DNMT3L compete for the same surface on DNMT3A. DNMT3A, DNMT3L, and TDG were preincubated at 1:1:1 (150 nM) in reaction buffer for 1h at 37 °C prior to initiating the reaction by the addition of DNA (5

μM bp poly(dI-dC)). To further challenge whether TDG also binds DNMT3A at the tetramer interface, DNMT3A and DNMT3L (1:1 at 150 nM) were preincubated for 1h at 37 °C, the reaction was initiated by the addition of 5 μM bp poly(dI-dC) and 150 nM TDG was added to the active heterotetramer at 30 min. Using similar conditions, a reciprocal reaction in which a preformed TDG–DNMT3A complex was challenged by the addition of DNMT3L was performed. As controls, reactions involving DNMT3A only, DNMT3A with either DNMT3L or TDG, and all three proteins together at the beginning of the reaction were performed. Data reflect the results from at least three independent co-incubation reactions.

Binding affinity of TDG or DNMT3L to DNMT3A

To assess the binding affinities of TDG or DNMT3L to DNMT3A, the effect of increasing concentrations of TDG or DNMT3L (10 –300 nM) were tested on a fixed concentration of DNMT3A (10 nM). DNMT3A was preincubated in reaction buffer for 1 h at 37 °C with varying concentrations of TDG or DNMT3L, reactions were initiated by the addition of 5 μM bp poly(dI-dC) and run for 1 h. Apparent affinity ($K_{D,app}$) were determined from a one-site specific binding model using Prism (version 6.01). Data reflect the results from at least three independent co-incubation reactions.

DNA sequences

DNA used for substrates include poly(dI-dC) (Sigma) and *p15*-pCpGL and pCpGL (non-CpG substrate) plasmids that were prepared as described in Holz-Schietinger *et al.* (21). Concentrations for DNA substrates are given in bp and were calculated from absorbance at 260 nm using the following extinction coefficients as previously determined: 6.9 $\text{mM}^{-1} \text{cm}^{-1}$ for poly(dI-dC) and 6.8 $\text{mM}^{-1} \text{cm}^{-1}$ for *p15*-pCpGL and pCpGL plasmids (21). The *p15*-pCpGL extinction coefficient considers

both *p15* promoter and pCpGL plasmid sequences to define the *p15*-pCpGL substrate concentration in number of base pairs.

Generation of doxycycline-inducible DNMT3A expressing cell line

Generation of doxycycline-inducible DNMT3A constructs was previously reported (52). In brief, full-length DNMT3A cDNA, which fused with a GFP sequence, was cloned into pDONR223 using a Gateway cloning BP clonase II enzyme mix. Two DNMT3A mutations, S714C and R771Q, were generated in pDONR–DNMT3A–GFP vectors using a QuikChange II site-directed mutagenesis kit. DNMT3A^{WT}, DNMT3A^{S714C}, and DNMT3A^{R771Q} GFP fusion cDNA were then Gateway- cloned into a pinducer20-BSD vector using Gateway LR clonase II enzyme mix.

DNMT3A/3B DKO mESCs were previously described (53). Lentiviral particles of DNMT3A/S714C/R771Q fusion GFP were generated using a previous published protocol (54) and then infected into DKO mESCs for 48 h. Lentivirus-infected DKO mESCs were treated with 4 µg/ml of blasticidin for 72 h and then recovered after 1 week and treated with 4 µg/ml of blasticidin for 1 week. DNMT3A-GFP expressing cells were then sorted using a FACSArial II sorter after 2 weeks of doxycycline induction and DNA was then extracted using a Purelink DNA extraction kit.

Dot-blot assay

A 5-mC dot-blot assay was previously described (55). In short, 500 ng of DNA was serially diluted and then treated with 1 M NaOH, 25 mM EDTA at 95 °C for 10 min. Ice-cold 2 M ammonium acetate was added to NaOH-treated DNA and incubated on ice for 10 min. Membranes of the dot-blot apparatus (Bio-Rad) were washed with 200 – 400 µl of TE buffer, loaded with denatured DNA, and then washed with 200 – 400 µl of 2× SSC and air-dried for 20 min. Membranes were baked in 80 °C for 2 h,

blocked using 5% nonfat milk TBST for 1 h, and incubated with 1:1000 anti-5-mC antibody at 4 °C overnight. The next day, membranes were washed with TBST for 10 min four times and then incubated with horseradish peroxidase- conjugated anti-rabbit secondary antibody at room temperature for 1 h. Membranes were washed with TBST for 10 min four times and reacted with ECL.

Supplementary Material

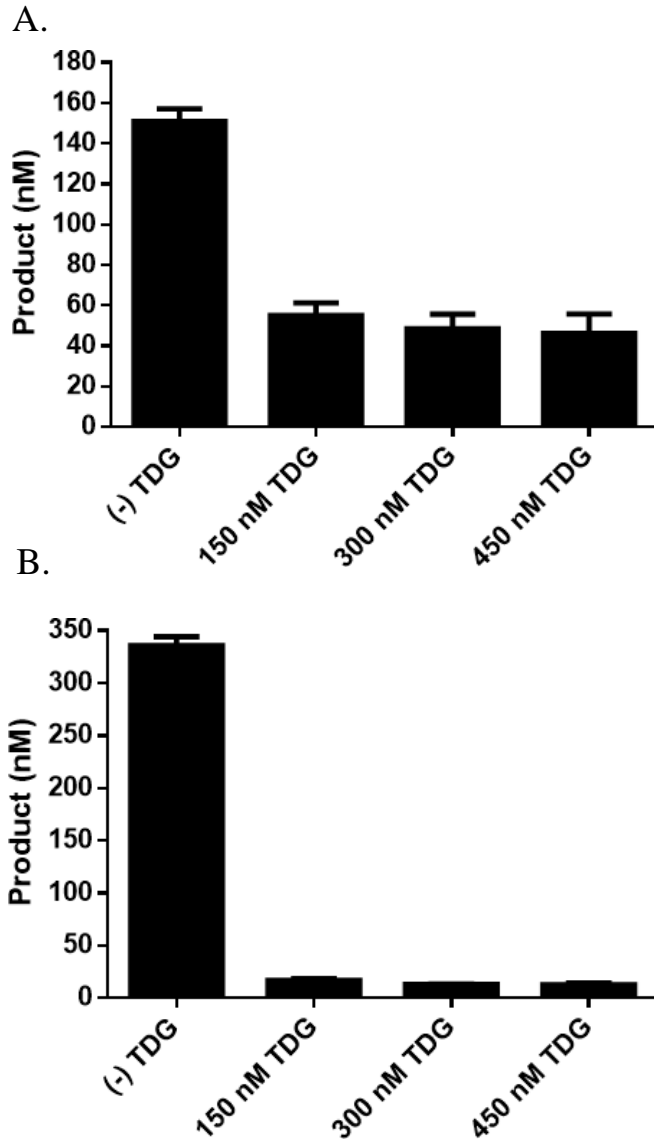


Figure S1. Equal concentration of TDG to active DNMT3A tetramer maximally inhibits methylation by DNMT3A. **A.** Wild type DNMT3A and **B.** R771Q at 150 nM tetramer were pre-incubated for 1 hour with increasing concentrations of TDG prior to starting the reaction by the addition of 5 μ M bp poly dI-dC. Product formation was measured after the reaction was run for 1 hour. 1:1, 1:2 and 1:3 concentrations of DNMT3A to TDG led to comparable levels of inhibition for wild type and R771Q.

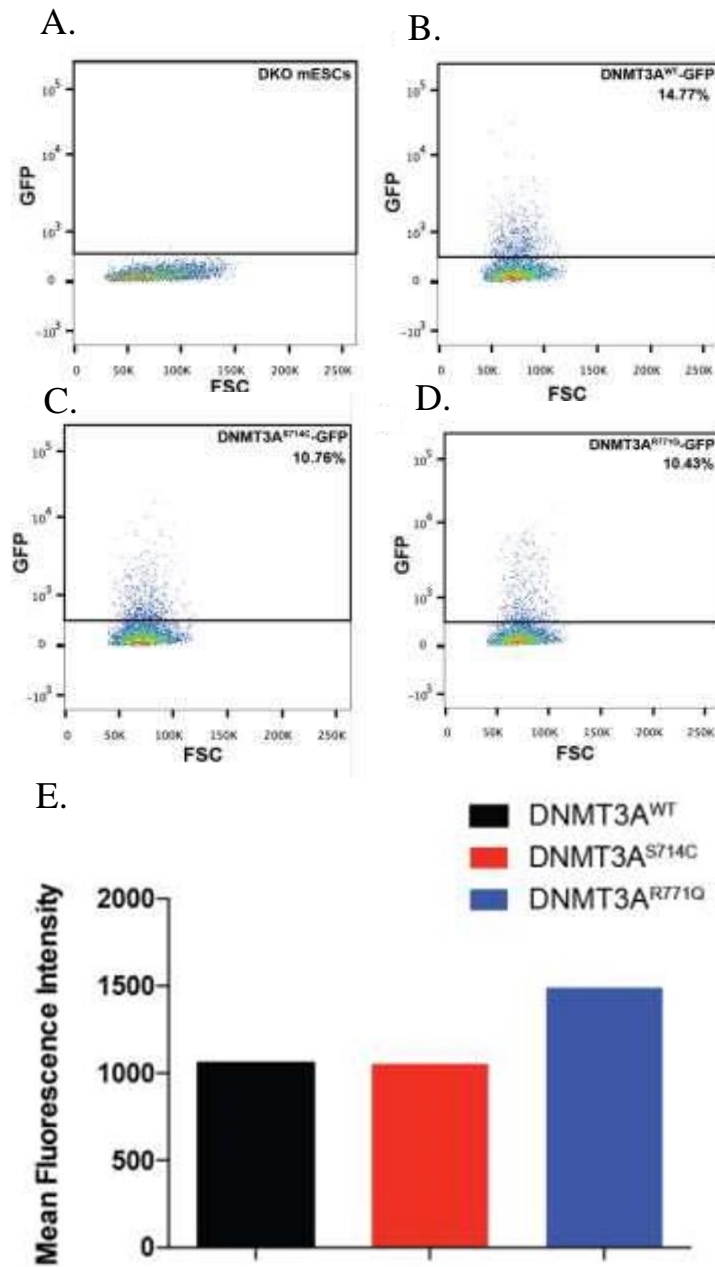


Figure S2. Cell sorting by flow cytometry following a two-week doxycycline induction. The graphs depict the GFP expression percentage as determined by flow cytometry in DNMT3A mutant expressing DKO mESCs after doxycycline induction for two weeks (a-d). The graph depicts the mean fluorescence intensity of the DNMT3A mutant expressing DKO mESCs after induction as determined by flow cytometry (e).

Chapter III: The R882H substitution in the human *de novo* DNA methyltransferase DNMT3A disrupts allosteric regulation by the tumor suppressor p53

Abstract

A myriad of protein partners modulate the activity of the human DNA methyltransferase 3A (DNMT3A), whose interactions with these other proteins are frequently altered during oncogenesis. We show here that the tumor suppressor p53 decreases DNMT3A activity by forming a heterotetramer complex with DNMT3A. Mutational and modeling experiments suggested that p53 interacts with the same region in DNMT3A as does the structurally characterized DNMT3L. We observed that the p53-mediated repression of DNMT3A activity is blocked by amino acid substitutions within this interface, but surprisingly, also by a distal DNMT3A residue, R882H. DNMT3A R882H occurs frequently in various cancers, including acute myeloid leukemia, and our results suggest that the effects of R882H and other *DNMT3A* mutations may go beyond changes in DNMT3A methylation activity. To further understand the dynamics of how protein–protein interactions modulate DNMT3A activity, we determined that p53 has a greater affinity for DNMT3A than for DNMT3L and that p53 readily displaces DNMT3L from the DNMT3A:DNMT3L heterotetramer. Interestingly, this occurred even when the preformed DNMT3A:DNMT3L complex was actively methylating DNA. The frequently identified p53 substitutions (R248W and R273H), while able to regulate DNMT3A function when forming the DNMT3A:p53 heterotetramer, no longer displaced DNMT3L from the DNMT3A:DNMT3L heterotetramer. The results of our work highlight the complex interplay between DNMT3A, p53, and DNMT3L and how these interactions are further modulated by clinically derived mutations in each of the interacting partners.

Introduction

Transcriptional regulation, genomic imprinting and cellular differentiation, including 5-methylcytosine patterning on DNA (1-7), relies on diverse protein-protein and protein-nucleic acid interactions. In the crowded intracellular environment, formation of biologically significant complexes relies on the kinetic accessibility to specific protein surfaces and the thermodynamic stability of the resultant complexes (8-11). For example, *de novo* DNA methylation by the DNA methyltransferase 3A (DNMT3A) involves the formation of complexes which include a wide-range of regulatory partners, such as histones, histone-modifying enzymes, transcription factors and RNA (2), (4), (12), (13). Such interactions are frequently altered during oncogenesis, resulting in the disruption to DNMT3A genomic localization and/or regulation of enzyme activity (14). The tumor suppressor p53 is well-known to interact with components of the epigenetic machinery, including DNMT3A; however, a functional understanding of p53-DNMT3A interactions remains largely unknown (15), (16).

In addition to directly activating transcription of genes essential for cell cycle arrest and apoptosis in response to genotoxic stress, the interactions between p53 and histone modifying enzymes are a key driver of gene activation (17), (18). The progressive accumulation of p53 mutations leads to the recruitment of histone modifying enzymes (19-21). Several studies suggest a link between p53 and DNA methylation. For example, while DNMT1 (the maintenance DNA methyltransferase) represses expression of the p53 gene (22), p53 binding to DNMT1 stimulates DNMT1-mediated methylation (23). In addition, p53 represses the expression of *DNMT3A* and *DNMT3B* while DNMT3A has been shown to repress the transcriptional activity of p53 (24), (25). However, definitive evidence of the functional consequences of a DNMT3A-p53 complex on DNMT3A activity remains elusive.

Our interest lies in exploring whether p53 binding to DNMT3A alters DNMT3A activity, and if well studied DNMT3A and p53 mutants, such as R882H (DNMT3A) and p53 mutants R248W and R273H, alter this regulation.

Located at the dimer interface, the major DNA binding site, the R882H substitution in DNMT3A disrupts tetramerization and processive catalysis, both of which can be restored by DNA-methyltransferase 3-like (DNMT3L) (26), (27), (28). Additionally, R882H displays altered interactions with components of the Polycomb Repressive Complex 1 (PRC1) compared to wild type DNMT3A, thereby leading to transcriptional silencing in a DNA methylation-independent manner (29). These observations suggest that compared to WT DNMT3A, the R882H substitution may lead to altered binding and/or regulation by partner proteins. Given that the *p53* gene is a recurring target for mutations in a wide-range of human cancers, there is growing interest in understanding how mutations in *p53* contribute to disease onset and progression (30), (31). In addition to a high mutation frequency, p53 R273H and R248W form aberrant protein complexes that affect the activity of interacting partner proteins (32), (33), (34). Our goal is to understand the dynamics and functional consequences of complex assembly involving the WT catalytic domain of DNMT3A (DNMT3A^{WT}) and the R882H substitution (DNMT3A^{R882H}) under a variety of conditions. Furthermore, we seek to better understand the functional consequences of protein complexes involving two or more proteins to better understand the cellular basis of enzyme function.

Results

Wild type (p53^{WT}) and mutant p53 inhibit the DNA methylation activity of full length and catalytic domain DNMT3A^{WT}

Previous cell-based evidence implicates direct and indirect DNMT3A and p53 interactions (24), (25). In mouse embryonic stem cells, p53 indirectly regulates DNMT3A-mediated methylation by restricting the expression of DNMT3A (24). Alternatively, direct binding of DNMT3A to p53 suppresses p53-mediated transcription of *p21* in a DNA methylation-independent manner, implying that DNMT3A may allosterically regulate p53 activity (25). Based on this evidence, we sought to determine whether p53 has any effect on the DNA methylation activity of DNMT3A. Given that the DNMT3A catalytic domain and full-length enzyme have comparable kinetic parameters (k_{cat} , K_m^{DNA} , K_m^{AdoMet} , processivity and DNMT3L stimulation), the catalytic domain of DNMT3A has proven to be a suitable model for *in vitro* studies and is commonly employed (35), (36). However, the N-terminal domains in full-length DNMT3A, including the ATX-DNMT3A-DNMT3L (ADD) and PWWP domains, are known to interact with numerous partner proteins that may modulate the enzymatic activities of DNMT3A (37), (38). Therefore, we compared the effect of p53^{WT} on the methylation activity of DNMT3A catalytic domain and full-length enzymes by pre-incubating p53 with equimolar concentrations of DNMT3A for 1 hour prior to initiating the reaction by the addition of poly dI-dC. We observed comparable levels of p53^{WT}-mediated DNMT3A inhibition with the catalytic domain (Figure 1 A. and B.) or the full-length DNMT3A (Figure 1 A. and C.). The comparable inhibition indicates that the N-terminal portion of DNMT3A is not essential for p53^{WT}-DNMT3A interactions and does not perturb p53^{WT} acting on the catalytic domain of DNMT3A. The consensus DNA binding sequence of p53 (5'-RRRC(A/T) (A/T)GYYY_{0-14 bases} RRRC(A/T)(A/T)GYYY-3'; R=A,G

and Y=C/T) differs from that of DNMT3A, which displays a strong preference towards CpG sites (39). However, it is possible that p53^{WT} inhibition of DNMT3A (full-length and catalytic domain) enzymatic activity is attributable to the DNA binding ability of p53. To assess whether the inhibitory effect of p53^{WT} on DNA methylation is specific to DNMT3A, the activity of the bacterial methyltransferase M.HhaI, which recognizes 5'GCGC3' sites in double stranded DNA, was challenged with increasing concentrations of p53^{WT}. Although p53^{WT} led to roughly a 50% decrease in DNMT3A (full-length and catalytic domain) activity (Figure 1), DNA methylation by M.HhaI was unaltered in similar reactions involving p53 at 1:1 and 3:1 relative to M.HhaI (Figure 1 A. and D.). Like DNMT3A, M.HhaI is a C-5 cytosine-specific methyltransferase which possesses a remarkably similar structure to that of the DNMT3A catalytic domain (40). Despite the shared similarities of DNMT3A and M.HhaI, here we show that p53 inhibition is specific to DNMT3A.

To further characterize the interactions between DNMT3A^{WT} and p53, the apparent binding affinities (K_D^{app}) of p53^{WT} and p53^{R248W} for DNMT3A^{WT} were determined. For comparison, we also determined the K_D^{app} of DNMT3L for DNMT3A^{WT} which has a well characterized interaction. K_D^{app} was assessed by measuring the activity of DNMT3A^{WT} with increasing levels of DNMT3L (Supplementary Figure 1 A.) or p53 (Supplementary Figure 1 B.), and subsequently determining the fold stimulation or inhibition by DNMT3L or p53^{WT} and R248W, respectively. While DNMT3L resulted in a K_D^{app} of 80 ± 12 nM, p53^{WT} displayed a nearly 5-fold stronger binding affinity for DNMT3A^{WT} with a K_D^{app} of 17 ± 3 nM, followed by p53^{R248W} which resulted in a K_D^{app} of 41 ± 6 nM (calculated from Supplementary Figure 1 A. and B.). Thus, compared to the DNMT3A^{WT}-DNMT3L complex, DNMT3A^{WT}- p53^{WT} and R248W complexes are more energetically favorable.

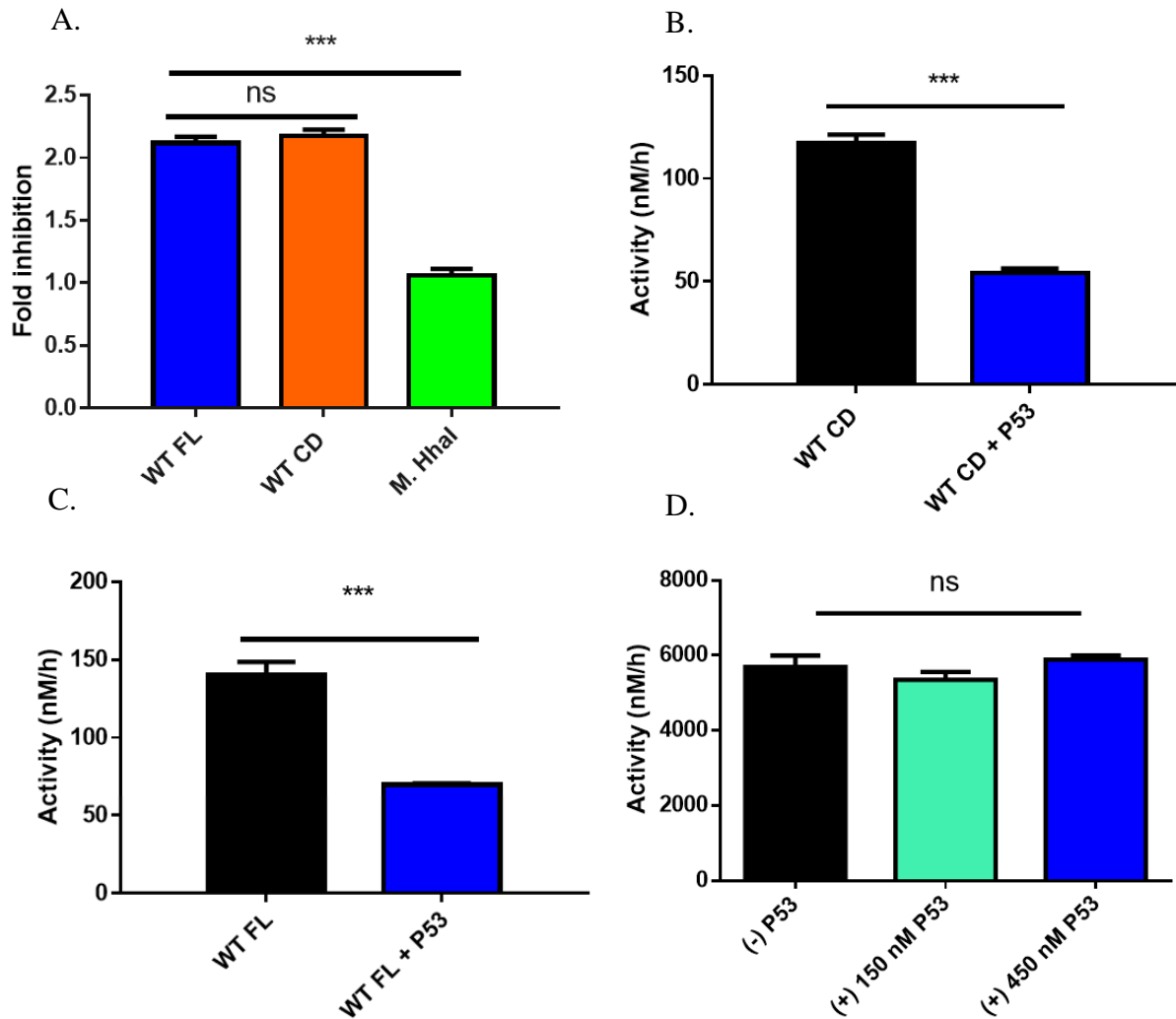


Figure 1. p53^{WT}-dependent inhibition of DNA methylation is specific to DNMT3A. A. Fold inhibition calculated by product formed by WT DNMT3A (full length or catalytic domain enzymes) or M. HhaI divided by product formed by DNMT3A (full length or catalytic domain enzymes) or M. HhaI without p53^{WT} from reactions in (B.-D.). Co-incubation of DNMT3A full length (A. ■ calculated from B.) and catalytic domain (A. ■ calculated from C.) enzymes with p53^{WT} (1:1 at 150 nM) leads to comparable levels of inhibition. Similar reactions involving the bacterial methyltransferase M. HhaI (A. ■ calculated from D.) with excess p53^{WT} (1:3) failed to inhibit DNA methylation. In all co-incubations, proteins were held at 37 °C for 1 hour prior to the start of the reaction by the addition of DNA (5 μM bp poly dI-dC). Data reflect the mean and standard deviation of 3 experiments; one-way analysis of variance was used to compare values of all three reactions; ***, $p < 0.001$; ns, $p > 0.05$.

Mutational mapping suggests p53^{WT} interacts with the tetramer interface DNMT3A

Previous work by Wang *et al.* suggests that DNMT3A interacts with the C-terminal tetramerization domain of p53 (amino acids 319-393, Supplementary Figure 3) (25). No such information is available for the region on DNMT3A that associates with. We previously used alanine scanning to identify residues on the DNMT3A tetramer interface that largely contribute to tetramer stability and alter the ability of DNMT3A to form higher order complexes (41). In a similar manner, we employed docking-based modeling of protein-protein interfaces using monomeric forms of DNMT3A (PDB: 5YX2; residues 628-914) and p53 (PDB: 3TS8; 94-356) to predict a surface on DNMT3A for interactions with p53. Computational models generated in ZDOCK and RosettaDock servers were used to predict the DNMT3A tetramer interface as a likely surface for DNMT3A-p53 interactions (Supplementary Figure 2) (42), (43). Based on this rationale, p53^{WT} inhibition of DNMT3A catalytic activity was assessed in a subset of alanine mutations on the DNMT3A tetramer interface (R729A, E733A, R736A, R771A) which are also commonly observed in AML (26) (Figure 2 A.). The extent of p53^{WT} inhibition varied across the mutations examined in this study: the fold inhibition of DNMT3A^{R771A} (Figure 2 B. and C. ■) and DNMT3A^{E733A} (Figure 2 B. and C. ■) was greater than wild type, whereas the fold inhibition of DNMT3A^{R729A} (Figure 2 B. and C. ■) was less than wild type and DNMT3A^{R736A} (Figure 2 B. and C. ■) displayed no inhibition. The results obtained implicate the DNMT3A tetramer interface as a potential surface on DNMT3A for interactions with p53 and suggest that residue R736 on the DNMT3A tetramer interface contributes to the necessary contacts for p53 inhibition of DNMT3A.

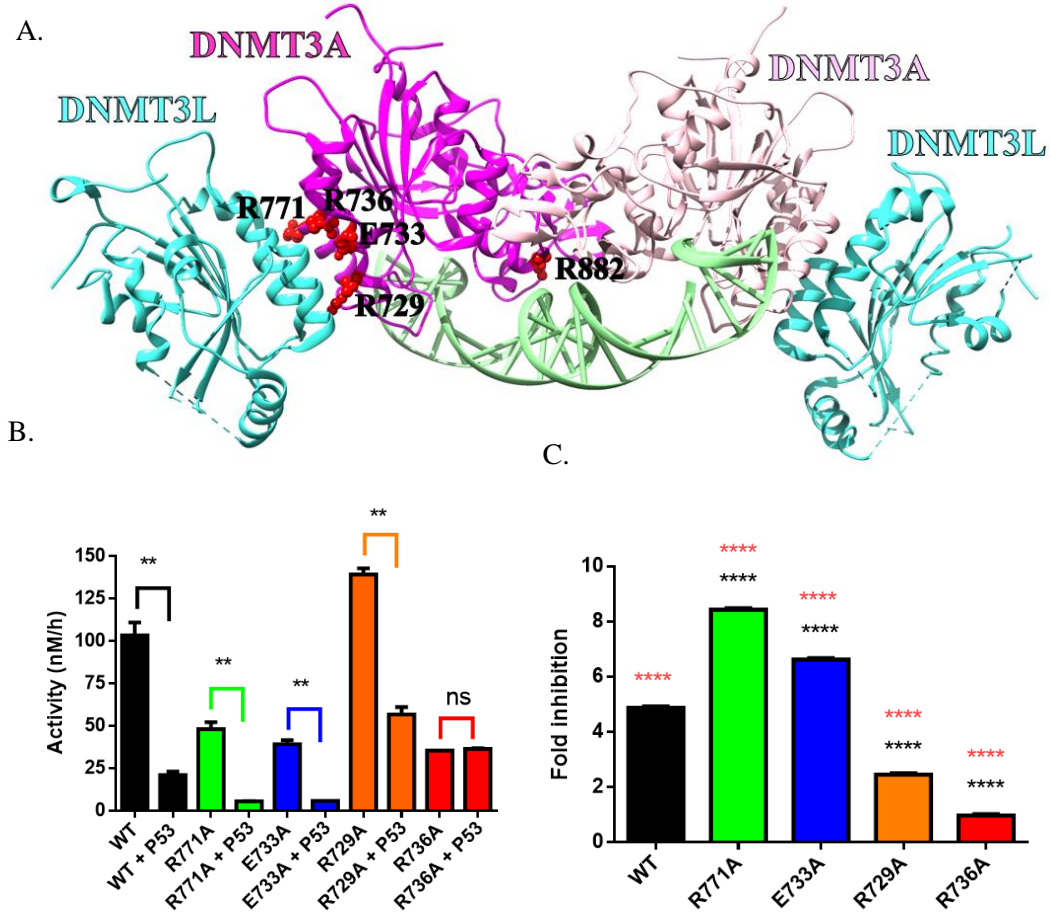


Figure 2. DNMT3A^{WT} tetramer interface mutants show highly variable response to p53^{WT} inhibition. Crystal structure of a DNMT3A^{WT}-DNMT3L complex (Adapted from PDB: 5YX2) denoting critical residues for DNMT3A^{WT} oligomerization (A.) (36), (50). While the extent of p53^{WT} inhibition varies across DNMT3A^{WT} mutants harboring a single alanine substitution within the tetramer interface, the DNMT3A^{R736A} was unresponsive to p53^{WT} inhibition (B. and C.). All reactions consisted of 150 nM DNMT3A^{WT} and were initiated by the addition of 5 μ M bp poly dI-dC. For co-incubations, DNMT3A^{WT} and p53^{WT} (1:1) were pre-incubated for 1 hour at 37 °C prior to starting the reaction by the addition of substrate DNA. Fold inhibition was calculated by product formed by DNMT3A (WT and mutants) divided by product formed by DNMT3A (WT and mutants) without p53^{WT}. All reactions were performed in duplicates. In (B.), a Student's unpaired *t* test was used to compare values within each set of reactions; **, $p < 0.01$; ns, $p > 0.05$. For (C.), a one-way analysis of variance was used to compare the values of each mutant to wild type (****, $p < 0.001$) and across all samples (****, $p < 0.001$). Data reflect the mean and standard deviation of 3 experiments.

The regulation of DNMT3A^{WT} by p53^{WT} is dominant to that of DNMT3L

Given that DNMT3A exists in several multiprotein complexes associated with transcriptional regulation, we sought to assess the extent of DNMT3A modulation in the presence of multiple regulatory partner proteins (5), (44), (45). Our mutational mapping and modeling results suggest that the DNMT3A tetramer interface (Figure 2 and Supplementary Figure 2) interacts with both DNMT3L and p53. Given that the DNMT3A-DNMT3L co-crystal structure (46) presents the DNMT3A tetramer interface as an established surface for regulation of DNMT3A activity by an additional partner protein, we assessed whether DNMT3L and p53^{WT} regulation of DNMT3A^{WT} is mutually exclusive using poly dI-dC as a substrate. After demonstrating DNMT3A^{WT} is responsive to DNMT3L (Figure 3 A. ■) and p53^{WT} (Figure 3 A. ■), we observed that p53^{WT} modulation of DNMT3A^{WT} is dominant over that of DNMT3L in DNMT3A^{WT}-DNMT3L- p53^{WT} co-incubations (Figure 3 A. ■). We previously showed that p53^{WT} inhibition of DNMT3A^{WT} does not rely on DNA binding by p53 (Figure 1). Therefore, the use of poly dI-dC as a substrate allowed us to investigate the isolated effects of p53-mediated inhibition of DNMT3A activity. Inspired by our previous studies using human promoters, we also studied the *Cyclin Dependent Kinase Inhibitor 1A/P21* promoter, which is a common target for DNMT3A and p53 (102), (25). As we observed for poly dI-dC, p53^{WT}-dependent inhibition of DNMT3A^{WT} activity is dominant over DNMT3L stimulation as DNMT3A^{WT}-p53^{WT}-DNMT3L co-incubations (Figure 3 B. ■) displayed comparable levels of activity as reactions consisting of DNMT3A^{WT}-p53^{WT} (Figure 3 B. ■) with the *Cyclin Dependent Kinase Inhibitor 1A/P21* promoter as a DNA substrate. Furthermore, equimolar concentrations of all proteins were used in DNMT3A^{WT}-DNMT3L- p53^{WT} co-incubations (Figure 3 A. and B.), suggesting that the dominant modulation of DNMT3A^{WT} activity by p53^{WT} over DNMT3L was not due to

stoichiometric differences. The stability of the DNMT3A^{WT}-p53^{WT} complex is greater than the DNMT3A^{WT}-DNMT3L complex (Supplementary Figure 1) and DNMT3L and p53 likely share a binding interface on DNMT3A (Figure 2). To further investigate the dynamics of DNMT3A^{WT}-DNMT3L-p53^{WT} interactions, we next assessed the effect of adding regulatory proteins to actively catalyzing heterotetrameric complexes, which is arguably a better representation of what occurs within the cell. We observed that addition of p53^{WT} disrupts the DNMT3A^{WT}-DNMT3L complex during catalysis (Figure 3 C. ■). This not only supports our observation that the DNMT3A^{WT}-p53^{WT} complex is more stable, but that it can access the DNMT3A^{WT}-DNMT3L complex and displace DNMT3L during catalysis. In contrast, adding DNMT3L to an actively methylating DNMT3A^{WT}-p53^{WT} complex failed to disrupt the modulatory effect of p53^{WT} (Figure 3 E. ■). In fact, comparable levels of DNMT3A^{WT}-dependent methylation activity were observed in reactions consisting of DNMT3A^{WT}-p53^{WT} (Figure 3 E. ■) and functional DNMT3A^{WT}-p53^{WT} complexes to which DNMT3L was added (Figure 3 E. ■). In sum, our results consistently suggest the regulatory effect of p53^{WT} on DNMT3A^{WT} is dominant compared to DNMT3L regulation and provides insights into the dynamics of p53^{WT} and DNMT3L binding on DNMT3A^{WT}.

p53^{WT} fails to inhibit the methylation activity of DNMT3A^{R882H}

Identified as the most common mutation in DNMT3A in AML patients, *in vitro* evidence suggests the R882H substitution leads to altered binding and/or regulation by partner proteins (26). Although R882H is unable to form homotetramers, the addition of DNMT3L leads to the formation of heterotetramers and restores processive catalysis (28). In addition, immunoprecipitation experiments using HEK293T cells reveal R882H displays increased binding to components of the PRC1 complex compared to wild type DNMT3A

(29). These observations suggest that while R882H is located at the dimer interface (Figure 2 A.), which is distal from the tetramer interface and proximal to the DNA interface (Figure 2 A.), R882H appears to allosterically affect the ability of DNMT3A to interact with partner proteins. While DNMT3A^{R882H} is responsive to DNMT3L activation (Figure 3 A. ■), it is unresponsive to the modulatory effect of p53^{WT} in DNMT3A^{R882H}-p53^{WT} (Figure 3 A. ■) and mixed DNMT3A^{R882H}-p53^{WT}-DNMT3L co-incubations (Figure 3 A. ■). In fact, DNMT3A^{R882H}-p53^{WT} (Figure 3 A. ■) co-incubations led to comparable levels of product formed as DNMT3A^{R882H} only (Figure 4 A. ■) and mixed DNMT3A^{R882H}-p53^{WT}-DNMT3L co-incubations (Figure 3 A. ■) reflected similar levels of activity as DNMT3A^{R882H}-DNMT3L co-incubations (Figure 3 A. ■). Thus, the R882H substitution appears to disrupt the modulatory effect of p53^{WT} on DNA methylation. To additionally challenge this notion, we evaluated the effect of adding DNMT3L or p53^{WT} to actively methylating DNMT3A^{R882H}-p53^{WT} or DNMT3A^{R882H}-DNMT3L co-incubations. Consistent with the hypothesis that p53^{WT} fails to modulate DNMT3A^{R882H} activity, the addition of p53^{WT} failed to disrupt functional DNMT3A^{R882H}-DNMT3L heterotetramers (Figure 3 D. ■) unlike that observed in similar reactions involving DNMT3A^{WT} (Figure 3 C. ■). However, the addition of DNMT3L failed to stimulate DNMT3A^{R882H} in actively catalyzing DNMT3A^{R882H}-p53^{WT} co-incubations (Figure 3 F. ■).

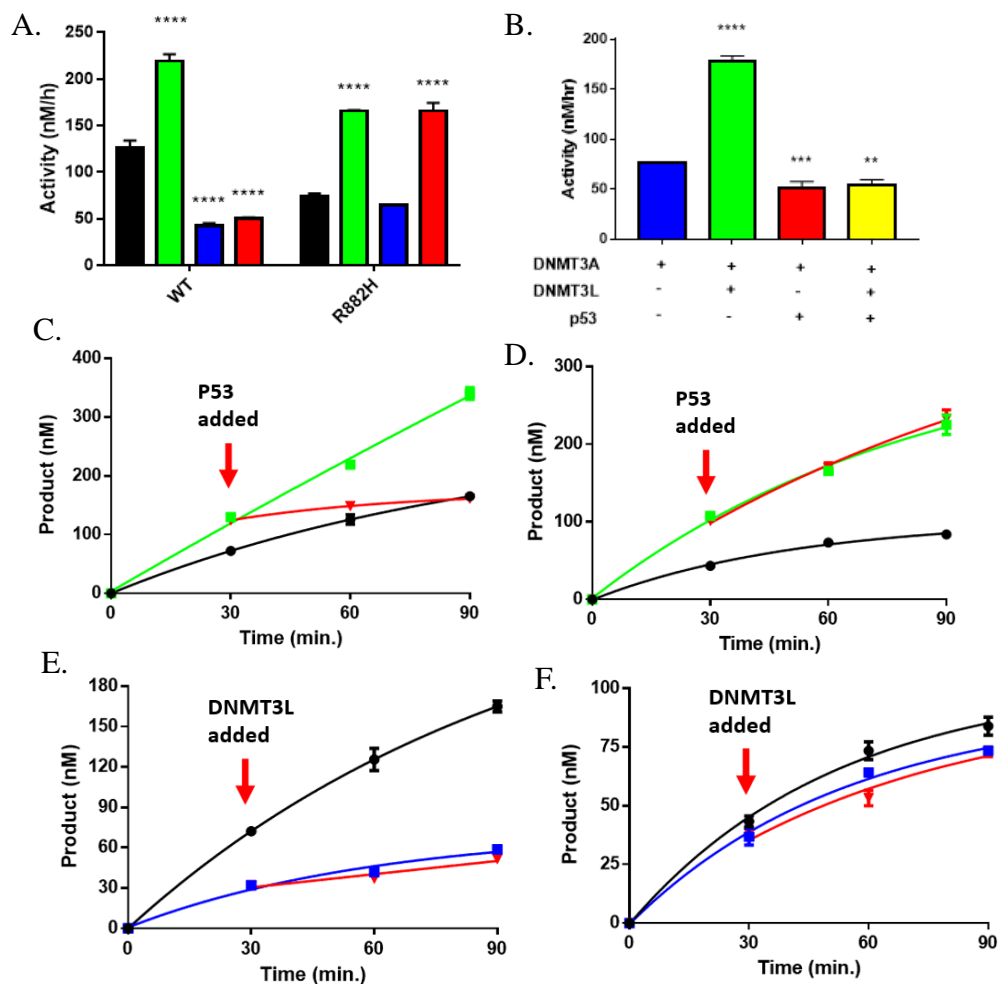


Figure 3. DNMT3A^{WT} and DNMT3A^{R882H} are differentially responsive to modulation by p53^{WT}. p53^{WT}-dependent inhibition of DNMT3A^{WT} activity is dominant in DNMT3A^{WT}-p53^{WT}-DNMT3L co-incubations (A. ■) while p53^{WT} fails to inhibit DNMT3A^{R882H} in DNMT3A^{R882H}-p53^{WT} (A. ■) and DNMT3A^{R882H}-p53^{WT}-DNMT3L co-incubations (A. ■) using poly dI-dC (5 μ M bp) as a substrate. B. p53^{WT}-dependent inhibition of DNMT3A^{WT} activity is dominant in DNMT3A^{WT}-p53^{WT}-DNMT3L co-incubations (■) with *p21*-pCpG^L (10 μ M) as a substrate. p53^{WT} (C. ■) disrupts DNMT3L stimulation of DNMT3A^{WT} in catalytically active DNMT3A^{WT}-DNMT3L complexes (C. ■), while catalytically active DNMT3A^{R882H}-DNMT3L (D. ■) are unaltered by the addition of p53^{WT} (D. ■). Reactions consisting of catalyzing p53^{WT}-DNMT3A^{WT} (E. ■) or DNMT3A^{R882H}-p53^{WT} (F. ■) were unaltered by the addition of DNMT3L (E. and F. ■). The following reactions were also performed as controls: DNMT3A^{WT} (A., C., and E. ■), DNMT3A^{R882H} (A., D., and F. ■), DNMT3A^{WT}-DNMT3L co-incubations (A. and C. ■), DNMT3A^{R882H}-DNMT3L co-incubations (A. and D. ■), DNMT3A^{WT}-p53^{WT} co-incubations (A. and E. ■) and DNMT3A^{R882H}-p53^{WT} co-incubations (A. and F. ■). In all reactions performed, protein concentrations were 150 nM and were initiated by the addition of substrate DNA. For co-incubations, proteins were placed at 37 °C for 1 hour prior to the addition of substrate DNA. All reactions were performed in triplicates. Values in (A. ■, ■, ■) were compared to either DNMT3A^{WT} (A. ■) or DNMT3A^{R882H} (A. ■) using a one-way analysis of variance; ****, $p < 0.001$. Data reflect the mean and standard deviation of 3 experiments.

p53^{R248W} and p53^{R273H} display altered regulation of DNMT3A^{WT} in the presence of DNMT3L

Mutated in over half of all human cancers, the majority of p53 mutations are missense mutations throughout the p53 DNA-binding domain (47-50). Two of these “hot spot” substitutions, p53 R248W and R273H, display altered interactions and regulation of several partner proteins compared to WT p53 (32), (33), (34). Although p53 R248W and R273H are outside of the region on p53 known to interact with DNMT3A (Figure S3), we compared the effect of p53^{WT} with p53^{R248W} and p53^{R273H} substitutions on the enzymatic activity of DNMT3A^{WT} based on their recurrence in a wide range of cancers. While p53^{WT} (Figure 3 A. ■), p53^{R248W} (Figure 4 A. ■) and p53^{R273H} (Figure 4 A. ■) displayed comparable levels of DNMT3A^{WT} inhibition, p53^{R248W} and p53^{R273H} failed to reverse the stimulatory effect of DNMT3L in DNMT3A^{WT}-p53^{R248W}-DNMT3L co-incubations (Figure 4 A. ■) or in DNMT3A^{WT}-p53^{R273H}-DNMT3L co-incubations (Figure 4 A. ■) as previously observed in similar reactions involving DNMT3A^{WT} and p53^{WT} (Figure 3 A. ■). In fact, DNMT3A^{WT}-DNMT3L co-incubations with p53^{R248W} (Figure 4 A. ■) or p53^{R273H} (Figure 4 A. ■) displayed comparable levels of product formation as DNMT3A^{WT}-DNMT3L co-incubations (Figure 4 A. ■). To further challenge the dominant regulatory effect of DNMT3L over p53^{R248W} and p53^{R273H} on DNMT3A^{WT} observed, we then assessed the outcome of adding DNMT3L to DNMT3A^{WT}-p53^{R248W} (or -p53^{R273H}) co-incubations, as well as the addition of p53^{R248W} (or p53^{R273H}) to catalyzing DNMT3A^{WT}-DNMT3L complexes. In contrast to similar experiments involving p53^{WT} (Figure 3 C. and E. ■), the addition of p53^{R248W} (Figure 4 B. ■) or p53^{R273H} (Figure 4 C. ■) to a catalyzing DNMT3A^{WT}-DNMT3L complexes did not disrupt DNMT3L-mediated stimulation, whereas the addition of DNMT3L to functional DNMT3A^{WT}-p53^{R248W} (Figure 4 D. ■) or DNMT3A^{WT}-p53^{R273H} (Figure 4 E. ■) assemblies led to an increase in DNMT3A^{WT} activity. These findings support

the notion that the regulatory effect of DNMT3L on DNMT3A^{WT} activity is dominant over that of p53^{R248W} or p53^{R273H}. Here we show that while p53^{WT}, p53^{R248W} and p53^{R273H} display comparable levels of DNMT3A^{WT} inhibition, p53^{R248W} and p53^{R273H} displayed altered regulation of DNMT3A^{WT} in the presence of DNMT3L compared to p53^{WT}. This presents an example in which p53^{R248W} and p53^{R273H} display altered protein-protein interactions compared to p53^{WT} in the context of DNA methylation and in addition to those previously reported (32), (33), (34).

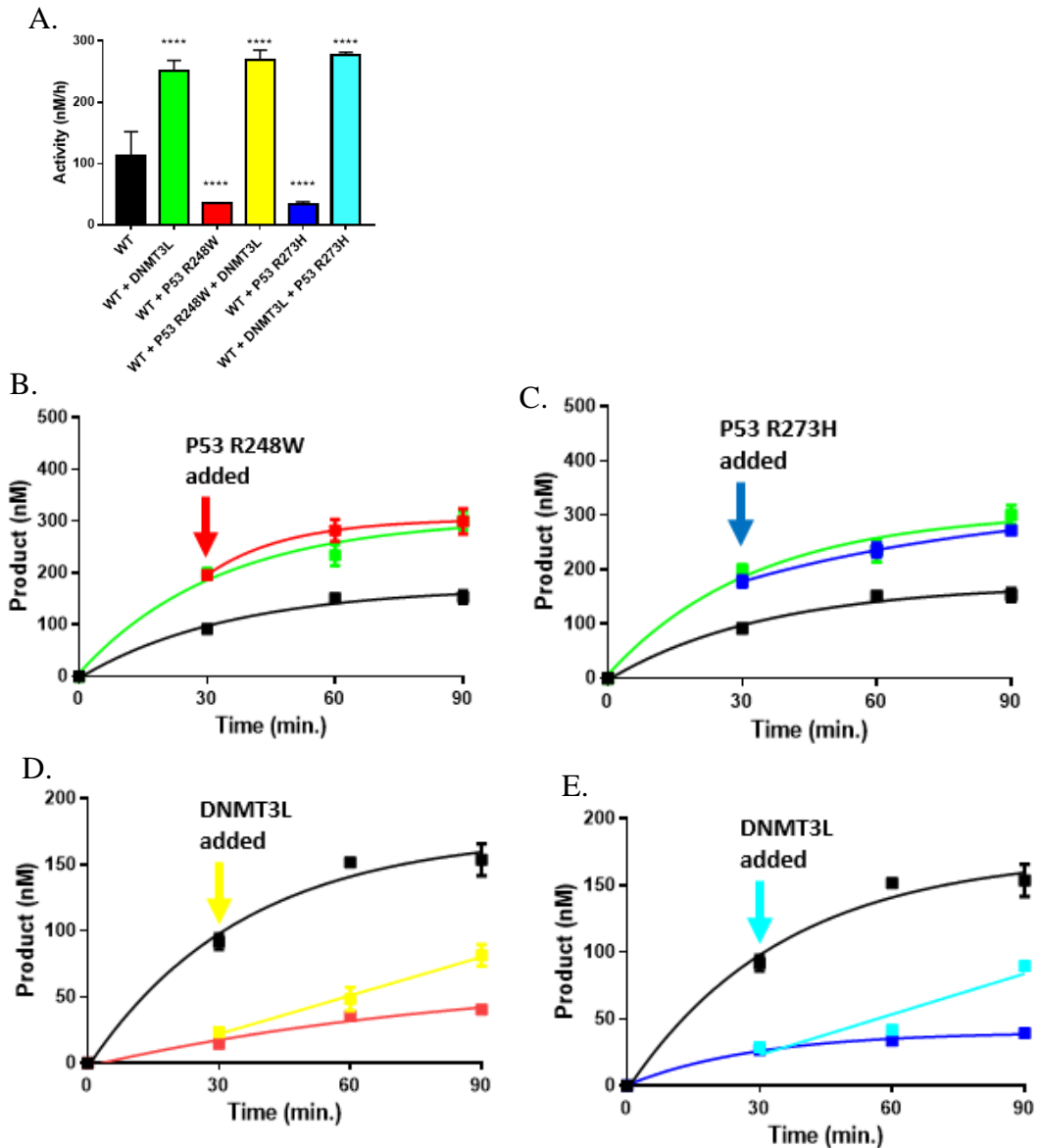


Figure 4. p53^{R248W} and p53^{R273H} fail to disrupt stimulation of DNMT3A^{WT} by DNMT3L. The stimulatory effect of DNMT3A^{WT} activity by DNMT3L is dominant in DNMT3A^{WT}-p53^{R248W}-DNMT3L (A. ■) or DNMT3A^{WT}-p53^{R273H}-DNMT3L co-incubations (A. ■). Catalytically active DNMT3A^{WT}-DNMT3L heterotetramers are unaffected by the addition of p53^{R248W} (B. ■) or p53^{R273H} (D. ■), while the addition of DNMT3L leads to an increase in DNMT3A^{WT}-p53^{R248W} (C. ■) or DNMT3A^{WT}-p53^{R273H} (C. ■) co-incubations. The following reactions were also performed as controls: DNMT3A^{WT} (A.-E. ■), DNMT3A^{WT}-DNMT3L co-incubations (A., B., and D. ■), DNMT3A^{WT}- p53^{R248W} co-incubations (A. and C. ■) and DNMT3A^{WT}-p53^{R273H} co-incubations (A. and C. ■). Protein concentrations were 150 nM for all reactions and were initiated by the addition of 5 μ M bp poly dI-dC as a substrate. For co-incubations, proteins were preincubated at 37 °C for 1 hour prior to the addition of DNA. All reactions were performed in triplicates and all values in (A.) were compared to wild type (A. ■) using a one-way analysis of variance; ****, $p < 0.001$. Data reflect the mean and standard deviation of 3 experiments.

p53 binds DNMT3A^{WT} and DNMT3A^{R882H} to form of heterotetramers

The ability of partner proteins to impact DNMT3A function is dependent on the formation of a complex, although this may not be sufficient. Anisotropy measurements are widely employed to assess protein-DNA, protein-protein interactions and estimate the oligomeric state of proteins (51-58). We previously used a 30-base pair 5' 6-FAM-labeled duplex DNA (GCbox30), which contains a single recognition site for DNMT3A, to resolve the oligomeric state of DNMT3A (28), (41). We relied on this approach and fluorescence anisotropy to assess the dynamics of DNMT3A^{WT}-p53^{WT} interactions on DNA (GCbox30). Increasing concentrations of p53^{WT} or DNMT3L (Figure 5 A. ■) to a fixed concentration of DNA-bound DNMT3A^{R882H} (Figure 5 A. ▼) resulted in a corresponding increase to the initial anisotropy value, thereby suggesting the formation of higher order complexes on DNA. Under identical conditions, we observed that increasing concentrations of DNMT3L (Figure 5 A. ●), p53^{WT} (Figure 5 A. ▲) or p53^{R248W} (Figure 5 A. ◆) did not result in a detectable change to the initial anisotropy value of DNMT3A^{WT}. DNMT3A^{R882H} binds DNA as a homodimer and forms heterotetramers with DNMT3L on DNA (28), (36). The titration of p53^{WT} to DNMT3A^{R882H} led to similar final anisotropy values as those observed for DNMT3A^{WT} in the absence and presence of DNMT3L, p53^{WT} and p53^{R248W} (approximately 0.19; Figure 7 A.). To confirm whether the increased anisotropy observed with DNMT3A^{R882H} (Figure 5 A. ▼) is due to formation of a higher order structure (likely a tetramer), we performed gel shift assays of DNMT3A^{R882H} with varying concentrations of p53^{WT} using GCbox30 as a substrate. Consistent with the results of the fluorescence anisotropy assays, an increase in the concentration of p53^{WT} to a fixed concentration of DNMT3A^{R882H} (Figure 5 B. and C., lanes 3-5) led to a super-shift and disappearance of the band corresponding to DNA-bound DNMT3A^{R882H} (Figure 5 B., lane 1). In sum, our results

indicate that p53 interacts with DNMT3A to form heterotetramers and that inhibition does not arise from disrupting the ability of DNMT3A to bind DNA.

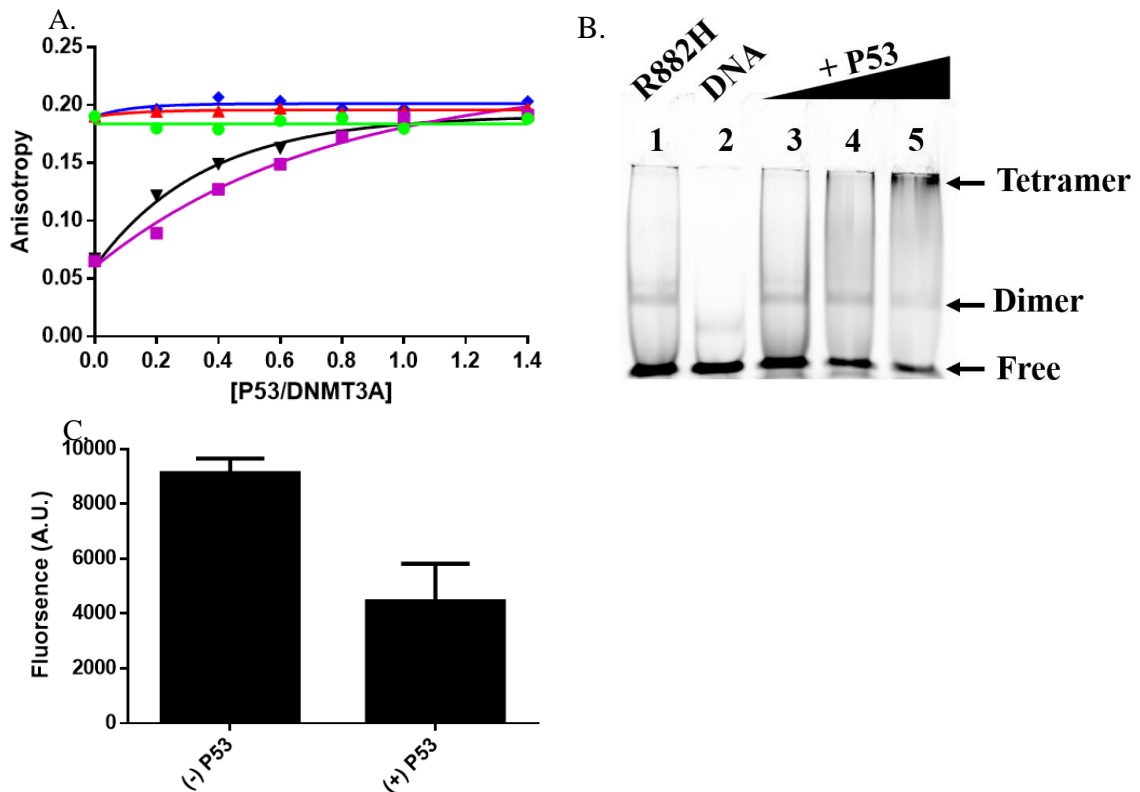


Figure 5. p53 heterodimerizes with WT and R882H DNMT3A. **A.** Increasing concentrations of DNMT3L (■) or p53^{WT} (▼) to a fixed concentration of DNMT3A^{R882H} led to a robust increase in Anisotropy, whereas DNMT3A^{WT} did not display a significant change in anisotropy by the titration of DNMT3L (●), p53^{WT} (▲) or p53^{R248W} (◆). **B.** EMSA and **C.** EMSA band densitometry (lanes 1 and 5) show increasing concentrations of p53^{WT} (lanes 3-5) to a constant concentration of DNMT3A^{R882H} leads to disappearance of the DNMT3A^{R882H} band and formation of a higher order structure (see arrows, lanes 3-5). In **A.**, DNMT3A^{WT} and DNMT3A^{R882H} concentrations were 2.5 μM. Single point anisotropy measurements were taken after increasing concentrations of DNMT3L (●), p53^{WT} (▲) and p53^{R248W} (◆) were added to DNA bound (250 nM 5' 6-FAM-labeled GCbox30) DNMT3A^{WT} and DNMT3A^{R882H} and allowed to incubate at room temperature for 5 minutes. Measurements were taken using a *fluorometer equipped with polarizing filters* (excitation: 485 nm, emission 520 nm). In **B.**, gel shift assays were carried out as described in Holz-Schietinger et al. (28) other than samples were run on native 4.5% polyacrylamide gels and binding reactions were performed at 37 °C (lane 1). For p53^{WT} super shifting, varying concentrations of p53^{WT} were preincubated for 30 minutes at 37 °C with DNMT3A^{R882H} before the addition of DNA. **A.** and **C.** reflect the results (mean and standard deviation) of 2 independent experiments.

Discussion

Although p53 has been extensively investigated, much less is known about whether or how this protein influences epigenetic pathways, particularly DNA methylation (17), (18), (30), (47-50). Reports on the crosstalk between p53 and members of the DNA methyltransferase (DNMT) family include the loss of global methylation by 5-aza-2'-deoxycytidine treatment induces a p53 DNA damage response pathway (59), deletion of the DNMT1 gene activates p53-mediated apoptosis (60) and p53 directly stimulates DNMT1-mediated methylation (23). In the context of the *de novo* DNA methyltransferases, p53 transcriptionally represses *DNMT3A* and *DNMT3B* while DNMT3A inhibits p53-mediated transcription (24). Based on this evidence and the association of DNMT3A and p53 in various human cancers (26), (47-50), we sought to characterize the dynamics and regulation of DNMT3A activity by p53 under various conditions. We show that p53 and the well-characterized DNMT3L bind to the same region on DNMT3A, resulting in roughly a 2-fold inhibition of DNMT3A activity. The DNMT3A-p53 interaction is modulated by well-known mutations in DNMT3A and p53. Our results provide insights into the complexity of mutation-specific variation in the regulation of protein function and elucidates a molecular basis for the distinguishing DNA methylation phenotypes associated with the R882H substitution in DNMT3A (61), (62).

The interaction interface between proteins relies on well-defined single residue interactions within flat surfaces (63), (64). Factors like kinetic accessibility to specific protein surfaces, thermodynamic stability of the resultant complexes, along with structural properties of protein complexes, contribute to the formation of biologically significant assemblies (8-11), (65). Complexes with partner proteins regulate DNMT3A activity (12),

(13), (37), (38), (46), thereby contributing to normal and aberrant tissue-specific methylation patterns (2-5). Given that DNMT3A binds the C-terminal tetramerization domain of p53 (residues 319-393, Supplementary Figure 3) (25), we sought to identify the surface on DNMT3A that binds p53 and whether p53 directly impacts DNMT3A activity. Like DNMT3L (36), our results suggest that surfaces on the catalytic domain of DNMT3A are sufficient for p53-mediated inhibition of DNMT3A (Figure 1). Using docking-based computational models of DNMT3A (PDB: 5YX2; residues 628-914) and p53 (PDB: 3TS8; 94-356) monomers, we identified the tetramer interface on DNMT3A as a likely surface for DNMT3A-p53 interactions (Supplementary Figure 2). We challenged this finding by determining if mutations at this interface (Figure 2 A. and Figure 8 B.) (41) interfered with p53 interactions (Figure 2 B. and C.). Our results suggest an overlap between DNMT3L and p53 for binding and allosteric regulation of DNMT3A activity (Tetramer interface) (Figure 2 and Supplementary Figure 2) through the formation of heterotetramers with DNMT3A^{WT} (Figure 5). Our proposed complex for DNMT3A^{WT}-p53^{WT} is consistent with previously resolved p53 co-crystal structures (PDB 1KZY and 5ECG) which consist of p53 dimers bound to interacting partner proteins (66), (67). The structure and functional studies on DNMT3A interactions with another protein, DNMT3L provides a reliable “metric” to investigate a common surface on DNMT3A that facilitates allosteric regulation of enzymatic activity. We show that DNMT3A^{WT}-p53^{WT} complexes (K_D^{app} of 17 ± 3 nM) are more thermodynamically stable than DNMT3A^{WT}-DNMT3L complexes (K_D^{app} of 80 ± 12 nM). Consistent with these relative stabilities, DNMT3A^{WT}-p53^{WT} complexes appear to be more kinetically stable when all three proteins are combined (DNMT3A, DNMT3L and p53). Moreover, p53^{WT} can displace DNMT3L from the DNMT3A-DNMT3L heterotetrameric complex under catalytic conditions, which is arguably more relevant (Figure 3). We propose

that p53^{WT} replaces the outer pair of DNMT3A^{WT} monomers (Figure 6 A., III.) or DNMT3L (Figure 6 A., V.) monomers to allosterically inhibit the enzymatic activity of DNMT3A^{WT}.

Due to the energetic contributions of specific residues to protein-protein interactions (63), (64), (69), it is not surprising that mutations which alter protein complex formation have been linked to various human disorders and are over-represented amongst disease-causing mutations (70), (71). The R882H substitution in DNMT3A is the most common recurrent mutation in AML patients (26) and DNMT3A^{R882H} may be disruptive to protein-protein interactions (29), (72), (73). While DNMT3A^{R882H} is mildly impacted in function (28), it seems reasonable that altered interactions with partner proteins contribute to the aberrant methylation patterns observed in AML (61), (62). Previous work from our lab has shown that although R882H is a functional dimer on DNA, the addition of DNMT3L restores the formation of heterotetramers, and near-normal levels of catalysis (Figure 6 A., II.) (28). The comparable increase in anisotropy observed by the addition of DNMT3L or p53 to DNA-bound DNMT3A^{R882H} (Figure 5) supports the notion that p53^{WT} binds DNMT3A^{R882H} (Figure 5) to form heterotetramers but is unable to allosterically inhibit DNMT3A^{R882H} activity (Figure 3) (Figure 6 A., IV.). Furthermore, p53^{WT} fails to displace DNMT3L monomers in DNMT3A^{R882H}-DNMT3L heterotetramers (Figure 3) (Figure 6 A., V.). Like DNMT3A^{R882H}, certain mutations in p53 are disruptive to protein-protein interactions and alter regulation of partner proteins relative to wild type p53 (32-34), (74), (75). In addition, several observations suggest an interplay between components of the epigenetic machinery and mutations in p53 (76), (77). Although located outside of the DNMT3A^{WT}- p53^{WT} interface (residues 319-393, Supplementary Figure 3) (25), we investigated how p53^{R248W} and p53^{R273H} mutations alter interactions with DNMT3A^{WT} based on our previous findings on DNMT3A^{WT}- p53^{WT} interactions and high incidence in human

cancers (47-50). In spite of the greater stability of the DNMT3A^{WT}-p53^{R248W} heterotetramers (Figure 5) (K_D^{app} of 41 ± 6 nM) compared to the DNMT3A^{WT}-DNMT3L complexes (K_D^{app} of 80 ± 12 nM), DNMT3L modulation of DNMT3A^{WT} activity is dominant over that of p53^{R248W} and p53^{R273H} (Figure 4). We propose that p53 mutations do not compromise modulation of DNMT3A^{WT} (Figure 6 A., III.). These mutations may allosterically affect the DNMT3A-interacting interface (p53 residues 319-393, Supplementary Figure 3) (25) such that the affinity of mutant p53 in DNMT3A^{WT}-mutant p53 complexes is compromised when presented with DNMT3L (Figure 6 A., V.).

The ongoing discovery of “hot spots” in protein-protein interfaces, discrete regions that confer most of the binding energy, has sparked an interest in the pharmacological intervention of protein-protein interactions (78-82). In fact, successful modulation of protein-protein interactions by small molecules has been reported in p53 (83-89). We describe how, in the context of DNMT3A interactions with partner proteins, mutations at protein-protein interfaces may lead to diverse changes in protein interactions and modulation of protein activity. In addition, we provide examples in two important cancer-related proteins of how mutations located distally from protein-protein interfaces may affect modulation of enzymatic activity, thereby contributing to the diverse phenotypic consequences of mutations in epigenetic enzymes like DNMT3A (61), (62). The findings in this study broaden our understanding of regulation of DNMT3A activity and emphasize the potential use of small molecules to target protein-protein interactions in diseases, like acute myeloid leukemia (AML), where DNMT3A and p53 are implicated (26) (90).

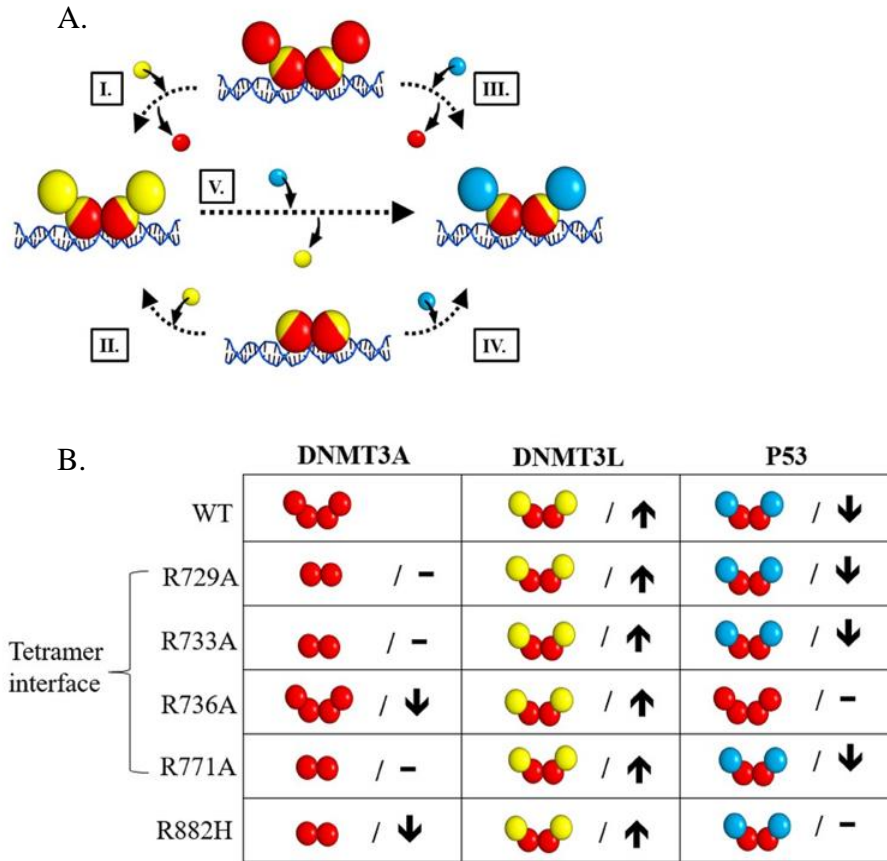


Figure 6. Mutations in DNMT3A lead to diverse interactions with p53. **A.** the addition of DNMT3L (*yellow square*) to DNMT3A homotetramers or homodimers (*red square* tetramer interface depicted in *yellow*) leads to the formation of DNMT3A (*red square*)-DNMT3L (*yellow square*) heterotetramers (*I* and *II*). Similarly, p53 (*blue square*) interacts with DNMT3A (*red square*)-homodimers or homodimers (*red square*) to form DNMT3A (*red square*)-p53 (*blue square*) heterotetramers (*III* and *IV*). Furthermore, the addition of p53 (*blue square*) to DNMT3A (*red square*)-DNMT3L (*yellow square*) heterotetramers displaces monomers at the tetramer interface and leads to the formation of DNMT3A- P53 (*blue square*) heterotetramers (*V*). **B.** summary of the oligomeric states of DNMT3A mutants in complex with DNMT3L (28, 36) and p53 as well as the effects on the catalytic function of DNMT3A. DNMT3A mutants display no change (-) or decreased (2) activity (*k_{cat}*) relative to WT. Although all the DNMT3A mutants are responsive to DNMT3L stimulation (1), DNMT3A mutants display varying p53 inhibition (2). Although DNMT3A R736A and R882H are unresponsive to p53 inhibition (-), p53 binds R882H to form heterotetramer.

Methods

Expression constructs

The plasmids used for expression of recombinant DNMT3A full length and catalytic domain (WT and R882H) proteins include pET28a-hDNMT3ACopt and pET28a-hDNMT3A_catalytic_domain ($\Delta 1-611$) (37). pTYB1-3L was used to express full length human DNMT3L (38). pET15b-human p53 (1-393) (Addgene) was used for expression of recombinant full length human p53 as a template to generate R248W and R273H substitutions by site-directed mutagenesis (91).

Protein Expression

DNMT3A full length and catalytic domain (WT and R882H), DNMT3L and P53 (WT, R248W and R273H) were expressed in NiCo21(DE3) Competent *E. coli* cells (New England Biolabs). Cells were grown in LB media at 37 °C to an $A_{600\text{ nm}}$ of 0.9 (DNMT3A full length), 0.7 (DNMT3A catalytic domain [WT and R882H]), 0.4 (DNMT3L), and 0.6 (P53 [WT, R248W and R273H]). Protein expression was induced by the addition of 1 mM isopropyl- β -D-thiogalactopyranoside (GoldBio) after lowering the temperature to 28 °C. Induction was 5 hours for DNMT3A full length and catalytic domain (WT and R882H) and 16 hours for DNMT3L and P53 (WT, R248W and R273H). Cells pellets were harvested by centrifugation at 5,000g for 15 minutes and stored at -80 °C.

Protein Purification

Cell pellets from 1 L of bacterial culture were resuspended in 30 mL lysis buffer (50 mM HEPES pH 7.8, 500 mM NaCl, 50 mM imidazole, 10% glycerol and PMSF) and lysed by sonication. Following sonication, lysates were centrifuged at 11,000g for 1 hour and the supernatant was retained for affinity chromatography. Recombinant proteins were purified using ÄKTA Fast Protein Liquid Chromatography (FPLC) system (GE healthcare)

containing a 5 mL HisTrap HP nickel-charged IMAC column (GE healthcare). Columns were preequilibrated with 50 mL of loading buffer (50 mM HEPES pH 7.8, 500 mM NaCl, 50 mM imidazole, 10% glycerol). After flowing the supernatant through the column, resins were washed using 47.5 mL of wash buffer (50 mM HEPES pH 7.8, 500 mM NaCl, 75 mM imidazole, 10% glycerol). 0.5 mL fractions were eluted with elution buffer (50 mM HEPES pH 7.8, 500 mM NaCl, 500 mM imidazole, 10% glycerol) using a linear imidazole gradient (0-100%) over 15 mL. The eluate containing the proteins of interest was desalted and concentrated into storage buffer (50 mM Tris-Cl, 200 mM NaCl, 1 mM EDTA, 20% (v/v) glycerol, pH 7.8, with 0.5 mM DTT) using a 0.5 mL Centrifugal Filter (10K device) supplied by Millipore. Proteins were stored at -80°C for later use.

Computational Modeling

Using a DNMT3A (PDB: 5YX2, chain A) (92) and a P53 monomer (PDB: 3TS8, chain B) (93), the protein docking server ZDOCK was initially used to predict the interface on DNMT3A involved with DNMT3A-P53 interactions (42). In addition, identical modeling was performed using a DNMT3A monomer (PDB: 5YX2, chain A) (92) and a DNMT3L monomer (PDB: 2QRV, chain B) (47) for comparison as the interface on DNMT3A for DNMT3A-DNMT3L interactions has been previously resolved (92), (47). ZDOCK performs a rigid-body search of possible docking orientations between the proteins of interest (42). This docking server relies on the Fast Fourier Transform algorithm to perform a global docking search and explores all possible binding modalities by combining translation and rotation of the ligand. To rank each possible docking pose, ZDOCK applies a combination of shape complementarity, electrostatics and statistical potential terms (94), (95). To predict the interface on DNMT3A involved with DNMT3A-P53 interactions, known contacting residues on P53 were considered (residues 319-393) (25). The local

refinement on the RosettaDock server was then employed to perform rigid-body minimization and side-chain conformation optimization (43). The local refinement function involves side chain repacking to improve rotameric side-chain conformations and a Monte Carlo-based recovery of near-native protein structures (43). RosettaDock employs an energy-based scoring function that calculates the energy of interactions by amino acids (43).

Methylation Assays

Assays were carried out to measure the ability of DNMT3A to incorporate tritiated methyl groups transferred from cofactor AdoMet onto DNA substrate under various experimental conditions. Reactions were carried out at 37 °C in a buffer consisting of 50 mM KH₂PO₄/K₂HPO₄, 1 mM EDTA, 1mM DTT, 0.2 mg/mL BSA, 20 mM NaCl with saturating AdoMet (15 μM) at pH 7.8. 50 μM ([³H]methyl-labeled: unlabeled) AdoMet stocks were made using 32 mM unlabeled AdoMet (NEB) and [³H]methyl-labeled AdoMet (X Ci/mmol) supplied by PerkinElmer in 10 mM H₂S O₄. In all assays, 15 μL aliquots were taken from a larger reaction and quenched by mixing with 0.1% SDS (1:1). Samples were spotted onto Hybond-XL membranes (GE healthcare), washed, dried and methylation was using a Beckman LS 6000 liquid scintillation Counter as previously established (96). Due to the large number of potential methylation sites, poly dI-dC is commonly used as a DNA substrate to study the enzymatic activity of DNA modifying enzymes (97-101). In addition, the use of poly dI-dC as a DNA substrate allowed us to investigate the isolated modulatory effect of p53 on DNMT3A activity. On this basis, 5 μM poly dI-dC (Sigma-Aldrich) was used as a DNA substrate. Previous work from our lab has provided insights into the mechanism of DNMT3A activity on human promoters (102). Given that *Cyclin Dependent Kinase Inhibitor 1A/P21* is a common target for DNMT3A and p53 (102), (25), we additionally employed *Cyclin Dependent Kinase Inhibitor 1A/P21*-pCpG^L as a substrate.

All radiochemical assays were performed in triplicates from a single purification and statistical analysis was performed using Prism v7 (GraphPad).

P53 assays

To test modulation of DNMT3A (full length, catalytic domain and mutant enzymes) or M. HhaI methylation activity by P53^{WT}, proteins were preincubated in reaction buffer with AdoMet for 1 hour at 37 °C before initiating the reaction by the addition of substrate DNA. Reactions were then run for 1 hour, stopped as stated above and methylation was counted. All proteins (DNMT3A, M. HhaI or P53^{WT}) were at a ratio of 1:1 (150 nM) in the 1-hour preincubation. Fold inhibition was calculated by product formed by DNMT3A variants (or M. HhaI) divided by product formed by DNMT3A variants (or M. HhaI) without P53^{WT}. Statistical analysis was performed using Graphpad software (Version 6.0).

DNMT3L and P53 assays

To evaluate regulation of DNMT3A activity by DNMT3L or P53 under a binary (protein pairs) approach, proteins (1:1:1 at 150 nM) were preincubated in reaction buffer with AdoMet for 1 hour at 37 °C before starting the reaction by the addition of substrate DNA. To assess modulation of DNMT3A activity under a co-complex (groups of proteins) approach, DNMT3A was preincubated with DNMT3L (or P53) (1:1 at 150 nM) for 1 hour at 37 °C prior to initiating the reaction by the addition of substrate DNA and enzyme were allowed to carry out catalysis for 30 minutes before the addition of P53 (or DNMT3L) (150 nM). Reactions were then monitored for an additional hour, stopped and methylation was counted as stated above.

Apparent binding affinities (K_D^{app})

Modulation of DNMT3A activity by varying DNMT3L, P53^{WT}, or P53^{R248W} concentrations from 10 to 300 nM with 10 nM DNMT3A was tested to determine apparent

affinities (K_D^{app}). DNMT3A^{WT} was preincubated with varying concentrations of DNMT3L, P53^{WT}, or P53^{R248W} in reaction buffer with AdoMet for 1 hour at 37 °C prior initiating the reaction by the addition of substrate DNA. Following the addition of DNA, reactions were run for 1 hour at 37 °C, stopped and methylation was counted as stated above. Fold stimulation was calculated by product formed by DNMT3A^{WT} with DNMT3L divided by product formed by DNMT3A^{WT} without DNMT3L. Fold inhibition was by P53^{WT} or P53^{R248W} was calculated as stated above. The data were fit to a one site-specific binding equation using Graphpad software (Version 6.0).

Fluorescence Anisotropy

Fluorescence anisotropy measurements were performed using a Horiba Fluoromax fluorescence spectrophotometer equipped with excitation and emission polarizers (excitation: 485 nm, emission 520 nm). Fluorescence anisotropy measurements of DNA-bound DNMT3A^{WT} or DNMT3A^{R882H} (both at 2.5 μ M) were taken following the titration of DNMT3L (DNMT3A^{WT} and DNMT3A^{R882H} reactions), P53^{WT} (DNMT3A^{WT} and DNMT3A^{R882H} reactions) or P53^{R248W} (DNMT3A^{WT} reactions). Anisotropy values were obtained following a 5-minute preincubation at room temperature. The substrate DNA (Gcbox30) consisted of a fluorescein (6-FAM) label on the 5' end of the top strand of the duplex (5'/6-FAM/TGGATATCTAGGGGCGGCTATGATATCT-3') and was supplied by Integrated DNA Technologies; the recognition site for DNMT3A is underlined.

Electrophoretic mobility shift assay (EMSA)

Experiments were carried out as described in Holz-Schietinger et al. (28). In brief, DNMT3A^{R882H} (150 nM) was incubated at 37 °C for 15 min with 200 nM duplex 5' 6-FAM GCbox30 in reaction buffer with 50 μ M Sinefungin (Sigma-Aldrich) and 10% glycerol. For P53^{WT} super shifting, varying concentrations of P53^{WT} were preincubated with

DNMT3A^{R882H} under identical conditions for 30 minutes at 37 °C before the addition of GCbox30. Samples were run on a native 4.5% (75:1) polyacrylamide gel in 0.25× Tris-Boric acid EDTA, pH 7.8, at 250 V for 50 minutes. Gels were visualized for fluorescein using a Typhoon scanner and data were analyzed using ImageJ.

Supplementary Material

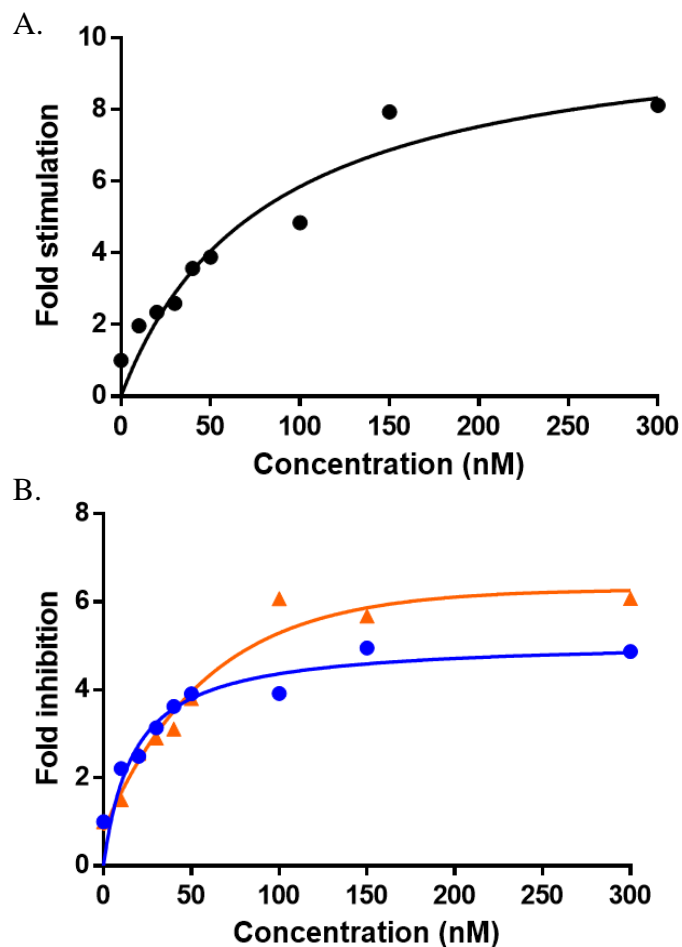


Figure S1. p53^{WT} and p53^{R248W} display stronger affinity for DNMT3A^{WT} binding than DNMT3L. **A.** Titration curves of 10 nM DNMT3A^{WT} co-incubated for 1 hour at 37 °C with increasing concentrations of DNMT3L (**A. ■**), p53^{WT} (**B. ■**) or p53^{R248W} (**C. ■**) prior to the start of the reaction by the addition of DNA were used to determine apparent affinities (KD^{app}). Fold stimulation (**A.**) was defined as the product formed by DNMT3A^{WT} with DNMT3L divided by product formed by DNMT3A^{WT} without DNMT3L. Fold inhibition (**B.** and **C.**) was determined by product formed by DNMT3A^{WT} alone divided by product formed by DNMT3A^{WT} with p53^{WT} or p53^{R248W}. Reactions were carried out at 37 °C for 1 hour following the addition of DNA (5 μ M bp poly dI-dC). Data reflect the results of 3 experiments.

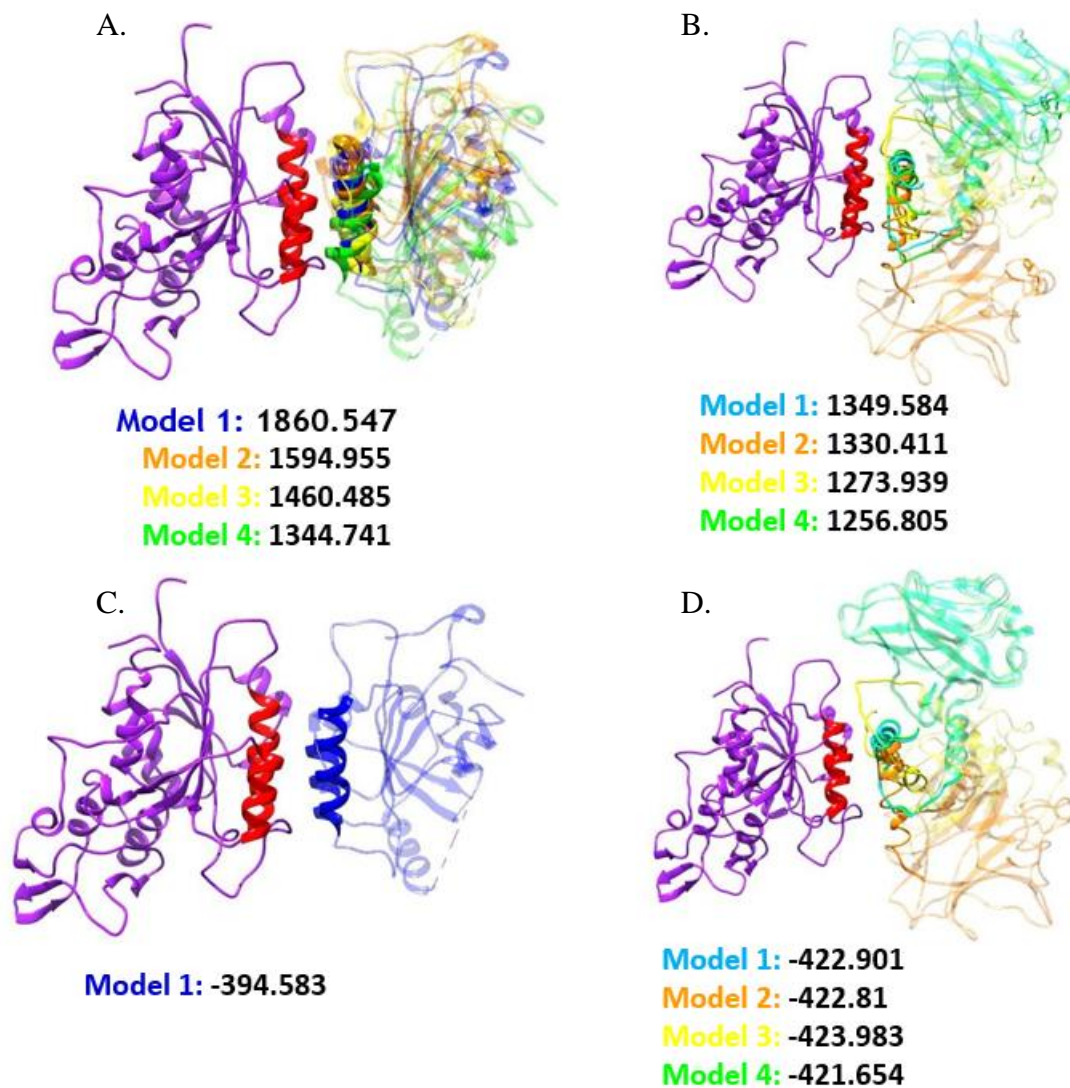


Figure S2. Models to identify p53 binding surface on DNMT3A. ZDOCK (A. and B.) and RosettaDock (C. and D.) models of DNMT3A^{WT} (PDB: 5YX2)-p53^{WT} (PDB: 3TS8) complexes to identify a potential p53 binding surface on DNMT3A. In all models (A.-D.), DNMT3A (■; ■ Tetramer interface) was defined as the receptor and either DNMT3L (A.; no transparency on identified binding surface) or p53 (B.; no transparency on identified binding surface) were defined as the ligand. DNMT3L (■)-DNMT3A (■) model 1 generated using ZDOCK was submitted to RosettaDock (C) DNMT3A (■; ■ Tetramer interface)-p53 models 1-4 generated using ZDOCK were submitted to RosettaDock (D.).

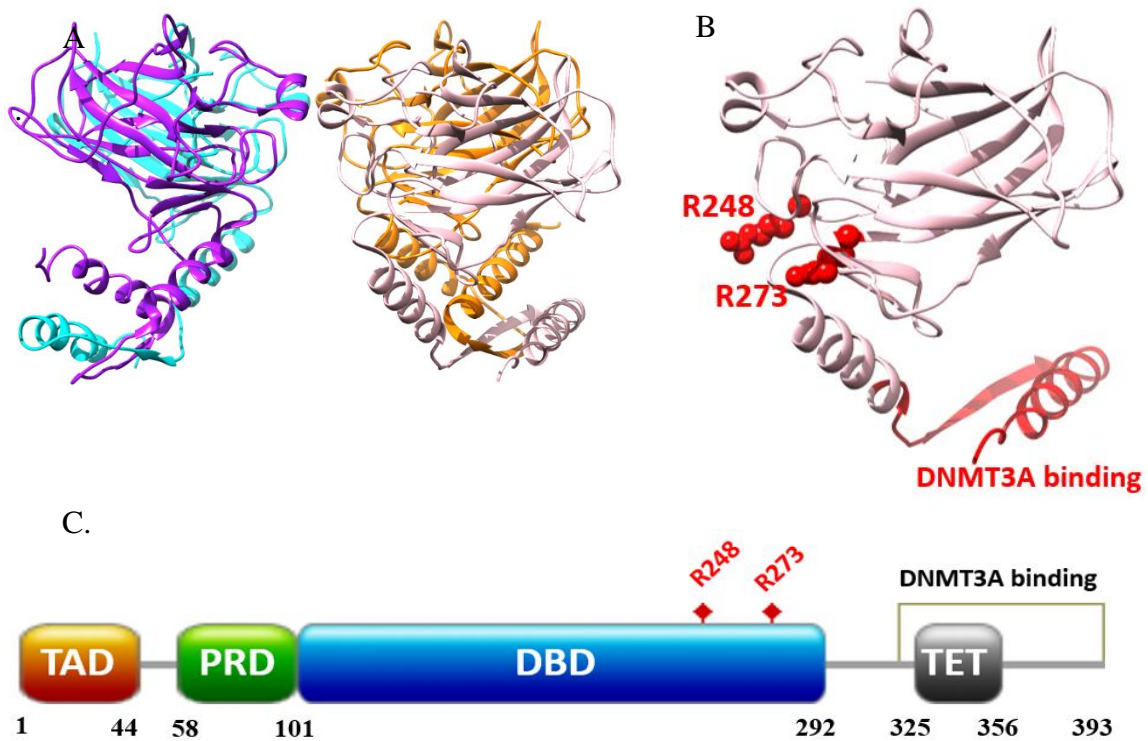


Figure S3. Depiction of p53^{WT} mutations and region on p53^{WT} for binding by DNMT3A. **A.** p53^{WT} homotetramer (adapted from PDB: 3TS8). **B.** p53^{WT} monomer (adapted from PDB: 3TS8) displaying residues assessed in this study (R248 and R273) as well as the region on p53^{WT} for DNMT3A binding (25). **C.** Domains in full-length p53^{WT}: transactivation domain (TAD) (1-44), proline-rich domain (PRD) (58-101), DNA-binding domain (DBD) (102-292) and tetramerization domain (TET) (325-356) (80). DNMT3A has been shown to bind residues 319-393 (25).

Chapter IV: p53 and TDG are dominant in regulating the activity of the human de novo DNA methyltransferase DNMT3A on nucleosome

Abstract

DNA methylation and histone tail modifications are interrelated mechanisms involved in a wide range of biological processes, and disruption of this crosstalk is linked to diseases like acute myeloid leukemia (AML). In addition, DNMT3A activity is modulated by several regulatory proteins, including p53 and TDG. However, the relative role of histone tails and regulatory proteins in the simultaneous coordination of DNMT3A activity remains obscure. We observed that DNMT3A binds H3 tails and p53 or TDG at distinct allosteric sites to form DNMT3A-H3 tail-p53 or -TDG multiprotein complexes. Functional characterization of DNMT3A-H3 tail-p53 or -TDG complexes on human-derived synthetic histone H3 tails, mono- or polynucleosomes shows p53 and TDG play dominant roles in the modulation of DNMT3A activity. Intriguingly, this dominance occurs even when DNMT3A is actively methylating nucleosome substrates. The activity of histone-modifiers is influenced by their ability to sense modifications on histone tails within the same nucleosome or histone tails on neighboring nucleosomes. In contrast, we show here that DNMT3A acts on DNA within a single nucleosome, on nucleosomal DNA within adjacent nucleosomes, and DNA not associated with the DNMT3A-nucleosome complex. Our findings have direct bearing on how the histone code drives changes in DNA methylation and highlight the complex interplay between histone tails, epigenetic enzymes and modulators of enzymatic activity.

Introduction

Carried out by DNA methyltransferase 3A (DNMT3A), *de novo* 5-methylcytosine patterning of mammalian DNA is a major epigenetic modification frequently associated with transcriptional repression (1), (2). The plethora of post-translational modifications to specific residues within the amino-terminal tails of core histones (H2A, H2B, H3, and H4) forms another epigenetic process leading to the activation or repression of genes (3). Mammalian transcriptional regulation relies on the extensive crosstalk between histone modifications and DNA methylation, and changes in this interplay are a major contributor to human cancers. For example, genome-wide epigenetic profiling reveals that genomic loci with H3K36me_{2/3}, H3K9me₃ and H3K4me₀ correlate with enrichment of *de novo* DNA methylation (4-6); more specifically, DNMT3A-mediated methylation follows H3K9me₃ and H3K36me₃ patterning (7), (8). Furthermore, alterations to the interplay between DNA methylation and modifications to H3K4/K27 contribute to the altered expression of the *cyclin-dependent kinase inhibitor 2B* (*CDKN2B* or *p15*) gene observed in AML (9). However, the mechanisms that underpin these correlations between changes in histone modifications and DNA methylation remain obscure, as is the contribution of regulatory proteins in this context. We envision two plausible situations (Figure 1 B.), starting with the physical recruitment of DNMT3A (Figure 1 B., I.), or DNMT3A in complex with distinct regulatory proteins (Figure 1 B., II and V.), through its well-known interactions with histone tails. In this model DNMT3A acts as a reader of histone marks (Figure 1 B., I, II., and V.) with histone tails modulating enzymatic activity (Figure 1 B., I, II. And V), or alternatively with histone tails primarily recruiting DNMT3A and regulatory proteins playing a dominant role in the modulation of enzymatic activity (Figure 1 B., II., and V.). An additional scenario derives not from a physical association of DNMT3A and particular histone marks, but rather the regulatory proteins associated with DNMT3A serving as a reader of histone

marks (Figure 1 B., VI.), and the enzymatic activity of DNMT3A modulated by regulatory proteins, or a combination of regulatory protein-histone tail interactions (Figure 1 B., VI.). Clearly, these mechanisms are not mutually distinctive.

The crystal structure of a DNMT3A- DNA Methyltransferase 3 Like (DNMT3L) heterotetramer in complex with a histone H3 peptide (residues 1-21) reveals that DNMT3A binds histone tails via its conserved ATRX-DNMT3-DNMT3L (ADD) domain while simultaneously accommodating DNMT3L at the tetramer interface (Figure 1 A.) (10). To date, insights on the combinatorial effect of regulatory proteins and histone H3 tails in the modulation of DNMT3A activity have focused solely on DNMT3L, which is complicated by the fact that both DNMT3A and DNMT3L bind H3 tails via the ADD domain (Figure 1 B., V. and VI.) (10-12). The interactions between DNMT3A and nucleosomes and regulatory proteins like DNMT3L is further modulated by other regulatory proteins such as tumor suppressor p53 (p53) or Thymine DNA Glycosylase (TDG), which involve DNMT3A surface regions that are shared with DNMT3L (13), (14). While there is no evidence for the direct interactions of p53 or TDG with histone tails, their genomic locations are associated with specific histone modifications and indirectly mediating changes to the modifications of histone tails (15), (16). Thus, these proteins clearly contribute to the modulation of epigenetic mechanisms. Although the related interactions between DNMT3A and nucleosomes remains largely uncharacterized, several studies have investigated this relationship in histone modifying enzymes. For example, the chromodomain helicase DNA-binding protein 4 (CHD4) associates with histone H3 tails within a single nucleosome (intra-nucleosomal interactions) while heterochromatin protein 1 α (HP1 α) binds individual histone H3 tails in adjacent nucleosomes (inter-nucleosomal interactions) (17), (18). The relationship between DNMT3A and histone H3 tails is inherently intricate as DNMT3A

plays a dual role as a reader of histone H3 tails and a writer on nucleosomal DNA (10). Furthermore, when the possible combinations of biologically significant complexes involving regulatory proteins are considered (Figure 1 B.), the complexity of the dynamics associated with epigenetic control is evident. Our current understanding of the allosteric modulation of DNMT3A activity is limited to studies focusing on the individual roles of histone H3 tails, regulatory proteins, or the interplay between DNMT3L and histone H3 tails. (7), (10-14), (19).

Our interest here is to explore the relative role (dominant or passive) of histone H3 tails and regulatory proteins in the modulation of DNMT3A activity to better understand the potential crosstalk between histone H3 tails and regulatory proteins, and how this translates into meaningful biological outcomes. Our approaches rely on human-derived synthetic histone H3 tails, mono- or polynucleosomes, the regulatory proteins p53 and TDG, and a modified pulse-chase assay along with fluorescence anisotropy assays. Our work provides novel insights into the dynamic interplay between distinct epigenetic mechanisms as well as a better understanding of the regulation of enzyme activity in protein complexes consisting of modulators that bind distinct allosteric sites.

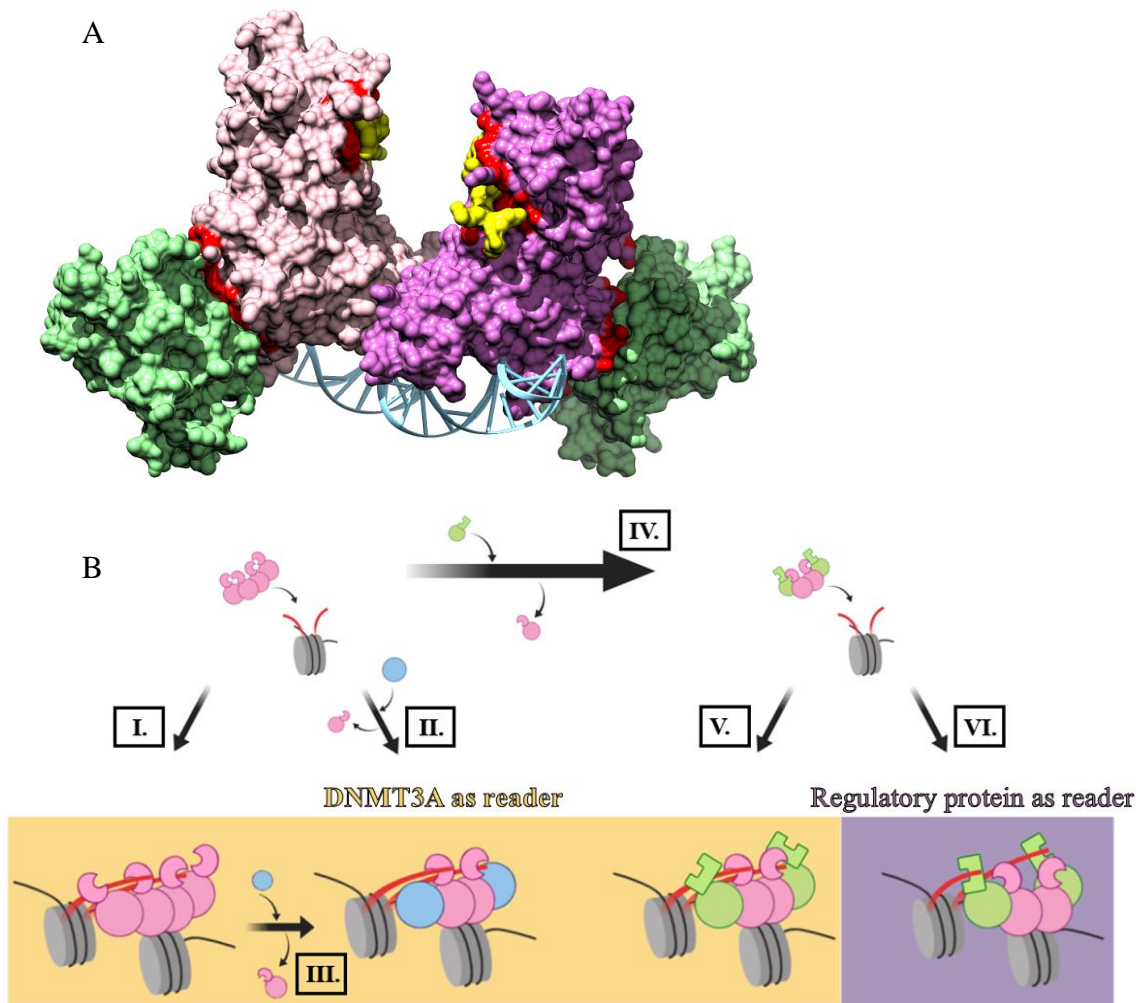


Figure 1. DNMT3L and H3 tails bind distinct surfaces on DNMT3A for modulation of enzymatic activity. **A.** Surface model of a DNMT3A heterotetramer (■ and ■) (residues 468-912) bound by DNMT3L (■) (residues 171-379) and Histone H3 N-terminal peptide (■) (residues 1-12) (adapted from PDB 4U7T) (10). The DNA (blue) binding interface on PDB 4U7T was modelled based on the structural similarity to a DNA-bound DNMT3A-DNMT3L crystal structure (PDB 5YX2) (48). (■) denote interacting surfaces on DNMT3A for DNMT3L or H3 peptide interactions (< 5 Å). **B.** Depiction of proposed interactions associated with the targeting of DNMT3A homotetramers (I.) or heterotetramers (II.-IV.) to nucleosome substrates. The yellow panel encompasses complexes in which DNMT3A is acting as the reader of histone marks (I., II., and V.), whereas the purple panel represents complexes in which regulatory proteins associated with DNMT3A serve as the reader of histone marks (VI.). Pink represents DNMT3A, blue denotes regulatory proteins that lack a histone reading domain and green represents regulatory proteins of DNMT3A that additionally act as readers of histone marks.

Results

Regulation of full-length DNMT3A activity by p53 or TDG is dominant in DNMT3A-p53-H3 tail or DNMT3A-TDG-H3 tail complexes

DNMT3A simultaneously accommodates DNMT3L and histone H3 tails through interactions at distinct surfaces (Figure 1 A.) (10). In conjunction with a distinct co-crystal structure of DNMT3L bound to H3K4me0 peptide (PDB 2PVC) (11), functional studies of the interactions between DNMT3A, DNMT3L and H3 peptide have led to a model in which recognition of H3K4me0 by DNMT3L leads to the recruitment of DNMT3A (10-12). However, this model does not entirely explain the relationship between DNMT3L and histone H3 tails in the simultaneous regulation of DNMT3A activity in DNMT3A-DNMT3L-H3 complexes as the same activation is observed in the absence of DNMT3L (19). Furthermore, this model leaves unanswered whether histone tails primarily recruit DNMT3A, while DNMT3L plays a dominant role in the modulation of DNMT3A activity (Figure 1 B., V.), or DNMT3L primarily recruits DNMT3A and the activity of DNMT3A is modulated by DNMT3L, or a combination of DNMT3L-histone H3 peptide interactions (Figure 1 B., VI.). To elucidate the role of histone H3 tails and regulatory proteins in the coordination of DNMT3A activity, we assessed the dynamics and functional consequences of complexes involving DNMT3A, histone H3 peptides (H3K4me0 and H3K4me3) and two previously characterized regulatory proteins of DNMT3A (p53 or TDG) whose cellular functions have been associated with the presence of specific histone modifications (13-16).

We previously used fluorescence anisotropy to characterize the interactions between the catalytic domain of DNMT3A and p53 on a fluorophore-labeled oligonucleotide (5' 6-FAM-labeled duplex DNA [GCbox30]) containing a single recognition site for DNMT3A (14). We relied on this approach to assess the dynamics between H3K4me0 and DNMT3A-

p53 or DNMT3A TDG on DNA. Importantly, the modulation of DNMT3A activity on DNA by p53 and TDG does not occur with other DNA cytosine methyltransferases, which argues against these effects deriving from competition by these regulatory proteins resulting from DNA binding (13), (14). Consistent with previous findings (10), increasing concentrations of unlabeled H3K4me0 peptide to a fixed concentration of DNA-bound DNMT3A (Figure 2 A. ■) increases the fluorescence anisotropy signal, reflecting the formation of DNA-bound DNMT3A-H3K4me0 complexes. Similarly, pre-formed DNMT3A-p53 (Figure 2 A. ■) or DNMT3A-TDG (Figure 2 A. ■) complexes on DNA displayed an increase to the initial anisotropy signal with a corresponding increase in H3K4me0 peptide concentration, suggesting the formation of higher order DNMT3A heterotetramers in complex with H3K4me0 peptide on DNA. Given that DNA-bound DNMT3A heterotetramers with p53 (Figure 2 A. ■) or TDG (Figure 2 A. ■) can accommodate H3K4me0 peptide, we sought to assess the relative role of H3K4 and regulatory proteins (p53 or TDG) in the simultaneous modulation of DNMT3A enzymatic activity.

As previously observed (19), pre-incubation of DNMT3A with H3K4me0 peptide results in activation of enzymatic activity (Figure 2 B. ■) while pre-incubation of DNMT3A with H3K4me3 peptide (Figure 2 A. ■) results in comparable levels of activity as reactions without H3 peptides (Figure 2 B. ■), although DNMT3A binds both peptides *in vitro* (10). Additionally, we observed a roughly 50% decrease in DNMT3A activity in control reactions consisting of DNMT3A-p53 (Figure 2 B. ■) or DNMT3A-TDG (Figure 2 B. ■) pre-incubations as previously reported (13), (20). In equilibrium reactions where DNMT3A and H3K4me0 peptide were pre-incubated with individual regulatory proteins, we observed that inhibition of DNMT3A activity by p53 (Figure 2 B. ■) or TDG (Figure 2 B. ■) is dominant

over H3K4me0 peptide activation of DNMT3A (Figure 2 A. ■). Under similar experimental conditions, the presence of H3K4me3 peptide does not disrupt modulation of DNMT3A methylation activity by p53 (Figure 2 B. ■) or TDG (Figure 2 B. ■). In fact, pre-incubation of DNMT3A with p53 or TDG in the presence of H3K4me0 or H3K4me3 peptides led to comparable levels of DNMT3A-dependent methylation as reactions consisting of DNMT3A with only p53 (Figure 2 B. ■) or TDG (Figure 2 B. ■). To further challenge the dominant modulatory effect of p53 or TDG over H3K4me0 or H3K4me3 peptides on DNMT3A observed, we then evaluated the functional outcome of adding equimolar concentrations of individual regulatory proteins (ratio of 1:1 regulatory protein to 150 nM tetramer DNMT3A) to DNMT3A- H3K4me0 or DNMT3A- H3K4me3 complexes that are actively methylating DNA. Like reactions at equilibrium (Figure 2 B), the addition of p53 (Figure 2 C. ■) or TDG (Figure 2 D. ■) to actively methylating DNMT3A- H3K4me0 complexes disrupted H3K4me0 peptide-mediated stimulation of DNMT3A activity (Figure 2 C. and D. ■). Furthermore, actively catalyzing DNMT3A- H3K4me3 peptide complexes (Figure 2 E. and F. ■) are responsive to the addition of p53 (Figure 2 E. ■) or TDG (Figure 2 F. ■). While H3K4me0 is associated with gene silencing, trimethylated histone H3K4 (H3K4me3) sites are associated with active gene promoters (21). These results do not derive from direct p53 or TDG competition with DNMT3A binding to the DNA (Figure S6) (13), (14). Our results indicate that in DNMT3A-H3 tail-regulatory protein complexes (Figure 2 A.), regulatory proteins play a dominant role in the simultaneous coordination of DNMT3A activity despite the methylation state H3K4 (Figure 2 B.-F.).

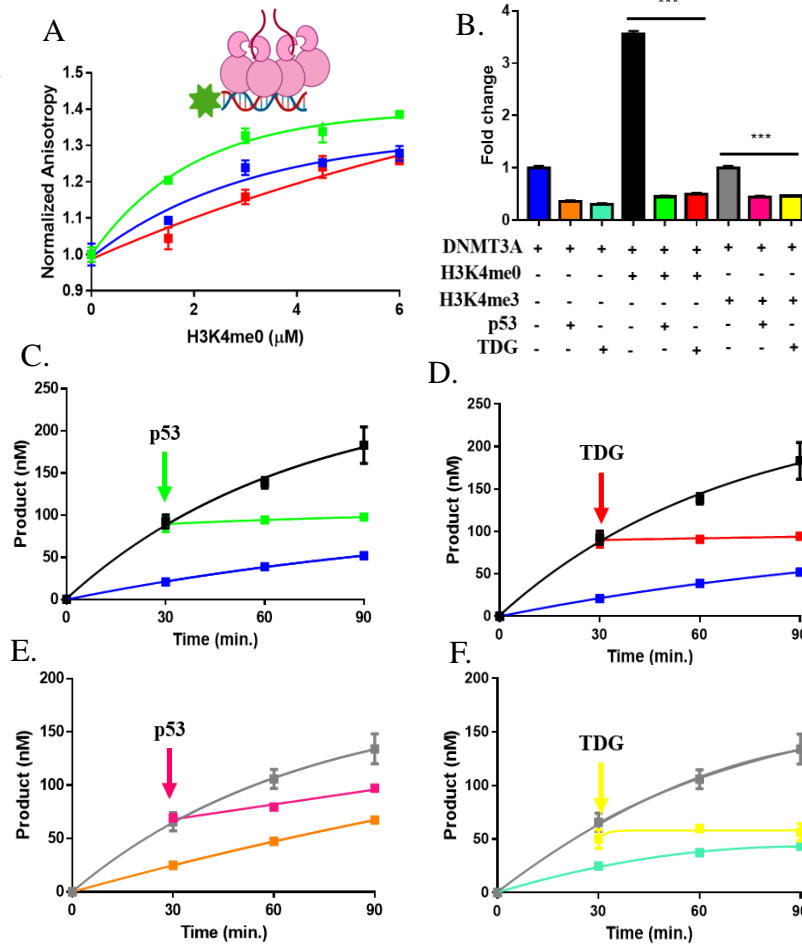





Figure 2. Modulation of DNMT3A activity by regulatory proteins is dominant in the presence of H3K4me0 or H3K4me3 peptides. **A.** The addition of H3K4me0 peptide (unlabeled) increases the FA of DNA-bound DNMT3A (■), DNMT3A-p53 (■) or DNMT3A-TDG (■) complexes. In **A.**, 50 nM DNA (5' 6-FAM-labeled GCbox30; see methods for sequence) was pre-incubated with DNMT3A or DNMT3A with individual regulatory proteins (1 μM at 1:1 to DNMT3A tetramer). Data **A.** are normalized to FA values in the absence of H3K4me0. **(B.)** The presence of H3K4me0 or H3K4me3 does not disrupt inhibition of DNMT3A enzymatic activity by p53 or TDG in equilibrium reactions. In **B.**, data were normalized to the DNA methylation activity observed in DNMT3A on poly dI-dC as a substrate and are representative of reactions carried out for 1 hour. The addition of p53 (**C.** ■, **E.** ■) or TDG (**D.** ■, **F.** ■) disrupts actively catalyzing DNMT3A- H3K4me0 (**C.** and **D.** ■) or DNMT3A- H3K4me3 (**E.** and **F.** ■) complexes. Reactions consisting of DNMT3A only (**C.** and **D.** ■), DNMT3A-p53 (**B.** and **E.** ■) or -TDG (**B.** and **E.** ■) co-incubations were performed as controls. For co-incubations, proteins were placed at 37 °C for 1 hour prior to the addition of substrate DNA. Except for **E.** and **F.** with proteins at 50 nM (1:1 to DNMT3A tetramer), DNA methylation reactions consisted of proteins at 150 nM (1:1 to DNMT3A tetramer), H3K4 peptides were at 4 μM and were initiated by the addition of 5 μM bp poly dI-dC. Data reflect the mean ± S.D. of 3 experiments; **B.** one-way analysis of variance was used to compare the values of p53 or TDG with DNMT3A to similar reactions but in the presence of H3K4me0 or H3K4me3; ***, p < 0.001; ns, p > 0.05.

Full-length DNMT3A methylates inter-nucleosomal DNA

Elucidating the spatial relationship between epigenetic enzymes and their substrates (intra- or inter-nucleosomal action, Figure 3 A.) is essential to truly understand nucleosome-protein interactions and the structural basis of epigenetic gene regulation. Several studies have characterized this relationship in the context of histone-modifying enzymes (17), (18). However, the molecular arrangement between DNMT3A and nucleosome substrates remains less well characterized (Figure 3 A.). The primary focus has been on whether the enzyme methylates linker DNA or the DNA wrapped to form the nucleosome, which at this point remains unclear. To provide insights into the orientation of DNMT3A relative to nucleosome substrates, we assessed the accessibility of exogenous (non-nucleosomal substrate) H3K4me0 peptide or DNA to DNMT3A-monomucleosome complexes (Figure 3 B.-F.). We initially assessed whether the N-terminus of DNMT3A contributes to DNMT3A-monomucleosome interactions. Consistent with previous findings, the catalytic domain of DNMT3A ($\Delta 1-611$) (Figure S1 ) and the prokaryotic CpG DNA methyltransferase M. SssI (Figure S1 ) displayed reduced activity on unmodified mononucleosomal substrates relative to full length DNMT3A (Figure S1 ) (12), (22). We then assessed the effect of increasing concentrations of H3K4me0 peptide on the activity of DNMT3A using mononucleosomes as a substrate (Figure 3 B.). Unlike reactions consisting of free DNA (Figure 2), an increase in the concentration of H3K4me0 peptide did not alter the enzymatic activity of DNMT3A on mononucleosomal DNA (Figure 3 B.). Thus, the association of DNMT3A to intrinsic (mononucleosomal) H3 tails appears to perturb the activation of DNMT3A by H3K4me0 peptide. To additionally challenge this notion, we then monitored changes in the fluorescence anisotropy of FAM-labelled H3K4me0 (1-21)-DNMT3A complexes by the addition unlabeled mononucleosomes (Figure 3 C.). The

addition of DNMT3A (150 nM tetramers) to 2 μ M FAM-labelled H3K4me0 peptide leads to saturating anisotropy (Figure S5). Under these conditions, we observed that the addition of unlabeled mononucleosomes (0-2 μ M) led to a robust decrease to the initial fluorescence anisotropy of FAM-labelled H3K4me0 peptide bound by DNMT3A (Figure 3 C.). The results obtained are consistent with H3 tails in mononucleosomes displacing FAM-H3K4me0 peptide in DNMT3A- H3K4me0 peptide complexes.

To evaluate the accessibility of extrinsic DNA (non-nucleosome) to DNMT3A, we monitored DNMT3A-mediated methylation following the addition of a twenty-fold excess of pCpG^L (a plasmid with ~3,800 base pairs and no CpG sites) or Poly dI-dC (a synthetic DNA substrate with ~2,000 base pairs and 800 CpG sites) to DNMT3A acting on mononucleosomal DNA (1 μ M) (Figure 3 D. and E.). The robust activity of DNMT3A on Poly dI-dC, and poor activity on pCpG^L, allow for effective monitoring of any changes to DNMT3A activity on mononucleosomal DNA. Initial controls were performed in which reactions were initiated by the addition of a mixture of excess (twenty-fold) pCpG^L to mononucleosomes (Figure 3 D. ■) or a mixture of excess (twenty-fold) Poly dI-dC to mononucleosomes (Figure 3 E. ■). We found that reactions initiated by the addition of a mixture of pCpG^L and mononucleosomes (Figure 3 D. ■) or Poly dI-dC and mononucleosomes (Figure 3 E. ■) resulted in comparable levels of activity as reactions initiated by the addition of only pCpG^L (Figure 3 D. ■) or Poly dI-dC (Figure 3 E. ■). The addition of pCpG^L (Figure 3 D. ■) or Poly dI-dC (Figure 3 E. ■) 60 minutes into the reaction resulted in a respective decrease (Figure 3 D. ■) or increase (Figure 3 E. ■) to the activity of DNMT3A catalyzing on mononucleosomal DNA (Figure 3 D. and E. ■). Thus, DNMT3A appears to act on extrinsic DNA (pCpG^L or Poly dI-dC) while bound and acting on mononucleosomes. We then challenged this notion by tracking the fluorescence anisotropy

of FAM-labeled Gcbox30 DNA after the addition of pre-formed DNMT3A-mononucleosome to assess the ability of DNMT3A-mononucleosome complexes to bind non-nucleosomal DNA (Gcbox30). An increase in the concentration of pre-formed DNMT3A-mononucleosome complexes (Figure 3 F. ■) led to a greater increase to the initial fluorescence anisotropy of FAM-labeled Gcbox30 DNA relative to the addition of DNMT3A only (Figure 3 F. ■), indicating the formation of a higher order complex composed of pre-formed DNMT3A-mononucleosome complexes bound to DNA (Gcbox30). Thus, our combined results are most consistent with an inter-nucleosomal mechanism (Figure 3 A., I.) in which DNMT3A that is already bound to a nucleosome can act on another DNA molecule, which is not part of the initial DNMT3A-nucleosome complex.

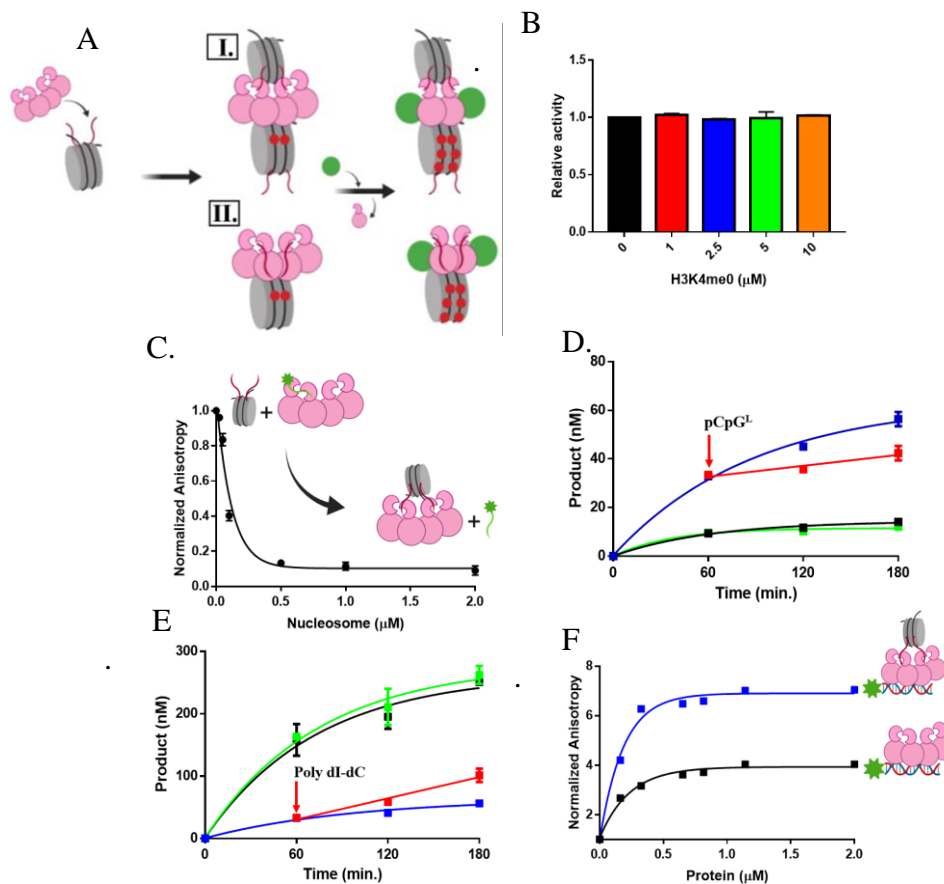


Figure 3. DNMT3A remains bound to histone tails in mononucleosomes when acting on free DNA. **A.** Proposed interactions for DNMT3A, or DNMT3A in complex with regulatory proteins, with nucleosomes: I. inter-nucleosomal and II. Intra-nucleosomal. **B.** Increasing the concentration of H3K4me0 peptide does not disrupt the enzymatic activity of DNMT3A in equilibrium reactions. In **B.**, data were normalized to the DNA methylation activity of DNMT3A in the absence of H3K4me0 and are representative of reactions carried out for 1 hour. **C.** The addition of unlabeled mononucleosomes disrupts DNMT3A (150 nM tetramer) bound to FAM-labelled H3K4me0 (2 μM); data are normalized to FA values in the absence of mononucleosomes. Catalytically active DNMT3A on mononucleosomal DNA as a substrate (**D.** and **E.** ■) is responsive to the addition of excess (20X) endogenous pCpG^L (**D.** ■) or Poly dI-dC (**E.** ■). In (**D.** and **E.**) reactions consisted of DNMT3A at 150 nM tetramer and mononucleosomes at 1 μM (**B.-E.**) and the following reactions were also performed as controls: pCpG^L only (**D.** ■), mixture of pCpG^L and mononucleosomes (**D.** ■), Poly dI-dC only (**E.** ■) and mixture of Poly dI-dC and mononucleosomes (**E.** ■). Increasing concentrations of pre-formed DNMT3A-monomucleosome complexes to FAM-labeled DNA (15 nM; see methods for sequence) (**F.** ■) led to a greater change in FA relative to similar binding reactions in the absence of mononucleosomes (**F.** ■). Data reflect the results of 2 independent experiments.

Modulation of Full-length DNMT3A activity by p53 or TDG is not impeded by nucleosomes

Studies of the EZH2 (Enhancer of Zeste 2 Polycomb Repressive Complex 2 Subunit) histone H3 methyltransferase reveal that EZH2 exhibits a 5-fold increase in histone methylation activity on polynucleosomes (>10) relative to mononucleosomes (23). MNase digestion of native chromatin isolated from mouse embryonic stem cell nuclei shows that DNMT3A primarily binds mono- or poly-nucleosomes (< 7), and higher-order polynucleosomes (>12) to a lesser extent (24). Based on these observations and previous work on p53 and TDG along with their links to the regulation of distinct epigenetic mechanisms, we assessed the catalytic activity of DNMT3A as well as the ability of p53 or TDG to modulate DNMT3A using mononucleosome or polynucleosome substrates (Figure 4) (13-16). We initially relied on DNA methylation assays across a range of mononucleosome or polynucleosome concentrations to generate saturation curves for DNMT3A on each substrate (Figure S2). DNMT3A displayed an increased K_M on polynucleosome (336 ± 51 nM; Figure S2 ■) relative to mononucleosomes (86.9 ± 14 nM; Figure S2 ■). DNMT3A had comparable maximal velocity (approximately 0.8 nM product/min) at saturating mononucleosome or polynucleosome concentrations (Figure S2). Thus, DNMT3A requires saturating polynucleosome concentrations to overcome the hindered accessibility to DNA, which likely stems from the structural complexity of polynucleosomes.

DNMT3A moves along DNA substrates carrying out multiple cycles of methylation on the same piece of DNA prior to dissociating and the DNA-bound DNMT3A is accessible for modulation by distinct regulatory proteins (13), (14), (25), (26). Given that DNMT3A acts on nucleosomal DNA without dissociating from *histone* N-Terminal tails (Figure 3. B.-

F.; Figure S1), we assessed whether mononucleosomal or polynucleosomal DNA-bound DNMT3A is accessible for modulation by p53 or TDG (Figure 4). In equilibrium reactions using mononucleosomal DNA, the presence of p53 (Figure 4 A. ■) or TDG (Figure 4 A. ■) results in decreased DNMT3A-mediated methylation relative to reactions consisting of DNMT3A only (Figure 4 A. ■). Moreover, we observed that the modulatory effect on DNMT3A activity by p53 (Figure 4 A. ■) or TDG (Figure 4 A. ■) observed in equilibrium reactions persisted in reactions with actively catalyzing DNMT3A on mononucleosomal DNA (B. and C. ■) challenged by the addition of p53 (Figure 4 B. ■) or TDG (Figure 4 C. ■) at equimolar concentrations relative to DNMT3A (150 nM tetramer). Therefore, the association of DNMT3A to histone tails while catalyzing mononucleosomal DNA does not occlude the accessibility of p53 or TDG to DNMT3A. Polynucleosomes challenge the ability of DNMT3A to access DNA compared to mononucleosomes (Figure S2). Therefore, we also examined the ability of p53 or TDG to access and modulate DNMT3A activity on polynucleosome substrates. Like reactions with mononucleosomes (Figure 4 A.), equimolar concentrations of p53 (Figure 4 A. ■) or TDG (Figure 4 A. ■) relative to DNMT3A (150 nM tetramer) inhibit DNMT3A acting on polynucleosomal DNA (Figure 4 A. ■) in equilibrium reactions. Surprisingly, the addition of equimolar amounts of p53 (Figure 4 D. ■) or TDG (Figure 4 E. ■) relative to DNMT3A (150 nM tetramer) methylating polynucleosomal DNA (Figure 4 D. and E. ■) did not disrupt DNMT3A activity. Modulation of DNMT3A in transient reactions was only observed by the addition of excess (500 nM tetramer) p53 (Figure 4 D. ■) or TDG (500 nM dimer) (Figure 4 E. ■) compared to DNMT3A (150 nM tetramer). Our results show that although the structural complexity of polynucleosomes challenges the accessibility of p53 or TDG to actively catalyzing DNMT3A, p53 or TDG bind and modulate the enzymatic activity of DNMT3A in a

concentration-dependent manner under catalytic conditions. In sum, our findings indicate that in DNMT3A-histone tail- regulatory protein (p53 or TDG) complexes, histone tails primarily sequester DNMT3A to nucleosomes and p53 or TDG play a dominant role in the modulation of DNMT3A activity (Figure 1 B., II. and III.).

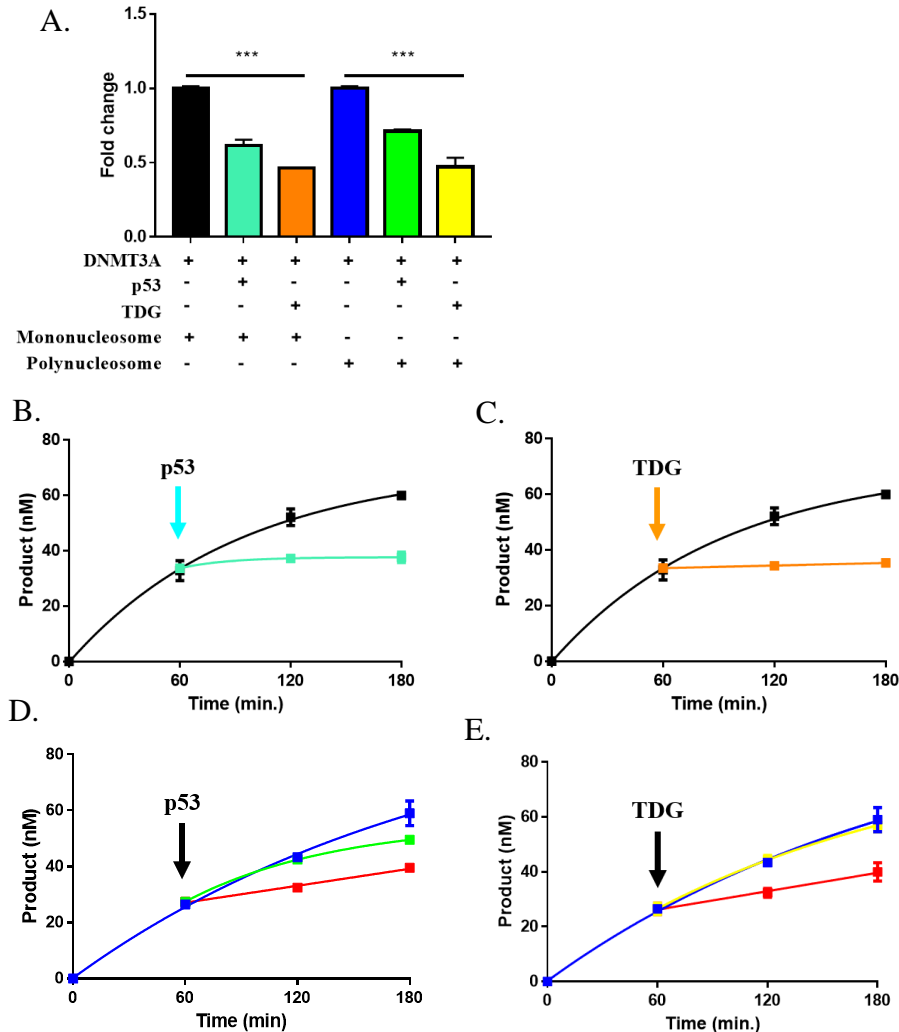


Figure 4. Modulation of DNMT3A activity by p53 or TDG using human mono- or polynucleosomes. **B.** Modulation of DNMT3A activity by p53 or TDG is unaffected in equilibrium reactions with mono- or polynucleosomal DNA as a substrate (1 μ M). The modulatory effect on DNMT3A activity observed in equilibrium reactions **A.**, persists in actively catalyzing DNMT3A on mononucleosomal DNA (**B.** and **C.** ■) challenged by the addition of p53 (**B.** ■) or TDG (**C.** ■). The addition of p53 or TDG disrupts actively catalyzing DNMT3A on polynucleosomal DNA at excess concentrations p53 (**D.** ■) or TDG (**E.** ■) but not at equimolar amounts p53 (**D.** ■) or TDG (**E.** ■). DNA methylation reactions consisted of proteins at 150 nM (1:1 to 150 nM tetramer DNMT3A) or excess regulatory proteins at 500 nM (see methods) (**D.** ■ and **E.** ■). In (**A.**), reactions consisting of mononucleosomes or polynucleosomes (1 μ M) and individual regulatory proteins (p53 or TDG, 1:1 at 150 nM) were initiated by the addition of DNMT3A. In (**B.**), actively catalyzing DNMT3A with mononucleosomes or polynucleosomes (1 μ M) as a substrate was challenged by the addition of p53 or TDG (1:1 at 150 nM) after 1 hour. Data from reactions in (**A.**) were normalized to the DNA methylation activity observed in DNMT3A on mono- or polynucleosomes and are representative of reactions carried out for 1 hour. Data reflect the mean \pm S.D. of 3 experiments; **A.** one-way analysis of variance was used to compare the values of p53 or TDG to those of DNMT3A for each substrate; ***, $p < 0.001$; ns, $p > 0.05$.

Discussion

Studies aiming to characterize the mammalian epigenetic landscape show DNA methylation and histone tail modifications are highly interrelated mechanisms that regulate gene expression. Evidence of the crosstalk between DNA methylation and histone tail modifications include the positive correlation of DNA methylation with H3K36me₂, H3K9me₃ and H3K4me₀ along with the altered expression of tumor-suppressor genes from changes to this crosstalk observed in AML (4-9). While histone marks evidently provide cues for DNA methylations, the mechanisms underlying these correlations along with the role of regulatory proteins in the interplay between DNA methylation and histone marks remain unclear. The ADD domains of DNMT3A, DNMT3B and DNMT3L bind H3K4me₀ with comparable specificity while carrying out distinct biological functions, thereby suggesting ADD domain-H3 tail interactions are not entirely responsible for the individual differences in cellular activity (7), (8), (11), (12), (27), (28). Given that DNMT3A activity is modulated by a wide range of protein partners, interactions with regulatory proteins provide an additional mechanism to alter DNMT3A function (13), (14), (20), (29). Although studies of histone-modifying enzymes have included interactions with respect to nucleosomes (intra- or inter-nucleosomal interactions; Figure 3 A.), the mechanism of substrate engagement by DNMT3A remains obscure (17), (18). Based on this evidence and the previously characterized activities of p53 and TDG in the modulation of DNA methylation and histone tail modifications (13-16), we sought to characterize the dynamics and simultaneous coordination of DNMT3A activity by p53 or TDG in the presence of H3 tails. Furthermore, we provide insights into the spatial relationship between DNMT3A and nucleosome substrates to better understand the interactions associated with DNMT3A acting as a reader of histone marks and how these interactions influence the modulation of its enzymatic activity. We show that modulation of DNMT3A methylation activity by p53 or

TDG is dominant in the presence of histone H3 peptides or with the use of mono- or polynucleosome substrates. Furthermore, we provide evidence for DNMT3A methylating inter-nucleosomal DNA. Our findings provide insights into the intricate interactions of key epigenetic players and provide a molecular basis for how these interactions contribute to epigenetic transcriptional regulation.

Previous work from our lab has shown DNMT3L, p53 and TDG bind a common surface on DNMT3A (tetramer interface, Figure 1A.), which differs from the surface H3 tail binds on DNMT3A (ADD domain, Figure 1A.) (13), (14). Given that p53 and TDG lack a structural domain that directly associates with histone H3 tails, we propose that the crosstalk between p53 or TDG and histone H3 tails in the simultaneous modulation of DNMT3A activity (Figure 1B., I.) is fundamentally different than DNMT3L in DNMT3A-DNMT3L-H3 tail complexes as DNMT3A and DNMT3L bind H3 tails (Figure 1B., V. or VI.) (11-16). We initially challenged this notion by assessing whether DNMT3A-p53 or DNMT3A-TDG heterotetramers can bind H3K4me0 peptide. The increase in anisotropy observed following the addition of H3K4me0 peptide to FAM-labelled DNA bound by DNMT3A-p53 or -TDG complexes shows that binding of H3 tails and these regulatory proteins is not mutually exclusive (Figure 2 A.) and that DNMT3A-H3 tail-p53 or -TDG complexes remain bound to DNA. Based on findings from distinct studies, p53 or TDG appear to display a stronger affinity for DNMT3A relative to H3 peptides (10), (13), (14), (19). Consistent with this notion, we found that inhibition of DNMT3A activity by p53 or TDG in DNMT3A-H3 tail-p53 or -TDG complexes is dominant in the presence of H3K4me0 or H3K4me3 peptide (Figure 2 B.) in reactions at equilibrium. Moreover, the dominant modulatory effect on DNMT3A activity by p53 or TDG persists in actively methylating DNMT3A- H3K4me0 (Figure 2 C. and D.) or -H3K4me3 (Figure 2 E. and F.) complexes. The results of transient

reactions (Figure 2 C.-F.) better model the cellular interactions of these epigenetic mechanisms and show that binding of H3 to its allosteric site does not induce conformational changes of DNMT3A that hinder the modulation of DNMT3A activity by p53 or TDG. Furthermore, equimolar concentrations of p53 and TDG relative to DNMT3A (150 nM tetramer) were used in all reactions (Figure 2 B.-F.), suggesting that the dominant modulation of DNMT3A activity by p53 and TDG over H3 peptides was not due to stoichiometric differences. We propose that DNMT3A simultaneously accommodates H3 tails and p53 or TDG to form complexes that are similar to the DNMT3A-DNMT3L-H3 tail co-crystal structure (Figure 1 A.) and in which the primary role of p53 or TDG is to modulate DNMT3A activity.

The spatial relationship between nucleosomes and nucleosome-interacting proteins (intra- or inter-nucleosomal, Figure 3 A.) provides a greater understanding of the interactions *associated* with readers, writers and erasers within chromatin. Compared to the interactions of histone-modifying enzymes and tails within a single nucleosome, the interactions of histone-modifying enzymes and histone tails on adjacent nucleosomes have proven more challenging to study due to the difficulty in generating suitable substrates that distinguish the two types of interactions. However, some studies have successfully characterized these two types of interactions in histone-modifying enzymes (17), (18). Structural analysis of DNMT3A and nucleosomes suggests steric hindrance from the comparable sizes (length, diameter and height) of the DNMT3A homotetramer and nucleosomes may pose a challenge for DNMT3A to act on intra-nucleosomal DNA (Figure S3). We sought to explore the spatial relationship between DNMT3A and nucleosome substrates (intra- or inter-nucleosomal, Figure 3 A.) in more detail prior to assessing the ability of p53 or TDG to modulate the enzymatic activity of DNMT3A on nucleosomes. We

initially assessed the extent to which the N-terminus of DNMT3A contributes to DNMT3A-monomucleosome interactions by comparing the enzymatic activity of full length DNMT3A (residues 1-912) on nucleosomes to that of the catalytic domain of DNMT3A (residues 634-912) and the prokaryotic DNA methyltransferase M. SssI. We show the N-terminal domains of DNMT3A (ADD and PWWP) enhance the enzymatic activity of DNMT3A on nucleosomes, likely by retaining DNMT3A on nucleosome substrates (Figure S1) (10), (12), (22). The H3K4me0 peptide allosterically activates the enzymatic activity of DNMT3A on a variety of oligonucleotide substrates (Figure 2) (10), (19). We therefore examined whether extrinsic H3K4me0 peptide (non-nucleosomal) stimulates the activity of DNMT3A on mononucleosomal DNA, or if binding of DNMT3A to intrinsic (nucleosomal) H3 tails perturbs the activation of DNMT3A by H3K4me0 peptide (Figure 3 B.). We show binding of histone tails within nucleosomes and the short H3 peptide to DNMT3A are mutually exclusive and nucleosome bound DNMT3A is not accessible to H3 peptides (Figure 3 B. and C.). To further distinguish between intra- or inter-nucleosomal interactions (Figure 3 A.), we then assessed the interactions of DNMT3A bound to nucleosomes with extrinsic DNA (non-nucleosomal). We show DNMT3A-nucleosome complexes can bind (Figure 3 F.) and act on distinct extrinsic DNA substrates (Figure 3 D. and E.) as the changes in DNMT3A activity observed by the addition of pCpG^L or Poly dI-dC (Figure 3 D. and E.) may only be achieved by DNMT3A employing an inter-nucleosomal mechanism (Figure 3 A., I.). Taken together, nucleosome bound DNMT3A is not limited to methylating intra-nucleosomal DNA and can act on inter-nucleosomal substrates (Figure 3 A., I.). These results suggest that cues provided by particular histone modifications may result in DNMT3A-mediated methylation of nucleosomal DNA in a particular region, encompassing DNA not directly associated with the nucleosome to which the enzyme is bound.

Functional characterization of DNMT3A-H3 tail-regulatory protein complexes indicates that regulatory proteins play a dominant role over histone H3 peptide in the regulation of DNMT3A activity (Figure 2). To better approximate the simultaneous modulation of DNMT3A activity within cells, we then assessed the relative role (dominant or passive) of histone H3 tails *and* regulatory proteins using human-derived mono- or polynucleosome substrates. Like histone-modifying enzymes, which are differentially regulated on nucleosomes compared to peptide substrates and whose enzymatic activity is influenced by nucleosome number (mono- or polynucleosome), we found that a higher concentration of polynucleosomes compared to mononucleosomes is required for DNMT3A to reach comparable maximal velocities on either substrate (Figure S2). This may result from the greater challenge for DNMT3A to access DNA in polynucleosome due to the structural complexity of this substrate. We show that equimolar concentrations of p53 or TDG relative to DNMT3A (150 nM tetramer) sufficiently modulate the enzymatic activity of DNMT3A in equilibrium (Figure 4 A.) or transient (Figure 4 B. and C.) reactions with mononucleosome substrates. In contrast, we found that the activity of DNMT3A on polynucleosomes is modulated by equimolar concentrations of p53 or TDG (1:1 relative to 150 nM tetramer DNMT3A) only in equilibrium reactions (Figure 4 A.) and that transient reactions require the addition of excess p53 (500 nM tetramer) or TDG (500 nM dimer) (Figure 4 D. and E.). P53 and TDG complexes with DNMT3A are more stable than DNMT3A-nucleosome complexes (Figure S2) (13), (14). Therefore, the results of reactions with polynucleosomes in which equimolar concentration of p53 or TDG to DNMT3A modulate the enzymatic activity of DNMT3A could be attributed to the thermodynamic regulation of the interactions between DNMT3A, regulatory proteins and mononucleosomes (Figure 4 A., B. and C.) or polynucleosomes (Figure 4 A.). *Interactions between the N-*

terminal domains of DNMT3A (ADD and PWWP) and histone H3 tails not only promote the retention of DNMT3A to polynucleosomes (Figure S1), but present additional interactions that may pose a challenge for allosteric regulators of DNMT3A to access DNMT3A under catalytic conditions. We show that an excess concentration of p53 or TDG to DNMT3A is necessary to overcome this challenge and modulate the enzymatic activity of DNMT3A (Figure 4 D. and E.), which is likely an appropriate representation of what occurs within cells as the expression of p53 or TDG is highly dynamic (30), (31). We propose that the histone code represents a network of specific modifications which creates a focal point for recruitment of DNMT3A (Figure 1 B.). Thus, DNMT3A-H3 tail interactions in DNMT3A-H3 tail-p53 or -TDG complexes increase the local concentration of DNMT3A at specific regions while the primary role of p53 or TDG is to modulate DNMT3A activity (Figure 1 B., II. And III.).

Genome-wide epigenetic profiling has provided unprecedented information about the links between specific histone marks and DNA methylation (4-9). However, these associations do not consider the role of regulatory proteins and their dynamics with epigenetic enzymes in transcriptional regulation, though many aspects of epigenetic transcriptional regulation stem from the direct modulation of epigenetic enzymes by protein partners (13-16). Most histone modifications do not work in isolation but rather form a histone code, with the combination of all modifications influencing the recognition and activity of readers, writers or erasers (32). When the role of proteins that modulate readers, writers or erasers is considered in addition to cues presented by the histone code, the complexity of the dynamics associated with epigenetic transcriptional regulation becomes clear. To date, biochemical work aiming to explore the interactions between DNMT3A, regulatory proteins and histone tails have solely focused on DNMT3L (10-12). We provide

insights into two important cancer-related proteins that directly (DNA methylation) and indirectly (histone modifications) affect key epigenetic mechanisms of how the simultaneous binding of regulatory proteins and H3 tails at distinct surfaces may affect enzymatic activity, thereby providing insights into the interactions that contribute to mammalian DNA methylation (13-16). The expression of DNMT3L is limited to germ cells and early developmental stages, whereas the expression of p53 and TDG, like DNMT3A, is not only highly dynamic, but p53, TDG and DNMT3A are active in a wide range of cellular contexts (15), (16), (30), (31), (33-37). Furthermore, disruptions to the cellular activity of DNMT3A, p53 or TDG have been implicated in human cancers such as AML and we have shown in previous work that clinically identified mutations in p53 disrupt the interactions of DNMT3A with additional partner proteins (3), (38-40). *Future* studies will be required to explore whether mutations in allosteric regulators of DNMT3A, like p53 and TDG, disrupt the interactions of DNMT3A with histone *H3 tails and lead to* differential functional outcomes. Thus, the findings in this study expand our understanding of the interactions associated with the modulation of readers and writers of epigenetic marks by regulatory proteins with broad biological implications.

Methods

Expression constructs

The following plasmids were used for expression of recombinant human proteins: pET28a-hDNMT3ACopt for DNMT3A full length (41), pET28a-hDNMT3A_catalytic_domain for DNMT3A catalytic domain (Δ 1–611) pET28a-hDNMT3A_catalytic_domain (Δ 1–611) (26), pET15b-human p53 (1-393) for p53 (42) and pET28a-hTDG for TDG (43).

Protein Expression

DNMT3A full length and catalytic domain, p53 and TDG were expressed in NiCo21(DE3) Competent *E. coli* cells (New England Biolabs). Cells were grown in LB media at 37 °C to an $A_{600\text{ nm}}$ of 0.9 (DNMT3A full length), 0.7 (DNMT3A catalytic domain), 0.6 (p53) and 0.8 (TDG). Protein expression was induced by the addition of 1 mM isopropyl- β -D-thiogalactopyranoside (GoldBio) after lowering the temperature to 28 °C. Induction times were 5 hours for DNMT3A full length and catalytic domain and 16 hours for p53. Cell pellets were harvested by centrifugation at 5,000g for 15 minutes and stored at -80 °C.

Protein Purification

Cell pellets from 1 L of bacterial culture were resuspended in 30 mL lysis buffer (50 mM HEPES pH 7.8, 500 mM NaCl, 50 mM imidazole, 10% glycerol and 1 mM PMSF) and lysed by sonication. Following sonication, lysates were centrifuged at 11,000g for 1 hour and the supernatant was retained for affinity chromatography. Recombinant proteins were purified using ÄKTA Fast Protein Liquid Chromatography (FPLC) system (GE healthcare) containing a 5 mL HisTrap HP nickel-charged IMAC column (GE healthcare). Columns were equilibrated with 50 mL of loading buffer (50 mM HEPES pH 7.8, 500 mM NaCl, 50 mM imidazole, 10% glycerol). After flowing the supernatant through the column, resins were washed using 47.5 mL of wash buffer (50 mM HEPES pH 7.8, 500 mM NaCl, 75 mM imidazole, 10% glycerol). 0.5 mL fractions were eluted with increasing amounts of imidazole (50 mM HEPES pH 7.8, 500 mM NaCl, 75-500 mM imidazole, 10% glycerol) over 15 mL. The fractions containing the proteins of interest was desalted and concentrated into storage buffer (50 mM Tris-Cl, 200 mM NaCl, 1 mM EDTA, 20% (v/v) glycerol, pH 7.8, with 0.5 mM DTT) using a 0.5 mL Centrifugal Filter (Millipore 10K device) supplied by Millipore and were stored at -80°C for later use. Protein concentrations were determined

using 280 nm extinction coefficients ($142,010 \text{ M}^{-1} \text{ cm}^{-1}$ for full length DNMT3A, $38,180 \text{ M}^{-1} \text{ cm}^{-1}$ for the catalytic domain of DNMT3A, $36,035 \text{ M}^{-1} \text{ cm}^{-1}$ for p53 and $33,725 \text{ M}^{-1} \text{ cm}^{-1}$ for TDG) and reflect the oligomeric state in all experimental conditions (nM of tetramers for full length DNMT3A, the catalytic domain of DNMT3A and p53; nM of dimers for TDG). A summary gel of the purified recombinant proteins used in this study is in Figure S4.

Methylation Assays

Radiochemical assays were carried out to measure the ability of DNMT3A to incorporate tritiated methyl groups transferred from cofactor AdoMet onto distinct DNA substrates and under varying experimental conditions. In this study DNMT3A refers to the full-length protein (912 amino acids), unless noted otherwise. Reactions were carried out at $37 \text{ }^{\circ}\text{C}$ in a buffer consisting of $50 \text{ mM KH}_2\text{PO}_4/\text{K}_2\text{HPO}_4$, 1 mM EDTA , 1 mM DTT , 0.2 mg/mL BSA , 20 mM NaCl with saturating AdoMet ($15 \text{ } \mu\text{M}$) at pH 7.8. For the Radiochemical assays, $50 \text{ } \mu\text{M}$ (^3H) methyl-labeled: unlabeled, 1:10) AdoMet stocks were made using 32 mM unlabeled AdoMet (NEB) and ^3H methyl-labeled AdoMet (80 Ci/mmol) supplied by PerkinElmer in $10 \text{ mM H}_2\text{S O}_4$. $15 \text{ } \mu\text{L}$ aliquots were taken from a larger reaction, quenched by mixing with 0.1% SDS (1:1) and spotted onto Hybond-XL membranes (GE healthcare). Samples were then washed, dried and counted using a Beckman LS 6000 liquid scintillation Counter as previously established (44).

Methylation Assays with H3K4me0 or H3K4me3 peptides in combination with p53 and TDG

Synthetic peptides (N-ARTKQTARKSTGGKAPRKQLA-C) derived from human Histone H3.1 were supplied by Active Motif (45). In equilibrium reactions containing H3K4me0 or H3K4me3 peptides, $4 \text{ } \mu\text{M}$ of either peptide was pre-incubated with DNMT3A and individual regulatory proteins (p53 tetramers or TDG dimers, 1:1 at 150 nM) in reaction

buffer with AdoMet for 1 hour at 37 °C before initiating the reaction by the addition of saturating substrate DNA (5 μM poly dI-dC). In transient reactions, DNMT3A was pre-incubated with individual peptides (4 μM of H3K4me0 or H3K4me3) in reaction buffer with AdoMet for 1 hour at 37 °C, reactions were initiated by the addition of DNA (5 μM poly dI-dC) and allowed to carry out catalysis for 30 minutes prior to the addition of p53 or TDG.

Methylation Assays with human mono- or polynucleosomal DNA

Unmodified recombinant human mononucleosomes consisting of two molecules of each of the four core histones (H2A, H2B, H3.1 and H4) bound by the Widom 601 positioning sequence (147 base pairs and 13 CpG sites) were supplied by Active Motif (46). Human polynucleosomes were generated from HeLa cell nuclear extracts subjected to *micrococcal nuclease digestion*. Purified HeLa polynucleosomes consisting of predominantly trimers of the histone octamer (two each of the four core histones, H2A, H2B, H3 and H4) wrapped by 147 base pairs of human genomic DNA were supplied by EpiCypher (47). The concentrations of mono- or polynucleosomes were determined by the absorbance at 280 nm, using the molecular weight of histone octamer (108 kDa). Equilibrium reactions consisting of reaction buffer with AdoMet, mononucleosomes or polynucleosomes (1 μM) and individual regulatory proteins (p53 or TDG, 1:1 at 150 nM) were initiated by the addition of DNMT3A. In transient reactions, p53 or TDG (1:1 at 150 nM) were added to actively catalyzing DNMT3A on mononucleosomes or polynucleosomes (1 μM) after 1 hour. To assess the accessibility of exogenous peptides to DNMT3A acting on mononucleosomes, additional equilibrium and transient experiments were performed. Equilibrium reactions consisting of reaction buffer with AdoMet, mononucleosomes (1 μM) and increasing levels of H3K4me0 were initiated by the addition of DNMT3A (150 nM). In transient reactions, increasing levels of H3K4me0 were added to actively catalyzing DNMT3A on

mononucleosomes (1 μM) after 1 hour. The accessibility of exogenous DNA was also assessed by the addition of excess Poly dI-dC or pCpG^L (20X) to actively catalyzing DNMT3A (150 nM) on mononucleosomes (1 μM). The concentrations of Poly dI-dC or pCpG^L are given in base pairs and were determined by the absorbance at 260 nm using the following molar absorptive coefficients: 6.9 $\text{mM}^{-1} \text{cm}^{-1}$ for Poly dI-dC and 6.6 $\text{mM}^{-1} \text{cm}^{-1}$ for pCpG^L.

Fluorescence Anisotropy

Fluorescence anisotropy measurements were obtained using a Horiba Fluoromax fluorescence spectrophotometer equipped with excitation and emission polarizers (excitation: 485 nm, emission 520 nm). The DNA substrate (Gcbox30) consisted of a fluorescein (6-FAM) label on the 5' end of the top strand of the duplex (5'/6-FAM/TGGATATCTAGGGGCGCTATGATATCT-3') was supplied by Integrated DNA Technologies. The recognition site for DNMT3A is underlined. In DNA binding experiments of homo- or heterotetrameric complexes, unlabeled H3K4me0 peptide was titrated to pre-formed DNMT3A or DNMT3A-regulatory protein (p53 and TDG) complexes (1 μM). Anisotropy values were obtained following the addition of unlabeled H3K4me0. To assess the ability of nucleosome-bound DNMT3A to bind non-nucleosomal DNA, increasing concentrations of pre-formed DNMT3A-monomucleosome complexes (or DNMT3A only) were added to 15 nM Gcbox30. For peptide binding experiments, H3K4me0 peptides were labelled with FAM-NHS on the N-terminus. Unlabeled mononucleosomes were then added to FAM-labelled H3K4me0 (2 μM) bound by DNMT3A (150 nM). Anisotropy values were obtained following a 5-minute incubation at room temperature for all experiments.

Supplementary Material

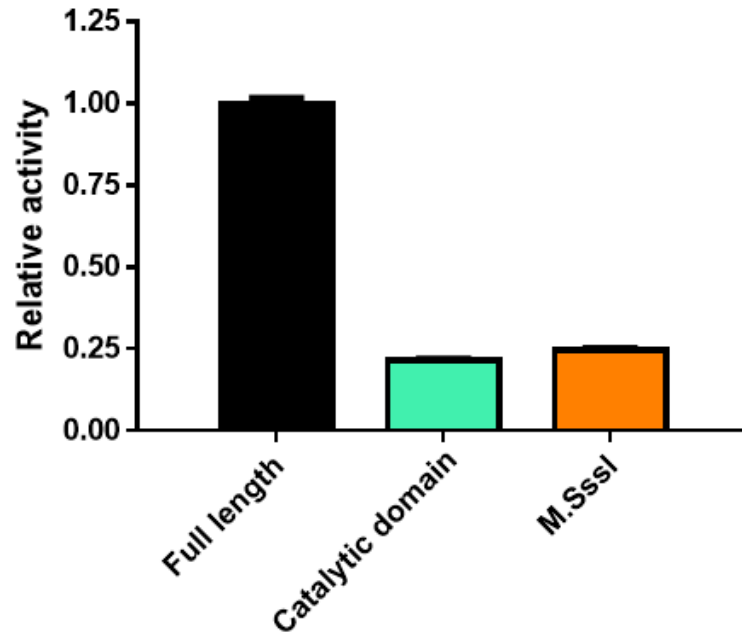


Figure S1. Interactions between the N-terminus of DNMT3A and nucleosomes increase catalytic activity on nucleosomal DNA.

Compared to full length DNMT3A (150 nM) (■), the catalytic domain of DNMT3A (150 nM) (■) and the bacterial CpG DNA methyltransferase *M. SssI* (0.2 units/ μ L) (■) are less catalytically active on mononucleosomal DNA (1 μ M) as a substrate. Data were normalized to the DNA methylation activity observed in full length DNMT3A and reflect the results of 2 independent experiments.

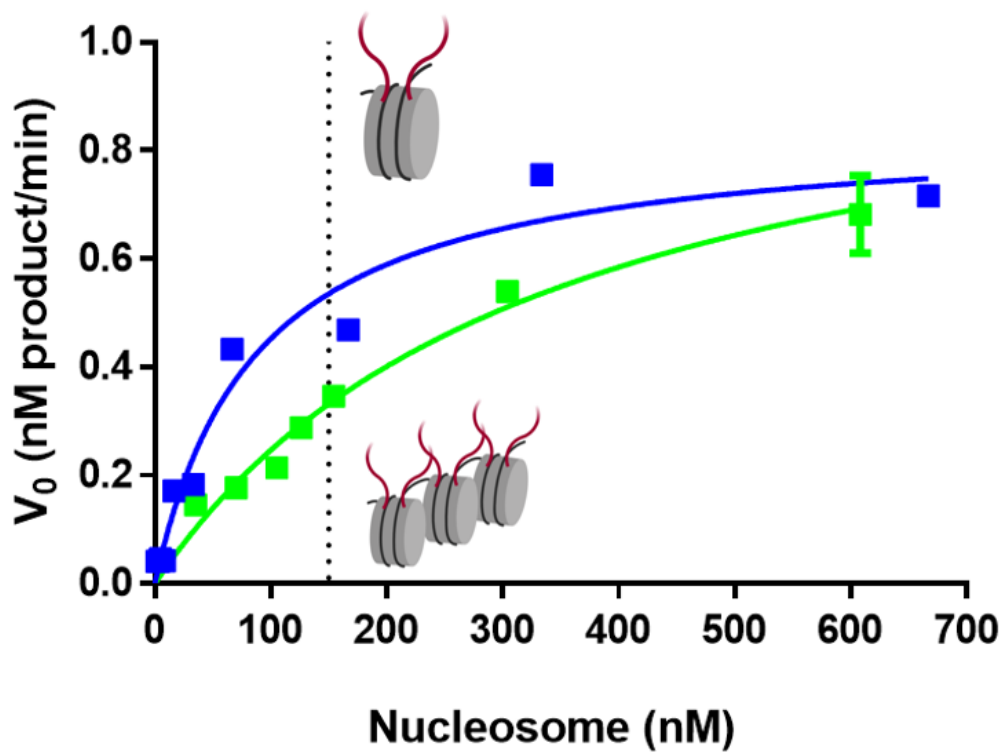


Figure S2. Binding curve of DNMT3A with mono- or poly-nucleosomal DNA as a substrate. Titration of (■) mono- or (■) poly-nucleosomes to DNMT3A (150 nM tetramer). Dashed line indicates equal concentration of mono- or poly-nucleosomes (150 nM) relative to DNMT3A. Data are representative of reactions carried out for 60 minutes and reflect the results of 2 independent experiments.

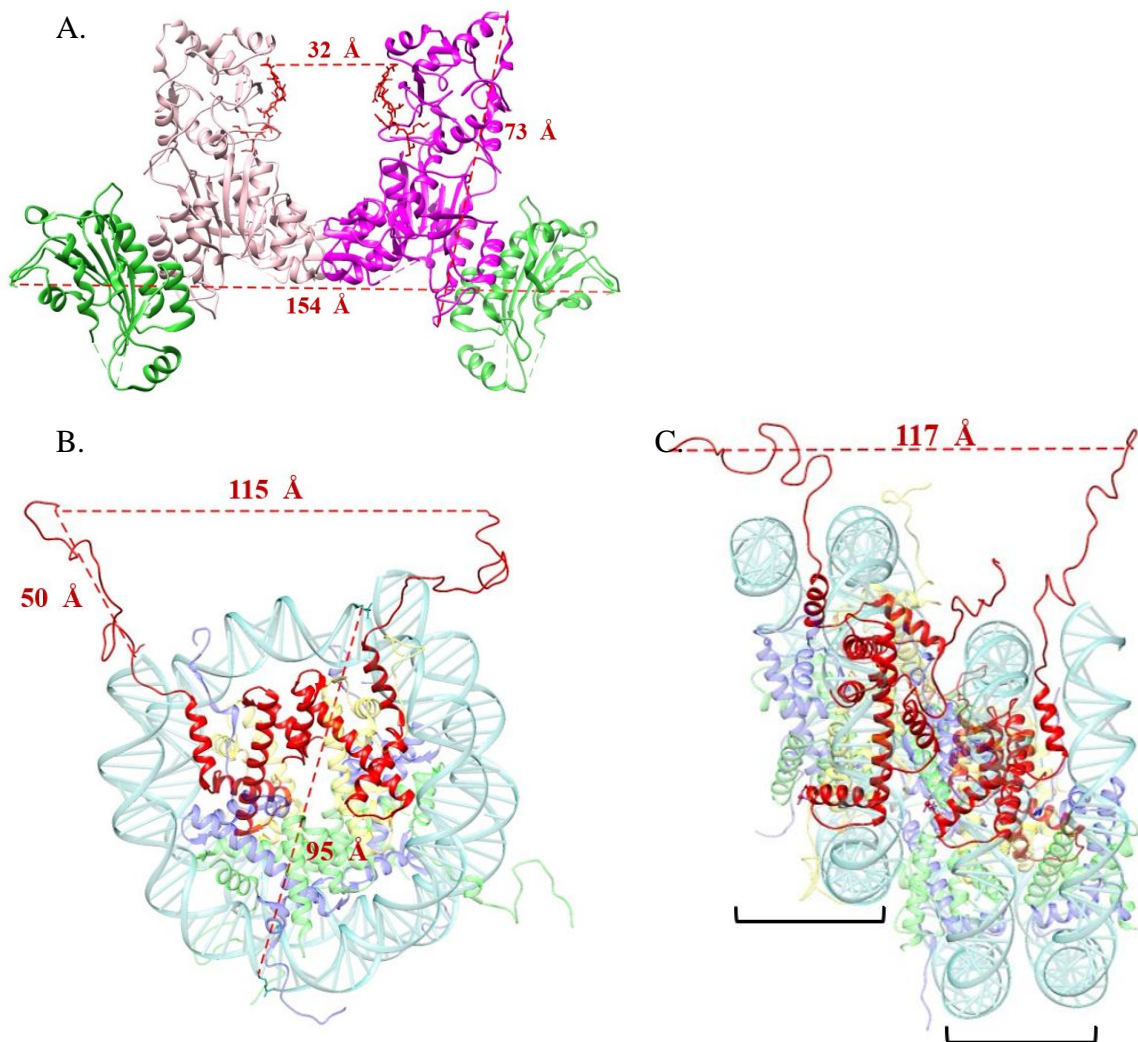


Figure S3. Distances in DNMT3A-Nucleosome interactions. **A.** Distances on a DNMT3A-DNMT3L heterotetramer in complex with Histone H3 N-terminal peptide (adapted from PDB 4U7T) (10). Distance between **B.** intra and **C.** inter -nucleosomal H3 N-terminal tails as well as nucleosome diameter and height of H3 N-terminal tail **B.**. To generate a model of a di-nucleosome containing H3 N-terminal tails **B.**, H3 (chain A) from PDB 1KX5 (49) was superimposed to H3 (chains A, E, K, O; $\Delta 1-40$) from PDB 5GSE (RMSD < 0.4 Å) (50). Modelling and distances were generated in UCSF Chimera.

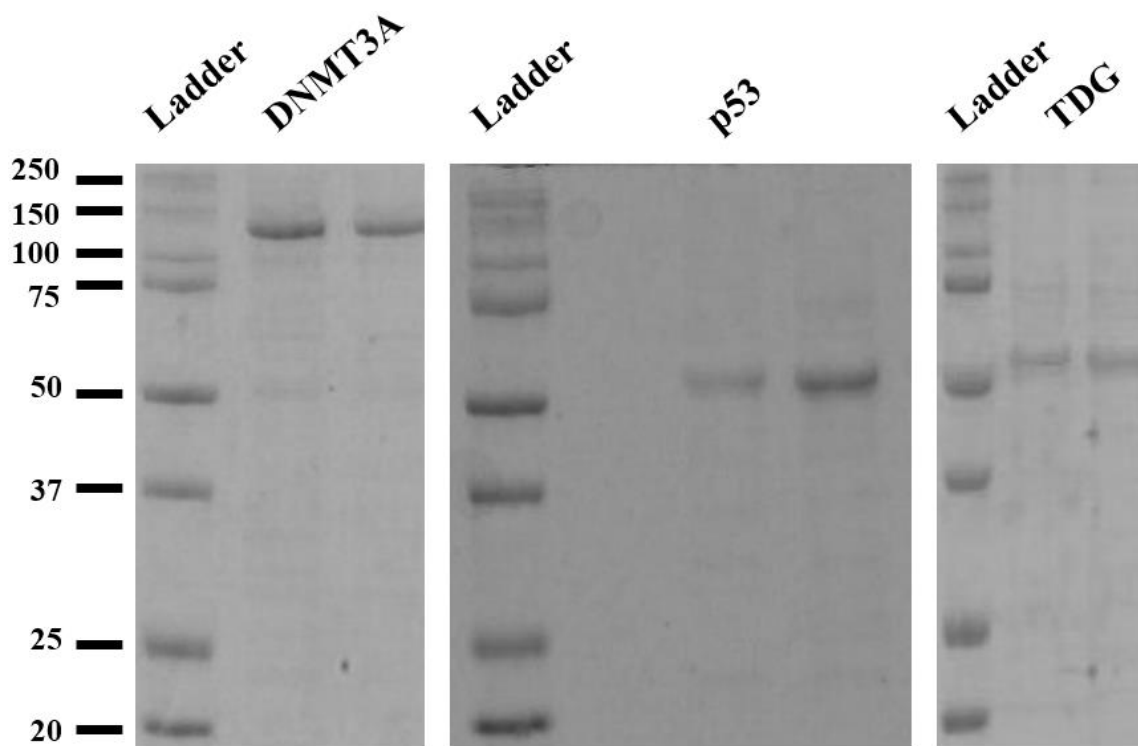


Figure S4. 10% SDS-PAGE gel of the purified proteins. Bio-rad Precision Plus Protein Dual Color was used as a size standard. The estimated molecular weight of purified proteins are as follows: 130 kDa for full length DNMT3A, 53 kDa for p53 and 55 kDa for TDG. Two lanes were loaded from pooled fractions of each purified protein.

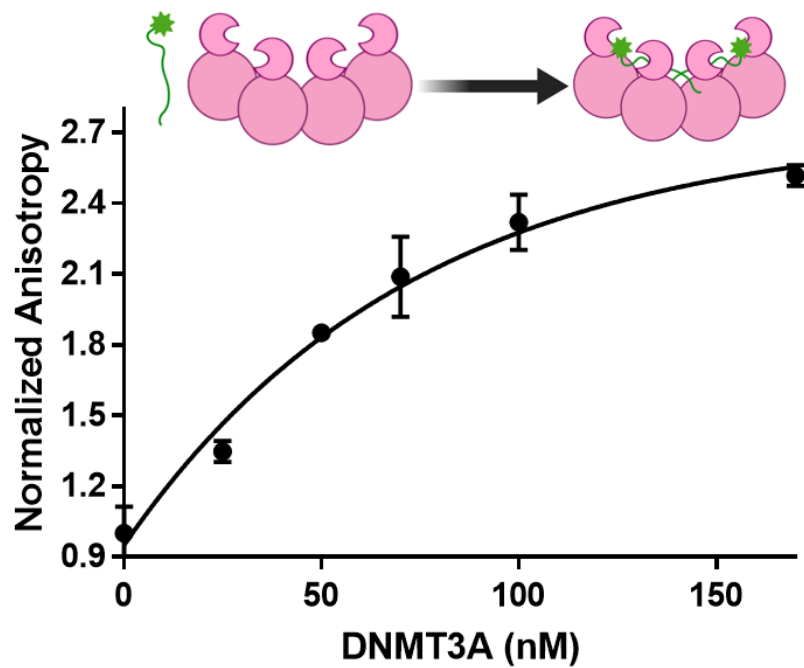


Figure S5. Binding curve DNMT3A to FAM-labeled H3K4me0 peptides. Increasing concentrations of full-length DNMT3A (0-170 nM) leads to a concomitant increase in the fluorescence anisotropy of FAM-labelled H3K4me0 (2 μ M) (residues 1-21). Data are normalized to fluorescence anisotropy values in the absence of DNMT3A.

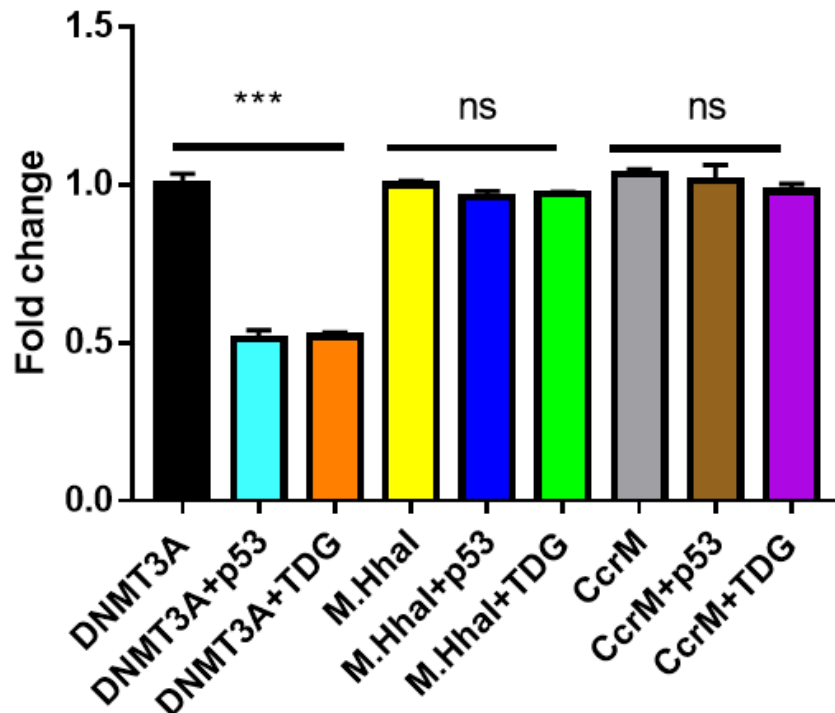


Figure S6. p53 and TDG specifically inhibit the DNA methylation activity of DNMT3A. The activity of bacterial CpG methyltransferase *M.HhaI* and adenine methyltransferase *CcrM* was assessed in the presence of *p53* or *TDG* to assess the specificity of the modulation of *DNMT3A* activity by *p53* and *TDG*. In all reactions, DNA methyltransferase (*DNMT3A*, *M.HhaI* and *CcrM*) were at 150 nM while *p53* and *TDG* were at 500 nM. For co-incubations with *p53* or *TDG*, proteins were placed at 37 °C for 1 hour prior to the addition of substrate DNA (Poly dI-dC at 5 μM for *M.HhaI* and *DNMT3A*; dsDNA 29 mer 5' TCACTGTACTCTGACTCGCCTGACATGAC 3' for *CcrM*). Data were normalized to the DNA methylation activity observed in the absence of *p53* or *TDG* and are representative of reactions carried out for 1 hour. Data reflect the mean ± S.D. of 3 experiments; one-way analysis of variance was used to compare the values of reactions with *p53* or *TDG* to those with DNA methyltransferases only; ***, $p < 0.001$; ns, $p > 0.05$. Data were normalized to the DNA methylation activity observed in the absence of *p53* or *TDG* and are representative of reactions carried out for 1 hour. Data reflect the mean ± S.D. of 3 experiments; one-way analysis of variance was used to compare the values of reactions with *p53* or *TDG* to those with DNA methyltransferases only; ***, $p < 0.001$; ns, $p > 0.05$.

Chapter V: Mechanism of non-coding RNA regulation of DNMT3A and its relation to histones, regulatory proteins, and clinically relevant mutations

Abstract

De novo DNA methylation by DNMT3A is a fundamental epigenetic modification for transcriptional regulation during cellular development and differentiation. Histone tails and regulatory proteins regulate DNMT3A, and the crosstalk between these epigenetic mechanisms ensures appropriate DNA methylation patterning. Based on findings showing that Fos Proto-Oncogene (*Fos*) extra-coding RNA (ecRNA) inhibits DNMT3A activity in neurons, we sought to characterize *Fos* ecRNA-DNMT3A interactions and provide insights into the relationship of histone tails, regulatory proteins and RNAs in the simultaneous regulation of DNMT3A. We show that *Fos* ecRNA and mRNA strongly correlate in primary cortical neurons on a single cell level and provide evidence that *Fos* ecRNA modulation of DNMT3A at these actively transcribed sites occurs in a sequence-independent manner. Our results are consistent with a model for RNA regulation of DNMT3A that relies on localized production of short RNAs binding to a nonspecific site on the protein, rather than models invoking formation of localized RNA/DNA structures. Through computational modeling and mutational mapping, we show that DNMT3A-*Fos-1* ecRNA occur at the DNMT3A tetramer interface. While substitutions to clinically relevant residues on the DNMT3A tetramer interface disrupt ecRNA-mediated regulation, formation of heterotetramers with DNMT3L restores inhibition of activity. Using DNMT3L and *Fos* ecRNA in the presence of synthetic histone H3 tails or reconstituted polynucleosomes, we show regulatory RNAs play dominant roles in the modulation of DNMT3A activity. Our

results expand on the modulation of DNMT3A and present a mechanism by which non-coding RNAs regulate DNMTs to contribute to neuronal function and memory formation.

Introduction

The establishment of mammalian *de novo* DNA methylation patterns by the DNA methyltransferase 3A (DNMT3A) involves the modulation of DNMT3A activity by a wide range of biological molecules, including histone tails, regulatory proteins, and RNA (1-8). Although there is a growing interest in understanding these regulatory mechanisms, few studies have identified specific interactions by which the crosstalk between *de novo* DNA methylation, histone modifications, regulatory proteins, and RNA translates into meaningful biological outcomes (9-11). For instance, the loss of H3K4me₂, H4 acetylation, and gain of H3K27me₃ on one X chromosome attenuate the biallelic expression of *Tsix* RNA (antisense) and activate *Xist* expression (sense) at the onset of X chromosome inactivation (12). The presence of H3K4me₂, H4 acetylation and continual *Tsix* RNA expression on the other X chromosome sequester DNMT3A and activate DNMT3A activity to silence *Xist* expression (12). In addition to playing a critical role in mammalian development, DNMT3A activity is linked to many aspects of neuronal function as well as memory formation and maintenance (13-16). Furthermore, there is growing evidence that this role of DNMT3A in neurons, along with other epigenetic mechanisms, is influenced by regulatory RNAs in the central nervous system (17). Savell et al. showed that extra-coding RNAs (ecRNAs), defined as non-polyadenylated RNAs originating from the sense strand of regions outside gene boundaries (transcription start and end sites), are critical modulators of DNMT3A activity in neurons (1). More specifically, this occurs with FOS proto-oncogene ecRNA (*Fos* ecRNA), whose protein counterpart serves as a marker for neuronal activation (1), (18). Furthermore, *Fos* ecRNA synthesis is increased by neuronal activation, leads to

hypomethylation of the *Fos* gene through the direct inhibition of DNMT3A, and contributes to long-term fear memory formation in adult rats (1). However, the underlying mechanism and extent of the modulation of DNMT3A activity by RNA generally, and *Fos* ecRNA in the presence of additional epigenetic mechanisms, like histone tails and regulatory proteins, remains unexplored.

Previous studies have demonstrated that distinct classes of regulatory RNAs, such as non-coding RNAs and microRNAs, play essential roles in the modulation of DNA methylation by directly associating with DNA methyltransferases (DNMTs) (2), (19), (20). Furthermore, mechanistic studies of this modulation show that antisense CCAAT/enhancer-binding protein α (asCEBPA) RNA is a mixed inhibitor of DNMT1 and antisense *E-cadherin* (*CHD*) RNA is a non-competitive or mixed inhibitor of DNMT3A (2), (19). While these studies on short regulatory RNAs (< 25 nucleotides) provide compelling evidence that RNA and DNA substrates bind to the same form of the enzyme, in addition to enzyme-DNA complexes, these findings are inconsistent with RNA binding to the active site of the enzyme and leave the surface on DNMT3A that binds regulatory RNAs uncharacterized. Furthermore, while the precise mechanism of RNA-induced inhibition of DNMTs in cells remains unknown, current models for the direct inhibition of DNMTs by RNAs in cells predict RNAs target DNMTs to specific genomic regions in a sequence specific manner (1) (21). For example, the restricted expression observed in specific types of regulatory RNAs with short half-lives and expressed from enhancer regions suggests that regulatory RNAs may limit the modulation of DNMTs to local genomic microenvironments (21). An alternative possibility, which stems from the prevalence of R-loops in DNA regulatory elements, is that regulatory RNAs form triplex structures by annealing to duplex DNA, provide a binding site for DNMTs and anchor DNMTs to specific loci (20), (22), (23). The

characterization of protein-RNA interactions has proven challenging due to the inherent flexibility of RNAs and the diversity of local RNA-binding surfaces on proteins (24). However, structural analysis of the surfaces of proteins that bind both DNA and RNA reveal nucleic acid-specific differences in features like surface topology, solvent accessibility, and distribution of secondary structures (25). For example, while the core domain of p53 (residues 98-292) binds DNA in a sequence-specific manner, regulatory RNAs bind the C-terminal tetramerization domain (residues 300-393) with no known sequence specificity (26). Intriguingly, the tetramerization domain of p53 enables the formation of p53 homotetramers and p53-DNMT3A heterotetramers (3), (27), thus suggesting that surfaces associated with protein-protein interactions may also be involved in protein-RNA interactions, which excludes the need for DNA-RNA sequence complementarity in RNA-mediated modulation of proteins that bind both DNA and RNA.

Given the emerging role of regulatory RNAs in diseases like Acute Myeloid Leukemia (AML) and Uterine corpus endometrial *carcinoma* (*UCEC*) (28), (29), two diseases that also display aberrant DNA methylation (30), (31), there is a growing interest in understanding the crosstalk among distinct epigenetic mechanisms. Previous work from our lab has shown that some proteins that regulate DNMT3A play a dominant role over histone N-terminal tails (32). We sought to expand on these findings by providing insights into how RNA modulates DNMT3A, and the dynamics and functional consequences of the simultaneous modulation of DNMT3A activity by histone tails, regulatory proteins, and RNA. For the latter, we relied on DNMT3L as an example of a partner protein whose physical interaction and functional perturbations of DNMT3A are well known (6), (33). With the use of mutational mapping and biochemical assays consisting of DNMT3A, *Fos-1/-2* ecRNA, *CHD* RNA, DNMT3L and reconstituted polynucleosomes under various

conditions, we show that *Fos-1* and *CHD* RNAs bind to the tetramer interface of DNMT3A and that these regulatory RNAs play a dominant role in modulating the enzymatic activity of DNMT3A in DNMT3A-Histone tail-DNMT3L- *Fos-1* or *CHD* RNA complexes. We also show *Fos* ecRNA accumulates at actively transcribed genomic regions of primary neurons and provide evidence that the modulation of DNMT3A activity by RNA transcripts does not rely entirely on sequence specificity, and contrary to the current models, inhibition of DNMTs by RNAs may involve transcripts that are nonspecific to the target gene (1), (20). Lastly, we found that DNMT3L restores *Fos-1* ecRNA inhibition of substitutions in DNMT3A to residues that are correlated with AML and UCEC (R729, R736 and R771) and are differentially responsive to *Fos-1* ecRNA.

Results

Single molecule fluorescent *in situ* hybridization (smFISH) reveals correlation between *Fos* ecRNA and mRNA on a single cell level

Previous studies show that the direct binding of *Fos-1* ecRNA to DNMT3A inhibits DNA methylation activity, results in hypomethylation of the *Fos* gene, and is required for the formation of long-term fear memories in rats (1). To further understand how *Fos* ecRNA modulates *de novo* DNA methylation, we sought to gain insights into the distribution of ecRNAs and their response to stimulation by performing single molecule fluorescent *in situ* hybridization (smFISH), a technique that allows visualization of individual ecRNA and mRNA transcripts on a single cell level. Using this tool, we investigated whether the number of RNA transcripts of interest changed in response to neuronal activation. Additionally, we investigated whether ecRNA and mRNA expression are correlated across individual neurons. Primary cortical neurons were depolarized with potassium chloride (KCl, 25mM) for 1 hr prior to fixation, permeabilization, and

hybridization with fluorescently labeled smFISH probes. We designed custom probe sets to selectively target and mark individual *Fos* mRNA transcripts, as well as *Fos* ecRNA (Fig. 1 A.-B.). To determine whether ecRNA and mRNA levels are correlated at the single-cell level, we multiplexed probe sets targeting *Fos* mRNA and *Fos* ecRNA. These experiments revealed a significant correlation of *Fos* ecRNA and *Fos* mRNA transcript numbers on a single cell level (Fig. 1 C.), with higher mRNA levels found in cells with more ecRNA foci.

As shown in Fig. 1 D.-F., the number of *Fos* ecRNA transcripts increased in response to KCl-mediated neuronal depolarization. It is possible that this effect is stronger than represented in our analysis due to overlapping signal in neurons with high transcript abundance (which would potentially cause overlapping or nearby spots to be counted together). Interestingly, we detected only a few, but very discrete puncta per cell with the ecRNA probe set. Larger high-intensity foci are typically associated with active transcription sites as they indicate an accumulation of transcripts. We observed this phenomenon frequently in the quantification of *Fos* mRNA signal, where active transcription is expected in response to depolarization. However, for ecRNAs, we found such high-intensity puncta to occur much more frequently in both treatment groups, suggesting an accumulation of transcripts at these sites. Notably, we also observed that KCl treatment only increased *Fos* mRNA counts in cells where *Fos* ecRNA was present, and neurons with ecRNA signal exhibited more *Fos* mRNA puncta in both vehicle and KCl-stimulated neurons. Taken together, these findings indicate that ecRNAs contribute to transcriptional regulation of their target genes not only on a cell population level but also on a single cell level.

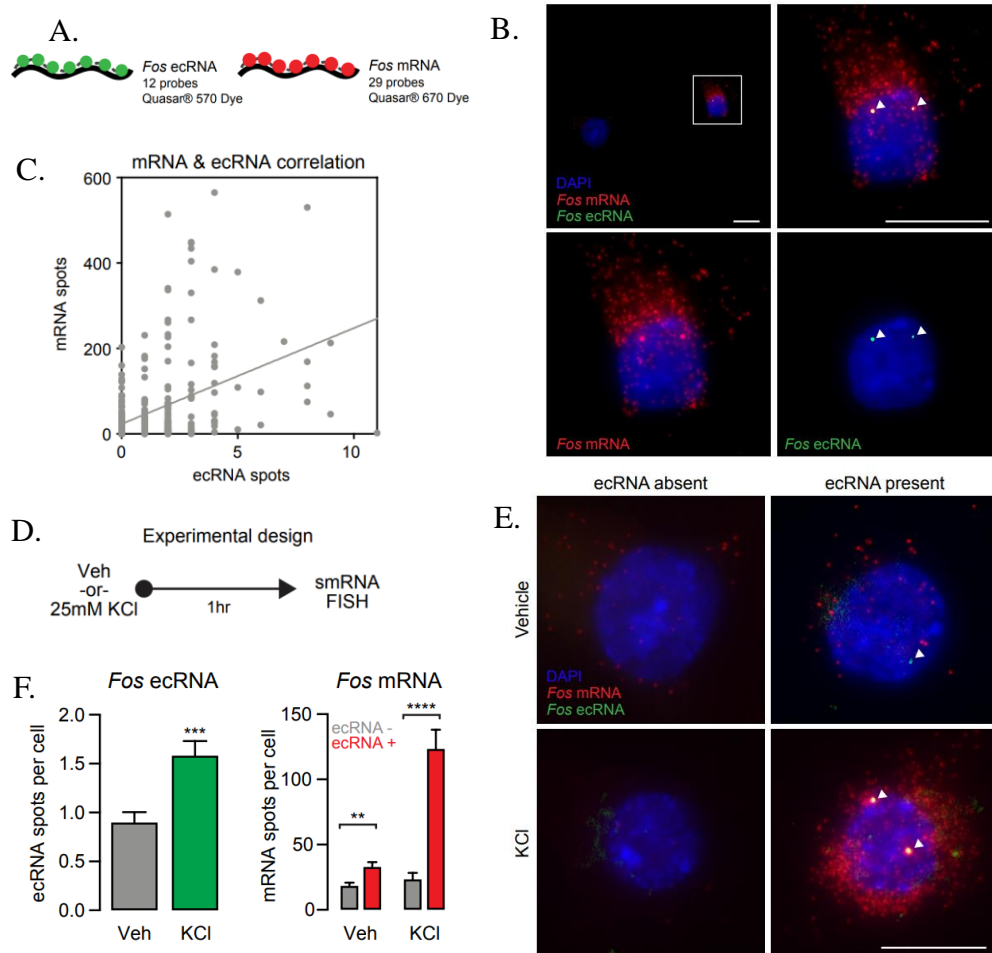


Figure 1. Cellular localization of *Fos* ecRNA and mRNA. **A.** Illustration of smFISH probe sets indicating number of probes, dye, and LUT. **B.** Representative smFISH images for *Fos* ecRNA (Quasar® 570) and *Fos* mRNA (Quasar® 670) transcripts. Cell nuclei are stained with DAPI (blue), RNA transcripts are marked by smFISH probes (red, green). Scale bar = 5 μ m. **C.** Comparison and correlation of detected *Fos* mRNA, and *Fos* ecRNA spots per cell reveal a significant positive correlation on a single cell level (Pearson correlation, $R^2=0.1869$, $p<0.0001$). **D.** Experimental design for neuronal depolarization experiments. **E.** Representative images of *Fos* ecRNA (Quasar® 570) and *Fos* mRNA (Quasar® 670) transcripts with or without neuronal depolarization. Cell nuclei are stained with DAPI (blue), RNA transcripts are marked by smFISH probes (red, green). Scale bar = 5 μ m. **F.** Summary data of ecRNA (left panel) and mRNA (right panel) after 1 hr of Veh or 25mM KCl treatment demonstrate ecRNA levels increase in response to stimulation (unpaired t-test with Welch's correction $n(\text{Veh}) = 158$, $n(\text{KCl}) = 178$, $t = 3.725$, $p = 0.0002$). Cells that express ecRNA express more *Fos* mRNA transcripts at baseline and in response to KCl (Multiple t-tests with fewer assumptions and Holm-Sidak correction $n(\text{Veh}) = 179$, $t = 3.35662$, $p = 0.000966$, $n(\text{KCl}) = 161$, $t = 5.58467$, $p < 0.000001$). Data expressed as mean \pm s.e.m. Multiple comparisons, * $p<0.05$, ** $p<0.01$, *** $p<0.001$, **** $p<0.0001$.

DNMT3A_CD tetramer interface mutants are differentially responsive to inhibition of enzymatic activity by *Fos-1* and *CHD* RNAs and inhibition does not require a DNA-*Fos* ecRNA complex

Work from our lab has provided insights into the mechanisms of RNA-mediated inhibition of DNMT3A using a wide-range of biologically significant RNA sequences (2). However, the surface on DNMT3A that binds regulatory RNAs and how regulatory RNAs restrict DNMT3A function to a specific locus remain uncharacterized. To probe whether inhibition of DNMT3A by *Fos* ecRNA requires the formation of an ecRNA-DNA complex, we monitored the fluorescence anisotropy of a 5' 6-FAM-labeled *Fos-1* ecRNA (5'-GGGGACACGCCCUCUGUUCCCUUAU-3') as well as a 5' 6-FAM-labeled 18-mer RNA designed to form a complex with the human *Fos* gene (NCBI Gene ID 2353, 3'- 500 nucleotide duplex) (SI appendix, Fig. S1 A.) (Fig. 2 A.). We employed this segment of the *Fos* gene due to its proximity to the sites of *Fos* ecRNA synthesis (1). Increasing concentrations of *Fos* DNA (10 or 30 nM) increases the fluorescence anisotropy of the 5' 6-FAM-labeled 18-mer RNA (Fig. 2 A. ■) but not of 5' 6-FAM-labeled *Fos-1* ecRNA (Fig. 2 A. ■), indicating that *Fos-1* ecRNA does not form a complex with this portion of the *Fos* gene. We previously used computational modeling and mutational mapping to implicate the tetramer interface of DNMT3A as a potential surface on DNMT3A for interactions with p53 (3), and in a similar manner, we employed a hybrid docking algorithm of template-based modeling and free docking to predict a surface on DNMT3A for interactions with *Fos-1* ecRNA (34). We initially sought to confirm that the previously reported inhibition by *Fos-1* ecRNA is specific to DNMT3A, and consistent with previous findings, we found that reactions initiated by a mixture of *Fos-1* ecRNA (5'-GGGGACACGCCCUCUGUUCCCUUAU-3') and Poly dI-dC as a DNA substrate (Fig. 2

B. ■) displayed roughly a 50% decrease in DNMT3A_CD activity compared to reactions consisting of Poly dI-dC only (Fig. 2 B. ■) (1). Additionally, this decrease in DNA methylation by *Fos-1* ecRNA was observed in reactions consisting of DNMT3A_CD (SI appendix, Fig. S1 B. ■) and DNMT1 (SI appendix, Fig. S1 B. ■) but not M. HhaI (SI appendix, Fig. S1 B. ■), a bacterial CpG methyltransferase. No inhibition to DNMT3A activity was observed in similar reactions involving a mixture of *Fos-1* ecRNA and Poly dI-dC that was treated with RNase prior to assaying for methylation activity (Fig. 2 B. ■) or a mixture of Poly dI-dC and a non-specific RNA (5'-CGACCGCCUACUGAAAGAGGGC-3') previously employed as a material for nanoparticle construction (Fig. 2 B. ■) (35). Furthermore, we observed that *Fos-2* ecRNA (5'-GUCUGUGCACCGUGUGCAUAUACAG-3') (SI appendix, Fig. S1 C. ■) is a more potent inhibitor of DNMT3A_CD activity compared to *Fos-1* ecRNA (SI appendix, Fig. S1 C. ■) and leads to nearly the same degree of inhibition as the previously characterized *CHD* RNA (5'-GGGGUGACGGGGACAGGCGGGGCUG-3') (SI appendix, Fig. S2 B. ■). Given previous work by Savell et al. showing that modulation of DNMT3A activity by *Fos-1* ecRNA is essential for neuronal DNA methylation dynamics and work from our lab characterizing DNMT3A-CHD RNA interactions, we focused on these RNA molecules for further biochemical characterization (1), (2).

We previously used alanine scanning to identify residues on the DNMT3A tetramer interface that largely contribute to the formation of higher order complexes and docking-based modeling of protein-protein interfaces to predict a surface on DNMT3A for interactions with p53 (3), (36). In a similar manner, previous studies have relied on a hybrid docking algorithm of template-based modeling and free docking (HDOCK server) to predict protein surfaces for protein-RNA interactions (34), (37-39). Using the monomeric form of

DNMT3A (PDB: 5YX2; residues 628-914) and the *Fos-I* ecRNA sequence, we relied on this approach to predict a surface on DNMT3A for interactions with *Fos-I* ecRNA (34), (40). Computational models generated in the HDOCK server were used to predict the DNMT3A tetramer interface as a likely surface for DNMT3A-*Fos-I* ecRNA interactions (SI appendix, Fig. S2). Based on these predictions, we assessed *Fos-I* ecRNA or *CHD* RNA inhibition of DNMT3A activity in a subset of alanine substitutions to residues at the DNMT3A tetramer interface (R729A, E733A, R736A, R771A) that are frequently mutated in AML or UCEC patients (TCGA) (41). We observed that the extent of *Fos-I* ecRNA inhibition varied across the mutations examined relative to DNMT3A_CD^{WT} (Fig. 2 B. ■) with DNMT3A_CD^{R736A} (Fig. 2 B. ■), DNMT3A_CD^{R729A} (Fig. 2 B. ■) and DNMT3A_CD^{E733A} (Fig. 2 B. ■) displaying a greater inhibition than wild type, while DNMT3A_CD^{R771A} (Fig. 2 B. ■) displayed no inhibition. Interestingly, we observed that a subset of the DNMT3A_CD tetramer interface mutants were differentially responsive to *CHD* RNA (Fig. 2 C.) or *Fos-I* ecRNA (Fig. 2 C.) and compared to DNMT3A_CD^{WT}. In reactions with *Fos-I* ecRNA (Fig. 2 B.) or *CHD* RNA (Fig. 2 C.), DNMT3A_CD^{R771A} was not inhibited (Fig. 2 B. ■) and DNMT3A_CD^{R736A} displayed increased inhibition compared to wild type (Fig. 2 B. ■). In contrast, in the presence of *CHD* RNA only (Fig. 2 C.), DNMT3A_CD^{E733A} was minimally responsive (Fig. 2 C. ■) and DNMT3A_CD^{R729A} displayed comparable levels of inhibition as wild type (Fig. 2 C. ■). We then sought to assess whether the lack of *Fos-I* ecRNA inhibition of DNMT3A_CD^{R771A} is due to the inability of DNMT3A_CD^{R771A} to bind *Fos-I* ecRNA (Fig. 2 D.) by monitoring the fluorescence anisotropy of DNMT3A complexes on DNA, an approach previously employed to monitor interactions at the DNMT3A tetramer interface (3). The addition of *Fos-I* ecRNA resulted in a corresponding increase to the initial anisotropy of DNA-bound

DNMT3A_CD^{WT} (Fig. 2 D. ■), DNMT3A_CD^{R736A} (Fig. 2 B. ■), DNMT3A_CD^{R729A} (Fig. 2 B. ■) but not of DNMT3A_CD^{R771A} (Fig. 2 D. ■). Thus, the addition of *Fos-I* ecRNA to DNA-bound DNMT3A_CD^{R771A} does not lead to the formation of higher order complexes on DNA (Fig. 2 D. ■). The tetramer interface of DNMT3A is well characterized as is the regulation of DNMT3A activity by a wide range of regulatory proteins with distinct functional outcomes (3-5). Our results suggest that modulation of DNMT3A activity by RNA also occurs through direct interactions with the tetramer interface of DNMT3A and does not rely on the formation of a DNA-*Fos* ecRNA complex (Fig. 6 A.).

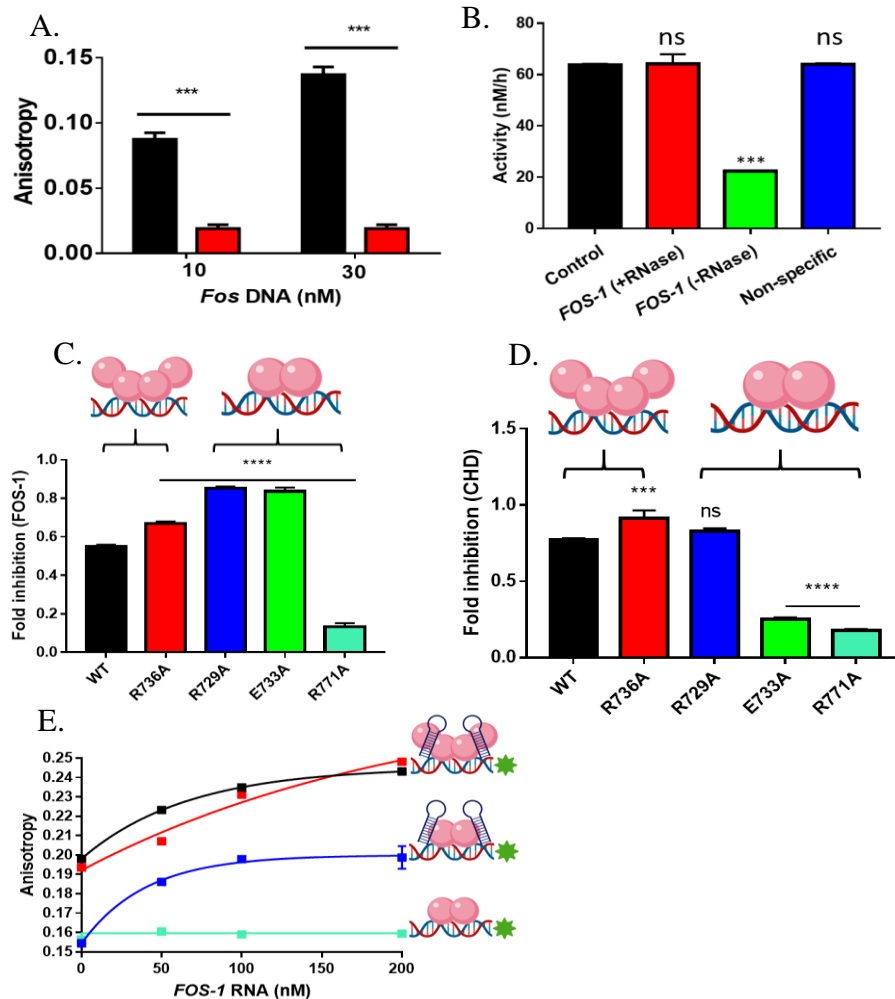


Figure 2. Mutations at the DNMT3A_CD tetramer interface disrupt RNA-mediated inhibition. **A.** The addition of *Fos* DNA (NCBI Gene ID 2353, 3'-500 nucleotide duplex DNA) increases the fluorescence anisotropy of a 5' FAM-6-labeled 18-mer positive control RNA (■) but not that of 5' 6-FAM-labeled *Fos-I* ecRNA (■). **B.** Reactions consisting of (■) no RNA, (■) RNase treatment of *Fos-I* ecRNA prior to the start of the reaction, (■) *Fos-I* RNA and (■) a non-specific RNA show that *Fos-I* ecRNA specifically inhibits DNMT3A_CD^{WT} activity. DNMT3A_CD tetramer interface mutants are differentially responsive to modulation of enzymatic activity by **C.** CHD and **D.** *Fos-I* RNAs. **E.** The addition of *Fos-I* ecRNA increases the fluorescence anisotropy of DNA-bound (10 nM of 5' FAM-6-labeled GCbox30 duplex) (■) WT, (■) R736A and (■) R729A but not (■) R771A DNMT3A_CD enzymes (1 μM). Reactions in **A.** consisted of 500 nM of each FAM-labelled RNA. Except for **B.** (50 nM enzyme), all other DNA methylation reactions consisted of 150 nM DNMT3A and were initiated by the addition of Poly dI-dC (5 μM) only or a pre-mixture of RNA (1 μM) and Poly dI-dC (5 μM). Data reflect the mean and standard deviation of 3 experiments. A one-way analysis of variance was used to compare values to a control **B.** or of each mutant to wild type (**C.** and **D.**) (****, $p < 0.001$; ***, $p < 0.001$; ns, $p > 0.05$).

The oligomeric state of DNMT3A_CD affects the mechanism of allosteric inhibition by *Fos-1* ecRNA

Studies aiming to probe the mechanism of DNMT1 inhibition by asCEBPA suggest that this short non-coding RNA (23 nucleotides) is a mixed inhibitor of DNMT1; thus, inhibition may occur through the direct binding of asCEBPA to DNMT1 or to the DNMT1–hemimethylated DNA complex (19). Similarly, mechanism of inhibition studies involving DNMT3A and *CHD* RNA support non-competitive or mixed type models (2). We previously showed that the oligomeric state of DNMT3A tetramer interface mutants affects processive catalysis and modulation by distinct partner proteins (3), (4), (42). Given that DNMT3A_CD tetramer interface mutants are differentially responsive to *Fos-1* ecRNA inhibition relative to DNMT3A_CD^{WT} (Fig. 2 B.), we sought to assess whether the altered oligomeric state of DNMT3A_CD tetramer interface mutants influences the mechanism of inhibition by *Fos-1* ecRNA. In addition, we sought to examine whether *Fos-1* ecRNA-mediated inhibition of DNMT3A_CD derives from direct *Fos-1* ecRNA competition with substrate DNA binding to DNMT3A_CD. For this approach, we carried out methylation assays with varying DNA concentrations and saturating RNA (SI appendix, Fig. S1 C.) using a dimeric DNMT3A_CD tetramer interface mutant (R729A) that is responsive to *Fos-1* ecRNA inhibition (Fig. 2 B.). While the addition of *Fos-1* ecRNA to DNMT3A_CD^{WT} led to a reduced V_{MAX} but did not affect K_M (Fig. 3 A. and B.), the addition of *Fos-1* ecRNA led to reduced K_M and V_{MAX} in reactions consisting of DNMT3A_CD^{R729A} (Fig. 3 C. and D.). Thus, the inhibition data for DNMT3A_CD^{WT} (Fig. 3 A. and B.) best fits a noncompetitive model while the results for DNMT3A_CD^{R729A} (Fig. 3 C. and D.) are more consistent with an uncompetitive model. While our results show the oligomeric state of DNMT3A affects inhibition by *Fos-1* ecRNA, our data exclude any mechanism that invokes

competition with substrate DNA and supports an allosteric mechanism of inhibition (Figure 3).

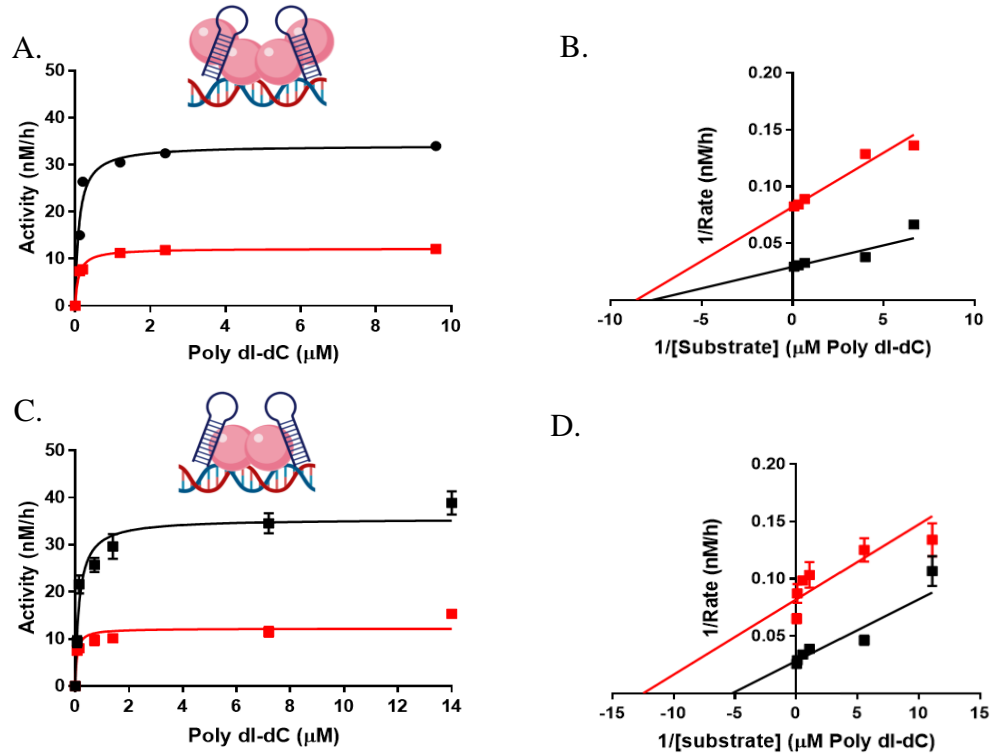


Figure 3. The oligomeric state of DNMT3A_CD affects modulation of enzymatic activity by *Fos-1* RNA. Velocity curves of **A.** DNMT3A_CD^{WT} homotetramers or **C.** DNMT3A_CD^{R729A} homodimers in the presence of excess *Fos-1* ecRNA (1 μM) with increasing concentration of Poly dI-dC as a DNA substrate. **B.** and **D.** double reciprocal plots for **A.** and **C.**, respectively. In **A.** and **C.**, reactions consisting of 30 nM enzymes were initiated by the addition of a pre-mixture of *Fos-1* ecRNA (1 μM) and Poly dI-dC (5 μM). Data reflect the mean and standard deviation of 3 experiments.

DNMT3L restores inhibition of DNMT3A_CD^{R771A} by *Fos-1* ecRNA

DNMT3L, the inactive homolog of DNMT3A, serves as a stimulatory factor of *de novo* methylation by DNMT3A and is essential for the establishment of appropriate methylation patterns of maternally imprinted genes (33). Furthermore, tetramerization of DNMT3A dimer mutants with DNMT3L restores processive catalysis (36), (42). Based on this evidence, we sought to examine whether formation of DNMT3A_CD^{R771A}-DNMT3L heterotetramers restores inhibition of enzymatic activity by *Fos-1* ecRNA as DNMT3L provides a well-studied model system for how partner proteins regulate the activity of DNMT3A mutants with altered oligomeric states (Fig. 2 C. and E.). Initial reactions show *Fos-1* ecRNA decreases the DNA methylation activity of DNMT3A_CD^{WT}-DNMT3L heterotetramers (SI appendix, Fig. S3 ■) compared to similar reactions that did not include *Fos-1* ecRNA (SI appendix, Fig. S3 ■). Surprisingly, although DNMT3A_CD^{R771A} homodimers are unresponsive to the modulatory effect of *Fos-1* ecRNA (Fig. 4 A. ■ and ■), we found that *Fos-1* ecRNA inhibits the activity of DNMT3A_CD^{R771A}-DNMT3L heterotetramers (Fig. 4 A. ■ and ■). We then assessed whether the observed inhibition (Fig. 4 A. ■ and ■) is due to DNMT3A_CD^{R771A}-DNMT3L heterotetramers binding *Fos-1* ecRNA by monitoring the fluorescence anisotropy of DNA-bound (GCbox30) DNMT3A_CD^{R771A} homodimers or DNMT3A_CD^{R771A}-DNMT3L heterotetramers with increasing levels of *Fos-1* ecRNA (Fig. 4 B.). While the addition of *Fos-1* ecRNA consistently did not result in a detectable change to the initial anisotropy value of DNMT3A_CD^{R771A} homodimers (Fig. 2 E. ■ and Fig. 4 B. ■), the titration of *Fos-1* ecRNA led to a corresponding increase to the initial anisotropy value of DNA-bound of DNMT3A_CD^{R771A}-DNMT3L heterotetramers (Fig. 4 B. ■). To better model the cellular dynamics between DNMT3A mutants, regulatory proteins and RNAs, we examined whether

Fos-I ecRNA inhibition of DNMT3A_CD^{R771A}-DNMT3L heterotetramers in equilibrium reactions (Fig. 4 A.) persists in actively catalyzing protein complexes (Fig. 4 C. and D.). We show that the addition of *Fos-I* ecRNA (Fig. 4 C. ■) disrupts the activity of DNMT3A_CD^{R771A}-DNMT3L on DNA (Fig. 4 C. ■). We also found that when challenged by the addition of DNMT3L, reactions consisting of DNMT3A_CD^{R771A} initiated by the addition of a pre-mixture of *Fos-I* ecRNA and Poly dI-dC (Fig. 4 D. ■) are less catalytically active than similar reactions lacking *Fos-I* ecRNA (Fig. 4 D. ■). In sum, our findings indicate that the formation of DNMT3A_CD^{R771A} heterotetramers with DNMT3L restores the ability of *Fos-I* ecRNA to inhibit the methylation activity of DNMT3A_CD^{R771A}.

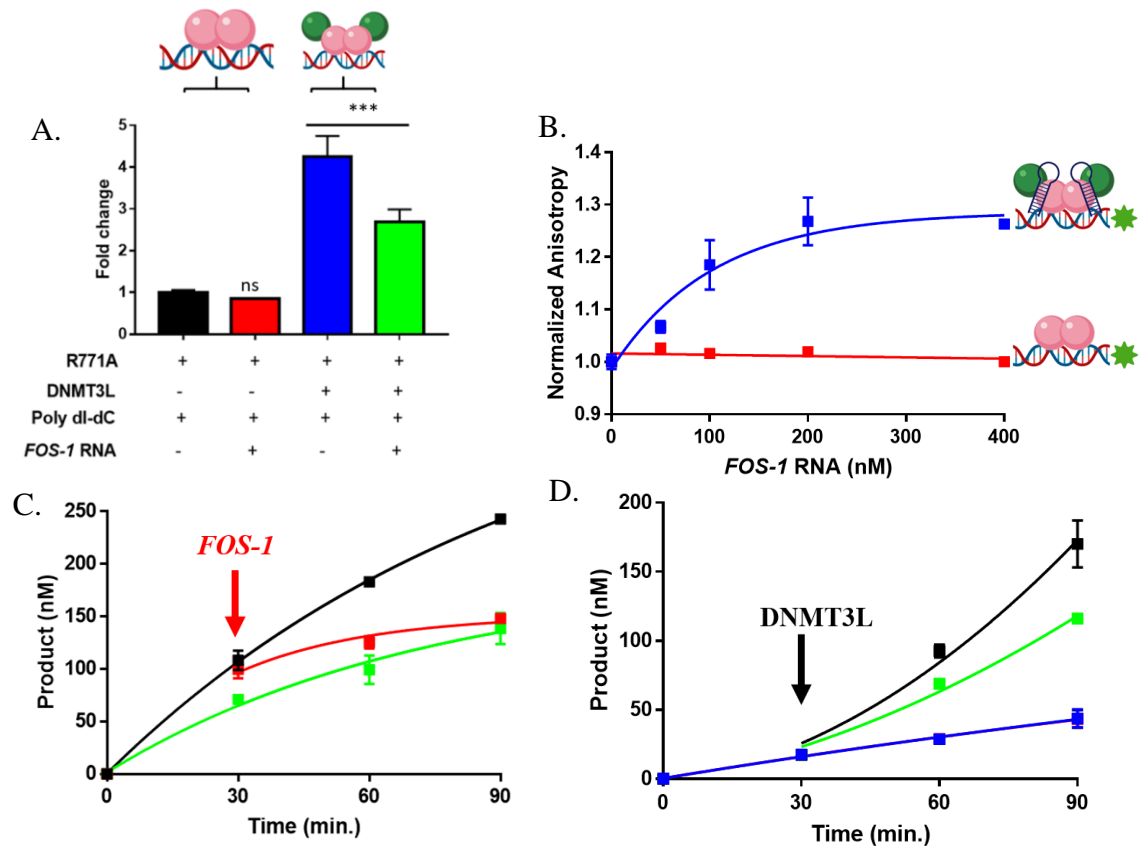


Figure 4. Formation of DNMT3A_CD^{R771A} heterotetramers with DNMT3L restores inhibition of enzymatic activity by *Fos-1* ecRNA. **A.** Although *Fos-1* ecRNA does not inhibit DNMT3A_CD^{R771A} homodimers (■), the addition of *Fos-1* ecRNA leads to the dominant inhibition of DNMT3A_CD^{R771A}-DNMT3L heterotetramers (■). All reactions in **A.** consisted of proteins at 150 nM (1:1 to DNMT3A tetramer) and were initiated by the addition of Poly dI-dC (5 μM) or a pre-mixture of *Fos-1* ecRNA (1 μM) with Poly dI-dC (5 μM). **B.** The addition of *Fos-1* ecRNA leads to an increase in the fluorescence anisotropy of DNA-bound (10 nM of 5' FAM-6-labeled GCbox30 duplex) DNMT3A_CD^{R771A}-DNMT3L heterotetramers (■) but not DNMT3A_CD^{R771A} homodimers (■). **C.** *Fos-1* ecRNA disrupts actively catalyzing DNMT3A_CD^{R771A}-DNMT3L heterotetramers (■). **D.** Reactions with DNMT3A_CD^{R771A} initiated by the addition of a pre-mixture of *Fos-1* ecRNA and Poly dI-dC challenged with the addition of DNMT3L (■) display reduced activity relative to similar reactions but in the absence of *Fos-1* ecRNA (■). The following reactions were performed as controls: DNMT3A_CD^{R771A}-DNMT3L with Poly dI-dC only (**C.** ■), DNMT3A_CD^{R771A}-DNMT3L with *Fos-1* ecRNA and Poly dI-dC at the start of the reaction (**C.** ■), or DNMT3A_CD^{R771A} with Poly dI-dC only (**D.** ■). Data reflect the mean and standard deviation of 3 experiments. In **A.**, a one-way analysis of variance was used to compare values to DNMT3A_CD^{R771A} (■) (***, $p < 0.001$; ns, $p > 0.05$).

Modulation of DNMT3A_FL^{WT} activity by *Fos-I* ecRNA is dominant in the presence of histone H3 tails and DNMT3L

In addition to modulating cellular activity of DNMT3A (1), (2), distinct classes of non-coding RNAs contribute to epigenetic gene regulation by directly and indirectly modulating the enzymatic activities of histone modifying enzymes (43-45) (46). Based on this evidence, there is growing interest in understanding the role regulatory non-coding RNAs play in epigenetic control (11), (47). However, much less is known about the crosstalk between non-coding RNAs, regulatory proteins and histone tails in the modulation of epigenetic enzymes. In the context of this crosstalk, we have shown that some regulatory proteins play a dominant role over histone N-terminal tails in the simultaneous modulation of DNMT3A (32). Given that DNMT3A activity is modulated through the direct interactions with non-coding RNAs, histone N-Terminal tails, and a wide range of regulatory proteins, we sought to expand on our findings by assessing the modulation of DNMT3A activity by *Fos-I* ecRNA in the presence of histone tails and DNMT3L (1-8). We relied on the use of DNMT3L as it provides a suitable model to study the simultaneous modulation of DNMT3A due to its well-characterized interactions with DNMT3A and predicted shared binding surface with *Fos-I* ecRNA (Fig. 2), (SI appendix, Fig. S2) (6), (33), (36), (42). Although our results indicate that *Fos-I* ecRNA and histone N-Terminal tails bind a distinct surface on DNMT3A (Fig. 2 and SI appendix, Fig. S2) (6-8), we initially assessed whether DNMT3A simultaneously accommodates *Fos-I* ecRNA and histone H3 tails by monitoring the fluorescence anisotropy of DNMT3A bound to FAM-labeled H3K4me0 peptide (residues 1-21; SI appendix, Fig. S4). While the addition of non-specific RNA did not lead to detectable changes in anisotropy of DNMT3A_FL^{WT}- FAM-labeled H3K4me0 peptide at maximum anisotropy (SI appendix, Fig. S4; Fig. 5 A. ■), the

addition of *Fos-I* ecRNA led to an increase to the initial anisotropy values of DNMT3A_FL^{WT}- FAM-labeled H3K4me0 peptide (Fig. 5 A. ■). Thus, *Fos-I* ecRNA can access DNMT3A in complex with histone H3 tails. Based on this finding, we then determined the functional consequences of a DNMT3A_FL^{WT}-H3K4me0 peptide- *Fos-I* ecRNA or -*CHD* RNA complex on DNMT3A_FL^{WT} activity (Fig. 5 B.). Initial controls show that while the presence of *Fos-I* ecRNA (Fig. 5 B. ■) or -*CHD* RNA (Fig. 5 B. ■) reduces the activity of a DNMT3A_FL^{WT} on of *p15* (nucleosome free) as a DNA substrate, formation of DNMT3A_FL^{WT}-H3K4me0 peptide complexes activates the enzymatic activity of DNMT3A (Fig. 5 B. ■), as previously reported (48). Interestingly, the activation of DNMT3A_FL^{WT} activity by H3K4me0 peptide (Fig. 5 B. ■) was disrupted in reactions initiated by a pre-mixture of *Fos-I* ecRNA (Fig. 5 B. ■) or -*CHD* RNA (Fig. 5 B. ■) with *p15* (Nucleosome free). Thus, modulation of DNMT3A_FL^{WT} methylation activity by *Fos-I* ecRNA or *CHD* RNA is dominant in DNMT3A_FL^{WT}-*Fos-I* ecRNA -H3 tail or DNMT3A_FL^{WT}-*CHD* RNA-H3 tail complexes. To better approximate the simultaneous modulation of DNMT3A activity within cells, we then assessed the functional outcomes of DNMT3A_FL^{WT}-*Fos-I* ecRNA -H3 tail or DNMT3A_FL^{WT}-*CHD* RNA-H3 tail complexes using *p15* assembled into polynucleosomes consisting of histone core proteins extracted from HeLa cells (Fig. 5 C.). We show that while 1 μM of *Fos-I* or *CHD* RNA sufficiently inhibits the enzymatic activity of DNMT3A_FL^{WT} on *p15* DNA (14 μM; Nucleosome free) (Fig. 5 B.; SI appendix, Fig. S5 A.), inhibition of DNMT3A_FL^{WT} with *p15* assembled into polynucleosomes (14 μM) as a substrate requires an excess concentration of *Fos-I* (Fig. 5 C. ■) or *CHD* RNAs (Fig. 5 C. ■) (SI appendix, Fig. S5 A. and B.). Furthermore, reactions initiated by a pre-mixture of 30 μM *Fos-I* ecRNA (Fig. 5 C. ■) or -*CHD* RNA (Fig. 5 C. ■) with *p15* assembled into polynucleosomes resulted in decreased activity compared to that of

DNMT3A_FL^{WT}-DNMT3L complexes using a similar substrate and protein concentrations (Fig. 5 C. ■). However, the enzymatic activity of DNMT3A_FL^{WT}-DNMT3L heterotetramers in the presence of *Fos-1* ecRNA (Fig. 5 C. ■) or *-CHD* RNA (Fig. 5 C. ■) was higher than that of similar reactions consisting of DNMT3A_FL^{WT} homotetramers and *Fos-1* ecRNA (Fig. 5 C. ■) or *-CHD* RNA (Fig. 5 C. ■) with *p15* assembled into polynucleosomes as a substrate. Using a biologically significant substrate, we show that modulation of DNMT3A methylation activity by regulatory RNAs is dominant in DNMT3A- histone H3 tails-regulatory protein-RNA complexes (Fig. 6 B.).

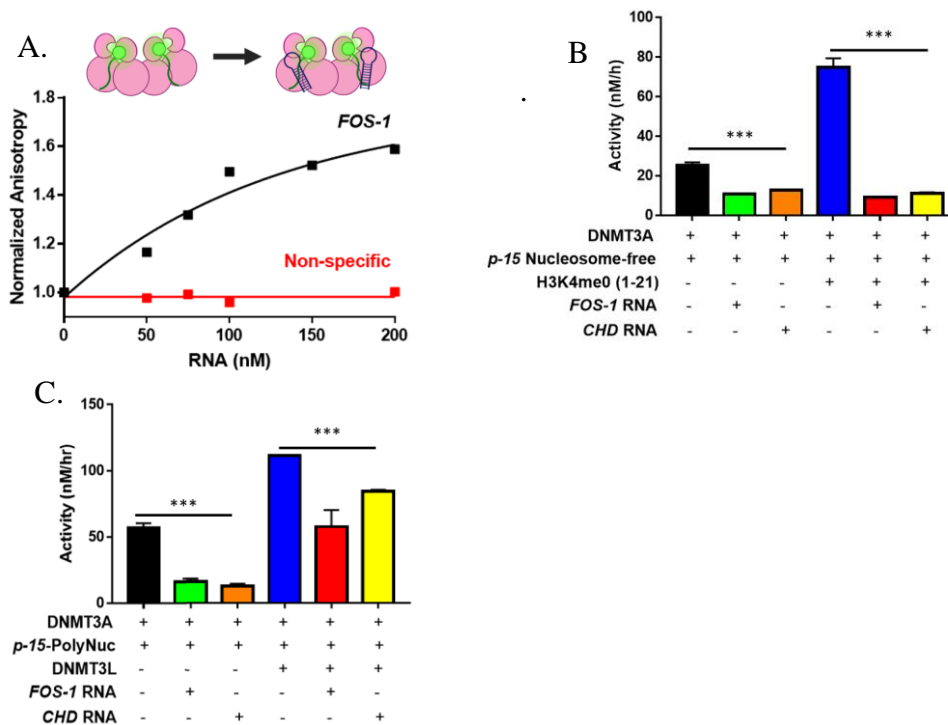


Figure 5. Modulation of DNMT3A enzymatic activity by RNA is dominant in DNMT3A_{FL}^{WT} - DNMT3L- H3 tail- RNA complexes.

A. The fluorescence anisotropy of DNMT3A_{FL}^{WT} (1 μ M) in complex with FAM-labeled H3K4me0 (residues 1-21; 10 nM) increases with the addition of *Fos-1* ecRNA (■) but not of non-specific RNA (■). **B.** *Fos-1* (■) or *CHD* (■) RNAs (1 μ M) in the presence of H3K4me0 peptide (5 μ M) disrupt stimulation of DNMT3A_{FL}^{WT} (50 nM) activity by H3K4me0 peptide (■) with nucleosome-free *p15* as a DNA substrate (14 μ M). Similar reactions consisting of *Fos-1* (■) or *CHD* (■) RNAs but in the absence of H3K4me0 peptide were performed as controls. **C.** Excess *Fos-1* (■) or *CHD* (■) RNAs (30 μ M; see SI appendix, Fig. S5) inhibit DNMT3A_{FL}^{WT} (150 nM) activity using *p15* assembled into polynucleosomes (HeLa core histones) as a DNA substrate (14 μ M). Furthermore, inhibition of DNMT3A_{FL}^{WT} activity by *Fos-1* (■) or *CHD* (■) RNAs is dominant in similar reactions containing DNMT3L 150 nM (1:1 to DNMT3A_{FL}^{WT} tetramer). DNA methylation reactions (**B.** and **C.**) were initiated by the addition of *p15* (Nucleosome free or polynucleosomes) or a pre-mixture of RNA (*Fos-1* or *CHD*) with *p15* (Nucleosome free or polynucleosomes). Data reflect the mean and standard deviation of 3 experiments. In **B.** and **C.**, a one-way analysis of variance was used to compare values the values of reactions with *Fos-1* or *CHD* RNAs to those of DNMT3A only or DNMT3A with H3K4me0 **B.** or DNMT3L **C.** (***, $p < 0.001$; ns, $p > 0.05$).

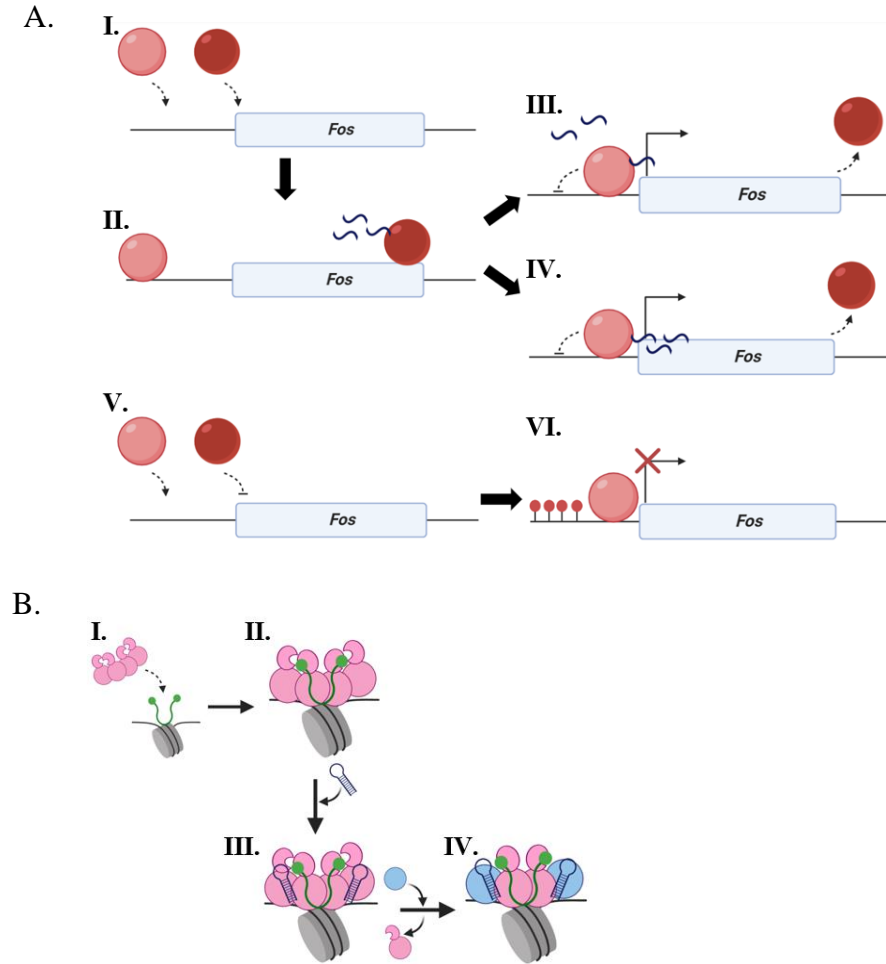


Figure 6. Models for eCRNA modulation of DNMT3A and interactions with additional components of the epigenetic machinery. **A.** The synthesis of eCRNA (■; II.) by RNA polymerase (■) can directly inhibit DNMT3A (■) through the absence (III.) or presence (IV.) of an eCRNA-DNA complex. **B.** Following the localization of DNMT3A (■) by histone tails (■) to specific genomic loci (I. and II.), eCRNA (■) can access and dominantly modulate the activity of DNMT3A homo- (III.) or heterotetramers (IV.).

Discussion

The modulation of DNMT3A activity in the establishment of appropriate genomic DNA methylation patterns calls for the simultaneous association with a wide range of biological molecules, yet few examples exist of the crosstalk between DNMT3A, histone modifications, regulatory proteins and RNAs as studies have largely focused on the individual effects of these modulators of DNMT3A (1-11). While the interactions between DNMT3A and its modulators play a multifaceted role in embryonic development, oncogenesis, and neuronal function (49), (13-16), recent work linking *Fos* ecRNA-mediated inhibition of DNMT3A activity in neurons to fear memory formation further highlight the role of regulatory RNAs in the control of epigenetic mechanisms involved in cognitive function (1), (9), (12), (27), (33). Based on these observations, along with the emerging role of regulatory RNAs as key modulators of the epigenetic machinery in a wide range of biological processes (1), (2), (11), (17), (28), (29), (43-45), (47), we sought to characterize the dynamics and relative role of histone tails, regulatory proteins, and RNA in the simultaneous coordination of DNMT3A activity. To further explore the cellular and structural basis of *Fos-1* ecRNA-DNMT3A interactions, we also assessed the distribution of ecRNA in primary neurons in response to stimuli on a single-cell level and aimed to determine the surface on DNMT3A for interactions with *Fos-1* ecRNA. We show that DNMT3A simultaneously accommodates H3 tails, regulatory proteins, and RNAs, and that regulatory RNAs play a dominant role in the modulation of DNMT3A methylation activity in these multiprotein-RNA complexes. We also show *Fos* ecRNA synthesis correlates with active transcription sites in primary neurons and provide evidence that the modulation of DNMT3A activity by ecRNA is not restricted to these sites through the formation of DNA-ecRNA complexes. Furthermore, we found that *Fos-1* ecRNA binds to the tetramer interface of DNMT3A. Although substitutions to clinically relevant residues at this

interface, such as R771A homodimers, are differentially responsive to *Fos-1* ecRNA, formation of hetero-tetramers between DNMT3A and partner proteins such as DNMT3L restores the inhibition of enzymatic activity by *Fos-1* ecRNA. These findings provide insights into the respective roles and interplay between RNA- and protein-based regulatory mechanisms of DNMT3A and elucidate a molecular basis for how these interactions contribute to the epigenetic control of gene expression.

RNA-binding proteins comprise as much as 13% of the eukaryotic proteome and are involved in a wide-range of biological processes including DNA repair, transcriptional and translational regulation (50-52). Despite the obvious biological importance of RNA-binding proteins, the mechanisms that underpin protein-RNA interactions remain obscure largely due to the challenges associated with the characterization of protein-RNA complexes, such as the conformational flexibility of RNA and structural diversity of RNA-binding surfaces on proteins (24), (53), (54). However, previous work from our lab has provided insights into how distinct classes of regulatory RNAs modulate DNMT3A and suggests these RNAs may bind a surface on DNMT3A outside the active site, although the precise surface on DNMT3A that binds regulatory RNAs and how DNMT3A function is restricted to a specific locus remain uncharacterized (2). Based on previous findings in distinct biological contexts, it has been previously proposed that the gene-specific modulation of DNMT3A by *Fos* ecRNA occurs in a DNA-RNA complex dependent or independent manner (Fig. 6 A., III or IV) (1), (20), (23). We show *Fos* ecRNA synthesis correlates with sites with active *Fos* transcription on a single-cell level (Fig. 1) and provide evidence that interactions between *Fos* ecRNA and DNA do not contribute to the modulation of DNMT3A by *Fos* ecRNA at a specific locus (Fig. 2 A.) (Fig. 6 A., III). In addition to our oligonucleotide binding assay (Fig. 2 A.), the fact that the regulatory RNAs and DNA substrate sequences employed in our

methylation assays are unrelated further suggests that the synthesis of regulatory RNAs in actively transcribed regions is a main contributor to the site-specific modulation of DNMT3A (Fig. 6 A). We then sought to characterize the surface on DNMT3A that binds *Fos-I* ecRNA to better understand the interactions between DNMT3A and *Fos* ecRNA following the synthesis of ecRNA. Using a hybrid docking algorithm to generate computational models of DNMT3A monomers (PDB 4U7T; residues 468-912) and *Fos-I* ecRNA, we identified the tetramer interface on DNMT3A as a potential surface on DNMT3A involved with DNMT3A-*Fos-I* ecRNA interactions (SI appendix, Fig. S2) (6), (34), (37-39). We found that mutations at the tetramer interface disrupt binding and inhibition of DNA methylation activity by *Fos-I* ecRNA, indicating that interactions between *Fos-I* ecRNA and key residues at this interface, such as R771, are essential for the formation of a DNMT3A- *Fos-I* ecRNA complex on DNA and modulation of DNMT3A activity (Fig. 2 C. and E.).

The tetramer interface of DNMT3A is a well-characterized surface on DNMT3A for the direct binding of distinct regulatory proteins to modulate essential biological functions of DNMT3A, such as kinetic parameters and cellular localization (3-5), (32), (36), (55). Our findings highlight the importance and versatility of the tetramer interface of DNMT3A by identifying a novel interacting partner of this surface of DNMT3A, which suggests that *Fos-I* ecRNA does not inhibit DNMT3A through direct competition with substrate DNA. We challenged this notion by probing the mechanism of inhibition by *Fos-I* ecRNA and additionally examined whether changes to the oligomeric state of DNMT3A, stemming from mutations at the tetramer interface, affect inhibition (Fig. 3) (42). We found that while *Fos-I* ecRNA does not compete with substrate DNA in DNMT3A homotetramers (Fig. 3 A. and B.) or homodimers (Fig. 3 C. and D.), the oligomeric state of DNMT3A affects the

mechanism of allosteric inhibition. Previous work from our lab shows that disruption of the oligomeric state of DNMT3A, due to mutations at the tetramer interface, additionally disrupt processive catalysis and that heterotetramerization of DNMT3A dimers with DNMT3L restores processivity (36), (42). Based on this observation and the apparent importance of the DNMT3A tetramer interface for interactions with *Fos-I* ecRNA (Fig. 2 B.-E. and Fig. 3), we assessed whether DNMT3L rescues modulation of DNMT3A_CD^{R771A} by *Fos-I* ecRNA (Fig. 2 C. and E.). Like that observed in the context of processivity (36), (42), we show that heterotetramerization of DNMT3A_CD^{R771A} with DNMT3L restores *Fos-I* ecRNA binding (Fig. 4 B.) and inhibition of DNMT3A_CD^{R771A} under distinct catalytic conditions (Fig. 4 A., C., and D.). We propose a model for a DNMT3A- *Fos-I* ecRNA complex that is consistent with previous findings showing p53 binds regulatory RNAs at a surface associated with protein-protein interactions (3), (26), (27), (56). Although H3 tails and p53 or TDG bind distinct allosteric sites on DNMT3A, we have previously shown that these regulatory proteins are dominant in the simultaneous modulation of DNMT3A activity (32). We show here that while *Fos-I* ecRNA binding to the DNMT3A tetramer interface does not perturb interactions between H3 tails and DNMT3A (Fig. 5 A.), *Fos-I* ecRNA disrupts activation of DNMT3A activity H3K4me0 (residues 1-21) (Fig. 5 B.) or DNMT3L in reactions with polynucleosome substrates (Fig. 5 C.). In sum, our results are inconsistent with models of RNA-mediated regulation of DNA methylation that requires some type of RNA-DNA hybridization and strongly supports a model in which DNA methylation changes result from allosteric binding of locally synthesized ecRNA to DNMT3A (Fig. 2 A.) (1), (20-23). What remains intriguing is that while the disruption of *Fos* ecRNA secondary structure does not disrupt binding to DNMT3A (1), a non-specific RNA of 22 nucleotides in length does not regulate DNMT3A activity (Fig. 2 B). This could be reconciled by the site

on DNMT3A that binds short RNA is largely non-specific, but the functional perturbation requires a particular sequence and length, both of which *Fos* ecRNA must contain but remains uncharacterized. The number of RNAs cells produce far exceeds the number of proteins that interact with these RNAs. In fact, a particular RNA may interact with multiple proteins and likewise proteins may interact with multiple RNA (68). Therefore, it has been proposed that this promiscuity and malleability of RNA-protein interactions contributes to the complex network of these interactions in cells (68). We propose that this is likely the case for DNMT3A-RNA interactions as it binds distinct RNA species in various biological contexts (1), (2), (12), (69-70).

Our work complements the extensive cell biological studies that reveal complex crosstalk between DNA methylation, histone modification, and non-coding RNA(1-8), (11). Clearly, our finding that non-coding RNA is a dominant form of DNMT3A regulation has implications on the extent to which distinct components of the epigenetic machinery contribute to the establishment of DNA methylation patterns. Furthermore, a major finding reported here is a model for RNA-mediated DNMT3A regulation in which RNA is produced locally (e.g., ecRNA, Fig. 6 A., I-IV.) resulting in regulation of proximal DNMT3A enzymes through a non-specific binding site at the DNMT3A tetramer interface, coupled with the well-known rapid degradation of RNA (21), (57). The relevance of this proposed mechanism to DNMT3B and DNMT1 remains to be determined. Short non-coding RNAs have been shown to inhibit DNMT1 activity by directly binding a distinct surface as DNA substrates (19). Although our proposed mechanism for DNMT3A (Fig. 6 A.) is consistent with these findings, how the production of short non-coding RNAs contributes to the regulation of other DNMTs remains uncertain. Furthermore, while mechanisms to explain how long non-coding RNA regulates DNMTs, histone modifying enzymes, and transcription

factors appear better supported by compelling data, how small non-coding RNA act in this capacity remains challenging (58), (59). This derives in part because many models invoke mechanisms (R-loop or RNA-DNA triplex) that have yet to be demonstrated to directly regulate the target protein (20), (22), (23). Finally, our implication of the tetramer interface as the site of RNA regulation, along with our prior identification of this interface in protein-protein interactions, highlights its potential for therapeutic intervention (3), (4), (36).

Methods

Single Molecule RNA FISH

smFISH Probe Design. To quantify and localize *Fos* ecRNA and mRNA transcripts in situ, we designed Stellaris® probe sets for fluorescent detection of *Fos* ecRNA (12 probes, conjugated to Quasar® 570) and mRNA (30 probes, conjugated to Quasar® 670). Probe sets consisted of multiple 14-20mer oligonucleotides targeting the same RNA molecule to optimize signal strength while minimizing background fluorescence. Target sequences of each probe set are provided in SI appendix, Table 1.

Sample Preparation and Hybridization. *Day 1:* Primary neuronal cultures (~250,000 neurons per coverslip/well) were treated with KCl (25mM) or vehicle treated for 1h. After treatment cells were cross-linked with 3.7% formaldehyde (paraformaldehyde in 1X PBS) for 10 min at room temperature (21°C) on a rocking platform. Wells were washed twice with PBS and permeabilized in 70% ethanol for at least 3h at 4°C. Wells were washed in Stellaris® Wash Buffer A for 5 min at room temperature. Coverslips were transferred to a humidifying chamber and incubated with hybridization buffer (0.5 nM mRNA probe, 0.5 nM ecRNA probe) for 14 hours at 37°C. *Day 2:* Coverslips were washed twice in Stellaris® Wash Buffer A for 60min at 37°C. After a 5 min wash in Stellaris® Wash Buffer B at room temperature coverslips were mounted using ProLong™ antifade with DAPI for imaging.

Quantification of Expression. smRNA FISH results were quantified using StarSearch (<http://rajlab.seas.upenn.edu/StarSearch/launch.html>), which was developed by Marshall J. Levesque and Arjun Raj at the University of Pennsylvania to automatically count individual RNAs. mRNA and ecRNA detection involved two major steps. First, images for each probe set as well as a DAPI image were merged, and cells were outlined. Next, punctae detection was carried out and additional adjustment of thresholds was performed. The same threshold range was used for all images, and this analysis was performed blind to treatment group.

Expression constructs

The plasmids used for expression of recombinant human proteins were as follows: pET28a-hDNMT3ACopt for DNMT3A full length (60), pET28a-hDNMT3A_catalytic_domain for wild type or mutants of DNMT3A catalytic domain ($\Delta 1-633$) (61), pTYB1-3L was used to express full-length human DNMT3L (62). Mutations to the DNMT3A catalytic domain pET28a-hDNMT3A_catalytic_domain as a template) were generated as described in (4) and (36).

Protein Expression

DNMT3A (human full length and catalytic domain) and DNMT3L (human full length) were expressed in NiCo21(DE3) Competent *E. coli* cells (New England Biolabs). Following growth in LB media at 37 °C to an $A_{600\text{ nm}}$ of 0.9 (DNMT3A full length) and 0.7 (DNMT3A catalytic domain and DNMT3L), induction occurred at room temperature (5 hours for DNMT3A full length and catalytic domain, and 16 hours for DNMT3L) with 1 mM IPTG (GoldBio). Cell pellets were harvested by centrifugation at 5,000g for 15 minutes and stored at -80 °C.

Protein Purification

Proteins were purified as stated in (3) and (32). Briefly, bacterial cell pellets were resuspended in lysis buffer (50 mM HEPES pH 7.8, 500 mM NaCl, 50 mM imidazole, 10% glycerol and 1 mM PMSF) and lysed by sonication. Cleared lysates (11,000g for 1 hour) were purified using ÄKTA Fast Protein Liquid Chromatography (FPLC) system with a 5 mL HisTrap HP nickel charged IMAC column (GE healthcare), which was previously equilibrated with loading buffer (50 mM HEPES pH 7.8, 500 mM NaCl, 50 mM imidazole, 10% glycerol). Resins were washed (50 mM HEPES pH 7.8, 500 mM NaCl, 75 mM imidazole, 10% glycerol) and an imidazole gradient was used to elute bound proteins (50 mM HEPES pH 7.8, 500 mM NaCl, 75-500 mM imidazole, 10% glycerol). Pooled fractions were desalted, concentrated into storage buffer (50 mM Tris-Cl, 200 mM NaCl, 1 mM EDTA, 20% (v/v) glycerol, pH 7.8, with 0.5 mM DTT) using a 15 mL Centrifugal Filter with a 10K MWCO supplied by MilliporeSigma™, and stored at -80°C for later use. Protein concentrations were determined using 280 nm extinction coefficients ($142,010\text{ M}^{-1}\text{ cm}^{-1}$ for full length DNMT3A, $38,180\text{ M}^{-1}\text{ cm}^{-1}$ for the catalytic domain of DNMT3A, $68380\text{ M}^{-1}\text{ cm}^{-1}$ for full length DNMT3L) and reflect the oligomeric state in all experimental conditions (nM of tetramers for the full length and the catalytic domain of DNMT3A). A summary gel of the purified recombinant proteins used in this study is in SI appendix, Fig. S6.

Computational Modeling

The HDOCK docking server was employed to predict the surface on DNMT3A that interacts with *Fos-1* ecRNA using a DNMT3A (PDB: 4U7T, chain A) monomer and the *Fos-1* ecRNA sequence (34). In the absence of any structures for *Fos-1* ecRNA or DNMT3A-RNA co-complexes, we relied on this approach as the HDOCK server utilizes a hybrid of global docking and a template-based modeling, which incorporates binding

interface information from protein-RNA complexes in the PDB and has been previously employed for similar purposes (34), (37-39). In the absence of a sequence, like in the case of *Fos-1* ecRNA, the server initially searches the PDB to generate a template based on the highest sequence similarity, coverage, and resolution. To generate models, HDock relies on a Fast Fourier Transform (FFT)-based docking algorithm to perform a global docking search to explore all possible binding modalities, which are then refined and scored by a knowledge-based scoring function as well as backbone flexibility (63).

Methylation Assays

In this study DNMT3A_FL refers to the full-length protein (912 amino acids) and DNMT3A_CD refers to the catalytic domain of DNMT3A (residues 634-912). DNA methylation reactions were carried out to assess the ability of DNMT3A to incorporate tritiated methyl groups from AdoMet onto distinct DNA substrates and experimental conditions. Assays were performed at 37 °C in a buffer consisting of 50 mM KH₂PO₄/K₂HPO₄ (pH 7.8), 1 mM EDTA, 1mM DTT, 0.2 mg/mL BSA, 20 mM NaCl with saturating AdoMet (15 μM). For the radiochemical assays, 50 μM ([³H] methyl-labeled: unlabeled, 1:10) AdoMet stocks were prepared from 32 mM unlabeled AdoMet (NEB) and [³H] methyl-labeled AdoMet (80 Ci/mmol; supplied by PerkinElmer) in 10 mM H₂SO₄. Reactions were quenched by mixing aliquots taken from a larger reaction with 0.1% SDS (1:1) and spotted onto Hybond-XL membranes (GE healthcare). Samples were then washed, dried, and counted using a Beckman LS 6000 liquid scintillation Counter as described in (64). Reactions with RNAs *Fos-1* (5' GGGGACACGCCUCUGUCCCCUUAU-3'), *Fos-2* (5'-GUCUGUGCACCGUGUGCAUAUACAG-3'), *CHD* (5' GGGGUGACGGGGACAGGCGGGGCUG-3') or non-specific (5'-

CGACCGCCUACUGAAAGAGGGC-3') were initiated by the addition of RNA pre-mixed with distinct DNA substrates (Poly dI-dC, nucleosomal or non-nucleosomal *p15*) as previously described in (2). The RNAs used in this study were purchased from IDT and HPLC purified. Where indicated, fold inhibition refers to 1 – (product formed with RNA/product formed without RNA) whereas fold change refers to data normalized to the activity of reactions consisting of DNMT3A only. In reactions consisting of additional modulators of DNMT3A activity (synthetic H3K4me0 peptide or DNMT3L), DNMT3A was pre-incubated with H3K4me0 or DNMT3L in reaction buffer for 1 hour at 37 °C prior to being initiated. Synthetic peptides derived from human Histone H3.1 (N-ARTKQTARKSTGGKAPRKQLA-C) were supplied by Active Motif (65). *In vitro* reconstitution of nucleosome core particles extracted from HeLa cells onto *p15*-pCpG^L DNA was performed with a salt gradient (61), (66), (67). For the high-salt histone extraction, HeLa cells (10⁷) were harvested (300g for 10 minutes) and re-suspended in hypotonic lysis buffer (10 mM Tris–Cl pH 8.0, 1 mM KCl, 1.5 mM MgCl₂ and 1 mM DTT). The nuclei were pelleted (10,000g for 10 minutes at 4 °C), re-suspended in extraction buffer (10 mM HEPES pH 7.9, 10 mM KCl, 1.5 mM MgCl₂, 0.34 M sucrose, 10% glycerol) and lysed in no-salt buffer (3 mM EDTA, 0.2 mM EGTA) by vortexing for 1 minute (10 seconds on and off). The chromatin was pelleted (6,500g for 5 minutes), re-suspended in high-salt solubilization buffer (50 mM Tris–Cl pH 8.0, 2.5 M NaCl) by vortexing for 2 minutes. DNA was pelleted (16,000g for 10 minutes) and the supernatant was transferred to a dialysis cassette (3,500 MWCO) against a no-salt dialysis buffer (10 mM Tris–Cl pH 8.0) for 2 hours at 4 °C and stored at -80 °C (66). Nucleosome core particles were reconstituted by salt gradient deposition, in which DNA and histone extracts were mixed in 2 M NaCl (30 minutes at 4 °C) followed by the addition of dilution buffer (10 mM Tris-HCl, pH 7.6;

1 hour at at 4 °C). Dilution buffer was then added (1 hour incubation at 4 °C per dilution) to obtain the following concentrations of NaCl (M): 0.8, 0.6, 0.2 and 0.1 (67).

Fluorescence Anisotropy

Fluorescence anisotropy measurements were obtained using a Horiba Fluoromax fluorescence spectrophotometer equipped with excitation and emission polarizers (excitation: 485 nm, emission 535 nm) following a 5-minute incubation at room temperature. Reactions involving DNMT3A (or DNMT3A-DNMT3L) complexes with FAM-labelled DNA or H3K4me0 peptide binding to *Fos-I* ecRNA were carried out in the following buffer: 50 mM KH₂PO₄/K₂HPO₄ (pH 7.8), 1 mM EDTA, 1 mM DTT, 0.2 mg/ml BSA, 20 mM NaCl with 50 µM Sinefungin. The DNA substrate (Gcbox30) consisted of a duplex with a fluorescein (6-FAM) label on the 5' end of the top strand (5'/6 FAM/TGGATATCTAGGGGCGCTATGATATCT-3'; the recognition site for DNMT3A is underlined) (36). Peptide binding experiments consisted of H3K4me0 (residues 1-21) with a FAM-NHS label on the N-terminus (32). Reactions involving a segment of the human *Fos* gene (NCBI Gene ID 2353, 3'- 500 nucleotide duplex DNA) and 5' FAM-6-labeled RNA were carried out in triplex buffer (20 mM Tris-HCl pH 7.4, 5 mM EDTA, 25 mM NaCl, 10 mM MgCl₂, 200 µM DTT) and incubated for 30 minutes at 37°C for 30 minutes prior to measuring the fluorescence anisotropy. The 5' 6-FAM-labeled RNAs employed were an 18-mer positive control RNA designed to complex with the *Fos* gene (NCBI Gene ID 2353, 3'- 500 nucleotide duplex DNA) or *Fos-I* ecRNA.

Supplementary Material

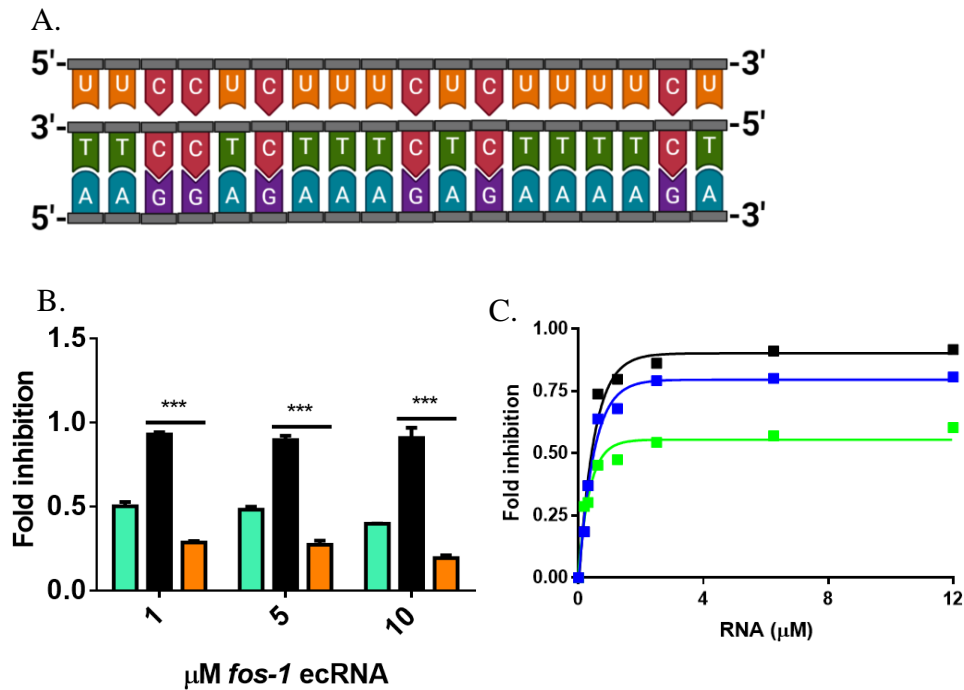


Figure S1. Functional characterization of RNA-mediated inhibition of DNMT3A_CD^{WT} activity and selectivity of *Fos-1* ecRNA for human DNMTs. **A.** sequences for oligonucleotide binding assays. The design relies on canonical principles for RNA-DNA triplex formation with Polypurine (bottom strand) and Polypyrimidine (top strand) DNA strands found within the *Fos* gene (NCBI Gene ID 2353, 3'- 500 nucleotide duplex DNA). **B.** The addition of a pre-mixture of Poly dI-dC (5 μM) and increasing concentrations of *Fos-1* ecRNA inhibits reactions consisting of DNMT3A_CD (■, 150 nM) and DNMT1 (■, 133 U/mL) but not M. HhaI (■, 150 nM). **B.** Inhibition curves for *CHD* (■), *Fos-2* (■) and *Fos-1* (■) RNAs with DNMT3A_CD^{WT}. Data in **B.** and **C.** reflect the mean and standard deviation of 3 experiments; In **C.**, a one-way analysis of variance was used to compare the values of each sample with increasing *Fos-1* ecRNA (***, $p < 0.001$; ns, $p > 0.05$).

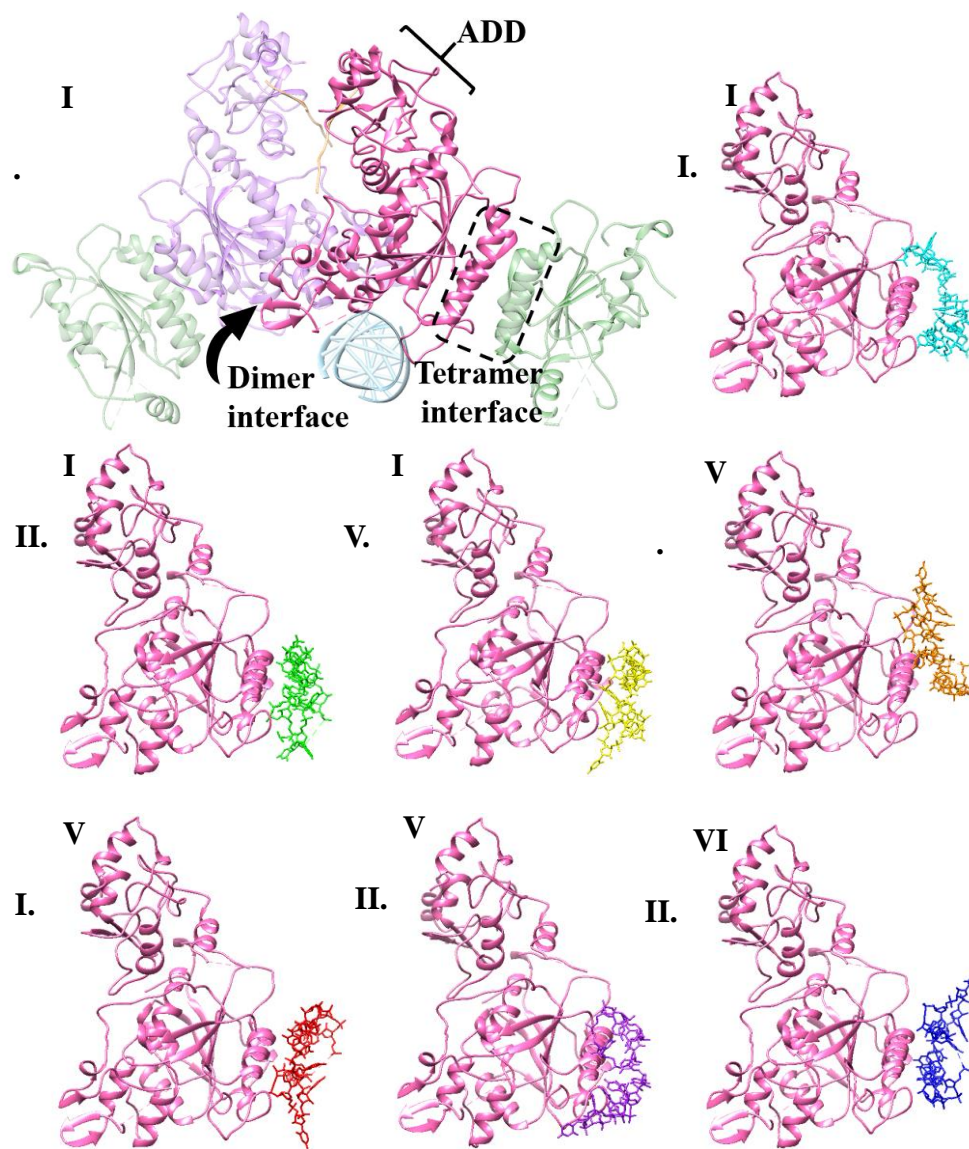


Figure S2. Computational models predict *Fos-1* ecRNA binds at the tetramer interface of DNMT3A. (I.) Crystal structure of a DNMT3A (■ and ■; residues 468-912) in complex with DNMT3L (■; residues 171-379) and H3 tail peptides (■; 1-21) (adapted from PDB 4U7T). (II.-VIII.) computational models of DNMT3A monomers in complex with *Fos-1* ecRNA.

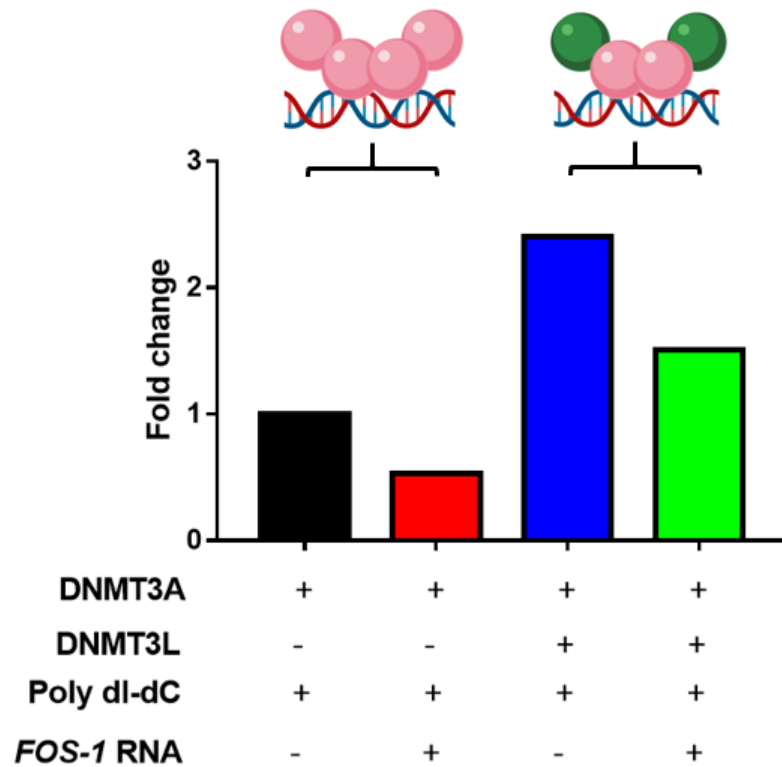


Figure S3. Modulation of DNMT3A_CD^{WT} enzymatic activity by *Fos-1* ecRNA is dominant in the presence of DNMT3L. *Fos-1* ecRNA inhibits enzymatic activity in reactions consisting of DNMT3A_CD^{WT} homotetramers (■) or DNMT3A_CD^{WT}-DNMT3L heterotetramers (■). Reactions consisted of proteins at 150 nM (1:1 to DNMT3A_CD^{WT}-tetramer) and were initiated by the addition of a pre-mixture of *Fos-1* ecRNA (1 μM) and Poly dI-dC (5 μM).

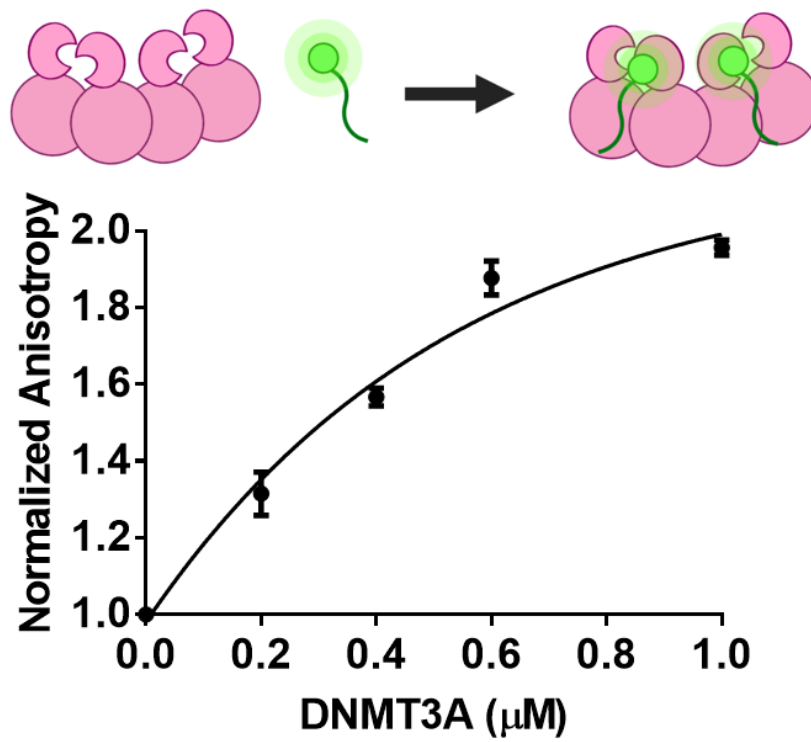


Figure S4. Binding of Full-length DNMT3A^{WT} to FAM-labeled H3K4me0 peptides. Increasing amounts of full-length DNMT3A^{WT} leads to a concomitant increase in the fluorescence anisotropy of 10 nM of 5' FAM-labeled H3K4me0 (residues 1-21).

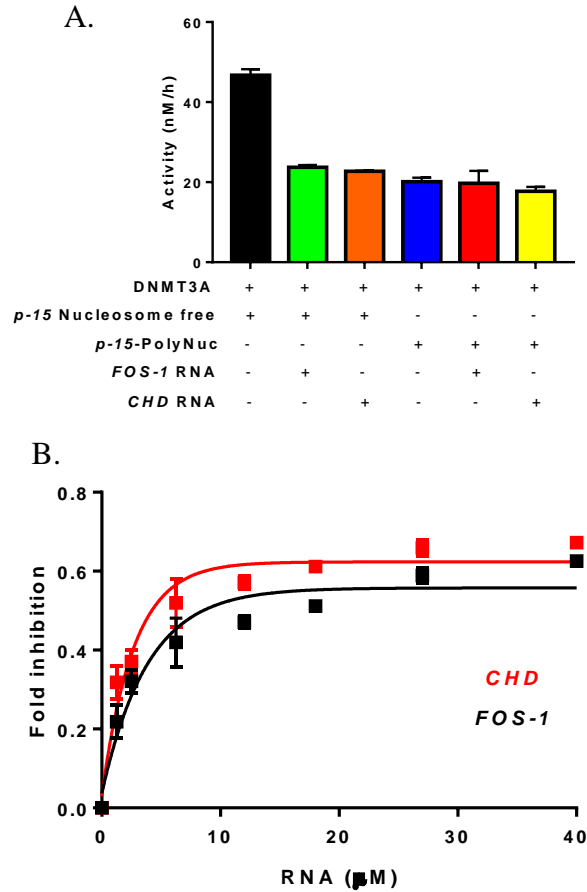


Figure S5. Excess *Fos-1* and *CHD* RNAs inhibit Full-length DNMT3A^{WT} activity with polynucleosomes as substrates. *Fos-1* or *CHD* RNA (1 μM) inhibit the enzymatic activity of full-length DNMT3A^{WT} (150 nM) with nucleosome-free *p15* as a substrate but not with the use of *p15* assembled into polynucleosomes **A.** Reactions consisted of 14 μM *p15* substrate (Nucleosome free or polynucleosomes) and were initiated by the addition of *p15* substrate (Nucleosome free or polynucleosomes) or a pre-mixture of RNA (*Fos-1* or *CHD*) with *p15* (Nucleosome free or polynucleosomes). **B.** Excess concentration of *Fos-1* or *CHD* inhibits full-length DNMT3A^{WT} (150 nM) with *p15* polynucleosomes (14 μM) as substrates.

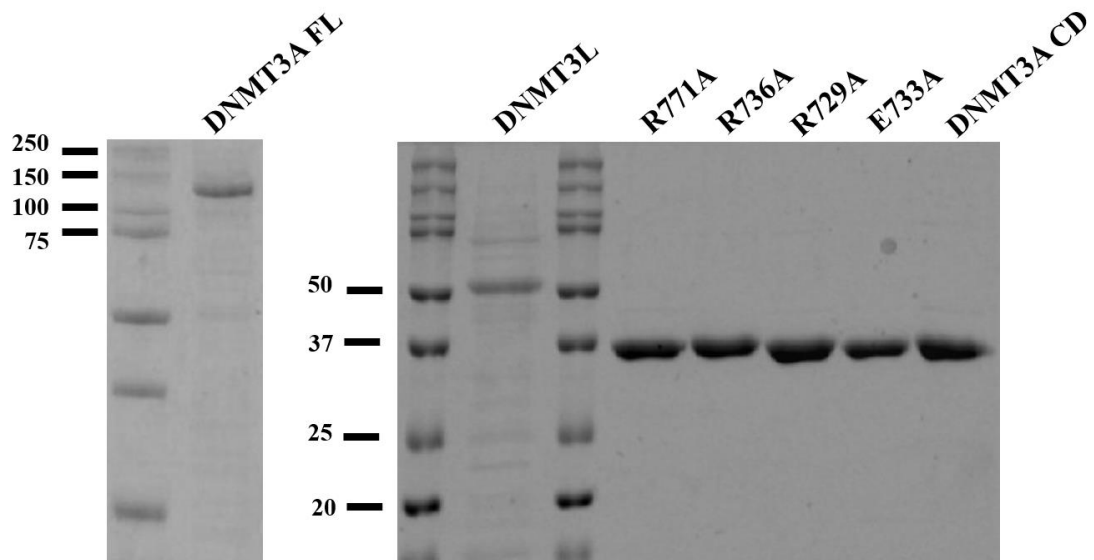


Figure S6. Summary gel of proteins used in this study. Proteins were run (150 Volts) on a 12% SDS-PAGE gel in 1X SDS electrophoresis buffer. Precision Plus Protein Dual Color (BIO-RAD) was used as a standard.

Chapter VI: A Novel Class of Selective Non-Nucleoside Inhibitors of Human DNA

Methyltransferase 3A

Abstract

Screening of a small chemical library (Pathogen Box (MMV)) identified two structurally related pyrazolone [1] and pyridazine [2] DNMT3A inhibitors with low micromolar inhibition constants. The uncompetitive and mixed type inhibition patterns with DNA and AdoMet suggest these molecules act through an allosteric mechanism, and thus are unlikely to bind to the enzyme's active site. Unlike the clinically used mechanism based DNMT inhibitors such as Decitabine or other candidates that act via the enzyme active site, the inhibitors described here could lead to the development of more selective drugs. Both inhibitors show promising selectivity for DNMT3A in comparison to DNMT1 and bacterial DNA cytosine methyltransferases.

Introduction

Epigenetic modifications of proteins and nucleic acids are crucial for normal development.(1), (2) Human DNA undergoes methylation largely at CpG dinucleotides, and the patterns are developmentally regulated and tissue-specific; these patterns contribute to the epigenetic code which is essential for viability.(3),(4) Aberrant methylation patterns can result in hypermethylation of gene promoters, leading to the silencing of critical tumor suppressor genes, resulting in tumorigenesis(4).

DNA methylation patterns are maintained by a class of DNA cytidine methyltransferases (DNMTs) in combination with TET enzymes engaged in removal of methyl moieties (5), (6) DNMTs rely on the methyl donor S-adenosyl methionine (AdoMet) and display both random and ordered kinetic mechanisms (7-11) DNA methylation patterns

are maintained by a housekeeping protein DNMT1, which primarily acts on hemimethylated DNA, and a family of *de novo* methyltransferases including DNMT3A and DNMT3B.(12) The DNMT3s, which also include a catalytically inactive regulatory protein DNMT3L, are mostly expressed during the early development phase of mammalian germ cells.(1), (3), (12) DNMT1, meanwhile, is expressed throughout the lifetime of mammalian somatic cells and is localized near replication forks.

All DNMTs share the same domain architecture with an N-terminal domain which contains the regulatory domains including the replication fork binding RFD domain in DNMT1 and the H3 binding ADD domain in DNMT3s.(1), (3) The C-terminal, or catalytic domain has the highly conserved methyltransferase motifs (I-X) that are found in both prokaryotic and eukaryotic methyltransferases (see Figure 1). These motifs are responsible for cofactor binding and catalysis.(3) DNMT3A forms tetramers with DNA binding occurring along the seam of the dimerization domain (see Figure 2).(13) Mutations that disrupt the oligomeric state of DNMT3A occur in diverse cancer patients, and in particular, acute myeloid leukemia patients.(4), (14–17) Both catalytically active DNMTs, and in particular, DNMT3A, interact with diverse partners and these interactions alter the function of DNMT3A and contribute to tumor-specific changes in methylation patterns.(4), (14)

The last twenty years have witnessed increasing interest in developing drugs that target epigenetic pathways, in particular histone and DNA modifying enzymes.(18–20) An obvious feature of these pathways is their inherent reversibility, unlike mutational changes which frequently demand therapeutic strategies leading to cytotoxic interventions. Interestingly, the FDA approved DNMT nucleoside inhibitors, azacytidine and Decitabine are highly cytotoxic. These prodrugs are converted to the triphosphates, incorporated into DNA and inhibit DNMTs through the formation of an irreversible suicide complex.(19) A

third variant, guadecitabine (SGI-110), a Decitabine dinucleotide, is in phase III clinical trials.(4), (19) The dose-limiting toxicity manifested by these drugs has led to the search for non-nucleoside inhibitors; interestingly, many of these act by binding the enzyme active site or act by unknown mechanisms (18), (19).

Our interest is to determine if new mechanistic classes of DNMT inhibitors can be identified with the long term goal of developing therapeutic approaches not hampered by the toxicity and related issues associated with currently used and recently described DNMT inhibitors.(18), (19) For example, DNMT3A has over 60 known biomolecular interacting partners,(21) which in many cases are implicated in directing DNMT3A to inappropriately methylate and regulate tumor suppressor genes (17), (22), could be the basis of tumor-specific protein-protein inhibitors (PPIs) (19), (23). Certainly, the recent progress in developing PPIs for diverse therapeutic targets forms a strong basis for such a strategy (24). Moreover, the clinically identified DNMT3A mutations in diverse cancers are known to alter the stability and functional outcomes of the complexes formed between DNMT3A and its partner proteins (17), (22), (25); thus, mutant and tumor-specific PPI's, which have been identified for other cancer targets may be possible. (26) Finally, allosteric enzyme modulators can provide a basis for enhanced selectivity and potentially, decreased toxicity.(27–29)

Here we describe our initial compound screening effort, relying on open source chemical library constructed from the *Medicines for Malaria Venture* (MMV) Pathogen Box. It consisted of 400 drug-like molecules with known activities against targets for neglected tropical diseases. The relative merits of using a library of well-established molecules that show good bio-activity versus other approaches have been well described. (30) Using 50 compounds of the library, we first determined that a compound concentration

of 60 μ M resulted in 5% of the molecules showing 90% or more inhibition. We then relied on a modified version of our standard radiochemical assay using tritiated AdoMet,(17) which measures DNA methylation (see Methods, Supplementary). The assay uses poly dIdC which is an excellent DNMT3A substrate, and the conditions allow for multiple catalytic turnovers with an excess of DNA.(17), (22) Importantly, many literature reports describing DNMT screens are actually done under conditions of excess enzyme over DNA, or less than a single catalytic cycle which compromise interpretation of any inhibition effects.(31–33)

Results and Discussion

Regulation of full-length DNMT3A activity by p53 or TDG is dominant in DNMT3A-p53-H3 tail or DNMT3A-TDG-H3 tail complexes

The screen of the 400 compounds in the library generated 12 compounds that showed at least 90% inhibition. A secondary assay was used to verify that these were actually positive results and only two compounds passed this second analysis (compounds 1 and 2, Figure 3). These compounds were previously identified as potential inhibitors of TbrPDEs, a class of phosphodiesterases found in *T. brucei* involved in trypanosomiasis (*African sleeping sickness*). (34) Compounds 1 and 2 both show potent inhibition of TbrPDE, good antitrypanosomal effects, and are part of an extensive study of TbrPDE inhibitors involving numerous analogs. (35)

The inhibition of DNMT3A by both compounds, against DNA or AdoMet, is inconsistent with a competitive mechanism. The best fit to the inhibition data is consistent with Mixed Type or Uncompetitive mechanisms. Importantly, both mechanisms require that compounds 1 and 2 bind allosterically, away from the active of the enzyme. The Mixed Type mechanism allows for scenarios in which the inhibitor binds the same form of the enzyme bound by either substrate, as well as the form of the enzyme already bound by one of the substrates. In contrast, the single Uncompetitive mechanism (Figure 3, Table 1,

Compound 2, using DNA (poly dIdC)) implicates a mechanism wherein the inhibitor only binds to the form of the enzyme already bound by the DNA. The mechanisms of other DNMT inhibitors, when reported, often display competitive mechanisms with DNA, AdoMet or both.(19), (32), (36) The simplest interpretation of these forms of inhibition is that the inhibitor binds the same site as DNA or AdoMet, or minimally, binds the same form of the enzyme bound by these substrates. (37)

The potencies (K_I values) of compounds 1 and 2 against DNMT3A range from 2.5 to 7.1 μM (AdoMet) and 11 to 41 μM (poly dI-dC), which compare favorably to numerous published efforts. (18), (19) The extensive SAR studies done against TbrPDEs, provide an opportunity to identify more potent DNMT3A inhibitors, develop a limited SAR, and determine if the selectivity of these compounds can be improved. The mechanisms and potencies of compounds 1 and 2 need to be considered in the context of the extensive screening, synthetic and computational efforts to develop DNMT3A inhibitors. (32), (38–41)

While the inhibition mechanisms of many of DNMT inhibitors are not reported, the majority of the assigned mechanisms appear to be competitive with DNA and in some cases AdoMet. (18), (19) Although many clinically used drugs act competitively with the endogenous substrates of the target enzyme, the widespread cellular reliance on AdoMet-dependent methyltransferases suggest that the development of drugs specific for DNA methyltransferases or drugs that distinguish between DNMT1 and DNMT3A will be challenging. The majority of DNA methyltransferase inhibitors are poorly selective for DNMT3A (refs). This likely contributes to the limiting toxicity displayed by these compounds. The inappropriate DNA methylation detected in patients with diverse cancers presumably results from the action of DNMT3A (and DNMT3B). DNMT3A is largely

missing in adult somatic cells, and is expressed in tumor cells, whereas DNMT1 is expressed in most somatic tissue. We tested the selectivity of both compounds (Figure 4) and found both show some selectivity, with inhibitor 2 being the more selective. Neither compound shows inhibition of the bacterial DNA cytosine methyltransferase M.SssI, even at 60 μ M. Both compounds show little inhibition of DNMT1 at 6 μ M, and compound 2 retains this selectivity even at 60 μ M. It is intriguing that both inhibitors show greater inhibition of the catalytic domain of DNMT3A (residues 628 to 912, see Figure 1) than the full length DNMT3A, suggesting that the large N-terminal segment interferes with the inhibition.

Inhibitors that act allosterically can potentially display lowered off target toxicity. (42), (43) The non-competitive and uncompetitive mechanisms displayed by compounds 1 and 2 (Figure 3) are not consistent with either of these binding to the enzyme active site, which is normally occupied by DNA and AdoMet. Thus, these molecules most likely bind allosterically, regulating the enzyme's function from a distal site. Small molecules that act in this way have, using standard SAR optimization methods, can lead to highly selective drugs. (43)

In summary, the screening of a small chemical library of known drugs against human DNMT3A identified two non-nucleoside molecules of low micromolar potency. Both molecules inhibit the enzyme by binding outside the active site, and not only selectively inhibit human over bacterial DNMTs, but also shows some promising preferential targeting of *de novo* over maintenance DNA methyltransferases. This highlights the potential use of these molecules for the treatment of malignancies associated with disruptions to DNMT3A activity. The large number of analogs of these two inhibitors which have been described provides a promising basis for further optimization of this new group of

DNMT3A inhibitors, with reasonable prospects of showing improved toxicity over known DNA methyltransferase drugs. (46)

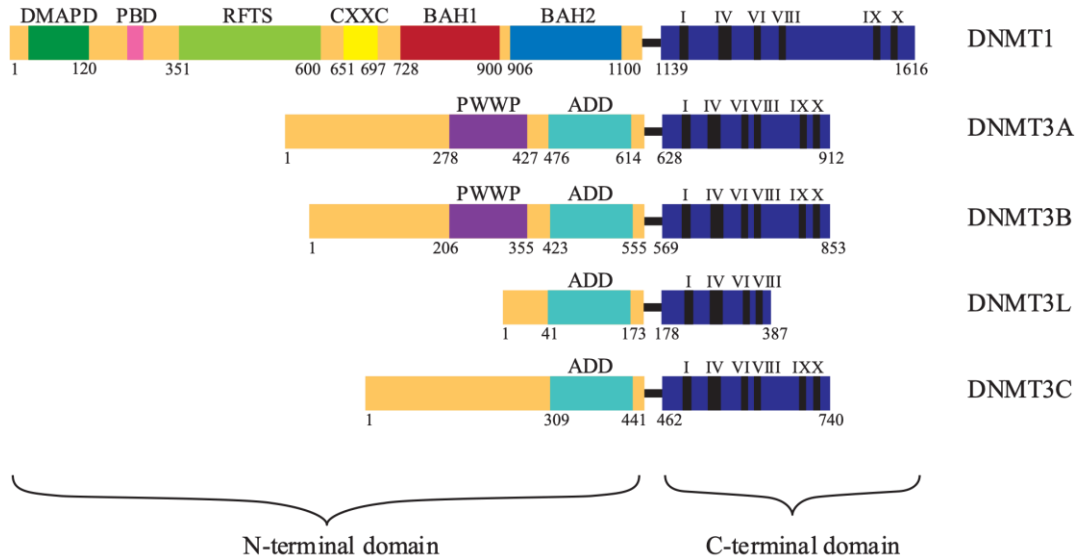


Figure 1. Comparison of the primary structures of human DNMTs. The C-terminal domain contains conserved motifs (I-X) and is active in the absence of the N-terminal domain. The N terminal domain has several conserved segments known to interact with regulatory proteins and histones. The abbreviations used are: DMAPD – DNA methyltransferase associated protein 1 interacting domain, PBD – PCNA binding domain, RFTS – Replication foci targeting domain, BAH – bromo-adjacent homology domain, ADD – ATRX-DNMT3-DNMT3L domain.

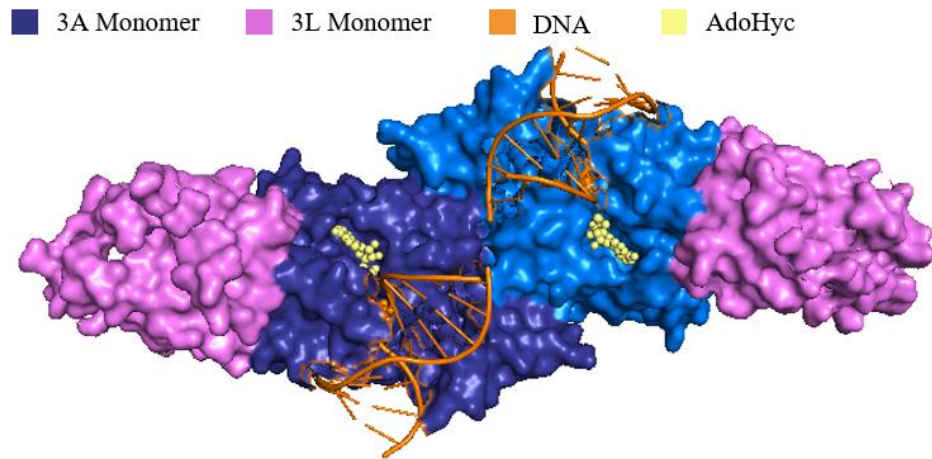


Figure 2. Comparison of the primary structures of human DNMTs. The C-terminal domain contains conserved motifs (I-X) and is active in the absence of the N-terminal domain. The N terminal domain has several conserved segments known to interact with regulatory proteins and histones. The abbreviations used are: DMAPD – DNA methyltransferase associated protein 1 interacting domain, PDB – PCNA binding domain, RFTS – Replication foci targeting domain, BAH – bromo-adjacent homology domain, ADD – ATRX-DNMT3-DNMT3L domain.

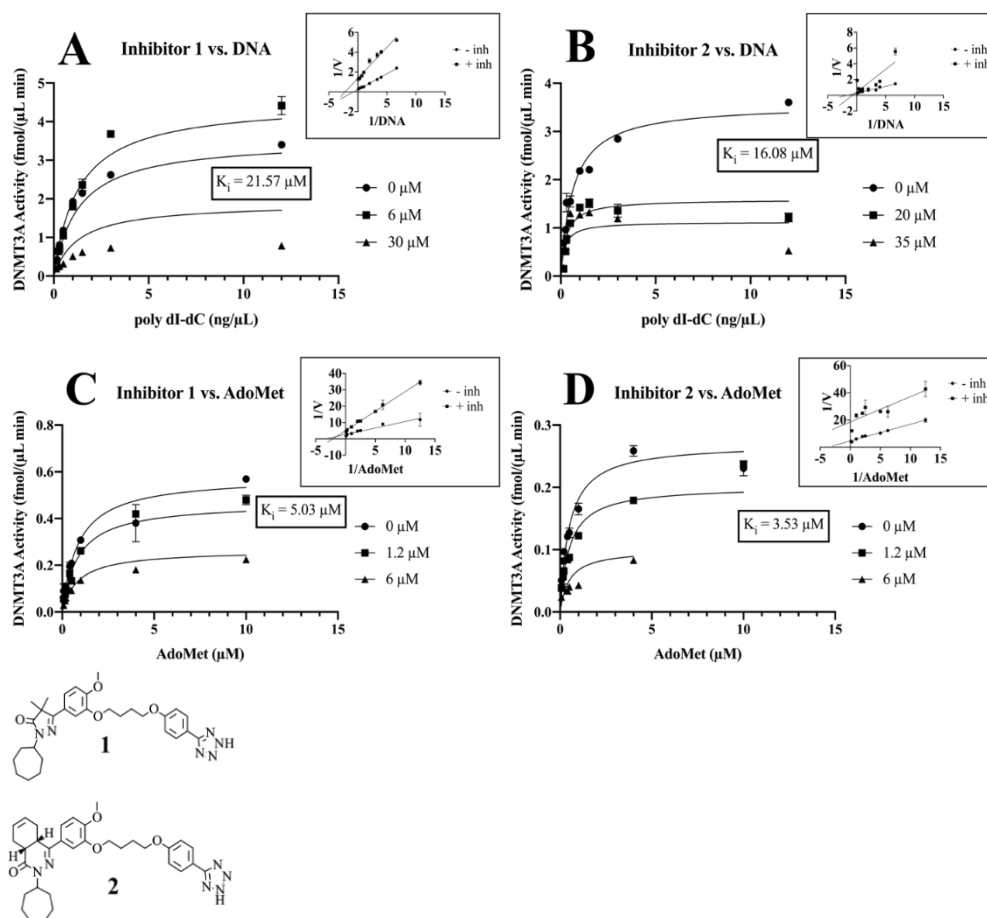


Figure 3. Best fit plots of the inhibition with respect to both substrates, poly dI-dC. A., B. and AdoMet C., D. Assays were performed with 150 nM DNMT3A with an excess of the substrate being held constant. Radiolabeled ^3H -AdoMet was used to determine product formation. All reactions were assayed for 30 min, then quenched with 0.1% SDS and spotted onto charged nylon membranes for detection. Extracted K_i values are boxed, while corresponding reciprocal plot with best-fit lines are shown in top right. Structures of inhibitors are shown (left).

Table 1. Values for the various fits of inhibitors with respect to both substrates. Fits were determined using the *Noncompetitive* and *Uncompetitive* nonlinear regression models in *Prism 8.4.3*. The reported bounds define the 95% confidence interval of the K_i value.

<i>Inhibitor</i>	1		2	
<i>Substrate</i>	<u>AdoMet</u>	<u>poly dI-dC</u>	<u>AdoMet</u>	<u>poly dI-dC</u>
<i>Best fit K_i (μM)</i>	3.70 – 7.06	12.64 – 40.56	2.53 – 5.09	11.37 – 23.34
<i>Best fit Mechanism</i>	<i>Mixed</i>	<i>Mixed</i>	<i>Mixed</i>	<i>Uncompetitive</i>
<i>Goodness of fit (R^2)</i>	0.957	0.831	0.945	0.891

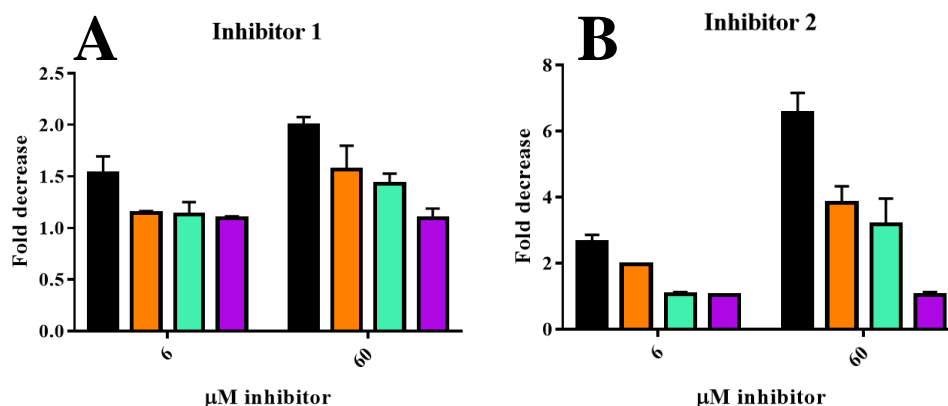


Figure 4. Inhibitors 1 (A) and 2 (B) modulate the activity of human DNMT3A_CD (■), DNMT3A_FL (■) and DNMT1 (■) DNA methyltransferases but not of the bacterial DNA methyltransferase M.SssI (■). To test the specificity of inhibitor 1 and 2 for these distinct types of enzymes, assays were performed with 150 nM DNMT3A_CD (■), DNMT3A_FL (■), 133 U/mL DNMT1 (■) and 266 U/mL M.SssI (A and B). Inhibitors 1 (A) and 2 (B) were tested at 6 and 60 μM with poly dIdC and AdoMet at a fixed concentration of 1.8 ng/μL and 5 μM, respectively. In all reactions (A and B), enzymes and inhibitor 1 or 2 were pre-incubated for 15 minutes at 37 °C in methylation reaction buffer (see methods) prior to initiating the reaction by the addition of DNA. Methylation reactions were assayed for 30 min, quenched with 0.1% SDS and spotted onto charged nylon membranes for detection of radiolabeled 3 H-AdoMet DNA. Data reflect the mean and standard deviation of at least 3 independent experiments.

Methods

Protein expression and purification

The isolated catalytic domain (CD) of DNMT3A (residues 634-912), which was used in all DNMT3A assays, has comparable kinetic parameters (k_{cat} , K_{mDNA} , $K_{mAdoMet}$) and similar regulatory responses to DNMT3L to the full length protein.^{1,2} The protein was expressed using codon optimized plasmids pET28a-hDNMT3A_CD ($\Delta 1-611$).³

All proteins were expressed in NiCo21 (DE3) competent *E. coli* cells (New England Biolabs). Using LB medium, cell cultures were grown at 37 °C until an $A_{600\text{ nm}}$ of 0.6 was reached. Following growth, expression was induced at 28 °C using 1 mM isopropyl β -D-thiogalactopyranoside (Gold Biotechnology). This addition marked the beginning of a 6 h induction time that ended with centrifugation and collection of the resulting cell pellet for storage at -80 °C. Further purification began with cell lysis via sonication in 50 mM HEPES, 500 mM NaCl, 50 mM imidazole, 10% glycerol and 1% phenylmethylsulfonyl fluoride (PMSF) at pH 7.8. The solution was clarified by centrifugation and then loaded into an AKTA start FPLC (GE Healthcare) for purification. This was performed using a nickel-nitrilotriacetic acid column (GE Healthcare), a 50 mM HEPES, 500 mM NaCl, 50 mM imidazole, 10% glycerol and 1% PMSF at pH 7.8 buffer for equilibration and a similar 70 mM imidazole buffer for washing. Elution of column bound protein was triggered with a 500 mM imidazole buffer equivalent. The storage of all collected proteins was done at -80 °C in 50 mM $\text{KH}_2\text{PO}_4/\text{K}_2\text{HPO}_4$, 20% glycerol buffer at pH 7.8. The activity of obtained DNMT3A was determined by methylation assay (described below).

Methylation Assays

In vitro methylation assays were used to determine the total amount of product (methylated poly dI-dC DNA) generated through the catalytic cycle of active DNMT3A. Reactions with 150 nM DNMT3A tetramer were carried out at 37 °C, pH 7.8 in 50 mM $\text{KH}_2\text{PO}_4/\text{K}_2\text{HPO}_4$, 1 mM DTT, 0.2 mg/mL BSA, 20 mM NaCl and 5 μM AdoMet (composed of 4.5 μM unlabeled and 0.5 μM 3H-methyl labeled cofactor). 20 μL assays were preincubated for 20 min at 37 °C followed by the addition of 1.8 ng/ μL poly dI-dC DNA. After the specified assay time, the reactions were quenched with 0.1% SDS and spotted onto Hybond-XL membranes (GE Healthcare). The membranes were washed with

both 50 mM KH₂PO₄/ K₂HPO₄ and ethanol. Following a drying period, samples were analyzed using a Beckmann LS6000 liquid scintillation counter.

Library screening

Screening was done in 96 conical well plates (Costar). The average maximum turnover rate from 8 wells with 150 nM DNMT3A WT served as control groups. A master mix contained reaction buffer (50 mM KH₂PO₄/K₂HPO₄, 1 mM EDTA, 1 mM DTT, 0.2 mg/ml of BSA, 20 mM NaCl), and 5 μM AdoMet (from a 50 μM stock composed of 45 μM unlabeled and 5 μM ³H-methyl labeled at pH 7.8) and 150 nM 3A were mixed and then aliquoted into each well. Chemical library compounds (Pathogen box) were added into each well at 60 μM and incubated at 37 °C for 60 mins after addition of 5 μM poly dI-dC. All wells were quenched with 0.1% SDS (1:1) after 1-hour. Samples (15μL) were spotted onto Hybond-XL membranes (GE Healthcare), washed, and dried.

Kinetic studies

To determine the dependence of inhibition on the individual cofactors, methylation assays (described above) were performed with inhibitor at three different concentrations (0 μM, ~IC₅₀, Excess), one cofactor held constant (5 μM AdoMet or 12.0 ng/μL poly dI-dC), and the other varied. For the variation of AdoMet, concentrations of 10, 4, 1, 0.5, 0.2, 0.16, and 0.08 μM were used, while for the variation of DNA, 0.15, 0.25, 0.3, 0.5, 1, 1.5, +3.0 and 12.0 ng/μL poly dI-dC DNA were used.

Data Analysis

Using *Prism 8.4.3*, all data was fit both to non-linear models and converted to double-reciprocal format and fitted to linear-models. Using the tabulated Goodness of Fit (R²) values, the most statistically likely mechanism of inhibition was chosen (Table 1S).

Specificity of inhibitors to human DNA methyltransferases

To assess the specificity of inhibitor 1 and 2 for DNMT3A, DNA methylation assays (described above) were performed with each inhibitor at two distinct concentrations (6 or 60 μM) with both poly dI-dC DNA (1.8 ng/μL) and AdoMet (5 μM) held at a constant concentration. The distinct types of DNA methyltransferases and their concentrations were as follows: 150 nM full-length (DNMT3A_FL) or catalytic domain DNMT3A

(DNMT3A_CD), 133 U/mL DNMT1 (purchased from NEB) and 266 U/mL M.SssI (purchased from NEB).

Supplementary Material

Table S1. R^2 values for the non-linear fits of the available inhibition data with respect to three generalized inhibition mechanisms: competitive, uncompetitive and noncompetitive (mixed type).

<i>Inhibitor</i>	1		2	
<i>Cofactor</i>	<u>AdoMet</u>	<u>poly dI-dC</u>	<u>AdoMet</u>	<u>poly dI-dC</u>
<i>Competitive Fit</i>	0.8927	0.7690	0.9507	0.5304
<i>Uncompetitive Fit</i>	0.9467	0.8124	0.9833	0.8909
<i>Noncompetitive Fit</i>	0.9571	0.8312	0.9804	0.8572

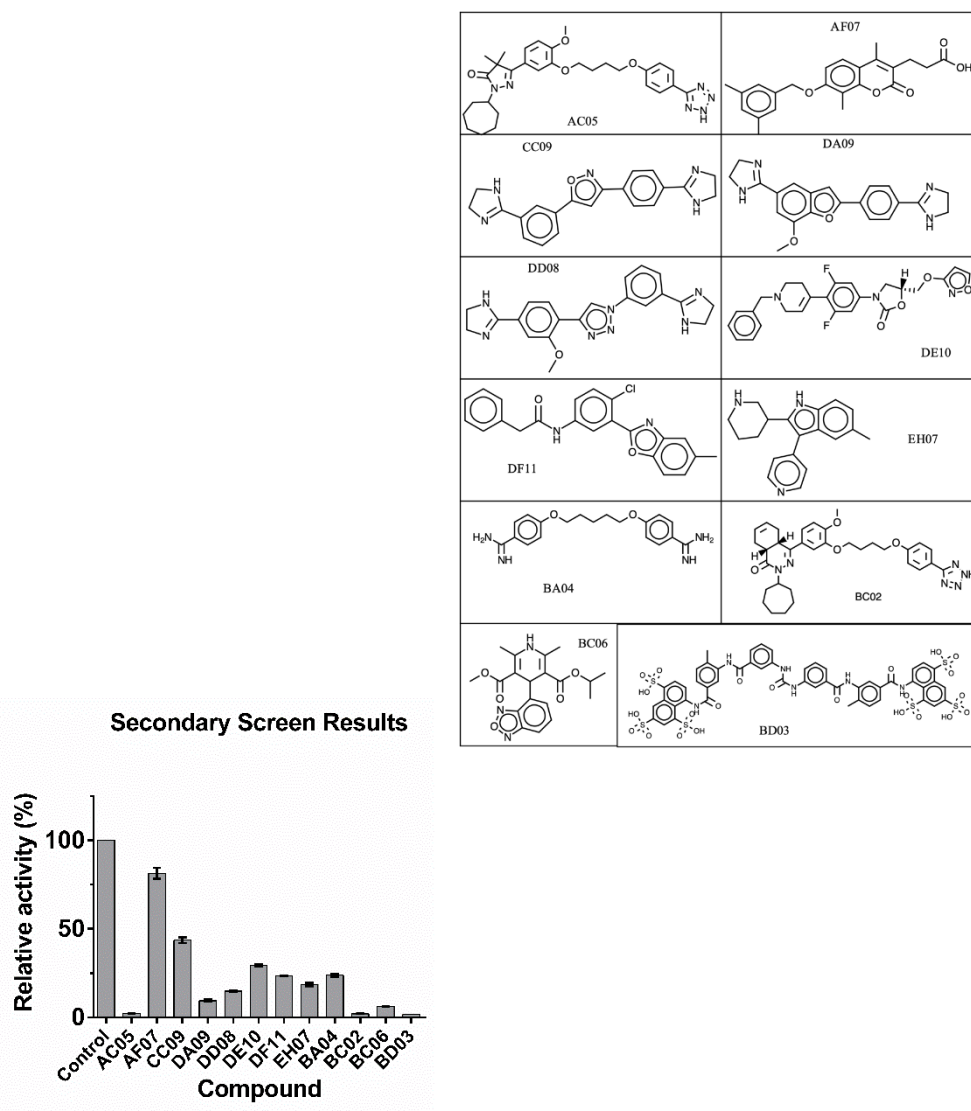


Figure S1. Results from the secondary screen. Compounds that exhibited more than 90% inhibition in the primary screen of the Pathogen Box library were subjected to duplicate (n=2) repetition of the inhibition. Activity assays were performed as described in the Methods. The compounds are designated by their location in the library and reference structures are provided below. Compound 1 is designated AC05 while compound 2 is BC02.

Chapter VII: Small molecule inhibition of DNMT3A regulation by partner proteins

Abstract

In a previous screening of a small chemical library (Medicines for Malaria Venture Pathogen Box) we identified two structurally related pyrazolone (inhibitor 1) and pyridazine (inhibitor 2) that act as allosteric inhibitors of DNMT3A and display low micromolar inhibition constants. With the use of mutational mapping, computational modeling, radiochemical and binding assays under various conditions, we show that these compounds bind and disrupt protein-protein interactions at the DNMT3A tetramer interface. This disruption is observed in tetrameric complexes involving DNMT3A and distinct partner proteins, like DNMT3L, p53 and TDG. To date, small molecules targeting DNMT3A are limited to competitive inhibitors of AdoMet or DNA as well as the highly cytotoxic nucleoside inhibitors. Our work is the first to identify small molecules with a mechanism of inhibition involving disruption of PPIs with DNMT3A. Future structure-activity relationship (SAR) studies and optimization of these compounds provides a promising basis for the treatment of diseases that display aberrant PPIs with DNMT3A, such as AML.

Introduction

The epigenetic machinery regulates a wide range of biological processes including parental imprinting, cellular development, and differentiation (1-4). Epigenetic regulation is a highly dynamic process that is achieved by the action and modulation of writers (DNMTs, HATs and HMTs) that catalyze the addition of specific modifications on DNA or histone tails, erasers that remove specific marks or readers that are recruited to specific modifications (5), (6). Given the reversibility of epigenetic modifications, interest in the development of therapeutics targeting epigenetic enzymes has increased in recent years,

especially allosteric modulators (7), (8). While some success has been realized for some epigenetic enzymes, like histone modifiers, others have proven challenging in this regard (9-12). For instance, the FDA approved nucleoside inhibitors (azacytidine and decitabine), which function as prodrugs that are incorporated into DNA to inhibit the human *de novo* DNA methyltransferase 3A (DNMT3A), are highly cytotoxic due to formation of an irreversible DNMT3A-DNA suicide complex (13-15). In addition to these substrate DNA competitive inhibitors of DNMTs, several molecules that act as cofactor S-adenosyl-l-methionine (AdoMet) competitors to inhibit DNMT3A have been described (16-20). However, the use of competitive inhibitors of DNMTs presents several disadvantages compared to allosteric inhibitors in terms of specificity within a family of related proteins, non-related proteins with shared cofactor or inability to target surfaces involved with modulation of enzymatic activity.

Epigenetic mechanisms are characterized by highly integrated pathways involving extensive crosstalk, and this crosstalk is often mediated by protein-protein interactions (PPIs) (21-23). For instance, DNMT3A interacts with the Polycomb repressive complexes 2 (PRC2), a multimeric complex associated with transcriptional silencing that is composed of various histone modifiers and long noncoding RNAs (24-30). Through this interaction, DNMT3A-mediated DNA methylation contributes to the silencing of PRC2 target genes (24-26). Therefore, the disruption of protein-protein complexes could be a route to develop highly specific drugs targeting epigenetic pathways. However, based on the unique physicochemical properties of surfaces involved with PPIs, small molecules targeting PPIs have proven more challenging to predict compared to molecules targeting a binding pocket. Therefore, studies targeting PPIs largely rely on high-throughput screens of many chemically diverse compounds (31), (32). Based on this approach, there has been some

success in efforts aiming to identify small molecule inhibitors of epigenetic protein-protein interactions, specifically in distinct types of histone reader proteins and scaffolding proteins of epigenetic complexes (33). In addition to being recurrently mutated in patients with Acute Myeloid leukemia (AML), the biological importance of DNMT3A is highlighted by the fact DNMT3A interacts with a wide range of proteins with distinct biological functions, some of which share a binding surface with DNMT3L (Figure 1 A.) (34-39). Thus, DNMT3A is a suitable target for the potential use of small molecules to target PPIs in diseases like AML.

Recent work from our lab identified two compounds that do not display a competitive mechanism with DNA or AdoMet, and inhibition of enzymatic activity is due to binding an allosteric region outside the active site (Supplementary Figure 1 A. and B.) (Figure 1 A.) (40). Given that the ATRX-DNMT3-DNMT3L (ADD) domain or the tetramer interface of DNMT3A present two well-characterized surfaces for allosteric modulation of enzymatic activity (Figure 1 A.), we assessed whether compounds 1 or 2 disrupt interactions at these surfaces (Figure 1 B.) (36), (41), (42). With the use of mutational mapping, radiochemical and binding assays under various conditions, we show that compounds 1 or 2 selectively inhibit DNMT3A activity by disrupting interactions at the tetramer interface and that this mechanism of inhibition persists even when DNMT3A is in complex with distinct partner proteins. This work presents the characterization of two novel compounds with the potential use for modulation of epigenetic pathways through disruption of PPIs, which are likely to not display the toxicity commonly observed with current therapeutics targeting DNMT3A (13-15).

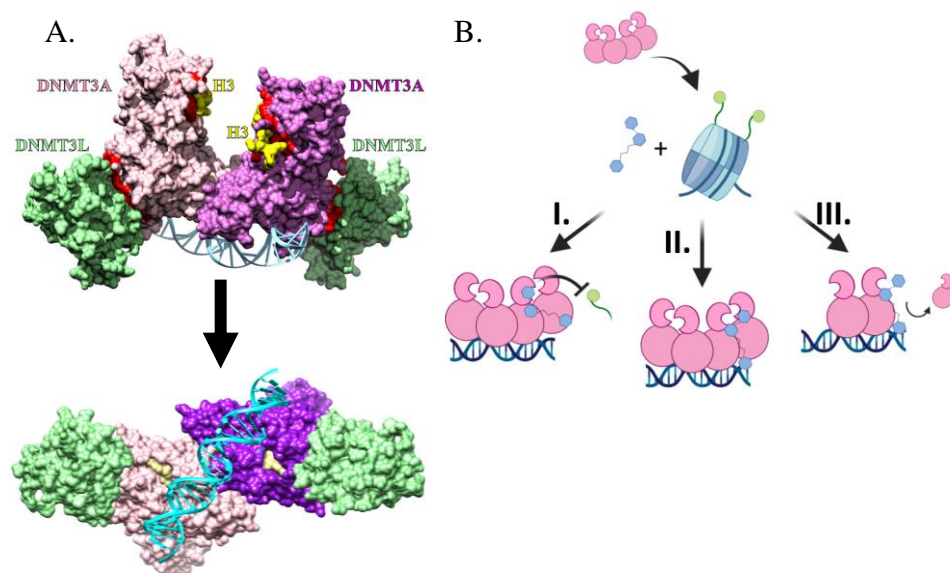


Figure 1. Surfaces involved with allosteric modulation of DNMT3A and models for disruption of modulation by compounds 1 and 2. **A.** Front and bottom view of a DNMT3A heterotetramer (■ and ■; a.a. 468-912) in complex with DNMT3L (■; a.a. 171-379) and Histone H3 peptides (■;1-12) with surfaces involved with interactions (■; < 5 Å) (adapted from PDB 4U7T). DNA (■) was modelled using the structure of a DNA-bound DNMT3A-DNMT3L complex (PDB 5YX2). **B.** Upon binding a target nucleosome, Compounds 1 or 2 may disrupt the allosteric modulation of DNMT3A by H3 tails (I.) or protein-protein interactions at the tetramer interface (II. and III.).

Results

Compounds 1 and 2 disrupt DNMT3A_WT homo- or heterotetramers but not Histone H3 tails- DNMT3A_WT interactions

While there have been several efforts to develop small-molecule inhibitors of DNMTs, to date, the FDA has only approved two nucleoside inhibitors (azacytidine and decitabine), which are highly cytotoxic (13), (15). We recently reported the discovery of two compounds (Supplementary Figure 1 A. and B.) that act as allosteric inhibitors of DNMT3A (i.e. not competitive with SAM or DNA) (40). However, the precise mechanism of action (Figure 1 B.) or the surface on DNMT3A bound by these inhibitors remain unknown (Figure 1 A.). Histone H3 tails and DNMT3L act as allosteric activators of

DNMT3A activity by binding the ADD domain or the tetramer interface of DNMT3A, respectively (36), (41), (42). Therefore, we assessed whether the allosteric inhibitors (Compound 1 or 2) disrupt the modulation of DNMT3A activity by Histone H3 tails or DNMT3L (Figure 2). We observed that the activity of DNMT3A_WT in reactions where DNMT3A_WT was pre-incubated with DNMT3L and Compound 1 (■ Figure 2 B.) or 2 (■, ■ Figure 2 B.) was lower compared to similar reactions with DNMT3A_WT, DNMT3L and DMSO (■ Figure 2 B. and E.; ***, $p < 0.001$). We found that under identical conditions other than pre-incubating DNMT3A_WT with Histone H3 tails and Compound 2 (■ Figure 2 A.), the activity of DNMT3A_WT in reactions with Compound 2 (■ Figure 2 A.) was not significantly different to that observed in reactions with DMSO (■ Figure 2 A.; ns, $p > 0.05$). Although DNMT3A and histone-modifying enzymes, like Lysine-specific demethylase 5A (KDM5A), modify distinct components of nucleosomes, both epigenetic enzymes are readers and writers of nucleosome substrates. We sought to determine whether Compounds 1 and 2 affect the activity of KDM5A to assess the specificity of these compounds for DNMT3A over an unrelated epigenetic enzymes and potential off-target effects in cells from non-specific interactions with other epigenetic readers and writers. We found that Compounds 1 and 2 minimally affect the demethylase activity of KDM5A relative to CPI-455, a well-established KDM5 inhibitor (Supplementary Figure 2). Based on the inhibition of DNMT3L-mediated stimulation of DNMT3A_WT activity by Compound 1 or 2 in reactions at equilibrium (Figure 2 B. and E.), we tested whether Compound 2 disrupts DNMT3A_WT homo- or heterotetramers carrying out DNA methylation (Figure 2 C. and D.). The addition of Compound 2 decreases the activity of DNMT3A_WT homotetramers (■ Figure 2 C.) or DNMT3A_WT-DNMT3L heterotetramers (■ Figure 2 D.) relative to similar reactions in which DMSO was added to catalytically active DNMT3A_WT

homotetramers (■ Figure 2 C.) or DNMT3A_WT-DNMT3L heterotetramers (■ Figure 2 D.).

In addition to DNMT3L, the activity of DNMT3A is modulated by distinct partner proteins through direct interactions with the tetramer interface of DNMT3A (7-11) (Figure 1 A.). Given that Compounds 1 and 2 disrupt the activation of DNMT3A activity by DNMT3L (Figure 2), we monitored the oligomeric state of DNMT3A_WT homo- or heterotetramers in the presence of these Compounds (Figure 1 B., II. or III.). For this approach, we measured the fluorescence anisotropy of a fluorescein (5'/6-FAM)-labelled 27-mer (GCbox30 duplex) in complex with DNMT3A_WT homo- or heterotetramers in the presence of Compounds 1 and 2 (Figure 3) (43), (44). We found that the addition of Compound 1 (■ Figure 3 A.) or 2 (■ Figure 3 B.) decreases the fluorescence anisotropy of DNA-bound DNMT3A_WT homotetramers compared to similar reactions with DMSO (■ Figure 3 A. and B.). Furthermore, increasing concentrations of DNMT3A_WT results in a lower change to the initial fluorescence anisotropy of FAM-DNA in reactions with Compound 1 (■ Figure 3 C.) or 2 (■ Figure 3 D.) relative to those with DMSO (■ Figure 3 C. and D.). Similarly, increasing concentrations of Compound 1 (■ Figure 3 E. and F.) or 2 (■ Figure 3 E. and F.) drastically decreases the initial fluorescence anisotropy of DNMT3A_WT-p53 (E.) or DNMT3A_WT-TDG (F.) heterotetramers bound to FAM-DNA compared to similar reactions consisting of DNMT3A_WT homotetramers (■ Figure 3 E. and F.) or heterotetramers with p53 (■ Figure 3 E.) or TDG (■ Figure 3 F.) challenged by the addition of DMSO. In fact, we observed that increasing levels of Compound 1 (■ Figure 3 E. and F.) or 2 (■ Figure 3 E. and F.) to DNMT3A_WT-p53 (Figure 3 E.) or DNMT3A_WT-TDG (Figure 3 F.) heterotetramers on FAM-DNA led to a final anisotropy value comparable to reactions with DNMT3A_WT homotetramers and Compound 2 (600

μM) at the start of the reaction (■ Figure 3 E. and F.). In sum, our observation that the addition of Compounds 1 and 2 under distinct conditions decreases the background subtracted (FAM-DNA only) initial fluorescence anisotropy of DNMT3A_WT homotetramers-FAM-DNA complexes (Figure 3) is consistent with the inhibition of enzymatic activity by these compounds involving disruptions to the oligomeric state of DNMT3A (Figure 1 B. III).

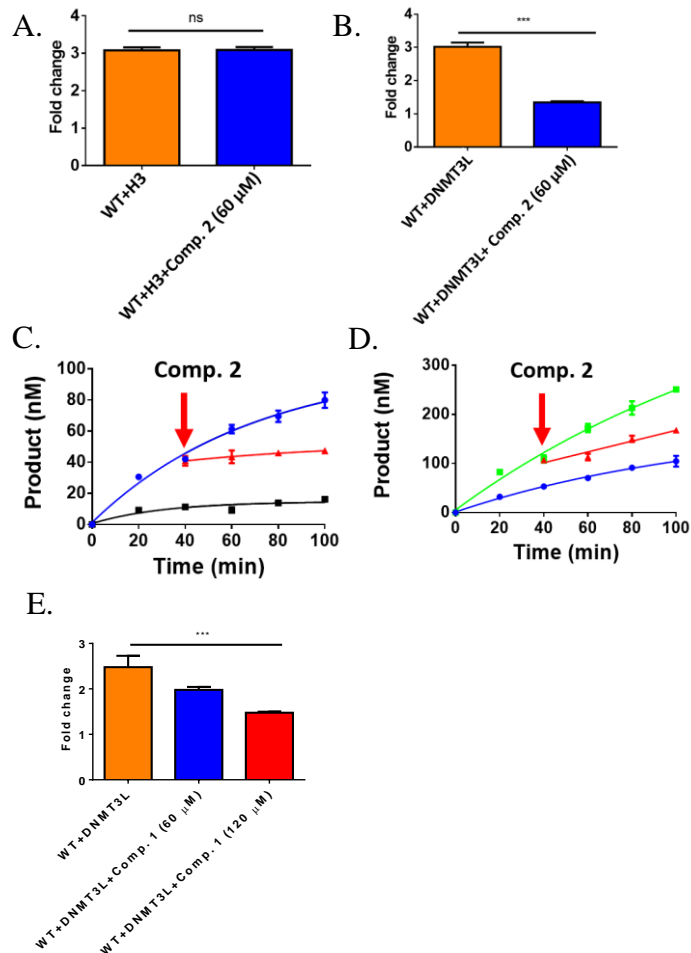


Figure 2. Compounds do not inhibit the activation of DNMT3A_WT by H3 peptides but disrupt DNMT3A-DNMT3L interactions at the DNMT3A tetramer interface. While compound 2 fails to disrupt the activation of full-length DNMT3A_WT **A.**, Compounds 1 and 2 inhibit the stimulation of DNMT3A_WT activity by DNMT3L in reactions at equilibrium (**B.** and **E.**) and actively methylating DNMT3A_WT homotetramers (**C.**; ■ DNMT3A_WT, ■ DNMT3A_WT with Comp. 2,) or DNMT3A_WT-DNMT3L heterotetramers (**D.**; ■ DNMT3A_WT, ■ DNMT3A_WT-DNMT3L). Reactions in (**A.**), (**B.**) and (**E.**) consisted of 150 nM DNMT3A_WT pre-incubated for 1 hour at 37°C with H3 peptides (5 μM; residues 1-21) (**A.**) or DNMT3L (150 nM; **B.** and **E.**) in buffer containing compound 1 (**E.**) or 2 (**A.** and **B.**). While reactions in (**C.**) and (**D.**) consisted of 50 nM DNMT3A_WT, reactions in (**D.**) consisted of DNMT3A_WT-DNMT3L (1:1 at 50 nM) that was pre-incubated for 1 hour at 37°C prior to the start of the reaction. All reactions (**A.-E.**) were initiated by the addition of Poly dI-dC (5 μM). Fold change (**A.-E.**) refers to data normalized to the activity of reactions consisting of DNMT3A_WT only. All data reflect the mean and s.d. of 3 independent experiments. A T-test (**A.** and **B.**) or one-way analysis of variance (**E.**) was used to compare the values of reactions containing compound 1 (**E.**) or 2 (**A.** and **B.**) to those without compound 1 or 2 (ns, $p > 0.05$; ***, $p < 0.001$).

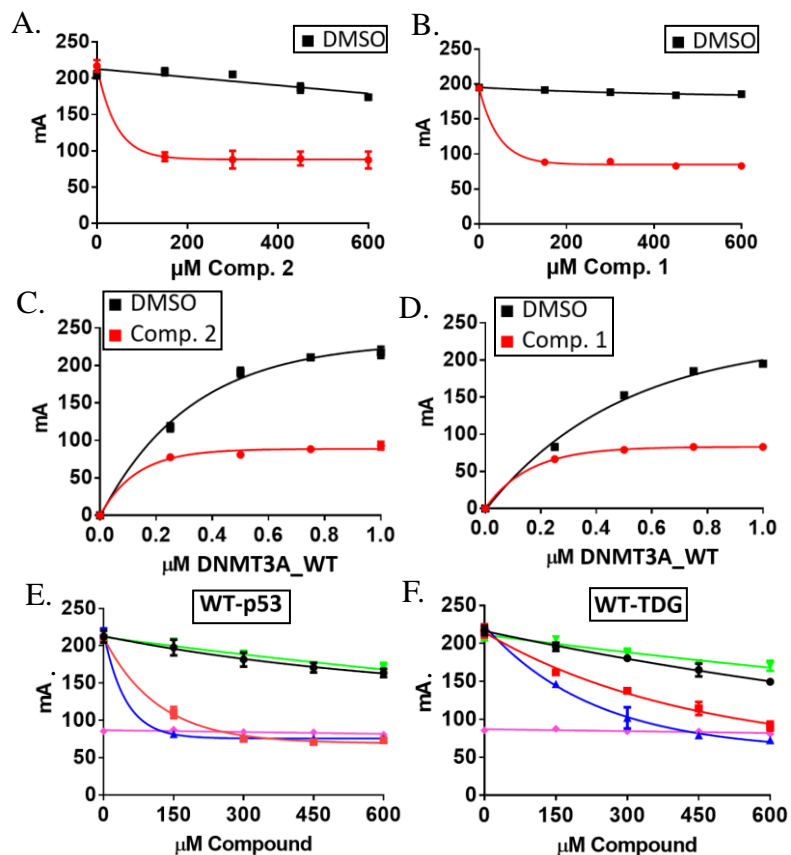


Figure 3. Compounds disrupt to DNA-bound DNMT3A_WT in complex with distinct partner proteins. While the addition of DMSO (A. and B.) does not disrupt DNA-bound (50 nM of 5' FAM-6-labeled GCbox30 duplex) DNMT3A_WT homotetramers (1 μM), increasing concentrations of Compound 1 (B.) or 2 (A.) decrease the fluorescence anisotropy (millianisotropy units (mA)) of DNMT3A_WT complexes on DNA. The addition of DNMT3A_WT to reactions consisting of Compound 1 (D.) or 2 (C.) leads to a lower change to the fluorescence anisotropy of FAM-labeled substrate DNA relative to similar reactions with DMSO (C. and D.). Increasing concentrations of Compound 1 (■ E. and F.) or 2 (■ E. and F.) decreases the fluorescence anisotropy of DNMT3A_WT-p53 (E.) or DNMT3A_WT-TDG (F.) complexes on DNA (GCbox30 duplex). The following reactions were performed as controls in (E.) and (F.): DNMT3A_WT with DMSO (■; E. and F.), DNMT3A_WT-p53 with DMSO (■ E.), DNMT3A_WT-TDG with DMSO (■ F.) and DNMT3A_WT with Compound 2 at the beginning of the reaction (■; E. and F.). Data reflect the mean and s.d. of 3 independent experiments.

Oligomerization of DNMT3A_R771A with DNMT3L restores inhibition by Compound 2

In previous work we show that substitutions to specific residues at the tetramer interface of DNMT3A disrupt the oligomeric state, processive catalysis and modulation by partner proteins (43), (45-47). Interestingly, inspection of the binding pose of Compound 2 to the DNMT3A tetramer interface predicted that Compound 2 stably interact with key residues involved in these processes (Supplementary Figure 3). Based on these observations and data showing Compounds 1 and 2 interfere with interactions at the tetramer interface of DNMT3A (Figure 1 B. and Figure 2), we assessed the effect of Compound 2 on DNMT3A tetramer interface Alanine substitutions (R729, E733, R736 and R771; Supplementary Figure 1 C.). Initially, we assessed the effect of Compound 1 or 2 on the activity of DNMT3A tetramer interface mutants in reactions initiated by the addition of substrate DNA following a short pre-incubation (10 minutes) with Compound 2 (Figure 4 A. and B.). While all the DNMT3A tetramer interface mutants (R729, E733, R736 and R771) were differentially responsive to Compound 2 relative to DNMT3A_WT (Figure 4 A.; ***, $p < 0.001$), we found that DNMT3A_R771A (■ Figure 4 B.) was the only mutant that was not inhibited by Compound 2 (ns, $p > 0.05$; *, $p < 0.01$). We then carried out similar reactions consisting of DNMT3A tetramer interface mutants that were pre-incubated with DNMT3L and Compound 2 prior to being initiated (Figure 4 C. and D.). Unlike reactions without DNMT3L (Figure 4 A. and B.), inhibition of DNMT3A tetramer interface mutants (R729, E733, R736 and R771) in complex with DNMT3L was comparable to that observed for DNMT3A_WT-DNMT3L heterotetramers (Figure 4 C.; ns, $p > 0.05$). Furthermore, Compound 2 inhibited the activity of DNMT3A_R771A in DNMT3A_R771A-DNMT3L heterotetramers (■ Figure 4 D.), which was not observed in reactions without DNMT3L (■ Figure 4 B.). To further examine the inhibition of DNMT3L-mediated activation of

DNMT3A tetramer interface mutants (■ Figure 4 D.), we then assessed the effect of Compound 2 on the fluorescence anisotropy of tetramer interface mutant DNMT3A-DNMT3L heterotetramers bound to FAM-DNA (Figure 4 E.). We initially monitored changes to the fluorescence anisotropy of dimeric DNMT3A tetramer interface mutants bound to FAM-DNA by the addition of DNMT3L to confirm the formation of tetramer interface mutant DNMT3A-DNMT3L heterotetramers. The increase to the fluorescence anisotropy of FAM-DNA bound by DNMT3A_R771A (■ Figure 4 E.) or DNMT3A_R729A (■ Figure 4 E.) observed by the addition of DNMT3L was comparable to fluorescence anisotropy values of DNMT3A_WT-DNMT3L heterotetramers in complex with FAM-DNA (■ Figure 4 E.). While the addition of DMSO did not alter the fluorescence anisotropy of these complexes (Figure 4 E., DNMT3L with ■ DNMT3A_WT, ■ DNMT3A_R771A or ■ DNMT3A_R729A), the addition of Compound 2 reduced the fluorescence anisotropy of FAM-DNA bound by DNMT3A_WT (■ Figure 4 E.), DNMT3A_R771A (■ Figure 4 E.) or DNMT3A_R729A (■ Figure 4 E.) in complex with DNMT3L to comparable levels as that observed prior to the addition of DNMT3L. Therefore, our data show the formation of DNMT3A_R771A-DNMT3L heterotetramers restores the ability of Compound 2 to inhibit DNMT3A_R771A activity by disrupting interactions at the tetramer interface (Figure 1 B.).

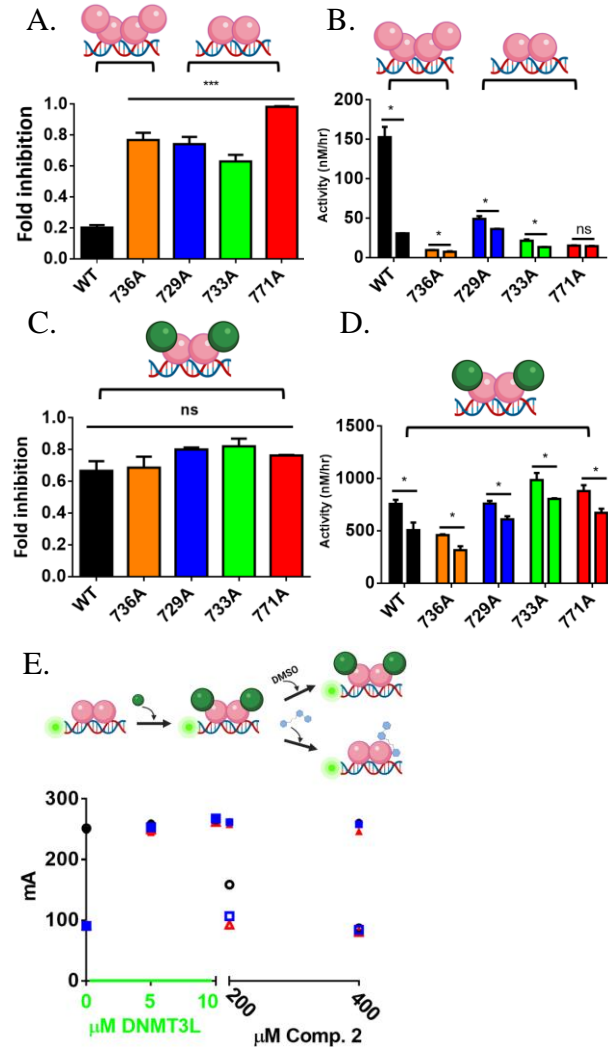


Figure 4. Compound 2 inhibits DNMT3A_R771A-DNMT3L heterotetramers but not DNMT3A_R771A homodimers. (A. and B.) DNMT3A tetramer interface mutants are differentially responsive to modulation by Comp. 2 relative to WT with R771A unresponsive to inhibition (B.). (C. and D.) Formation of mutant DNMT3A heterotetramers with DNMT3L leads to comparable levels of inhibition by Comp. 2 as WT-DNMT3L complexes and restores inhibition of R771A (D.). (E.) The addition of Comp. 2 decreases the fluorescence anisotropy of DNMT3L heterotetramers with DNMT3A WT (■), R771A (■) or R729A (■) bound to FAM-labeled DNA (GCbox30 duplex). Similar reactions consisting of DNMT3L in complex with DNMT3A WT (■), R771A (■) or R729A (■) to which DMSO was added were performed as controls. (A.-D.) consisted of 150 nM WT or mutant DNMT3A, 150 nM DNMT3L (C. and D.; pre-incubated for 1 hour at 37°C) and were initiated by the addition of Poly dI-dC (5 μM). Fold inhibition (C. and D.) refers to $1 - (\text{product formed with Comp. 2}/\text{product formed without Comp. 2})$. A one-way analysis of variance (A. and C.) was used to compare the values of reactions with DNMT3A mutants to those with WT. A T-test (B. and D.) was performed to compare the values of reactions containing comp. 2 to those without comp. 2 (ns, $p > 0.05$; ***, $p < 0.001$; *, $p < 0.01$). All data reflect the mean and s.d. of 3 independent experiments.

Compounds 1 and 2 disrupt interactions at the tetramer interface of DNMT3A_R882H

The DNMT3A R882H substitution is the most frequently detected *DNMT3A* mutation in AML patients (37-39). Although located at the major surface of DNMT3A for DNA binding (Supplementary Figure 1), the R882H substitution appears to alter the interactions between DNMT3A and distinct partner proteins, including those that bind the DNMT3A tetramer interface (42),(47), (48). Given the biological impact of R882H substitutions and the effect of R882H on protein-protein interactions involving DNMT3A, we explored the consequences of Compounds 1 or 2 on DNMT3A_R882H-DNMT3L heterotetramers (Figure 5). Like that observed in reactions with DNMT3A_WT (Figure 2 B.), we found that a one-hour pre-incubation of DNMT3A_R882H, DNMT3L and Compound 1 (■, ■ Figure 5 B.) or 2 (■, ■ Figure 5 A.) decreases the activation of DNMT3A_R882H by DNMT3L relative to similar reactions consisting of DNMT3A_R882H, DNMT3L and DMSO (■ Figure A. and B.; ***, $p < 0.001$). Furthermore, the addition of Compound 2 (■ Figure 5 C.; 120 μ M) decreases product formation (nM methylated DNA) in catalytically active DNMT3A_R882H-DNMT3L heterotetramers relative to reactions with DNMT3A_R882H-DNMT3L heterotetramers challenged with the addition of DMSO (■ Figure 5 C.). To further examine the effect of Compounds 1 or 2 on protein-protein interactions involving DNMT3A_R882H, and like that performed in reactions with DNMT3A_WT (Figure 3) and tetramer interface mutants (Figure 4), we monitored the fluorescence anisotropy of DNA-bound DNMT3A_R882H in complex with distinct partner proteins and under various conditions (Figure 6). As observed in tetramer interface mutants (R729A and R771A, Figure 4 E.), the addition of DNMT3L increases the initial fluorescence anisotropy of DNMT3A_R882H dimers on FAM-DNA (■, ■ Figure 6 A. and B.). Compared to reactions with DNMT3A_R882H-DNMT3L

heterotetramers to which DMSO was added (■ Figure 6 A. and B.), the addition of Compound 1 (■ Figure 6 B.) or 2 (■ Figure 6 A.) reduces the fluorescence anisotropy of DNA-bound DNMT3A_R882H-DNMT3L to similar levels as that observed prior to the addition of DNMT3L. Moreover, the addition of DNMT3L does not appear to change the initial fluorescence anisotropy of DNMT3A_R882H complexes on FAM-DNA in reactions with Compound 1 (■ Figure 6 D.) or 2 (■ Figure 6 C.) compared to similar reactions with DMSO (■ Figure 6 C. and D.). To assess whether this effect (Figure 6 A.-D.) is also observed in DNMT3A_R882H heterotetramers, we monitored the fluorescence anisotropy of DNA-bound DNMT3A_R882H in complex with p53 (Figure 6 E.) or TDG (Figure 6 F.) challenged with increasing concentrations of Compound 1 or 2. The addition of DMSO minimally reduces the fluorescence anisotropy of DNA-bound DNMT3A_R882H heterotetramers with DNMT3L (■ Figure 6 E. and F.), p53 (■ Figure 6 E.) or TDG (■ Figure 6 F.). However, increasing concentrations of Compound 1 (■, Figure 6 E. and F.) or 2 (■, Figure 6 E. and F.) decreased the fluorescence anisotropy of DNA-bound DNMT3A_R882H-p53 (E.) or DNMT3A_R882H-TDG (F.) heterotetramers to similar levels as that observed in controls consisting of DNMT3A_R882H, DNMT3L and Compound 2 from the start of the reaction (■, Figure 6 E. and F.). Here we show that Compounds 1 and 2 disrupt protein-protein interactions involving the biomedically relevant R882H substitution in DNMT3A and partner proteins with distinct biological functions.

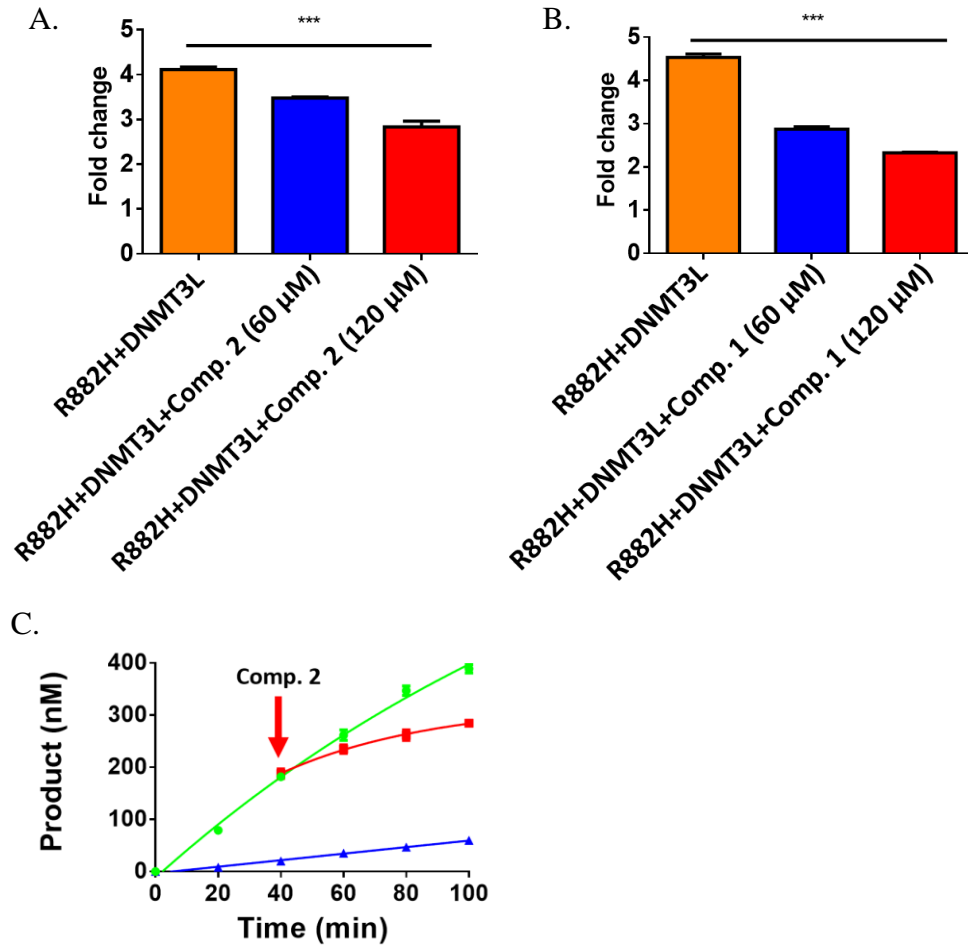


Figure 5. Compounds 1 and 2 inhibit the activation of DNMT3A_R882H by DNMT3L. (A. and B.) Compounds 1 and 2 disrupt the activation of DNMT3A_R882H enzymatic activity by DNMT3L in reactions at equilibrium (A. and B.) as well as actively methylating DNMT3A_R882H-DNMT3L complexes (■ C.). Reactions in (A. and B.) consisted of 150 nM DNMT3A_R882H pre-incubated for 1 hour at 37°C with DNMT3L (150 nM; B. and E.) in buffer containing compound 1 (E.) or 2 (A. and B.). Reactions in (C.) consisted of 50 nM DNMT3A_R882H (■) and DNMT3A_R882H-DNMT3L (■; 1:1 at 50 nM and pre-incubated for 1 hour at 37°C). All reactions (A.-C.) were initiated by the addition of Poly dI-dC (5 μM). Fold change (A. and B.) refers to data normalized to the activity of reactions consisting of DNMT3A_R882H only. A one-way analysis of variance (A. and B.) was carried out to compare the averages of reactions with DNMT3A_R882H-DNMT3L complexes under various conditions.

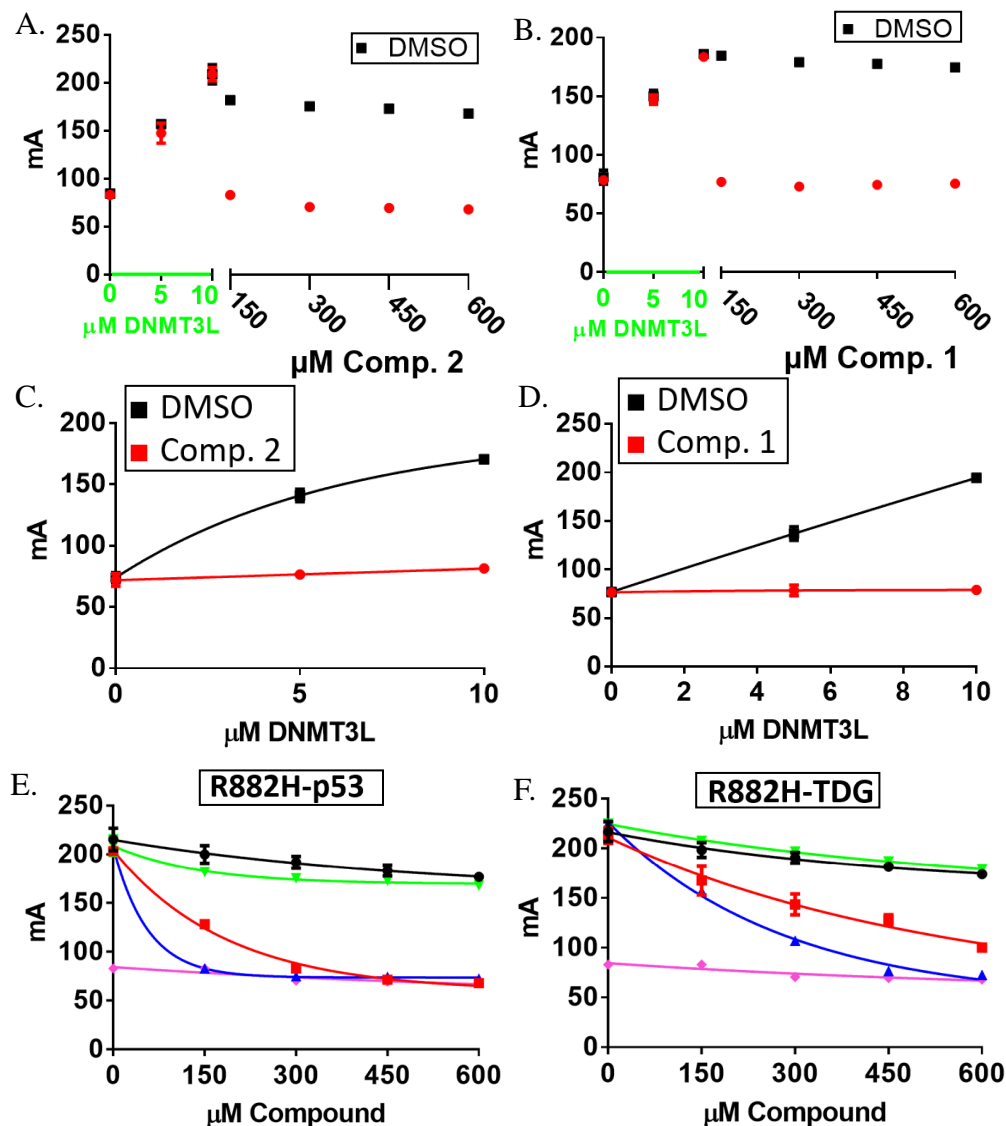


Figure 6. Compounds disrupt DNA-bound DNMT3A_R882H heterotetramers with distinct partner proteins. The addition of Compound 1 (B.) or 2 (A.) decreases the fluorescence anisotropy (millianisotropy units (mA)) of DNA-bound (50 nM of 5' FAM-6-labeled GCbox30 duplex) DNMT3A_R882H-DNMT3L complexes relative to similar reactions to which DMSO was added (A. and B.). While the addition of DNMT3L increases the fluorescence anisotropy of DNMT3A_R882H in complex with DNA in DMSO (C. and D.), increasing levels of DNMT3L do not change the fluorescence anisotropy of DNA-bound (GCbox30 duplex) DNMT3A_R882H in the presence of Compound 1 (D.) or 2 (C.). Increasing amounts of Compound 1 (■; E. and F.) or 2 (■; E. and F.) decrease the fluorescence anisotropy of DNMT3A_R882H-p53 (E.) or DNMT3A_R882H-TDG (F.) complexes on DNA (GCbox30 duplex). (E. and F.) The following reactions were performed as controls: DNMT3A_R882H-DNMT3L with DMSO (■; E. and F.), DNMT3A_R882H-p53 (■; E.) or -TDG (■; F.) with DMSO and DNMT3A_R882H-DNMT3L with Compound 2 at the beginning of the reaction (■; E. and F.). All data reflect the mean and s.d. of 3 independent experiments.

Discussion

There is expanding experimental evidence that epigenetic mechanisms are interdependent and comprise a regulatory network whose crosstalk contributes to transcriptional regulation (21-23). Given that this crosstalk involves the interactions of distinct multimeric protein complexes, therapeutics targeting PPIs of epigenetic writers, readers, and erasers are of keen interest (33). Small molecule therapeutics targeting DNMTs are limited to nucleoside inhibitors (azacytidine and decitabine) and molecules that act as competitive inhibitors of substrate DNA or cofactor AdoMet, which have been reported as being cytotoxic (13-20). These observations led us to screen a diverse chemical library in which we identified two structurally related pyrazolone (Compound 1) and pyridazine (Compound 2) allosteric inhibitors of DNMT3A (40). Here we present evidence that inhibition of enzymatic activity by Compound 1 or 2 is achieved through disruption of PPIs at the tetramer interface of DNMT3A in DNMT3A homo- or heterotetramers (Figure 1 B.). Compounds 1 and 2 are the only reported small molecule inhibitors of PPIs with DNMT3A to date. Therefore, our findings present the potential use of these compounds to chemically manipulate the modulation of DNMT3A and the treatment of malignancies associated with aberrant modulation of DNMT3A activity, like AML (37-39), (43), (46), (47).

Previously we reported two allosteric inhibitors that inhibit enzymatic activity by binding outside the active site (Figure 1 A.). Subsequently we assessed whether Compounds 1 and 2 disrupt interactions at the allosteric surfaces known to modulate DNMT3A (■, Figure 1 A.) to help define their mechanism of action. Given that Compounds 1 and 2 disrupt interactions at the tetramer interface of DNMT3A (Figure 2 B.-E.), but not at the ADD domain (Figure 2 A.), our data are consistent with these compounds acting as PPIs without impacting DNMT3A-H3 tail interactions (Figure 1 B., II. and III.). Our anisotropy results show that the addition of Compounds 1 or 2 results in the formation of a smaller

DNMT3A_WT-FAM-DNA complex, suggesting that both compounds disrupt interactions between DNMT3A and partner proteins (Figure 1 B. III.). Furthermore, this mechanism of action is not specific to WT DNMT3A-DNMT3A interactions at the tetramer interface because we obtain similar results for two partner proteins with a shared binding surface on DNMT3A but are associated with distinct biological functions (Figure 3 E. and F.) (33), (34), (42), (46). The direct association and functional cooperation between DNMT3A and partner proteins with distinct biological functions is well documented (24-26), (33), (34), (42), (46). In fact, it has been shown that DNMT3A may act as a scaffold for epigenetic regulatory complexes (24-26) in addition to directly influencing the activity of distinct partner proteins (33), (34). Thus, the use of small molecules targeting binding partners of DNMT3A, like Compounds 1 and 2, may serve to manipulate the DNA methylation-independent activities of DNMT3A.

Specific residues at the dimer (R882) and tetramer interface (R729, E733, R736 and R771) of DNMT3A are often mutated in AML patients and have been identified as major contributors to the oligomeric state, processive catalysis and modulation by partner proteins (36), (43), (45-47). We show Compounds 1 and 2 inhibit the activity of homodimer mutants (R729A, E733A and R882H) located at both the dimer (R882H, Figure 5 A.-C.) and tetramer (R729A and E733A, Figure 4 A. and B.) interfaces (Supplementary Figure 1 C.). Thus, inhibition of DNMT3A activity by Compounds 1 and 2 does not come entirely from disruptions of PPIs at the tetramer interface, and that once bound, these compounds further inhibit the catalytic activity of DNMT3A (Figure 1 B. III.). We also identified a dimer mutant located at the tetramer interface (R771A) (Supplementary Figure 1 C.) that was only responsive to inhibition of enzymatic activity (Figure 4 A.-D.) through disruption of PPIs by compound 2 in heterotetrameric complexes with DNMT3L (Figure 4 E.). These findings

provide insights into the amino acid side chain interactions that are essential for inhibition and provide a basis for future structure-activity relationship (SAR) studies to determine the precise molecular interactions involved with inhibition of DNMT3A activity by Compounds 1 and 2. Studies have shown that DNMT3A R882H contributes to leukemogenesis by silencing differentiation-associated genes in hematopoietic stem cell (HSC) in a DNA methylation-independent manner through the aberrant recruitment of the PRC1 complex (47). Here we show that Compounds 1 and 2 disrupt the activation of DNMT3A R882H through PPIs at the tetramer interface (Figure 5 A.-C.), and perhaps more notably, these compounds disrupt DNMT3A R882H complexes with distinct partner proteins (Figure 6 A.-F.). Given that the R882H substitutions impacts distal interactions at the tetramer interface (Supplementary Figure 1 C.) (42), (45), future SAR studies using Compounds 1 and 2 may additionally lead to the development of small molecules that specifically target DNMT3A R882H and the aberrant PPIs associated with this substitution, like that observed with PRC1 in leukemogenesis (47).

In summary, our study aiming to characterize the inhibition of DNMT3A activity by the recently described Compounds 1 and 2 revealed that the mechanism of inhibition involves disruption of PPIs at the tetramer interface. The ability to allosterically manipulate the DNA methylation activity and interactions involving DNMT3A provides a basis for improved toxicity, which is dose limiting for currently used drugs targeting DNA methylation (13-20). Further optimization of these compounds and the discovery of novel PPI inhibitors provides a promising approach for the treatment of diseases that display disruptions to the PPIs associated with DNMT3A, such as AML (47).

Methods

Expression constructs

The plasmids used for expression of recombinant human proteins were as follows: pET28a-hDNMT3ACopt for DNMT3A full length (49), pET28a-hDNMT3A_catalytic_domain for wild type or mutants of DNMT3A catalytic domain (Δ 1–633) (50), pTYB1–3L was used to express full-length human DNMT3L (35), pET15b-human p53 for expression of full-length (1–393) human p53 (51) and pET28a-hTDG for full-length TDG (1-410) (52). DNMT3A mutants were generated using pET28a-hDNMT3A_catalytic_domain as a template and described in (45).

Protein expression and purification

DNMT3A full length and catalytic domain (WT and mutants), DNMT3L, p53, and TDG were expressed in NiCo21(DE3) Competent *E. coli* cells (New England Biolabs). Cells were grown in LB media at 37 °C to an A600 nm of 0.9 (DNMT3A full length), 0.7 (DNMT3A catalytic domain WT and mutants), 0.7 (DNMT3L), 0.6 (p53), and 0.8 (TDG). Protein expression was induced by the addition of 1 mM isopropyl- β -D-thiogalactopyranoside (GoldBio) after lowering the temperature to 28 °C. Induction times were 5 h for DNMT3A full length and catalytic domain (WT and mutants), 5 h for DNMT3L, 5 h for TDG, 16 h for p53. Cell pellets were harvested by centrifugation at 5000g for 15 min and stored at –80 °C.

DNA methylation assays

DNA methylation reactions were carried out to monitor the ability of DNMT3A to incorporate tritiated methyl groups from AdoMet onto DNA substrates in the absence or presence of Compounds 1 and 2 under distinct experimental conditions involving biological modulators of DNMT3A (Histone tails and partner proteins). Assays were performed at 37 °C in a methylation reaction buffer consisting of 50 mM $\text{KH}_2\text{PO}_4/\text{K}_2\text{HPO}_4$ (pH 7.8), 1 mM

EDTA, 1mM DTT, 0.2 mg/mL BSA, 20 mM NaCl and with saturating AdoMet (15 μ M). For these reactions, 50 μ M (3 H) methyl-labeled: unlabeled, 1:10) AdoMet stocks were prepared from 32 mM unlabeled AdoMet (NEB) and 3 H methyl-labeled AdoMet (80 Ci/mmol; supplied by PerkinElmer) in 10 mM H₂SO₄. Poly dI-dC (5 μ M) was used as a substrate due to the increased activity of DNMT3A in this substrate, which allows a higher level of detection to changes in enzymatic activity. Reactions were quenched by mixing aliquots taken from a larger reaction with 0.1% SDS (1:1) and spotted onto Hybond-XL membranes (GE healthcare). Samples were then washed, dried, and counted using a Beckman LS 6000 liquid scintillation Counter as described in (53). In reactions assessing disruption of PPIs with DNMT3A at equilibrium, DNMT3A was incubated for 1 hour at 37 °C in methylation reaction buffer containing Compounds 1, 2 or DMSO prior to initiating the reaction by the addition of Poly dI-dC.

Fluorescence anisotropy

Changes to fluorescence anisotropy were monitored using a Tecan microplate reader equipped with excitation and emission polarizers (excitation: 485 nm, emission 535 nm) at room temperature. Reactions involving DNMT3A (or distinct DNMT3A heterotetramers) complexes with FAM-labelled DNA were carried out in the following buffer: 50 mM KH₂PO₄/K₂HPO₄ (pH 7.8), 1 mM EDTA, 1 mM DTT, 0.2 mg/ml BSA, 20 mM NaCl with 50 μ M Sinefungin. The DNA substrate (Gcbox30) for binding reactions consisted of a duplex with a fluorescein (6-FAM) label on the 5' end of the top strand (5'/6 FAM/TGGATATCTAGGGGGCGGCTATGATATCT-3'; the recognition site for DNMT3A is underlined) (44). Briefly, fluorescence anisotropy measurements of DNA-bound DNMT3A homo- or heterotetramers were taken following a 5-minute incubation after the addition of Compound 1, 2 or DMSO. Alternatively, Compounds were added to DNMT3A 40 minutes

following the addition of Poly dI-dC to assess whether these compounds inhibit catalytically active DNMT3A.

Computational docking

Using SWISS-MODEL a model of the catalytic domain (res 629-912) of DNMT3A was constructed using the solved crystal structure 4u7t as a template (54). This structure was then prepared for docking using AutoDock Tools (55). The structures of the small molecules were prepared using Gypsum-DL (56). The small molecules were docked to the protein surface using AutoDock Vina (56).

Computational dynamics

With the GROMACS 2020.04 molecular dynamics software package, the docked protein ligand complexes could be further evaluated (57-59). The CHARMM36m force field was used to parameterize the protein structure (60), (61). In order to parameterize the small molecules the CGenFF tool was used (62), (63). The assembled complex was solvated with TIP3P water molecules and neutralized with chloride counterions. This system was subsequently minimized and simulated for 100 ps first at constant volume and temperature (NVT) and then at constant pressure and temperature (NPT). Restraints were applied to the heavy atoms in the complex during these steps. This resulted in a protein-ligand system equilibrated at 300 K. The complexes were subjected to an unrestrained 10 ns dynamics simulation.

Computational affinity calculations

Using the trajectory file containing the positions, velocities, and forces for the atoms in the 10 ns protein-ligand simulation, molecular mechanics generalized-Born surface area (MM/GBSA) calculations were performed. This method approximates binding affinity using

five distinct energy terms examining the difference between bound and unbound (eq1).

These calculations were handled by the program gmx_MMPBSA (63).

$$\Delta G_{bind} = (\Delta E_{vdw} + \Delta V_{el} + \Delta V_{int}) + (\Delta G_{polar} + \Delta G_{non-polar})$$

The five energy terms can be divided into two groups. The Van der Waals', Coulombic and Internal energies are computed using standard molecule mechanics (MM) methods, while the changes in polar and non-polar energy are determined using the generalized-Born (GB) method and changes in solvent accessible surface area (SASA) respectively.

Supplementary Material

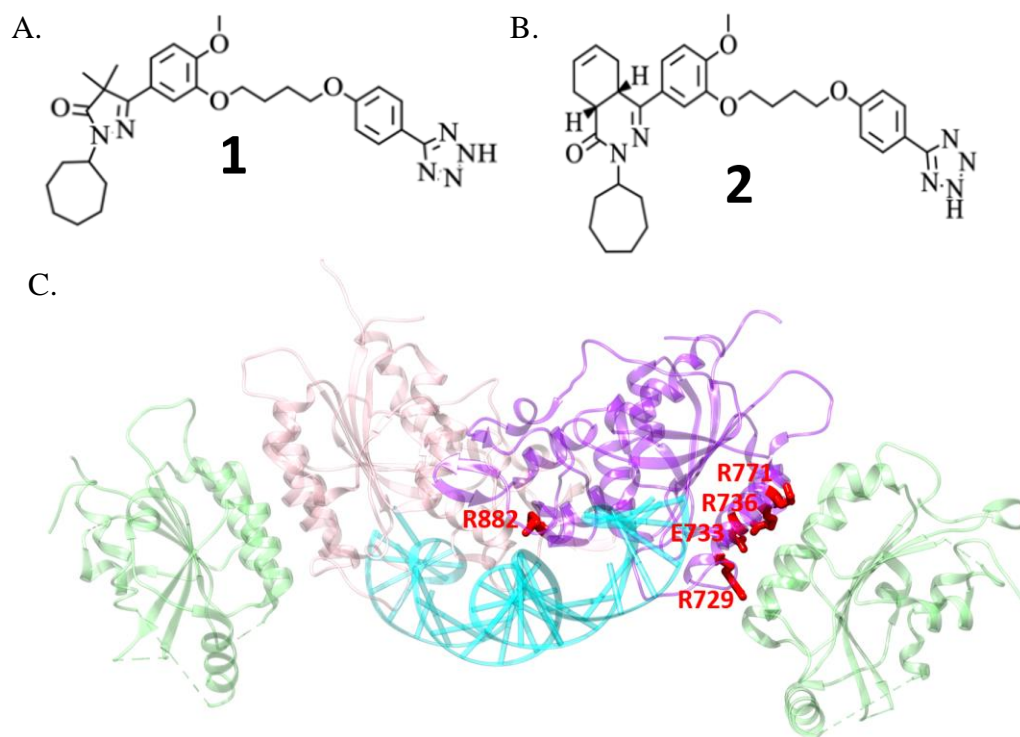


Figure S1. Structure of Compounds 1 or 2 as well as DNMT3A mutants explored in this study. (A. and B.) Structure of related pyrazolone (1) and pyridazine (2) inhibitors. (C.) Crystal structure of a DNA-bound DNMT3A-DNMT3L heterotetramer (adapted from PDB 5YX2) depicting tetramer interface (R729, E733, R736 and R771) and dimer interface (R882H) substitutions assayed in this study.

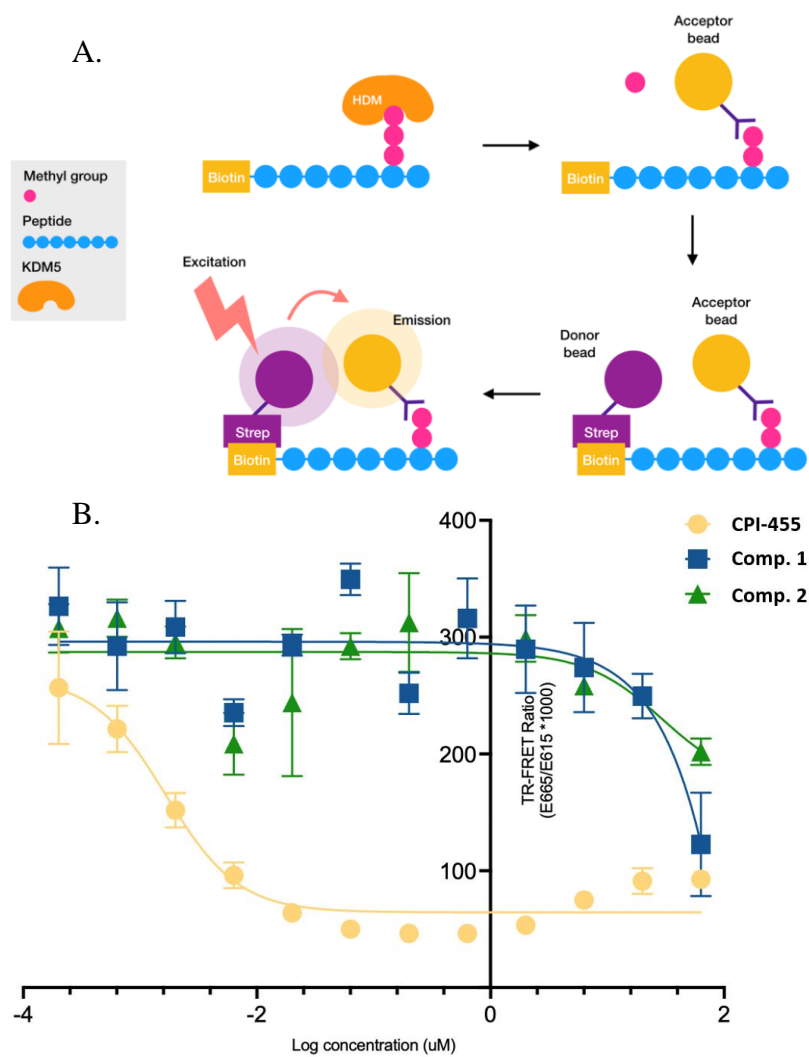


Figure S2. Compounds 1 and 2 do not inhibit the activity of the H3K4 histone demethylase KDM5.

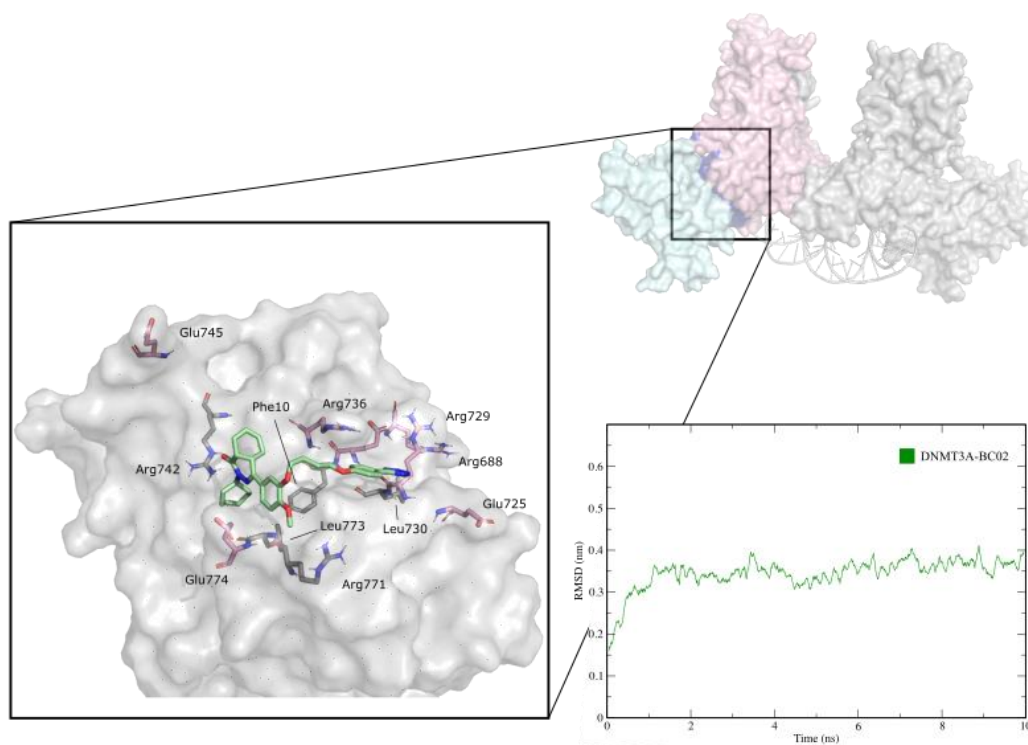


Figure S3. Inspection of the binding pose of Compound 2 on the tetramer interface. The position of the allosteric molecule Compound 2 in the tetramer interface of DNMT3A following a 10 ns simulation of Compound 2 with a single catalytic monomer is shown with its trajectory. A monomer (pink) is shown with the position of this interface (blue) shown relative to the entire crystal structure (PDB: 4u7t) with DNA modeled in (PDB: 6kda). The top contacts defined by their contribution to the MM/GBSA calculation are shown in pink and labeled. Conserved residues are in grey. (Note currently Arg742 and Arg771 are both conserved and top contacts). The Compound 2 scaffold lies over the conserved residues with strong coulombic contributions from surrounding PPI residues (mainly Arg and Glu).

References

Chapter I

1. Gibney, E. R., and Nolan, C. M. (2010) Epigenetics and gene expression. *Heredity*. **105**, 4–13
2. Kim, M., and Costello, J. (2017) DNA methylation: an epigenetic mark of cellular memory. *Exp Mol Med*. **49**, e322–e322
3. Hata, K., Okano, M., Lei, H., and Li, E. (2002) Dnmt3L cooperates with the Dnmt3 family of de novo DNA methyltransferases to establish maternal imprints in mice. *Development*. **129**, 1983–1993
4. Savell, K. E., Gallus, N. V. N., Simon, R. C., Brown, J. A., Revanna, J. S., Osborn, M. K., Song, E. Y., O'Malley, J. J., Stackhouse, C. T., Norvil, A., Gowher, H., Sweatt, J. D., and Day, J. J. (2016) Extra-coding RNAs regulate neuronal DNA methylation dynamics. *Nat Commun*. **7**, 12091
5. Challen, G. A., Sun, D., Jeong, M., Luo, M., Jelinek, J., Berg, J. S., Bock, C., Vasanthakumar, A., Gu, H., Xi, Y., Liang, S., Lu, Y., Darlington, G. J., Meissner, A., Issa, J.-P. J., Godley, L. A., Li, W., and Goodell, M. A. (2011) Dnmt3a is essential for hematopoietic stem cell differentiation. *Nat Genet*. **44**, 23–31
6. Sharma, S., Kelly, T. K., and Jones, P. A. (2010) Epigenetics in cancer. *Carcinogenesis*. **31**, 27–36
7. Bednar, J., Horowitz, R. A., Grigoryev, S. A., Carruthers, L. M., Hansen, J. C., Koster, A. J., and Woodcock, C. L. (1998) Nucleosomes, linker DNA, and linker histone form a unique structural motif that directs the higher-order folding and compaction of chromatin. *PNAS*. **95**, 14173–14178
8. Becker, P. B., and Workman, J. L. (2013) Nucleosome Remodeling and Epigenetics. *Cold Spring Harb Perspect Biol*. **5**, a017905
9. Miller, J. L., and Grant, P. A. (2013) The Role of DNA Methylation and Histone Modifications in Transcriptional Regulation in Humans. *Subcell Biochem*. **61**, 289–317
10. Weinberg, D. N., Papillon-Cavanagh, S., Chen, H., Yue, Y., Chen, X., Rajagopalan, K. N., Horth, C., McGuire, J. T., Xu, X., Nikbakht, H., Lemiesz, A. E., Marchione, D. M., Marunde, M. R., Meiners, M. J., Cheek, M. A., Keogh, M.-C., Bareke, E., Djedid, A., Harutyunyan, A. S., Jabado, N., Garcia, B. A., Li, H., Allis, C. D., Majewski, J., and Lu, C. (2019) The histone mark H3K36me2 recruits DNMT3A and shapes the intergenic DNA methylation landscape. *Nature*. **573**, 281–286
11. Lehnertz, B., Ueda, Y., Derijck, A. A. H. A., Braunschweig, U., Perez-Burgos, L., Kubicek, S., Chen, T., Li, E., Jenuwein, T., and Peters, A. H. F. M. (2003) Suv39h-mediated histone H3 lysine 9 methylation directs DNA methylation to major satellite repeats at pericentric heterochromatin. *Curr Biol*. **13**, 1192–1200
12. Hervouet, E., Peixoto, P., Delage-Mourroux, R., Boyer-Guittaut, M., and Cartron, P.-F. (2018) Specific or not specific recruitment of DNMTs for DNA methylation, an epigenetic dilemma. *Clinical Epigenetics*. **10**, 17

13. Bartke, T., Vermeulen, M., Xhemalce, B., Robson, S. C., Mann, M., and Kouzarides, T. (2010) Nucleosome-interacting proteins regulated by DNA and histone methylation. *Cell*. **143**, 470–484
14. Holz-Schietinger, C., and Reich, N. O. (2012) RNA modulation of the human DNA methyltransferase 3A. *Nucleic Acids Res.* **40**, 8550–8557
15. Zhang, G., Estève, P.-O., Chin, H. G., Terragni, J., Dai, N., Corrêa, I. R., and Pradhan, S. (2015) Small RNA-mediated DNA (cytosine-5) methyltransferase 1 inhibition leads to aberrant DNA methylation. *Nucleic Acids Res.* **43**, 6112–6124
16. Di Ruscio, A., Ebralidze, A. K., Benoukraf, T., Amabile, G., Goff, L. A., Terragni, J., Figueroa, M. E., De Figueiredo Pontes, L. L., Alberich-Jorda, M., Zhang, P., Wu, M., D’Alò, F., Melnick, A., Leone, G., Ebralidze, K. K., Pradhan, S., Rinn, J. L., and Tenen, D. G. (2013) DNMT1-interacting RNAs block gene-specific DNA methylation. *Nature*. **503**, 371–376
17. Bhat, S. A., Ahmad, S. M., Mumtaz, P. T., Malik, A. A., Dar, M. A., Urwat, U., Shah, R. A., and Ganai, N. A. (2016) Long non-coding RNAs: Mechanism of action and functional utility. *Non-coding RNA Research*. **1**, 43–50
18. Wang, K. C., and Chang, H. Y. (2011) Molecular mechanisms of long noncoding RNAs. *Mol Cell*. **43**, 904–914
19. Bestor, T., Laudano, A., Mattaliano, R., and Ingram, V. (1988) Cloning and sequencing of a cDNA encoding DNA methyltransferase of mouse cells. The carboxyl-terminal domain of the mammalian enzymes is related to bacterial restriction methyltransferases. *J Mol Biol*. **203**, 971–983
20. Okano, M., Xie, S., and Li, E. (1998) Cloning and characterization of a family of novel mammalian DNA (cytosine-5) methyltransferases. *Nat Genet*. **19**, 219–220
21. Bourc’his, D., Xu, G. L., Lin, C. S., Bollman, B., and Bestor, T. H. (2001) Dnmt3L and the establishment of maternal genomic imprints. *Science*. **294**, 2536–253
22. Tajima, S., Suetake, I., Takeshita, K., Nakagawa, A., and Kimura, H. (2016) Domain Structure of the Dnmt1, Dnmt3a, and Dnmt3b DNA Methyltransferases. in *DNA Methyltransferases - Role and Function* (Jeltsch, A., and Jurkowska, R. Z. eds), pp. 63–86, *Advances in Experimental Medicine and Biology*, Springer International Publishing, Cham, [10.1007/978-3-319-43624-1_4](https://doi.org/10.1007/978-3-319-43624-1_4)
23. Okano, M., Bell, D. W., Haber, D. A., and Li, E. (1999) DNA Methyltransferases Dnmt3a and Dnmt3b Are Essential for De Novo Methylation and Mammalian Development. *Cell*. **99**, 247–257
24. Rountree, M. R., Bachman, K. E., and Baylin, S. B. (2000) DNMT1 binds HDAC2 and a new co-repressor, DMAP1, to form a complex at replication foci. *Nat Genet*. **25**, 269–277
25. Dhayalan, A., Rajavelu, A., Rathert, P., Tamas, R., Jurkowska, R. Z., Ragozin, S., and Jeltsch, A. (2010) The Dnmt3a PWWP domain reads histone 3 lysine 36 trimethylation and guides DNA methylation. *J Biol Chem*. **285**, 26114–26120
26. Fuks, F., Burgers, W. A., Godin, N., Kasai, M., and Kouzarides, T. (2001) Dnmt3a binds deacetylases and is recruited by a sequence-specific repressor to silence transcription. *EMBO J*. **20**, 2536–2544
27. Brenner, C., Deplus, R., Didelot, C., Lorient, A., Viré, E., De Smet, C., Gutierrez, A., Danovi, D., Bernard, D., Boon, T., Giuseppe Pelicci, P., Amati, B., Kouzarides, T., de Launoit, Y., Di Croce, L., and Fuks, F. (2005) Myc represses transcription through recruitment of DNA methyltransferase corepressor. *EMBO J*. **24**, 336–346

28. Otani, J., Nankumo, T., Arita, K., Inamoto, S., Ariyoshi, M., and Shirakawa, M. (2009) Structural basis for recognition of H3K4 methylation status by the DNA methyltransferase 3A ATRX-DNMT3-DNMT3L domain. *EMBO Rep.* **10**, 1235–1241
29. Qiu, C., Sawada, K., Zhang, X., and Cheng, X. (2002) The PWWP domain of mammalian DNA methyltransferase Dnmt3b defines a new family of DNA-binding folds. *Nat Struct Mol Biol.* **9**, 217–224
30. Aapola, U., Lyle, R., Krohn, K., Antonarakis, S. E., and Peterson, P. (2001) Isolation and initial characterization of the mouse Dnmt3l gene. *CGR.* **92**, 122–126
31. Gao, L., Emperle, M., Guo, Y., Grimm, S. A., Ren, W., Adam, S., Uryu, H., Zhang, Z.-M., Chen, D., Yin, J., Dukatz, M., Anteneh, H., Jurkowska, R. Z., Lu, J., Wang, Y., Bashtrykov, P., Wade, P. A., Wang, G. G., Jeltsch, A., and Song, J. (2020) Comprehensive structure-function characterization of DNMT3B and DNMT3A reveals distinctive de novo DNA methylation mechanisms. *Nat Commun.* **11**, 3355
32. Kaneda, M., Okano, M., Hata, K., Sado, T., Tsujimoto, N., Li, E., and Sasaki, H. (2004) Essential role for de novo DNA methyltransferase Dnmt3a in paternal and maternal imprinting. *Nature.* **429**, 900–903
33. Bestor, T. H. (2000) The DNA methyltransferases of mammals. *Hum Mol Genet.* **9**, 2395–2402
34. Li, E., Bestor, T. H., and Jaenisch, R. (1992) Targeted mutation of the DNA methyltransferase gene results in embryonic lethality. *Cell.* **69**, 915–926
35. Sun, B. K., Deaton, A. M., and Lee, J. T. (2006) A transient heterochromatic state in Xist preempts X inactivation choice without RNA stabilization. *Mol Cell.* **21**, 617–628
36. Lopatina, N., Haskell, J. F., Andrews, L. G., Poole, J. C., Saldanha, S., and Tollefsbol, T. (2002) Differential maintenance and de novo methylating activity by three DNA methyltransferases in aging and immortalized fibroblasts. *Journal of Cellular Biochemistry.* **84**, 324–334
37. Jin, B., and Robertson, K. D. (2013) DNA Methyltransferases (DNMTs), DNA Damage Repair, and Cancer. *Adv Exp Med Biol.* **754**, 3–29
38. Bird, A. P. (1986) CpG-rich islands and the function of DNA methylation. *Nature.* **321**, 209–213
39. Jang, H. S., Shin, W. J., Lee, J. E., and Do, J. T. (2017) CpG and Non-CpG Methylation in Epigenetic Gene Regulation and Brain Function. *Genes (Basel).* **8**, 148
40. Jones, P. A. (2012) Functions of DNA methylation: islands, start sites, gene bodies and beyond. *Nat Rev Genet.* **13**, 484–492
41. Chodavarapu, R. K., Feng, S., Bernatavichute, Y. V., Chen, P.-Y., Stroud, H., Yu, Y., Hetzel, J. A., Kuo, F., Kim, J., Cokus, S. J., Casero, D., Bernal, M., Huijser, P., Clark, A. T., Krämer, U., Merchant, S. S., Zhang, X., Jacobsen, S. E., and Pellegrini, M. (2010) Relationship between nucleosome positioning and DNA methylation. *Nature.* **466**, 388–392
42. Shukla, S., Kavak, E., Gregory, M., Imashimizu, M., Shutinoski, B., Kashlev, M., Oberdoerffer, P., Sandberg, R., and Oberdoerffer, S. (2011) CTCF-promoted RNA polymerase II pausing links DNA methylation to splicing. *Nature.* **479**, 74–79
43. Zhu, H., Wang, G., and Qian, J. (2016) Transcription factors as readers and effectors of DNA methylation. *Nat Rev Genet.* **17**, 551–565

44. Yang, X., Han, H., De Carvalho, D. D., Lay, F. D., Jones, P. A., and Liang, G. (2014) Gene body methylation can alter gene expression and is a therapeutic target in cancer. *Cancer Cell*. **26**, 577–590
45. Flynn, J., Glickman, J. F., and Reich, N. O. (1996) Murine DNA Cytosine-C5 Methyltransferase: Pre-Steady- and Steady-State Kinetic Analysis with Regulatory DNA Sequences. *Biochemistry*. **35**, 7308–7315
46. Cheng, X., and Blumenthal, R. M. (2008) Mammalian DNA methyltransferases: a structural perspective. *Structure*. **16**, 341–350
47. Chen, T., Ueda, Y., Xie, S., and Li, E. (2002) A novel Dnmt3a isoform produced from an alternative promoter localizes to euchromatin and its expression correlates with active de novo methylation. *J Biol Chem*. **277**, 38746–38754
48. Li, E. (2002) Chromatin modification and epigenetic reprogramming in mammalian development. *Nat Rev Genet*. **3**, 662–673
49. Holz-Schietinger, C., and Reich, N. O. (2010) The Inherent Processivity of the Human de Novo Methyltransferase 3A (DNMT3A) Is Enhanced by DNMT3L. *J Biol Chem*. **285**, 29091–29100
50. Sandoval, J. E., Huang, Y.-H., Muise, A., Goodell, M. A., and Reich, N. O. (2019) Mutations in the DNMT3A DNA methyltransferase in acute myeloid leukemia patients cause both loss and gain of function and differential regulation by protein partners. *Journal of Biological Chemistry*. **294**, 4898–4910
51. Norvil, A. B., Petell, C. J., Alabdi, L., Wu, L., Rossie, S., and Gowher, H. (2018) Dnmt3b Methylates DNA by a Noncooperative Mechanism, and Its Activity Is Unaffected by Manipulations at the Predicted Dimer Interface. *Biochemistry*. **57**, 4312–4324
52. Pradhan, S., Bacolla, A., Wells, R. D., and Roberts, R. J. (1999) Recombinant Human DNA (Cytosine-5) Methyltransferase. *Journal of Biological Chemistry*. **274**, 33002–33010
53. Ahmad, I., and Rao, D. N. (1996) Chemistry and Biology of DNA Methyltransferases. *Critical Reviews in Biochemistry and Molecular Biology*. **31**, 361–380
54. Wood, R. J., McKelvie, J. C., Maynard-Smith, M. D., and Roach, P. L. (2010) A real-time assay for CpG-specific cytosine-C5 methyltransferase activity. *Nucleic Acids Research*. **38**, e107–e107
55. Handa, V., and Jeltsch, A. (2005) Profound flanking sequence preference of Dnmt3a and Dnmt3b mammalian DNA methyltransferases shape the human epigenome. *J Mol Biol*. **348**, 1103–1112
56. Wienholz, B. L., Karetka, M. S., Moarefi, A. H., Gordon, C. A., Ginno, P. A., and Chédin, F. (2010) DNMT3L Modulates Significant and Distinct Flanking Sequence Preference for DNA Methylation by DNMT3A and DNMT3B In Vivo. *PLOS Genetics*. **6**, e1001106
57. Ali, M. H., and Imperiali, B. (2005) Protein oligomerization: How and why. *Bioorganic & Medicinal Chemistry*. **13**, 5013–5020
58. Zhang, Z.-M., Lu, R., Wang, P., Yu, Y., Chen, D., Gao, L., Liu, S., Ji, D., Rothbart, S. B., Wang, Y., Wang, G. G., and Song, J. (2018) Structural basis for DNMT3A-mediated de novo DNA methylation. *Nature*. **554**, 387–391
59. Guo, X., Wang, L., Li, J., Ding, Z., Xiao, J., Yin, X., He, S., Shi, P., Dong, L., Li, G., Tian, C., Wang, J., Cong, Y., and Xu, Y. (2015) Structural insight into autoinhibition and histone H3-induced activation of DNMT3A. *Nature*. **517**, 640–644

60. Russler-Germain, D. A., Spencer, D. H., Young, M. A., Lamprecht, T. L., Miller, C. A., Fulton, R., Meyer, M. R., Erdmann-Gilmore, P., Townsend, R. R., Wilson, R. K., and Ley, T. J. (2014) The R882H DNMT3A Mutation Associated with AML Dominantly Inhibits Wild-Type DNMT3A by Blocking Its Ability to Form Active Tetramers. *Cancer Cell*. **25**, 442–454
61. Holz-Schietinger, C., Matje, D. M., Harrison, M. F., and Reich, N. O. (2011) Oligomerization of DNMT3A Controls the Mechanism of de Novo DNA Methylation. *J Biol Chem*. **286**, 41479–41488
62. Holz-Schietinger, C., Matje, D. M., and Reich, N. O. (2012) Mutations in DNA Methyltransferase (DNMT3A) Observed in Acute Myeloid Leukemia Patients Disrupt Processive Methylation. *J Biol Chem*. **287**, 30941–30951
63. Breyer, W. A., and Matthews, B. W. (2001) A structural basis for processivity. *Protein Sci*. **10**, 1699–1711
64. Moore, L. D., Le, T., and Fan, G. (2013) DNA Methylation and Its Basic Function. *Neuropsychopharmacol*. **38**, 23–38
65. Yang, L., Rau, R., and Goodell, M. A. (2015) DNMT3A in haematological malignancies. *Nat Rev Cancer*. **15**, 152–165
66. Ley, T. J., Ding, L., Walter, M. J., McLellan, M. D., Lamprecht, T., Larson, D. E., Kandoth, C., Payton, J. E., Baty, J., Welch, J., Harris, C. C., Lichti, C. F., Townsend, R. R., Fulton, R. S., Dooling, D. J., Koboldt, D. C., Schmidt, H., Zhang, Q., Osborne, J. R., Lin, L., O’Laughlin, M., McMichael, J. F., Delehaunty, K. D., McGrath, S. D., Fulton, L. A., Magrini, V. J., Vickery, T. L., Hundal, J., Cook, L. L., Conyers, J. J., Swift, G. W., Reed, J. P., Alldredge, P. A., Wylie, T., Walker, J., Kalicki, J., Watson, M. A., Heath, S., Shannon, W. D., Varghese, N., Nagarajan, R., Westervelt, P., Tomasson, M. H., Link, D. C., Graubert, T. A., DiPersio, J. F., Mardis, E. R., and Wilson, R. K. (2010) DNMT3A Mutations in Acute Myeloid Leukemia. *New England Journal of Medicine*. **363**, 2424–2433
67. Im, A. P., Sehgal, A. R., Carroll, M. P., Smith, B. D., Tefferi, A., Johnson, D. E., and Boyiadzis, M. (2014) DNMT3A and IDH mutations in acute myeloid leukemia and other myeloid malignancies: associations with prognosis and potential treatment strategies. *Leukemia*. **28**, 1774–1783
68. Vogelstein, B., Lane, D., and Levine, A. J. (2000) Surfing the p53 network. *Nature*. **408**, 307–310
69. Hainaut, P., Hernandez, T., Robinson, A., Rodriguez-Tome, P., Flores, T., Hollstein, M., Harris, C. C., and Montesano, R. (1998) IARC Database of p53 gene mutations in human tumors and cell lines: updated compilation, revised formats and new visualisation tools. *Nucleic Acids Res*. **26**, 205–213
70. Barbosa, K., Li, S., Adams, P. D., and Deshpande, A. J. (2019) The role of TP53 in acute myeloid leukemia: Challenges and opportunities. *Genes, Chromosomes and Cancer*. **58**, 875–888
71. Oren, M., and Rotter, V. (2010) Mutant p53 Gain-of-Function in Cancer. *Cold Spring Harb Perspect Biol*. **2**, a001107
72. Willis, A., Jung, E. J., Wakefield, T., and Chen, X. (2004) Mutant p53 exerts a dominant negative effect by preventing wild-type p53 from binding to the promoter of its target genes. *Oncogene*. **23**, 2330–2338
73. Wang, Y. A., Kamarova, Y., Shen, K. C., Jiang, Z., Hahn, M.-J., Wang, Y., and Brooks, S. C. (2005) DNA methyltransferase-3a interacts with p53 and represses p53-mediated gene expression. *Cancer Biol Ther*. **4**, 1138–1143

74. Ooi, S. K. T., Qiu, C., Bernstein, E., Li, K., Jia, D., Yang, Z., Erdjument-Bromage, H., Tempst, P., Lin, S.-P., Allis, C. D., Cheng, X., and Bestor, T. H. (2007) DNMT3L connects unmethylated lysine 4 of histone H3 to de novo methylation of DNA. *Nature*. **448**, 714–717
75. Zhang, Y., Jurkowska, R., Soeroes, S., Rajavelu, A., Dhayalan, A., Bock, I., Rathert, P., Brandt, O., Reinhardt, R., Fischle, W., and Jeltsch, A. (2010) Chromatin methylation activity of Dnmt3a and Dnmt3a/3L is guided by interaction of the ADD domain with the histone H3 tail. *Nucleic Acids Res.* **38**, 4246–4253
76. Michalak, E. M., Burr, M. L., Bannister, A. J., and Dawson, M. A. (2019) The roles of DNA, RNA and histone methylation in ageing and cancer. *Nat Rev Mol Cell Biol.* **20**, 573–589
77. Denis, H., Ndlovu, M. N., and Fuks, F. (2011) Regulation of mammalian DNA methyltransferases: a route to new mechanisms. *EMBO Rep.* **12**, 647–656
78. Wei, J.-W., Huang, K., Yang, C., and Kang, C.-S. (2017) Non-coding RNAs as regulators in epigenetics (Review). *Oncology Reports.* **37**, 3–9
79. Li, Y.-Q., Zhou, P.-Z., Zheng, X.-D., Walsh, C. P., and Xu, G.-L. (2007) Association of Dnmt3a and thymine DNA glycosylase links DNA methylation with base-excision repair. *Nucleic Acids Res.* **35**, 390–400
80. Viré, E., Brenner, C., Deplus, R., Blanchon, L., Fraga, M., Didelot, C., Morey, L., Van Eynde, A., Bernard, D., Vanderwinden, J.-M., Bollen, M., Esteller, M., Di Croce, L., de Launoit, Y., and Fuks, F. (2006) The Polycomb group protein EZH2 directly controls DNA methylation. *Nature*. **439**, 871–874
81. Chedin, F., Lieber, M. R., and Hsieh, C.-L. (2002) The DNA methyltransferase-like protein DNMT3L stimulates de novo methylation by Dnmt3a. *Proc Natl Acad Sci U S A.* **99**, 16916–16921
82. Sandoval, J. E., and Reich, N. O. (2019) The R882H substitution in the human de novo DNA methyltransferase DNMT3A disrupts allosteric regulation by the tumor suppressor p53. *J Biol Chem.* **294**, 18207–18219
83. Kanhere, A., Viiri, K., Araújo, C. C., Rasaiyaah, J., Bouwman, R. D., Whyte, W. A., Pereira, C. F., Brookes, E., Walker, K., Bell, G. W., Pombo, A., Fisher, A. G., Young, R. A., and Jenner, R. G. (2010) Short RNAs Are Transcribed from Repressed Polycomb Target Genes and Interact with Polycomb Repressive Complex-2. *Molecular Cell.* **38**, 675–688
84. Jin, B., Li, Y., and Robertson, K. D. (2011) DNA methylation: superior or subordinate in the epigenetic hierarchy? *Genes Cancer.* **2**, 607–617
85. Biswas, S., and Rao, C. M. (2018) Epigenetic tools (The Writers, The Readers and The Erasers) and their implications in cancer therapy. *Eur J Pharmacol.* **837**, 8–24
86. Ye, F., Huang, J., Wang, H., Luo, C., and Zhao, K. (2019) Targeting epigenetic machinery: Emerging novel allosteric inhibitors. *Pharmacology & Therapeutics.* **204**, 107406
87. Zucconi, B. E., and Cole, P. A. (2017) Allosteric regulation of epigenetic modifying enzymes. *Curr Opin Chem Biol.* **39**, 109–115
88. Qi, W., Zhao, K., Gu, J., Huang, Y., Wang, Y., Zhang, H., Zhang, M., Zhang, J., Yu, Z., Li, L., Teng, L., Chuai, S., Zhang, C., Zhao, M., Chan, H., Chen, Z., Fang, D., Fei, Q., Feng, L., Feng, L., Gao, Y., Ge, H., Ge, X., Li, G., Lingel, A., Lin, Y., Liu, Y., Luo, F., Shi, M., Wang, L., Wang, Z., Yu, Y., Zeng, J., Zeng, C., Zhang, L., Zhang, Q., Zhou, S., Oyang, C., Atadja, P., and Li, E. (2017) An allosteric PRC2

- inhibitor targeting the H3K27me3 binding pocket of EED. *Nat Chem Biol.* **13**, 381–388
89. Siarheyeva, A., Senisterra, G., Allali-Hassani, A., Dong, A., Dobrovetsky, E., Wasney, G. A., Chau, I., Marcellus, R., Hajian, T., Liu, F., Korboukh, I., Smil, D., Bolshan, Y., Min, J., Wu, H., Zeng, H., Loppnau, P., Poda, G., Griffin, C., Aman, A., Brown, P. J., Jin, J., Al-Awar, R., Arrowsmith, C. H., Schapira, M., and Vedadi, M. (2012) An allosteric inhibitor of protein arginine methyltransferase 3. *Structure.* **20**, 1425–1435
 90. Liu, F., Li, F., Ma, A., Dobrovetsky, E., Dong, A., Gao, C., Korboukh, I., Liu, J., Smil, D., Brown, P. J., Frye, S. V., Arrowsmith, C. H., Schapira, M., Vedadi, M., and Jin, J. (2013) Exploiting an Allosteric Binding Site of PRMT3 Yields Potent and Selective Inhibitors. *J. Med. Chem.* **56**, 2110–2124
 91. Santi, D. V., Norment, A., and Garrett, C. E. (1984) Covalent bond formation between a DNA-cytosine methyltransferase and DNA containing 5-azacytosine. *Proc Natl Acad Sci U S A.* **81**, 6993–6997
 92. Stresemann, C., and Lyko, F. (2008) Modes of action of the DNA methyltransferase inhibitors azacytidine and decitabine. *Int J Cancer.* **123**, 8–13
 93. Siedlecki, P., Garcia Boy, R., Musch, T., Brueckner, B., Suhai, S., Lyko, F., and Zielenkiewicz, P. (2006) Discovery of two novel, small-molecule inhibitors of DNA methylation. *J Med Chem.* **49**, 678–683
 94. Brueckner, B., Garcia Boy, R., Siedlecki, P., Musch, T., Kliem, H. C., Zielenkiewicz, P., Suhai, S., Wiessler, M., and Lyko, F. (2005) Epigenetic reactivation of tumor suppressor genes by a novel small-molecule inhibitor of human DNA methyltransferases. *Cancer Res.* **65**, 6305–6311
 95. Halby, L., Champion, C., Sénamaud-Beaufort, C., Ajjan, S., Drujon, T., Rajavelu, A., Ceccaldi, A., Jurkowska, R., Lequin, O., Nelson, W. G., Guy, A., Jeltsch, A., Guianvarc'h, D., Ferroud, C., and Arimondo, P. B. (2012) Rapid synthesis of new DNMT inhibitors derivatives of procainamide. *Chembiochem.* **13**, 157–16
 96. Datta, J., Ghoshal, K., Denny, W. A., Gamage, S. A., Brooke, D. G., Phiasivongsa, P., Redkar, S., and Jacob, S. T. (2009) A new class of quinoline-based DNA hypomethylating agents reactivates tumor suppressor genes by blocking DNA methyltransferase 1 activity and inducing its degradation. *Cancer Res.* **69**, 4277–4285
 97. Valente, S., Liu, Y., Schnekenburger, M., Zwergel, C., Cosconati, S., Gros, C., Tardugno, M., Labella, D., Florean, C., Minden, S., Hashimoto, H., Chang, Y., Zhang, X., Kirsch, G., Novellino, E., Arimondo, P. B., Miele, E., Ferretti, E., Gulino, A., Diederich, M., Cheng, X., and Mai, A. (2014) Selective non-nucleoside inhibitors of human DNA methyltransferases active in cancer including in cancer stem cells. *J Med Chem.* **57**, 701–713
 98. Christman, J. K. (2002) 5-Azacytidine and 5-aza-2'-deoxycytidine as inhibitors of DNA methylation: mechanistic studies and their implications for cancer therapy. *Oncogene.* **21**, 5483–549

Chapter II

1. Bird, A. (2002) DNA methylation patterns and epigenetic memory. *Genes Dev.* **16**, 6–21

2. Reik, W., Dean, W., and Walter, J. (2001) Epigenetic reprogramming in mammalian development. *Science* **293**, 1089–1093
3. Robertson, K. D. (2005) DNA methylation and human disease. *Nat. Rev. Genet.* **6**, 597–610
4. Figueroa, M. E., Lugthart, S., Li, Y., Erpelinck-Verschueren, C., Deng, X., Christos, P. J., Schifano, E., Booth, J., van Putten, W., Skrabanek, L., Campagne, F., *et al.* (2010) DNA methylation signatures identify biologically distinct subtypes in acute myeloid leukemia. *Cancer Cell* **17**, 13–27
5. Melnick, A. M. (2010) Epigenetics in AML. *Best Pract. Res. Clin. Haematol.* **23**, 463–468
6. Hou, H. A., and Tien, H. F. (2016) Mutations in epigenetic modifiers in acute myeloid leukemia and their clinical utility. *Expert Rev. Hematol.* **9**, 447–469
7. Rau, R. E., Rodriguez, B. A., Luo, M., Jeong, M., Rosen, A., Rogers, J. H., Campbell, C. T., Daigle, S. R., Deng, L., Song, Y., Sweet, S., *et al.* (2016) DOT1L as a therapeutic target for the treatment of DNMT3A-mutant acute myeloid leukemia. *Blood* **128**, 971–981
8. Holz-Schietinger, C., Matje, D. M., and Reich, N. O. (2012) Mutations in DNA methyltransferase (DNMT3A) observed in acute myeloid leukemia patients disrupt processive methylation. *J. Biol. Chem.* **287**, 30941–30951
9. Ley, T. J., Ding, L., Walter, M. J., McLellan, M. D., Lamprecht, T., Larson, D. E., Kandoth, C., Payton, J. E., Baty, J., Welch, J., Harris, C. C., *et al.* (2010) DNMT3A mutations in acute myeloid leukemia. *N. Engl. J. Med.* **363**, 2424–2433
10. Russler-Germain, D. A., Spencer, D. H., Young, M. A., Lamprecht, T. L., Miller, C. A., Fulton, R., Meyer, M. R., Erdmann-Gilmore, P., Townsend, R. R., Wilson, R. K., and Ley, T. J. (2014) The R882H DNMT3A mutation associated with AML dominantly inhibits wild-type DNMT3A by blocking its ability to form active tetramers. *Cancer Cell* **25**, 442–454
11. Forbes, S. A., Beare, D., Boutselakis, H., Bamford, S., Bindal, N., Tate, J., Cole, C. G., Ward, S., Dawson, E., Ponting, L., Stefancsik, R., *et al.* (2017) COSMIC: somatic cancer genetics at high-resolution. *Nucleic Acids Res.* **45**, D777–D783
12. Aggerholm, A., Guldberg, P., Hokland, M., and Hokland, P. (1999) Extensive intra- and interindividual heterogeneity of p15INK4B methylation in acute myeloid leukemia. *Cancer Res.* **59**, 436–441
13. Cameron, E. E., Baylin, S. B., and Herman, J. G. (1999) p15INK4B CpG island methylation in primary acute leukemia is heterogeneous and suggests density as a critical factor for transcriptional silencing. *Blood* **94**, 2445–2451
14. Esteller, M. (2002) CpG island hypermethylation and tumor suppressor genes: a booming present, a brighter future. *Oncogene* **21**, 5427–5440
15. Santini, V., Kantarjian, H. M., and Issa, J. P. (2001) Changes in DNA methylation in neoplasia: pathophysiology and therapeutic implications. *Ann. Int. Med.* **134**, 573–586
16. Ramsahoye, B. H., Biniszkiwicz, D., Lyko, F., Clark, V., Bird, A. P., and Jaenisch, R. (2000) Non-CpG methylation is prevalent in embryonic stem cells and may be mediated by DNA methyltransferase 3a. *Proc. Natl. Acad. Sci. U.S.A.* **97**, 5237–5242
17. Qu, Y., Lennartsson, A., Gaidzik, V. I., Deneberg, S., Karimi, M., Bengtsson, S., Höglund, M., Bullinger, L., Döhner, K., and Lehmann, S. (2014) Differential methylation in CN-AML preferentially targets non-CGI regions and is dictated by

- DNMT3A mutational status and associated with pre- dominant hypomethylation of HOX genes. *Epigenetics* **9**, 1108–1119
18. Li, Y. Q., Zhou, P. Z., Zheng, X. D., Walsh, C. P., and Xu, G. L. (2006) Association of Dnmt3a and thymine DNA glycosylase links DNA methylation with base-excision repair. *Nucleic Acids Res.* **35**, 390–400
 19. Esposito, M. T., and So, C. W. E. (2014). DNA damage accumulation and repair defects in acute myeloid leukemia: implications for pathogenesis, disease progression, and chemotherapy resistance. *Chromosoma.* **123**, 545–561
 20. Holz-Schietinger, C., Matje, D. M., Harrison, M. F., and Reich, N. O. (2011) Oligomerization of DNMT3A controls the mechanism of *de novo* DNA methylation. *J. Biol. Chem.* **286**, 41479–41488
 21. Holz-Schietinger, C., and Reich, N. O. (2010) The inherent processivity of the human *de novo* methyltransferase 3A (DNMT3A) is enhanced by DNMT3L. *J. Biol. Chem.* **285**, 29091–29100
 22. Laurent, L., Wong, E., Li, G., Huynh, T., Tsirigos, A., Ong, C. T., Low, H. M., Kin Sung, K. W., Rigoutsos, I., Loring, J., and Wei, C. L. (2010) Dynamic changes in the human methylome during differentiation. *Genome Res.* **20**, 320–331
 23. Hardeland, U., Bentele, M., Lettieri, T., Steinacher, R., Jiricny, J., and Schär, P. (2001) Thymine DNA glycosylase. *Prog. Nucleic Acid Res. Mol. Biol.* **68**, 235–253
 24. Purdy, M. M., Holz-Schietinger, C., and Reich, N. O. (2010) Identification of a second DNA binding site in human DNA methyltransferase 3A by substrate inhibition and domain deletion. *Arch. Biochem. Biophys.* **498**, 13–22
 25. Thillainadesan, G., Chitilian, J. M., Isovich, M., Ablack, J. N., Mymryk, J. S., Tini, M., and Torchia, J. (2012) TGF- β -dependent active demethylation and expression of the p15ink4b tumor suppressor are impaired by the ZNF217/CoREST complex. *Mol. Cell* **46**, 636–649
 26. Hervouet, E., Vallette, F. M., and Cartron, P. F. (2009) Dnmt3/transcription factor interactions as crucial players in targeted DNA methylation. *Epigenetics* **4**, 487–499
 27. Fuks, F., Burgers, W. A., Godin, N., Kasai, M., and Kouzarides, T. (2001) Dnmt3a binds deacetylases and is recruited by a sequence-specific repressor to silence transcription. *EMBO J.* **20**, 2536–2544
 28. Stirzaker, C., Song, J. Z., Ng, W., Du, Q., Armstrong, N. J., Locke, W. J., Statham, A. L., French, H., Pidsley, R., Valdes-Mora, F., Zotenko, E., and Clark, S. J. (2017) Methyl-CpG-binding protein MBD2 plays a key role in maintenance and spread of DNA methylation at CpG islands and shores in cancer. *Oncogene* **36**, 1328–1338
 29. Jia, D., Jurkowska, R. Z., Zhang, X., Jeltsch, A., and Cheng, X. (2007) Structure of Dnmt3a bound to Dnmt3L suggests a model for *de novo* DNA methylation. *Nature* **449**, 248–251
 30. Doherty, K. M., Sommers, J. A., Gray, M. D., Lee, J. W., von Kobbe, C., Thoma, N. H., Kureekattil, R. P., Kenny, M. K., and Brosh, R. M. (2005) Physical and functional mapping of the replication protein A interaction domain of the werner and bloom syndrome helicases. *J. Biol. Chem.* **280**, 29494–29505
 31. Chen, W., Lam, S. S., Srinath, H., Schiffer, C. A., Royer, W. E., and Lin, K. (2007) Competition between Ski and CREB-binding protein for binding to Smad proteins in transforming growth factor- β signaling. *J. Biol. Chem.* **282**, 11365–11376
 32. Shiba, N., Taki, T., Park, M. J., Shimada, A., Sotomatsu, M., Adachi, S., Tawa, A., Horibe, K., Tsuchida, M., Hanada, R., Tsukimoto, I., Arakawa, H., and Hayashi, Y.

- (2012) DNMT3A mutations are rare in childhood acute myeloid leukaemia, myelodysplastic syndromes and juvenile myelomonocytic leukaemia. *Br. J. Haematol.* **156**, 413–414
33. Stegelmann, F., Bullinger, L., Schlenk, R. F., Paschka, P., Griesshammer, M., Bliersch, C., Kuhn, S., Schauer, S., Döhner, H., and Döhner, K. (2011) DNMT3A mutations in myeloproliferative neoplasms. *Leukemia* **25**, 1217–1219
 34. Couronné, L., Bastard, C., and Bernard, O. A. (2012) TET2 and DNMT3A mutations in human T-cell lymphoma. *N. Engl. J. Med.* **366**, 95–96
 35. Grossmann, V., Haferlach, C., Weissmann, S., Roller, A., Schindela, S., Poetzinger, F., Stadler, K., Bellos, F., Kern, W., Haferlach, T., Schnittger, S., and Kohlmann, A. (2013) The molecular profile of adult T-cell acute lymphoblastic leukemia: mutations in RUNX1 and DNMT3A are associated with poor prognosis in T-ALL. *Genes Chromosomes Cancer* **52**, 410–422
 36. Suzuki, M., Yamada, T., Kihara-Negishi, F., Sakurai, T., Hara, E., Tenen, D. G., Hozumi, N., and Oikawa, T. (2006) Site-specific DNA methylation by a complex of PU.1 and Dnmt3a/b. *Oncogene* **25**, 2477–2488
 37. Fuks, F., Hurd, P. J., Deplus, R., and Kouzarides, T. (2003) The DNA methyltransferases associate with HP1 and the SUV39H1 histone methyltransferase. *Nucleic Acids Res.* **31**, 2305–2312
 38. Turker, M. S. (2002) Gene silencing in mammalian cells and the spread of DNA methylation. *Oncogene* **21**, 5388–5393
 39. Vardiman, J. W., Thiele, J., Arber, D. A., Brunning, R. D., Borowitz, M. J., Porwit, A., Harris, N. L., Le Beau, M. M., Hellström-Lindberg, E., Tefferi, A., and Bloomfield, C. D. (2009) The 2008 revision of the World Health Organization (WHO) classification of myeloid neoplasms and acute leukemia: rationale and important changes. *Blood* **114**, 937–951
 40. Du, J., Johnson, L. M., Jacobsen, S. E., and Patel, D. J. (2015) DNA methylation pathways and their crosstalk with histone methylation. *Nat. Rev. Mol. Cell Biol.* **16**, 519–532
 41. Matzke, M. A., and Mosher, R. A. (2014) RNA-directed DNA methylation: an epigenetic pathway of increasing complexity. *Nat. Rev. Genet.* **15**, 394–408
 42. Spencer, D. H., Russler-Germain, D. A., Ketkar, S., Helton, N. M., Lamprecht, T. L., Fulton, R. S., Fronick, C. C., O’Laughlin, M., Heath, S. E., Shinawi, M., Westervelt, P., *et al.* (2017) CpG island hypermethylation mediated by DNMT3A is a consequence of AML progression. *Cell* **168**, 801–816.e13
 43. Chen, D., Christopher, M., Helton, N. M., Ferguson, I., Ley, T. J., and Spencer, D. H. (2018) DNMT3A R882-associated hypomethylation patterns are maintained in primary AML xenografts, but not in the DNMT3A R882C OCI-AML3 leukemia cell line. *Blood Cancer J.* **8**, 38
 44. Pedrali-Noy, G., and Weissbach, A. (1986) Mammalian DNA methyltransferases prefer poly(dI-dC) as substrate. *J. Biol. Chem.* **261**, 7600–7602
 45. Galonska, C., Charlton, J., Mattei, A. L., Donaghey, J., Clement, K., Gu, H., Mohammad, A. W., Stamenova, E. K., Cacchiarelli, D., Klages, S., Timmermann, B., Cantz, T., Schöler, H. R., Gnirke, A., Ziller, M. J., and Meissner, A. (2018) Genome-wide tracking of dCas9-methyltransferase footprints. *Nat. Commun.* **9**, 597
 46. Lei, Y., Huang, Y. H., and Goodell, M. A. (2018) DNA methylation and demethylation using hybrid site-targeting proteins. *Genome Biol.* **19**, 187

47. Chen, T., Ueda, Y., Dodge, J. E., Wang, Z., and Li, E. (2003) Establishment and maintenance of genomic methylation patterns in mouse embryonic stem cells by Dnmt3a and Dnmt3b. *Mol. Cell. Biol.* **23**, 5594–5605
48. Hata, K., Okano, M., Lei, H., and Li, E. (2002) Dnmt3L cooperates with the Dnmt3 family of *de novo* DNA methyltransferases to establish maternal imprints in mice. *Development* **129**, 1983–1993
49. Kareta, M. S., Botello, Z. M., Ennis, J. J., Chou, C., and Chédin, F. (2006) Reconstitution and mechanism of the stimulation of *de novo* methylation by human DNMT3L. *J. Biol. Chem.* **281**, 25893–25902
50. Schuermann, D., Scheidegger, S. P., Weber, A. R., Bjørås, M., Leumann, C. J., and Schär, P. (2016) 3CAPS, a structural AP-site analogue as a tool to investigate DNA base excision repair. *Nucleic Acids Res.* **44**, 2187–2198
51. Peterson, S. N., and Reich, N. O. (2006) GATC flanking sequences regulate Dam activity: evidence for how Dam specificity may influence pap expression. *J. Mol. Biol.* **355**, 459–472
52. Su, J., Huang, Y. H., Cui, X., Wang, X., Zhang, X., Lei, Y., Xu, J., Lin, X., Chen, K., Lv, J., Goodell, M. A., and Li, W. (2018) Homeobox oncogene activation by pan-cancer DNA hypermethylation. *Genome Biol.* **19**, 108
53. Galonska, C., Charlton, J., Mattei, A. L., Donaghey, J., Clement, K., Gu, H., Mohammad, A. W., Stamenova, E. K., Cacchiarelli, D., Klages, S., Timmermann, B., *et al.* (2018) Genome-wide tracking of dCas9-methyltransferase footprints. *Nat. Commun.* **9**, 597
54. Huang, Y. H., Su, J., Lei, Y., Brunetti, L., Gundry, M. C., Zhang, X., Jeong, M., Li, W., and Goodell, M. A. (2017) DNA epigenome editing using CRISPR-Cas SunTag-directed DNMT3A. *Genome Biol.* **18**, 176
55. Gu, T., Lin, X., Cullen, S. M., Luo, M., Jeong, M., Estecio, M., Shen, J., Hardikar, S., Sun, D., Su, J., Rux, D., *et al.* (2018) DNMT3A and TET1 cooperate to regulate promoter epigenetic landscapes in mouse embryonic stem cells. *Genome Biol.* **19**, 88

Chapter III

1. Vertino, P. M., Sekowski, J. A., Coll, J. M., Applegreen, N., Han, S., Hickey, R. J., and Malkas, L. H. (2002) DNMT1 is a component of a multiprotein DNA replication complex. *Cell Cycle* **1**, 416–423
2. Viré, E., Brenner, C., Deplus, R., Blanchon, L., Fraga, M., Didelot, C., Morey, L., Van Eynde, A., Bernard, D., Vanderwinden, J. M., Bollen, M., *et al.* (2006) The Polycomb group protein EZH2 directly controls DNA methylation. *Nature* **439**, 871–874
3. Datta, J., Majumder, S., Bai, S., Ghoshal, K., Kutay, H., Smith, D. S., Crabb, J. W., and Jacob, S. T. (2005) Physical and functional interaction of DNA methyltransferase 3A with Mbd3 and Brg1 in mouse lymphosarcoma cells. *Cancer Res.* **65**, 10891–10900
4. Brenner, C., Deplus, R., Didelot, C., Loriot, A., Viré, E., De Smet, C., Gutierrez, A., Danovi, D., Bernard, D., Boon, T., Pelicci, P. G., *et al.* (2005) Myc represses transcription through recruitment of DNA methyltransferase corepressor. *EMBO J.* **24**, 336–346

5. Thillainadesan, G., Chitilian, J. M., Isovich, M., Ablack, J. N., Mymryk, J. S., Tini, M., and Torchia, J. (2012) TGF- β -dependent active demethylation and expression of the p15^{ink4b} tumor suppressor are impaired by the ZNF217/CoREST complex. *Mol. Cell* **46**, 636 – 649
6. Bird, A. (2002) DNA methylation patterns and epigenetic memory. *Genes Dev.* **16**, 6 – 21
7. Reik, W., Dean, W., and Walter, J. (2001) Epigenetic reprogramming in mammalian development. *Science* **293**, 1089 – 1093
8. Ellis, R. J. (2001) Macromolecular crowding: an important but neglected aspect of the intracellular environment. *Curr. Opin. Struct. Biol.* **11**, 114 – 119
9. Levy, E. D., De, S., and Teichmann, S. A. (2012) Cellular crowding imposes global constraints on the chemistry and evolution of proteomes. *Proc. Natl. Acad. Sci. U.S.A.* **109**, 20461 – 20466
10. Schreiber, G., Haran, G., and Zhou, H. X. (2009) Fundamental aspects of protein-protein association kinetics. *Chem. Rev.* **109**, 839 – 860
11. Chakravarty, D., Janin, J., Robert, C. H., and Chakrabarti, P. (2015) Changes in protein structure at the interface accompanying complex formation. *IUCr J.* **2**, 643 – 652
12. Guo, X., Wang, L., Li, J., Ding, Z., Xiao, J., Yin, X., He, S., Shi, P., Dong, L., Li, G., Tian, C., *et al.* (2015) Structural insight into autoinhibition and histone H3-induced activation of DNMT3A. *Nature* **517**, 640 – 644
13. Holz-Schietinger, C., and Reich, N. O. (2012) RNA modulation of the human DNA methyltransferase 3A. *Nucleic Acids Res.* **40**, 8550 – 8557
14. Yang, L., Rau, R., and Goodell, M. A. (2015) DNMT3A in haematological malignancies. *Nat. Rev. Cancer* **15**, 152 – 165
15. Biegging, K. T., Mello, S. S., and Attardi, L. D. (2014) Unravelling mechanisms of p53-mediated tumour suppression. *Nat. Rev. Cancer* **14**, 359 – 370
16. Kasthuber, E. R., and Lowe, S. W. (2017) Putting p53 in context. *Cell* **170**, 1062 – 1078
17. Espinosa, J. M., Verdun, R. E., and Emerson, B. M. (2003) p53 functions through stress- and promoter-specific recruitment of transcription initiation components before and after DNA damage. *Mol. Cell* **12**, 1015 – 1027
18. Williams, A. B., and Schumacher, B. (2016) p53 in the DNA-damage-repair process. *Cold Spring Harbor Perspect. Med.* **6**, a026070
19. Xie, P., Tian, C., An, L., Nie, J., Lu, K., Xing, G., Zhang, L., and He, F. (2008) Histone methyltransferase protein SETD2 interacts with p53 and selectively regulates its downstream genes. *Cell. Signal.* **20**, 1671 – 1678
20. Agalioti, T., Chen, G., and Thanos, D. (2002) Deciphering the transcriptional histone acetylation code for a human gene. *Cell* **111**, 381 – 392
21. Kaeser, M. D., and Iggo, R. D. (2004) Promoter-specific p53-dependent histone acetylation following DNA damage. *Oncogene* **23**, 4007 – 4013
22. Georgia, S., Kanji, M., and Bhushan, A. (2013) DNMT1 represses p53 to maintain progenitor cell survival during pancreatic organogenesis. *Genes Dev.* **27**, 372 – 377
23. Estève, P. O., Chin, H. G., and Pradhan, S. (2005) Human maintenance DNA (cytosine-5)-methyltransferase and p53 modulate expression of p53-repressed promoters. *Proc. Natl. Acad. Sci. U.S.A.* **102**, 1000 – 1005
24. Tovy, A., Spiro, A., McCarthy, R., Shipony, Z., Aylon, Y., Alton, K., Ainsbinder, E., Furth, N., Tanay, A., Barton, M., and Oren, M. (2017) p53 is essential for DNA

- methylation homeostasis in naïve embryonic stem cells, and its loss promotes clonal heterogeneity. *Genes Dev.* **31**, 959–972
25. Wang, Y. A., Kamarova, Y., Shen, K. C., Jiang, Z., Hahn, M. J., Wang, Y., and Brooks, S. C. (2005) DNA methyltransferase-3a interacts with p53 and represses p53-mediated gene expression. *Cancer Biol. Ther.* **4**, 1138–1143
 26. Ley, T. J., Ding, L., Walter, M. J., McLellan, M. D., Lamprecht, T., Larson, D. E., Kandoth, C., Payton, J. E., Baty, J., Welch, J., Harris, C. C., *et al.* (2010) DNMT3A mutations in acute myeloid leukemia. *N. Engl. J. Med.* **363**, 2424–2433
 27. Russler-Germain, D. A., Spencer, D. H., Young, M. A., Lamprecht, T. L., Miller, C. A., Fulton, R., Meyer, M. R., Erdmann-Gilmore, P., Townsend, R. R., Wilson, R. K., and Ley, T. J. (2014) The R882H DNMT3A mutation associated with AML dominantly inhibits wild-type DNMT3A by blocking its ability to form active tetramers. *Cancer Cell* **25**, 442–454
 28. Holz-Schietinger, C., Matje, D. M., and Reich, N. O. (2012) Mutations in DNA methyltransferase (DNMT3A) observed in acute myeloid leukemia patients disrupt processive methylation. *J. Biol. Chem.* **287**, 30941–30951
 29. Koya, J., Kataoka, K., Sato, T., Bando, M., Kato, Y., Tsuruta-Kishino, T., Kobayashi, H., Narukawa, K., Miyoshi, H., Shirahige, K., and Kurokawa, M. (2016) DNMT3A R882 mutants interact with polycomb proteins to block haematopoietic stem and leukaemic cell differentiation. *Nat. Commun.* **7**, 10924
 30. Vogelstein, B., Lane, D., and Levine, A. J. (2000) Surfing the p53 network. *Nature* **408**, 307–310
 31. Petitjean, A., Mathe, E., Kato, S., Ishioka, C., Tavtigian, S. V., Hainaut, P., and Olivier, M. (2007) Impact of mutant p53 functional properties on TP53 mutation patterns and tumor phenotype: lessons from recent developments in the IARC TP53 database. *Hum. Mutat.* **28**, 622–629
 32. Song, H., Hollstein, M., and Xu, Y. (2007) p53 gain-of-function cancer mutants induce genetic instability by inactivating ATM. *Nat. Cell Biol.* **9**, 573–580
 33. Strano, S., Fontemaggi, G., Costanzo, A., Rizzo, M. G., Monti, O., Bacca-rini, A., Del Sal, G., Levrero, M., Sacchi, A., Oren, M., and Blandino, G. (2002) Physical interaction with human tumor-derived p53 mutants inhibits p63 activities. *J. Biol. Chem.* **277**, 18817–18826
 34. Gaiddon, C., Lokshin, M., Ahn, J., Zhang, T., and Prives, C. (2001) A subset of tumor-derived mutant forms of p53 down-regulate p63 and p73 through a direct interaction with the p53 core domain. *Mol. Cell. Biol.* **21**, 1874–1887
 35. Purdy, M. M., Holz-Schietinger, C., and Reich, N. O. (2010) Identification of a second DNA binding site in human DNA methyltransferase 3A by substrate inhibition and domain deletion. *Arch. Biochem. Biophys.* **498**, 13–22
 36. Karetta, M. S., Botello, Z. M., Ennis, J. J., Chou, C., and Chédin, F. (2006) Reconstitution and mechanism of the stimulation of *de novo* methylation by human DNMT3L. *J. Biol. Chem.* **281**, 25893–25902
 37. Galonska, C., Charlton, J., Mattei, A. L., Donaghey, J., Clement, K., Gu, H., Mohammad, A. W., Stamenova, E. K., Cacchiarelli, D., Klages, S., Timmermann, B., Cantz, T., Schöler, H. R., Gnirke, A., Ziller, M. J., and Meissner, A. (2018) Genome-wide tracking of dCas9-methyltransferase footprints. *Nat. Commun.* **9**, 597
 38. Lei, Y., Huang, Y. H., and Goodell, M. A. (2018) DNA methylation and demethylation using hybrid site-targeting proteins. *Genome Biol.* **19**, 187
 39. el-Deiry, W. S., Kern, S. E., Pietenpol, J. A., Kinzler, K. W., and Vogelstein, B. (1992) Wt1 and p53: a molecular pathway for cell cycle arrest and apoptosis. *Mol. Cell. Biol.* **12**, 2243–2252

- B. (1992) Definition of a consensus binding site for p53. *Nat. Genet.* **1**, 45–49
40. Cheng, X., and Blumenthal, R. M. (2008) Mammalian DNA methyltransferases: a structural perspective. *Structure* **16**, 341–350
41. Holz-Schietinger, C., Matje, D. M., Harrison, M. F., and Reich, N. O. (2011) Oligomerization of DNMT3A controls the mechanism of *de novo* DNA methylation. *J. Biol. Chem.* **286**, 41479–41488
42. Pierce, B. G., Wiehe, K., Hwang, H., Kim, B. H., Vreven, T., and Weng, Z. (2014) ZDOCK server: interactive docking prediction of protein–protein complexes and symmetric multimers. *Bioinformatics* **30**, 1771–1773
43. Lyskov, S., and Gray, J. J. (2008) The RosettaDock server for local protein–protein docking. *Nucleic Acids Res.* **36**, W233–W238
44. Datta, J., Ghoshal, K., Sharma, S. M., Tajima, S., and Jacob, S. T. (2003) Biochemical fractionation reveals association of DNA methyltransferase (Dnmt) 3b with Dnmt1 and that of Dnmt 3a with a histone H3 methyltransferase and Hdac1. *J. Cell. Biochem.* **88**, 855–864
45. Neri, F., Krepelova, A., Incarnato, D., Maldotti, M., Parlato, C., Galvagni, F., Matarese, F., Stunnenberg, H. G., and Oliviero, S. (2013) Dnmt3L antagonizes DNA methylation at bivalent promoters and favors DNA methylation at gene bodies in ESCs. *Cell* **155**, 121–134
46. Jia, D., Jurkowska, R. Z., Zhang, X., Jeltsch, A., and Cheng, X. (2007) Structure of Dnmt3a bound to Dnmt3L suggests a model for *de novo* DNA methylation. *Nature* **449**, 248–251
47. Hollstein, M., Sidransky, D., Vogelstein, B., and Harris, C. C. (1991) p53 mutations in human cancers. *Science* **253**, 49–53
48. Levine, A. J., and Oren, M. (2009) The first 30 years of p53: growing ever more complex. *Nat. Rev. Cancer* **9**, 749–758
49. Harris, C. C., and Hollstein, M. (1993) Clinical implications of the p53 tumor-suppressor gene. *N. Engl. J. Med.* **329**, 1318–1327
50. Cho, Y., Gorina, S., Jeffrey, P. D., and Pavletich, N. P. (1994) Crystal structure of a p53 tumor suppressor–DNA complex: understanding tumorigenic mutations. *Science* **265**, 346–355
51. Anderson, B. J., Larkin, C., Guja, K., and Schildbach, J. F. (2008) Using fluorophore-labeled oligonucleotides to measure affinities of protein–DNA interactions. *Methods Enzymol.* **450**, 253–272
52. Gradinaru, C. C., Marushchak, D. O., Samim, M., and Krull, U. J. (2010) Fluorescence anisotropy: from single molecules to live cells. *Analyst* **135**, 452–459
53. Heyduk, T., Ma, Y., Tang, H., and Ebright, R. H. (1996) Fluorescence anisotropy: rapid, quantitative assay for protein–DNA and protein–protein interaction. *Methods Enzymol.* **274**, 492–503
54. Emperle, M., Rajavelu, A., Reinhardt, R., Jurkowska, R. Z., and Jeltsch, A. (2014) Cooperative DNA binding and protein/DNA fiber formation increases the activity of the Dnmt3a DNA methyltransferase. *J. Biol. Chem.* **289**, 29602–29613
55. Yan, Y., and Marriott, G. (2003) Analysis of protein interactions using fluorescence technologies. *Curr. Opin. Chem. Biol.* **7**, 635–640
56. Kreida, S., Roche, J. V., Olsson, C., Linse, S., and Törnroth-Horsefield, S. (2018) Protein–protein interactions in AQP regulation: biophysical characterization of AQP0–CaM and AQP2–LIP5 complex formation. *Faraday Disc.* **209**, 35–54

57. Oi, C., Treado, J. D., Levine, Z. A., Lim, C. S., Knecht, K. M., Xiong, Y., O'Hern, C. S., and Regan, L. (2018) A threonine zipper that mediates protein–protein interactions: structure and prediction. *Protein Sci.* **27**, 1969–1977
58. Singh, S. P., Kukshal, V., and Galletto, R. (2019) A stable tetramer is not the only oligomeric state that mitochondrial single-stranded DNA-binding proteins can adopt. *J. Biol. Chem.* **294**, 4137–4144
59. Karpf, A. R., Moore, B. C., Ririe, T. O., and Jones, D. A. (2001) Activation of the p53 DNA damage response pathway after inhibition of DNA methyltransferase by 5-aza-2'-deoxycytidine. *Mol. Pharmacol.* **59**, 751–757
60. Jackson-Grusby, L., Beard, C., Possemato, R., Tudor, M., Fambrough, D., Csankovszki, G., Dausman, J., Lee, P., Wilson, C., Lander, E., and Jaenisch, R. (2001) Loss of genomic methylation causes p53-dependent apoptosis and epigenetic deregulation. *Nat. Genet.* **27**, 31–39
61. Spencer, D. H., Russler-Germain, D. A., Ketkar, S., Helton, N. M., Lamprecht, T. L., Fulton, R. S., Fronick, C. C., O'Laughlin, M., Heath, S. E., Shinawi, M., Westervelt, P., *et al.* (2017) CpG island hypermethylation mediated by DNMT3A is a consequence of AML progression. *Cell* **168**, 801–816.e13
62. Chen, D., Christopher, M., Helton, N. M., Ferguson, I., Ley, T. J., and Spencer, D. H. (2018) DNMT3A R882-associated hypomethylation patterns are maintained in primary AML xenografts, but not in the DNMT3A R882C OCI-AML3 leukemia cell line. *Blood Cancer J.* **8**, 38
63. Rajamani, D., Thiel, S., Vajda, S., and Camacho, C. J. (2004) Anchor residues in protein–protein interactions. *Proc. Natl. Acad. Sci. U.S.A.* **101**, 11287–11292
64. Li, X., Keskin, O., Ma, B., Nussinov, R., and Liang, J. (2004) Protein–protein interactions: hot spots and structurally conserved residues often locate in complemented pockets that pre-organized in the unbound states: implications for docking. *J. Mol. Biol.* **344**, 781–795
65. Sowmya, G., Breen, E. J., and Ranganathan, S. (2015) Linking structural features of protein complexes and biological function. *Protein Sci.* **24**, 1486–1494
66. Joo, W. S., Jeffrey, P. D., Cantor, S. B., Finnin, M. S., Livingston, D. M., and Pavletich, N. P. (2002) Structure of the 53BP1 BRCT region bound to p53 and its comparison to the Brcal BRCT structure. *Genes Dev.* **16**, 583–593
67. Baldock, R. A., Day, M., Wilkinson, O. J., Cloney, R., Jeggo, P. A., Oliver, A. W., Watts, F. Z., and Pearl, L. H. (2015) ATM localization and heterochromatin repair depend on direct interaction of the 53BP1-BRCT2 domain with μ H2AX. *Cell Rep.* **13**, 2081–2089
68. Jubb, H. C., Pandurangan, A. P., Turner, M. A., Ochoa-Montano, B., Blundell, T. L., and Ascher, D. B. (2017) Mutations at protein-protein interfaces: small changes over big surfaces have large impacts on human health. *Prog. Biophys. Mol. Biol.* **128**, 3–13
69. David, A., Razali, R., Wass, M. N., and Sternberg, M. J. (2012) Protein–protein interaction sites are hot spots for disease-associated nonsynonymous SNPs. *Hum. Mutat.* **33**, 359–363
70. Engin, H. B., Kreisberg, J. F., and Carter, H. (2016) Structure-based analysis reveals cancer missense mutations target protein interaction interfaces. *PLoS ONE* **11**, e0152929

71. Yates, C. M., and Sternberg, M. J. (2013) The effects of non-synonymous single nucleotide polymorphisms (nsSNPs) on protein–protein interactions. *J. Mol. Biol.* **425**, 3949–3963
72. Trowbridge, J. J., and Orkin, S. H. (2011) Dnmt3a silences hematopoietic stem cell self-renewal. *Nat. Genet.* **44**, 13–14
73. Xu, J., Wang, Y. Y., Dai, Y. J., Zhang, W., Zhang, W. N., Xiong, S. M., Gu, Z. H., Wang, K. K., Zeng, R., Chen, Z., and Chen, S. J. (2014) DNMT3A Arg882 mutation drives chronic myelomonocytic leukemia through disturbing gene expression/DNA methylation in hematopoietic cells. *Proc. Natl. Acad. Sci. U.S.A.* **111**, 2620–2625
74. Freed-Pastor, W. A., and Prives, C. (2012) Mutant p53: one name, many proteins. *Genes Dev.* **26**, 1268–1286
75. Kim, M. P., and Lozano, G. (2018) Mutant p53 partners in crime. *Cell Death Differ.* **25**, 161–168
76. Zhu, J., Sammons, M. A., Donahue, G., Dou, Z., Vedadi, M., Getlik, M., Barsyte-Lovejoy, D., Al-awar, R., Katona, B. W., Shilatifard, A., Huang, J., Hua, X., Arrowsmith, C. H., and Berger, S. L. (2015) Gain-of-function p53 mutants co-opt chromatin pathways to drive cancer growth. *Nature* **525**, 206–211
77. Nieto, M., Samper, E., Fraga, M. F., González de Buitrago, G. G., Esteller, M., and Serrano, M. (2004) The absence of p53 is critical for the induction of apoptosis by 5-aza-2'-deoxycytidine. *Oncogene* **23**, 735–743
78. Jin, L., Wang, W., and Fang, G. (2014) Targeting protein-protein interaction by small molecules. *Annu. Rev. Pharmacol. Toxicol.* **54**, 435–456
79. Ivanov, A. A., Khuri, F. R., and Fu, H. (2013) Targeting protein–protein interactions as an anticancer strategy. *Trends Pharmacol. Sci.* **34**, 393–400
80. Petta, I., Lievens, S., Libert, C., Tavernier, J., and De Bosscher, K. (2016) Modulation of protein–protein interactions for the development of novel therapeutics. *Mol. Ther.* **24**, 707–718
81. Arkin, M. R., and Wells, J. A. (2004) Small-molecule inhibitors of protein–protein interactions: progressing towards the dream. *Nat. Rev. Drug Discov.* **3**, 301–317
82. Clackson, T., and Wells, J. A. (1995) A hot spot of binding energy in a hormone-receptor interface. *Science* **267**, 383–386
83. Vassilev, L. T., Vu, B. T., Graves, B., Carvajal, D., Podlaski, F., Filipovic, Z., Kong, N., Kammlott, U., Lukacs, C., Klein, C., Fotouhi, N., and Liu, E. A. (2004) *In vivo* activation of the p53 pathway by small-molecule antagonists of MDM2. *Science* **303**, 844–848
84. Vu, B., Wovkulich, P., Pizzolato, G., Lovey, A., Ding, Q., Jiang, N., Liu, J. J., Zhao, C., Glenn, K., Wen, Y., Tovar, C., Packman, K., Vassilev, L., and Graves, B. (2013) Discovery of RG7112: a small-molecule MDM2 inhibitor in clinical development. *ACS Med. Chem. Lett.* **4**, 466–469
85. Ray-Coquard, I., Blay, J. Y., Italiano, A., Le Cesne, A., Penel, N., Zhi, J., Heil, F., Rueger, R., Graves, B., Ding, M., Geho, D., Middleton, S. A., Vassilev, L. T., Nichols, G. L., and Bui, B. N. (2012) Effect of the MDM2 antagonist RG7112 on the P53 pathway in patients with MDM2-amplified, well-differentiated or dedifferentiated liposarcoma: an exploratory proof-of-mechanism study. *Lancet Oncol.* **13**, 1133–1140
86. Ding, Q., Zhang, Z., Liu, J. J., Jiang, N., Zhang, J., Ross, T. M., Chu, X. J., Bartkovitz, D., Podlaski, F., Janson, C., Tovar, C., Filipovic, Z. M., Higgins, B., Glenn,

- K., Packman, K., *et al.* (2013) Discovery of RG7388, a potent and selective p53–MDM2 inhibitor in clinical development. *J. Med. Chem.* **56**, 5979–5983
87. Zhao, Y., Aguilar, A., Bernard, D., and Wang, S. (2015) Small-molecule inhibitors of the MDM2–p53 protein–protein interaction (MDM2 inhibitors) in clinical trials for cancer treatment: miniperspective. *J. Med. Chem.* **58**, 1038–1052
88. Wang, S., Sun, W., Zhao, Y., McEachern, D., Meaux, I., Barrière, C., Stuckey, J. A., Meagher, J. L., Bai, L., Liu, L., Hoffman-Luca, C. G., Lu, J., Shangary, S., Yu, S., Bernard, D., *et al.* (2014) SAR405838: an optimized inhibitor of MDM2–p53 interaction that induces complete and durable tumor regression. *Cancer Res.* **74**, 5855–5865
89. Sun, D., Li, Z., Rew, Y., Gribble, M., Bartberger, M. D., Beck, H. P., Canon, J., Chen, A., Chen, X., Chow, D., Deignan, J., Duquette, J., Eksterowicz, J., Fisher, B., Fox, B. M., *et al.* (2014) Discovery of AMG 232, a potent, selective, and orally bioavailable MDM2–p53 inhibitor in clinical development. *J. Med. Chem.* **57**, 1454–1472
90. Cancer Genome Atlas Research Network, Ley, T. J., Miller, C., Ding, L., Raphael, B. J., Mungall, A. J., Robertson, A., Hoadley, K., Triche, T. J., Jr., Laird, P. W., Baty, J. D., Fulton, L. L., *et al.* (2013) Genomic and epigenomic landscapes of adult *de novo* acute myeloid leukemia. *N. Engl. J. Med.* **368**, 2059–2074
91. Ayed, A., Mulder, F. A., Yi, G. S., Lu, Y., Kay, L. E., and Arrowsmith, C. H. (2001) Latent and active p53 are identical in conformation. *Nat. Struct. Mol. Biol.* **8**, 756–760
92. Zhang, Z. M., Lu, R., Wang, P., Yu, Y., Chen, D., Gao, L., Liu, S., Ji, D., Rothbart, S. B., Wang, Y., Wang, G. G., and Song, J. (2018) Structural basis for DNMT3A-mediated *de novo* DNA methylation. *Nature* **554**, 387–391.
93. Emamzadah, S., Tropia, L., and Halazonetis, T. D. (2011) Crystal structure of a multidomain human p53 tetramer bound to the natural CDKN1A (p21) p53-response element. *Mol. Cancer Res.* **9**, 1493–1499
94. Mintseris, J., Pierce, B., Wiehe, K., Anderson, R., Chen, R., and Weng, Z. (2007) Integrating statistical pair potentials into protein complex prediction. *Proteins* **69**, 511–520
95. Chen, R., Li, L., and Weng, Z. (2003) ZDOCK: an initial-stage protein-docking algorithm. *Proteins* **52**, 80–87
96. Peterson, S. N., and Reich, N. O. (2006) GATC flanking sequences regulate Dam activity: evidence for how Dam specificity may influence pap expression. *J. Mol. Biol.* **355**, 459–472
97. Zhang, G., Estève, P. O., Chin, H. G., Terragni, J., Dai, N., Corrêa, I. R., Jr., and Pradhan, S. (2015) Small RNA-mediated DNA (cytosine-5) methyltransferase 1 inhibition leads to aberrant DNA methylation. *Nucleic Acids Res.* **43**, 6112–6124
98. Ponnaluri, V. C., Estève, P. O., Ruse, C. I., and Pradhan, S. (2018) S-Adenosylhomocysteine hydrolase participates in DNA methylation inheritance. *J. Mol. Biol.* **430**, 2051–2065
99. Mellini, P., Marrocco, B., Borovika, D., Polletta, L., Carnevale, I., Saladini, S., Stazi, G., Zwergel, C., Trapencieris, P., Ferretti, E., and Tafani, M. (2018). Pyrazole-based inhibitors of enhancer of zeste homologue 2 induce apoptosis and autophagy in cancer cells. *Philos. Trans. R. Soc. B Biol. Sci.* **373**, 20170150
100. Mao, S. Q., Ghanbarian, A. T., Spiegel, J., Cuesta, S. M., Beraldi, D., Di Antonio, M., Marsico, G., Hänsel-Hertsch, R., Tannahill, D., and Balasubramanian,

- S. (2018) DNA G-quadruplex structures mold the DNA methylome. *Nat. Struct. Mol. Biol.* **25**, 951–957
101. Balakrishnan, A., Guruprasad, K. P., Satyamoorthy, K., and Joshi, M. B. (2018) Interleukin-6 determines protein stabilization of DNA methyltransferases and alters DNA promoter methylation of genes associated with insulin signaling and angiogenesis. *Lab. Invest.* **98**, 1143–1158
102. Holz-Schietinger, C., and Reich, N. O. (2010) The inherent processivity of the human *de novo* methyltransferase 3A (DNMT3A) is enhanced by DNMT3L. *J. Biol. Chem.* **285**, 29091–29100

Chapter IV

1. Maunakea, A. K., Nagarajan, R. P., Bilenky, M., Ballinger, T. J., D'Souza, C., Fouse, S. D., Johnson, B. E., Hong, C., Nielsen, C., Zhao, Y., Turecki, G., Delaney, A., Varhol, R., Thiessen, N., Shchors, K., Heine, V. M., Rowitch, D. H., Xing, X., Fiore, C., Schillebeeckx, M., Jones, S. J. M., Haussler, D., Marra, M. A., Hirst, M., Wang, T., and Costello, J. F. (2010). Conserved Role of Intragenic DNA Methylation in Regulating Alternative Promoters. *Nature*, **466**, 253–257.
2. Jones, P. A. (1999). The DNA methylation paradox. *Trends in Genetics*, **15**, 34–37.
3. Berger, S. L. (2007). The complex language of chromatin regulation during transcription. *Nature*, **447**, 407–412.
4. Weinberg, D. N., Papillon-Cavanagh, S., Chen, H., Yue, Y., Chen, X., Rajagopalan, K. N., Horth, C., McGuire, J. T., Xu, X., Nikbakht, H., Lemiesz, A. E., Marchione, D. M., Marunde, M. R., Meiners, M. J., Cheek, M. A., Keogh, M.-C., Bareke, E., Djedid, A., Harutyunyan, A. S., Jabado, N., Garcia, B. A., Li, H., Allis, C. D., Majewski, J., and Lu, C. (2019). The histone mark H3K36me2 recruits DNMT3A and shapes the intergenic DNA methylation landscape. *Nature*, **573**, 281–286.
5. Lehnertz, B., Ueda, Y., Derijck, A. A. H. A., Braunschweig, U., Perez-Burgos, L., Kubicek, S., Chen, T., Li, E., Jenuwein, T., and Peters, A. H. F. M. (2003). Suv39h-Mediated Histone H3 Lysine 9 Methylation Directs DNA Methylation to Major Satellite Repeats at Pericentric Heterochromatin. *Current Biology*, **13**, 1192–1200.
6. Hervouet, E., Peixoto, P., Delage-Mourroux, R., Boyer-Guittaut, M., and Cartron, P.-F. (2018). Specific or not specific recruitment of DNMTs for DNA methylation, an epigenetic dilemma. *Clin Epigenet*, **10**, 17.
7. Ge, Y.-Z., Pu, M.-T., Gowher, H., Wu, H.-P., Ding, J.-P., Jeltsch, A., and Xu, G.-L. (2004). Chromatin Targeting of *de Novo* DNA Methyltransferases by the PWWP Domain. *J. Biol. Chem*, **279**, 25447–25454.
8. Lorincz, M. C., Dickerson, D. R., Schmitt, M., and Groudine, M. (2004). Intragenic DNA methylation alters chromatin structure and elongation efficiency in mammalian cells. *Nat Struct Mol Biol*, **11**, 1068–1075.
9. Paul, T. A., Bies, J., Small, D., and Wolff, L. (2010). Signatures of polycomb repression and reduced H3K4 trimethylation are associated with p15INK4b DNA methylation in AML. *Blood*, **115**, 3098–3108.
10. Guo, X., Wang, L., Li, J., Ding, Z., Xiao, J., Yin, X., He, S., Shi, P., Dong, L., Li, G., Tian, C., Wang, J., Cong, Y., and Xu, Y. (2015). Structural insight into autoinhibition and histone H3-induced activation of DNMT3A. *Nature*, **517**, 640–644.

11. Ooi, S. K. T., Qiu, C., Bernstein, E., Li, K., Jia, D., Yang, Z., Erdjument-Bromage, H., Tempst, P., Lin, S.-P., Allis, C. D., Cheng, X., and Bestor, T. H. (2007). DNMT3L connects unmethylated lysine 4 of histone H3 to de novo methylation of DNA. *Nature*, **448**, 714–717.
12. Zhang, Y., Jurkowska, R., Soeroes, S., Rajavelu, A., Dhayalan, A., Bock, I., Rathert, P., Brandt, O., Reinhardt, R., Fischle, W., and Jeltsch, A. (2010). Chromatin methylation activity of Dnmt3a and Dnmt3a/3L is guided by interaction of the ADD domain with the histone H3 tail. *Nucleic Acids Res*, **38**, 4246–4253.
13. Sandoval, J. E., and Reich, N. O. (2019). The R882H substitution in the human *de novo* DNA methyltransferase DNMT3A disrupts allosteric regulation by the tumor suppressor p53. *J. Biol. Chem*, **294**, 18207–18219.
14. Sandoval, J. E., Huang, Y.-H., Muise, A., Goodell, M. A., and Reich, N. O. (2019). Mutations in the DNMT3A DNA methyltransferase in acute myeloid leukemia patients cause both loss and gain of function and differential regulation by protein partners. *J. Biol. Chem*, **294**, 4898–4910.
15. Mungamuri, S. K., Benson, E. K., Wang, S., Gu, W., Lee, S. W., and Aaronson, S. A. (2012). p53-mediated heterochromatin reorganization regulates its cell fate decisions. *Nat Struct Mol Biol*, **19**, 478–484.
16. Garcia-Gomez, A., Li, T., Kerick, M., Català-Moll, F., Comet, N. R., Rodríguez-Ubreva, J., de la Rica, L., Branco, M. R., Martín, J., and Ballestar, E. (2017). TET2- and TDG-mediated changes are required for the acquisition of distinct histone modifications in divergent terminal differentiation of myeloid cells. *Nucleic Acids Research*, **45**, 10002–10017.
17. Feng, Y., Wang, J., Asher, S., Hoang, L., Guardiani, C., Ivanov, I., and Zheng, Y. G. (2011). Histone H4 Acetylation Differentially Modulates Arginine Methylation by an in Cis Mechanism. *J. Biol. Chem*, **286**, 20323–20334.
18. Azzaz, A. M., Vitalini, M. W., Thomas, A. S., Price, J. P., Blacketer, M. J., Cryderman, D. E., Zirbel, L. N., Woodcock, C. L., Elcock, A. H., Wallrath, L. L., and Shogren-Knaak, M. A. (2014). Human Heterochromatin Protein 1 α Promotes Nucleosome Associations That Drive Chromatin Condensation. *J. Biol. Chem*, **289**, 6850–6861.
19. Li, B.-Z., Huang, Z., Cui, Q.-Y., Song, X.-H., Du, L., Jeltsch, A., Chen, P., Li, G., Li, E., and Xu, G.-L. (2011). Histone tails regulate DNA methylation by allosterically activating de novo methyltransferase. *Cell Res*, **21**, 1172–1181.
20. Li, Y.-Q., Zhou, P.-Z., Zheng, X.-D., Walsh, C. P., and Xu, G.-L. (2007). Association of Dnmt3a and thymine DNA glycosylase links DNA methylation with base-excision repair. *Nucleic Acids Research*, **35**, 390–400.
21. Fischle, W. (2008). Talk is cheap—cross-talk in establishment, maintenance, and readout of chromatin modifications. *Genes & Development*, **22**, 3375–3382.
22. Gowher, H., Stockdale, C. J., Goyal, R., Ferreira, H., Owen-Hughes, T., and Jeltsch, A. (2005). De Novo Methylation of Nucleosomal DNA by the Mammalian Dnmt1 and Dnmt3A DNA Methyltransferases. *Biochemistry*, **44**, 9899–9904.
23. Cao, R., Wang, L., Wang, H., Xia, L., Erdjument-Bromage, H., Tempst, P., Jones, R. S., and Zhang, Y. (2002). Role of Histone H3 Lysine 27 Methylation in Polycomb-Group Silencing. *Science*, **298**, 1039–1043.
24. Velazquez Camacho, O., Galan, C., Swist-Rosowska, K., Ching, R., Gamalinda, M., Karabiber, F., De La Rosa-Velazquez, I., Engist, B., Koschorz, B., Shukeir, N., Onishi-Seebacher, M., van de Nobelen, S., and Jenuwein, T. (2017). Major satellite

- repeat RNA stabilize heterochromatin retention of Suv39h enzymes by RNA-nucleosome association and RNA:DNA hybrid formation. *eLife*, **6**, e25293.
25. Holz-Schietinger, C., Matje, D. M., Harrison, M. F., and Reich, N. O. (2011). Oligomerization of DNMT3A Controls the Mechanism of de Novo DNA Methylation. *J. Biol. Chem*, **286**, 41479–41488.
 26. Holz-Schietinger, C., and Reich, N. O. (2010). The Inherent Processivity of the Human *de Novo* Methyltransferase 3A (DNMT3A) Is Enhanced by DNMT3L. *J. Biol. Chem*, **285**, 29091–29100.
 27. Okano, M., Bell, D. W., Haber, D. A., and Li, E. (1999). DNA Methyltransferases Dnmt3a and Dnmt3b Are Essential for De Novo Methylation and Mammalian Development. *Cell*, **99**, 247–257.
 28. Kaneda, M., Okano, M., Hata, K., Sado, T., Tsujimoto, N., Li, E., and Sasaki, H. (2004). Essential role for de novo DNA methyltransferase Dnmt3a in paternal and maternal imprinting. *Nature*, **429**, 900–903.
 29. Wang, Y. A., Kamarova, Y., Shen, K. C., Jiang, Z., Hahn, M. J., Wang, Y., and Brooks, S. C. (2005). DNA methyltransferase-3a interacts with p53 and represses p53-mediated gene expression. *Cancer Biology & Therapy*, **4**, 1138–1143.
 30. Davey, C.A., Sargent, D.F., Luger, K., Maeder, A.W. and Richmond, T.J. (2002). Solvent mediated interactions in the structure of the nucleosome core particle at 1.9 Å resolution. *Journal of molecular biology*, **319**, 1097-1113.
 31. Kato, D., Osakabe, A., Arimura, Y., Mizukami, Y., Horikoshi, N., Saikusa, K., Akashi, S., Nishimura, Y., Park, S.Y., Nogami, J. and Maehara, K. (2017). Crystal structure of the overlapping dinucleosome composed of hexasome and octasome. *Science*, **356**, 205–208.
 32. Danilova, N., Sakamoto, K. M., and Lin, S. (2008). p53 family in development. *Mechanisms of Development*, **125**, 919–931.
 33. Xu, X., Watt, D. S., and Liu, C. (2015). Multifaceted roles for thymine DNA glycosylase in embryonic development and human carcinogenesis. *Acta Biochim Biophys Sin*, **48**, 82-89.
 34. Biel, M., Wascholowski, V. and Giannis, A. (2005). Epigenetics—An Epicenter of Gene Regulation: Histones and Histone-Modifying Enzymes. *Angewandte Chemie International Edition*, **44**, 3186–3216.
 35. Luo, Q., Beaver, J.M., Liu, Y. and Zhang, Z. (2017). Dynamics of p53: A Master Decider of Cell Fate. *Genes*, **8**, 66.
 36. Germanguz, I., Park, J.C., Cinkornpumin, J., Solomon, A., Ohashi, M. and Lowry, W.E. (2018). TDG regulates cell cycle progression in human neural progenitors. *F1000Res*, **7**, 497.
 37. Liao, H.F., Tai, K.Y., Chen, W.S.C., Cheng, L.C., Ho, H.N. and Lin, S.P. (2012). Functions of DNA methyltransferase 3-like in germ cells and beyond. *Biology of the Cell*, **104**, 571–587.
 38. Bayraktar, G. and Kreutz, M.R. (2018). Neuronal DNA Methyltransferases: Epigenetic Mediators between Synaptic Activity and Gene Expression? *Neuroscientist*, **24**, 171–185.
 39. Li, X., Zhang, Q., Ding, Y., Liu, Y., Zhao, D., Zhao, K., Shen, Q., Liu, X., Zhu, X., Li, N. and Cheng, Z. (2016). Methyltransferase Dnmt3a upregulates HDAC9 to deacetylate the kinase TBK1 for activation of antiviral innate immunity. *Nat Immunol*, **17**, 806–815.

40. Chen, B.F. and Chan, W.Y. (2014). The de novo DNA methyltransferase DNMT3A in development and cancer. *Epigenetics*, **9**, 669–677.
41. Barbosa, K., Li, S., Adams, P.D. and Deshpande, A.J. (2019). The role of TP53 in acute myeloid leukemia: Challenges and opportunities. *Genes, Chromosomes and Cancer*, **58**, 875–888.
42. Maynard, S., Schurman, S.H., Harboe, C., de Souza-Pinto, N.C. and Bohr, V.A. (2008). Base excision repair of oxidative DNA damage and association with cancer and aging. *Carcinogenesis*, **30**, 2–10.
43. Purdy, M.M., Holz-Schietinger, C. and Reich, N.O. (2010). Identification of a second DNA binding site in human DNA methyltransferase 3A by substrate inhibition and domain deletion. *Archives of biochemistry and biophysics*, **498**, 13–22.
44. Ayed, A., Mulder, F.A., Yi, G.S., Lu, Y., Kay, L.E. and Arrowsmith, C.H. (2001). Latent and active p53 are identical in conformation. *nature structural biology*, **8**, 5.
45. Schuermann, D., Scheidegger, S.P., Weber, A.R., Bjørås, M., Leumann, C.J. and Schär, P. (2016). 3CAPS – a structural AP–site analogue as a tool to investigate DNA base excision repair. *Nucleic Acids Res*, **44**, 2187–2198.
46. Peterson, S.N. and Reich, N.O. (2006). GATC flanking sequences regulate Dam activity: evidence for how Dam specificity may influence pap expression. *Journal of molecular biology*, **355**, 459–472.
47. Fuchs, S.M., Krajewski, K., Baker, R.W., Miller, V.L. and Strahl, B.D. (2011). Influence of combinatorial histone modifications on antibody and effector protein recognition. *Current biology*, **21**, 53–58.
48. Lowary, P.T. and Widom, J. (1998). New DNA sequence rules for high affinity binding to histone octamer and sequence-directed nucleosome positioning. *Journal of molecular biology*, **276**, 19–42.
49. Kuo, A.J., Cheung, P., Chen, K., Zee, B.M., Kioi, M., Lauring, J., Xi, Y., Park, B.H., Shi, X., Garcia, B.A. and Li, W. (2011). NSD2 links dimethylation of histone H3 at lysine 36 to oncogenic programming. *Mol Cell.*, **44**, 609–620.
50. Zhang, Z.M., Lu, R., Wang, P., Yu, Y., Chen, D., Gao, L., Liu, S., Ji, D., Rothbart, S.B., Wang, Y. and Wang, G.G. (2018). Structural basis for DNMT3A-mediated de novo DNA methylation. *Nature*, **554**, 387–391.

Chapter V

1. Savell, K. E., Gallus, N. V. N., Simon, R. C., Brown, J. A., Revanna, J. S., Osborn, M. K., Song, E. Y., O'Malley, J. J., Stackhouse, C. T., Norvil, A., Gowher, H., Sweatt, J. D., and Day, J. J. (2016) Extra-coding RNAs regulate neuronal DNA methylation dynamics. *Nature Communications*. **7**, 12091
2. Holz-Schietinger, C., and Reich, N. O. (2012) RNA modulation of the human DNA methyltransferase 3A. *Nucleic Acids Research*. **40**, 8550–8557J. E. Sandoval, N. O. Reich, The R882H substitution in the human de novo DNA methyltransferase DNMT3A disrupts allosteric regulation by the tumor suppressor p53. *Journal of Biological Chemistry* **294**, 18207–18219 (2019).
3. Sandoval, J. E., Huang, Y.-H., Muise, A., Goodell, M. A., and Reich, N. O. (2019) Mutations in the DNMT3A DNA methyltransferase in acute myeloid leukemia patients

- cause both loss and gain of function and differential regulation by protein partners. *Journal of Biological Chemistry*. **294**, 4898–4910
4. Jia, D., Jurkowska, R. Z., Zhang, X., Jeltsch, A., and Cheng, X. (2007) Structure of Dnmt3a bound to Dnmt3L suggests a model for de novo DNA methylation. *Nature*. **449**, 248–251
 5. Guo, X., Wang, L., Li, J., Ding, Z., Xiao, J., Yin, X., He, S., Shi, P., Dong, L., Li, G., Tian, C., Wang, J., Cong, Y., and Xu, Y. (2015) Structural insight into autoinhibition and histone H3-induced activation of DNMT3A. *Nature*. **517**, 640–644
 6. Ooi, S. K. T., Qiu, C., Bernstein, E., Li, K., Jia, D., Yang, Z., Erdjument-Bromage, H., Tempst, P., Lin, S.-P., Allis, C. D., Cheng, X., and Bestor, T. H. (2007) DNMT3L connects unmethylated lysine 4 of histone H3 to de novo methylation of DNA. *Nature*. **448**, 714–717
 7. Zhang, Y., Jurkowska, R., Soeroes, S., Rajavelu, A., Dhayalan, A., Bock, I., Rathert, P., Brandt, O., Reinhardt, R., Fischle, W., and Jeltsch, A. (2010) Chromatin methylation activity of Dnmt3a and Dnmt3a/3L is guided by interaction of the ADD domain with the histone H3 tail. *Nucleic Acids Res.* **38**, 4246–4253
 8. Michalak, E. M., Burr, M. L., Bannister, A. J., and Dawson, M. A. (2019) The roles of DNA, RNA and histone methylation in ageing and cancer. *Nature Reviews Molecular Cell Biology*. **20**, 573–589
 9. Denis, H., Ndlovu, 'Matladi N., and Fuks, F. (2011) Regulation of mammalian DNA methyltransferases: a route to new mechanisms. *EMBO reports*. **12**, 647–656
 10. Wei, J.-W., Huang, K., Yang, C., and Kang, C.-S. (2017) Non-coding RNAs as regulators in epigenetics (Review). *Oncology Reports*. **37**, 3–9
 11. Sun, B. K., Deaton, A. M., and Lee, J. T. (2006) A Transient Heterochromatic State in Xist Preempts X Inactivation Choice without RNA Stabilization. *Molecular Cell*. **21**, 617–628
 12. Greenberg, M. V. C., and Bourc'his, D. (2019) The diverse roles of DNA methylation in mammalian development and disease. *Nature Reviews Molecular Cell Biology*. **20**, 590–607
 13. Miller, C. A., and Sweatt, J. D. (2007) Covalent Modification of DNA Regulates Memory Formation. *Neuron*. **53**, 857–869
 14. Feng, J., Zhou, Y., Campbell, S. L., Le, T., Li, E., Sweatt, J. D., Silva, A. J., and Fan, G. (2010) Dnmt1 and Dnmt3a maintain DNA methylation and regulate synaptic function in adult forebrain neurons. *Nat Neurosci*. **13**, 423–430
 15. LaPlant, Q., Vialou, V., Covington, H. E., Dumitriu, D., Feng, J., Warren, B. L., Maze, I., Dietz, D. M., Watts, E. L., Iñiguez, S. D., Koo, J. W., Mouzon, E., Renthal, W., Hollis, F., Wang, H., Noonan, M. A., Ren, Y., Eisch, A. J., Bolaños, C. A., Kabbaj, M., Xiao, G., Neve, R. L., Hurd, Y. L., Oosting, R. S., Fan, G., Morrison, J. H., and Nestler, E. J. (2010) Dnmt3a regulates emotional behavior and spine plasticity in the nucleus accumbens. *Nat Neurosci*. **13**, 1137–1143
 16. Butler, A. A., Webb, W. M., and Lubin, F. D. (2015) Regulatory RNAs and control of epigenetic mechanisms: expectations for cognition and cognitive dysfunction. *Epigenomics*. **8**, 135–151
 17. Chung, L. (2015) A Brief Introduction to the Transduction of Neural Activity into Fos Signal. *Dev Reprod*. **19**, 61–67

18. Zhang, G., Estève, P.-O., Chin, H. G., Terragni, J., Dai, N., Corrêa, I. R., and Pradhan, S. (2015) Small RNA-mediated DNA (cytosine-5) methyltransferase 1 inhibition leads to aberrant DNA methylation. *Nucleic Acids Res.* **43**, 6112–6124
19. Di Ruscio, A., Ebralidze, A. K., Benoukraf, T., Amabile, G., Goff, L. A., Terragni, J., Figueroa, M. E., De Figueiredo Pontes, L. L., Alberich-Jorda, M., Zhang, P., Wu, M., D'Alò, F., Melnick, A., Leone, G., Ebralidze, K. K., Pradhan, S., Rinn, J. L., and Tenen, D. G. (2013) DNMT1-interacting RNAs block gene-specific DNA methylation. *Nature.* **503**, 371–376
20. Schaukowitch, K., Joo, J.-Y., Liu, X., Watts, J. K., Martinez, C., and Kim, T.-K. (2014) Enhancer RNA Facilitates NELF Release from Immediate Early Genes. *Molecular Cell.* **56**, 29–42
21. Sanz, L. A., Hartono, S. R., Lim, Y. W., Steyaert, S., Rajpurkar, A., Ginno, P. A., Xu, X., and Chédin, F. (2016) Prevalent, Dynamic, and Conserved R-Loop Structures Associate with Specific Epigenomic Signatures in Mammals. *Molecular Cell.* **63**, 167–178
22. Martianov, I., Ramadass, A., Serra Barros, A., Chow, N., and Akoulitchev, A. (2007) Repression of the human dihydrofolate reductase gene by a non-coding interfering transcript. *Nature.* **445**, 666–670
23. Liu, Z.-P., Liu, S., Chen, R., Huang, X., and Wu, L.-Y. (2017) Structure alignment-based classification of RNA-binding pockets reveals regional RNA recognition motifs on protein surfaces. *BMC Bioinformatics.* **18**, 27
24. Wang, W., Li, K., Lv, H., Zhang, H., Zhang, S., Zhou, Y., and Huang, J. (2019) Analyzing the Surface Structure of the Binding Domain on DNA and RNA Binding Proteins. *IEEE Access.* **7**, 30042–30049
25. Riley, K. J.-L., and Maher, L. J. (2007) p53 RNA interactions: New clues in an old mystery. *RNA.* **13**, 1825–1833
26. Wang, Y. A., Kamarova, Y., Shen, K. C., Jiang, Z., Hahn, M. J., Wang, Y., and Brooks, S. C. (2005) DNA methyltransferase-3a interacts with p53 and represses p53-mediated gene expression. *Cancer Biology & Therapy.* **4**, 1138–1143
27. Gourvest, M., Brousset, P., and Bousquet, M. (2019) Long Noncoding RNAs in Acute Myeloid Leukemia: Functional Characterization and Clinical Relevance. *Cancers.* **11**, 1638
28. Vallone, C., Rigon, G., Gulia, C., Baffa, A., Votino, R., Morosetti, G., Zaami, S., Briganti, V., Catania, F., Gaffi, M., Nucciotti, R., Costantini, F. M., Piergentili, R., Putignani, L., and Signore, F. (2018) Non-Coding RNAs and Endometrial Cancer. *Genes.* **9**, 187
29. Yang, X., Wong, M. P. M., and Ng, R. K. (2019) Aberrant DNA Methylation in Acute Myeloid Leukemia and Its Clinical Implications. *International Journal of Molecular Sciences.* **20**, 4576
30. Saghafinia, S., Mina, M., Riggi, N., Hanahan, D., and Ciriello, G. (2018) Pan-Cancer Landscape of Aberrant DNA Methylation across Human Tumors. *Cell Reports.* **25**, 1066-1080.e8
31. Sandoval, J. E., and Reich, N. O. (2021) p53 and TDG are dominant in regulating the activity of the human de novo DNA methyltransferase DNMT3A on nucleosomes. *Journal of Biological Chemistry.* **296**, 100058

32. Chédin, F., Lieber, M. R., and Hsieh, C.-L. (2002) The DNA methyltransferase-like protein DNMT3L stimulates de novo methylation by Dnmt3a. *PNAS*. **99**, 16916–16921
33. Yan, Y., Zhang, D., Zhou, P., Li, B., and Huang, S.-Y. (2017) HDOCK: a web server for protein–protein and protein–DNA/RNA docking based on a hybrid strategy. *Nucleic Acids Research*. **45**, W365–W373
34. Zakrevsky, P., K. Kasprzak, W., F. Heinz, W., Wu, W., Khant, H., Bindewald, E., Dorjsuren, N., A. Fields, E., Val, N. de, Jaeger, L., and A. Shapiro, B. (2020) Truncated tetrahedral RNA nanostructures exhibit enhanced features for delivery of RNAi substrates. *Nanoscale*. **12**, 2555–2568
35. Holz-Schietinger, C., Matje, D. M., Harrison, M. F., and Reich, N. O. (2011) Oligomerization of DNMT3A Controls the Mechanism of de Novo DNA Methylation. *Journal of Biological Chemistry*. **286**, 41479–41488
36. Deep, A., Tiwari, P., Agarwal, S., Kaundal, S., Kidwai, S., Singh, R., and Thakur, K. G. (2018) Structural, functional and biological insights into the role of Mycobacterium tuberculosis VapBC11 toxin–antitoxin system: targeting a tRNase to tackle mycobacterial adaptation. *Nucleic Acids Research*. **46**, 11639–11655
37. Tejera, B., López, R. E., Hidalgo, P., Cárdenas, R., Ballesteros, G., Rivillas, L., French, L., Amero, C., Pastor, N., Santiago, Á., Groitl, P., Dobner, T., and Gonzalez, R. A. (2019) The human adenovirus type 5 E1B 55kDa protein interacts with RNA promoting timely DNA replication and viral late mRNA metabolism. *PLOS ONE*. **14**, e0214882
38. Yeh, C.-C., Luo, J.-L., Phan, N. N., Cheng, Y.-C., Chow, L.-P., Tsai, M.-H., Chuang, E. Y., and Lai, L.-C. (2018) Different effects of long noncoding RNA NDRG1-OT1 fragments on NDRG1 transcription in breast cancer cells under hypoxia. *RNA Biology*. **15**, 1487–1498
39. Zhang, Z.-M., Lu, R., Wang, P., Yu, Y., Chen, D., Gao, L., Liu, S., Ji, D., Rothbart, S. B., Wang, Y., Wang, G. G., and Song, J. (2018) Structural basis for DNMT3A-mediated de novo DNA methylation. *Nature*. **554**, 387–391.
40. Weinstein, J. N., Collisson, E. A., Mills, G. B., Shaw, K. M., Ozenberger, B. A., Ellrott, K., Shmulevich, I., Sander, C., and Stuart, J. M. (2013) The Cancer Genome Atlas Pan-Cancer Analysis Project. *Nat Genet*. **45**, 1113–1120
41. Holz-Schietinger, C., Matje, D. M., and Reich, N. O. (2012) Mutations in DNA Methyltransferase (DNMT3A) Observed in Acute Myeloid Leukemia Patients Disrupt Processive Methylation. *Journal of Biological Chemistry*. **287**, 30941–30951
42. Velazquez Camacho, O., Galan, C., Swist-Rosowska, K., Ching, R., Gamalinda, M., Karabiber, F., De La Rosa-Velazquez, I., Engist, B., Koschorz, B., Shukeir, N., Onishi-Seebacher, M., van de Nobelen, S., and Jenuwein, T. (2017) Major satellite repeat RNA stabilize heterochromatin retention of Suv39h enzymes by RNA-nucleosome association and RNA:DNA hybrid formation. *eLife*. **6**, e25293
43. Yuan, J., Yang, F., Chen, B., Lu, Z., Huo, X., Zhou, W., Wang, F., and Sun, S. (2011) The histone deacetylase 4/SP1/microrna-200a regulatory network contributes to aberrant histone acetylation in hepatocellular carcinoma. *Hepatology*. **54**, 2025–2035
44. Kim, D. H., Sætrom, P., Snøve, O., and Rossi, J. J. (2008) MicroRNA-directed transcriptional gene silencing in mammalian cells. *PNAS*. **105**, 16230–16235

45. Bose, D. A., Donahue, G., Reinberg, D., Shiekhatar, R., Bonasio, R., and Berger, S. L. (2017) RNA Binding to CBP Stimulates Histone Acetylation and Transcription. *Cell*. **168**, 135-149.e22
46. Peschansky, V. J., and Wahlestedt, C. (2014) Non-coding RNAs as direct and indirect modulators of epigenetic regulation. *Epigenetics*. **9**, 3–12
47. Li, B.-Z., Huang, Z., Cui, Q.-Y., Song, X.-H., Du, L., Jeltsch, A., Chen, P., Li, G., Li, E., and Xu, G.-L. (2011) Histone tails regulate DNA methylation by allosterically activating de novo methyltransferase. *Cell Research*. **21**, 1172–1181
48. Chen, B.-F., and Chan, W.-Y. (2014) The de novo DNA methyltransferase DNMT3A in development and cancer. *Epigenetics*. **9**, 669–677
49. The Gene Ontology Consortium (2015) Gene Ontology Consortium: going forward. *Nucleic Acids Research*. **43**, D1049–D1056
50. Kai, M. (2016) Roles of RNA-Binding Proteins in DNA Damage Response. *International Journal of Molecular Sciences*. **17**, 310
51. Díaz-Muñoz, M. D., and Turner, M. (2018) Uncovering the Role of RNA-Binding Proteins in Gene Expression in the Immune System. *Front. Immunol.* [10.3389/fimmu.2018.01094](https://doi.org/10.3389/fimmu.2018.01094)
52. Jones, S. (2016) Protein–RNA interactions: structural biology and computational modeling techniques. *Biophys Rev*. **8**, 359–367
53. Jones, S., Daley, D. T. A., Luscombe, N. M., Berman, H. M., and Thornton, J. M. (2001) Protein–RNA interactions: a structural analysis. *Nucleic Acids Research*. **29**, 943–954
54. Jurkowska, R. Z., Rajavelu, A., Anspach, N., Urbanke, C., Jankevicius, G., Ragozin, S., Nellen, W., and Jeltsch, A. (2011) Oligomerization and Binding of the Dnmt3a DNA Methyltransferase to Parallel DNA Molecules: HETEROCHROMATIC LOCALIZATION AND ROLE OF Dnmt3L*. *Journal of Biological Chemistry*. **286**, 24200–24207
55. Poyurovsky, M. V., Katz, C., Laptenko, O., Beckerman, R., Lokshin, M., Ahn, J., Byeon, I.-J. L., Gabizon, R., Mattia, M., Zupnick, A., Brown, L. M., Friedler, A., and Prives, C. (2010) The C terminus of p53 binds the N-terminal domain of MDM2. *Nature Structural & Molecular Biology*. **17**, 982–989
56. Tani, H., Mizutani, R., Salam, K. A., Tano, K., Ijiri, K., Wakamatsu, A., Isogai, T., Suzuki, Y., and Akimitsu, N. (2012) Genome-wide determination of RNA stability reveals hundreds of short-lived noncoding transcripts in mammals. *Genome Res*. **22**, 947–956
57. Bhat, S. A., Ahmad, S. M., Mumtaz, P. T., Malik, A. A., Dar, M. A., Urwat, U., Shah, R. A., and Ganai, N. A. (2016) Long non-coding RNAs: Mechanism of action and functional utility. *Non-coding RNA Research*. **1**, 43–50
58. Wang, K. C., and Chang, H. Y. (2011) Molecular mechanisms of long noncoding RNAs. *Mol Cell*. **43**, 904–914
59. Purdy, M. M., Holz-Schietinger, C., and Reich, N. O. (2010) Identification of a second DNA binding site in human DNA methyltransferase 3A by substrate inhibition and domain deletion. *Archives of Biochemistry and Biophysics*. **498**, 13–22

60. Holz-Schietinger, C., and Reich, N. O. (2010) The Inherent Processivity of the Human de Novo Methyltransferase 3A (DNMT3A) Is Enhanced by DNMT3L*[S]. *Journal of Biological Chemistry*. **285**, 29091–29100
61. Kareta, M. S., Botello, Z. M., Ennis, J. J., Chou, C., and Chédin, F. (2006) Reconstitution and Mechanism of the Stimulation of de Novo Methylation by Human DNMT3L*. *Journal of Biological Chemistry*. **281**, 25893–25902
62. Huang, S.-Y., and Zou, X. (2014) A knowledge-based scoring function for protein-RNA interactions derived from a statistical mechanics-based iterative method. *Nucleic Acids Research*. **42**, e55–e55
63. Peterson, S. N., and Reich, N. O. (2006) GATC Flanking Sequences Regulate Dam Activity: Evidence for how Dam Specificity may Influence pap Expression. *Journal of Molecular Biology*. **355**, 459–472
64. Fuchs, S. M., Krajewski, K., Baker, R. W., Miller, V. L., and Strahl, B. D. (2011) Influence of Combinatorial Histone Modifications on Antibody and Effector Protein Recognition. *Current Biology*. **21**, 53–58
65. Shechter, D., Dormann, H. L., Allis, C. D., and Hake, S. B. (2007) Extraction, purification and analysis of histones. *Nature Protocols*. **2**, 1445–1457
- Dyer, P. N., Edayathumangalam, R. S., White, C. L., Bao, Y., Chakravarthy, S., Muthurajan, U. M., and Luger, K. (2003) Reconstitution of Nucleosome Core Particles from Recombinant Histones and DNA. in *Methods in Enzymology*, pp. 23–44, Chromatin and Chromatin Remodeling Enzymes, Part A, Academic Press, **375**, 23–44
66. Jankowsky, E., and Harris, M. E. (2015) Specificity and nonspecificity in RNA–protein interactions. *Nat Rev Mol Cell Biol*. **16**, 533–544
67. Jeffery, L., and Nakielnny, S. (2004) Components of the DNA methylation system of chromatin control are RNA-binding proteins. *J Biol Chem*. **279**, 49479–49487
68. WEINBERG, M. S., VILLENEUVE, L. M., EHSANI, A., AMARZGUIOUI, M., AAGAARD, L., CHEN, Z.-X., RIGGS, A. D., ROSSI, J. J., and MORRIS, K. V. (2006) The antisense strand of small interfering RNAs directs histone methylation and transcriptional gene silencing in human cells. *RNA*. **12**, 256–262

Chapter VI

1. Bergman Y, Cedar H. DNA methylation dynamics in health and disease. *Nat Struct Mol Biol*. 2013;20(3):274-281. doi:10.1038/nsmb.2518
2. Baylin SB, Jones PA. A decade of exploring the cancer epigenome-biological and translational implications. *Nat Rev Cancer*. 2011;11(10):726-734. doi:10.1038/nrc3130
3. Jeltsch A, Jurkowska RZ. Allosteric control of mammalian DNA methyltransferases - A new regulatory paradigm. *Nucleic Acids Res*. 2016;44(18):8556-8575. doi:10.1093/nar/gkw723
4. Wong KK, Lawrie CH, Green TM. Oncogenic Roles and Inhibitors of DNMT1, DNMT3A, and DNMT3B in Acute Myeloid Leukaemia. *Biomark Insights*. 2019;14. doi:10.1177/1177271919846454
5. Jeltsch A, Jurkowska RZ. New concepts in DNA methylation. *Trends Biochem Sci*. 2014;39(7):310-318. doi:10.1016/j.tibs.2014.05.002
6. Rasmussen KD, Helin K. Role of TET enzymes in DNA methylation, development, and cancer. *Genes Dev*. 2016;30(7):733-750. doi:10.1101/gad.276568.115

7. Gromova ES, Khoroshaev A V. Prokaryotic DNA methyltransferases: The structure and the mechanism of interaction with DNA. *Mol Biol.* 2003;37(2):300-314.
8. Wu JC, Santi D V. Kinetic and catalytic mechanism of HhaI methyltransferase. *J Biol Chem.* 1987;262(10):4778-4786.
9. Bheemanaik S, Reddy YVR, Rao DN. Structure, function and mechanism of exocyclic DNA methyltransferases. *Biochem J.* 2006;399(2):177-190. doi:10.1042/BJ20060854
10. Reich NO, Mashhoon N. Kinetic Mechanism of the EcoRI DNA Methyltransferase. *Biochemistry.* 1991;30(11):2933-2939. doi:10.1021/bi00225a029
11. Yokochi T, Robertson KD. Preferential Methylation of Unmethylated DNA by Mammalian de Novo DNA Methyltransferase Dnmt3a*. doi:10.1074/jbc.M106590200
12. Lyko F. The DNA methyltransferase family: A versatile toolkit for epigenetic regulation. *Nat Rev Genet.* 2018;19(2):81-92. doi:10.1038/nrg.2017.80
13. Zhang ZM, Lu R, Wang P, et al. Structural basis for DNMT3A-mediated de novo DNA methylation. *Nature.* 2018;554(7692):387-391. doi:10.1038/nature25477
14. Brunetti L, Gundry MC, Goodell MA. DNMT3A in Leukemia. *Cold Spring Harb Perspect Med.* 2017;7(2). doi:10.1101/cshperspect.a030320
15. Khrabrova DA, Loiko AG, Tolkacheva AA, et al. Functional analysis of DNMT3A DNA methyltransferase mutations reported in patients with acute myeloid leukemia. *Biomolecules.* 2020;10(1). doi:10.3390/biom10010008
16. Holz-Schietinger C, Matje DM, Reich NO. Mutations in DNA methyltransferase (DNMT3A) observed in acute myeloid leukemia patients disrupt processive methylation. *J Biol Chem.* 2012;287(37):30941-30951. doi:10.1074/jbc.M112.366625
17. Sandoval JE, Huang YH, Muise A, Goodell MA, Reich NO. Mutations in the DNMT3A DNA methyltransferase in acute myeloid leukemia patients cause both loss and gain of function and differential regulation by protein partners. *J Biol Chem.* 2019;294(13):4898-4910. doi:10.1074/jbc.RA118.006795
18. Gros C, Fahy J, Halby L, et al. DNA methylation inhibitors in cancer: Recent and future approaches. *Biochimie.* 2012;94(11):2280-2296. doi:10.1016/j.biochi.2012.07.025
19. Yu J, Xie T, Wang Z, et al. DNA methyltransferases: emerging targets for the discovery of inhibitors as potent anticancer drugs. *Drug Discov Today.* 2019;24(12):2323-2331. doi:10.1016/j.drudis.2019.08.006
20. Ganesan A, Arimondo PB, Rots MG, Jeronimo C, Berdasco M. The timeline of epigenetic drug discovery: From reality to dreams. *Clin Epigenetics.* 2019;11(1):1-17. doi:10.1186/s13148-019-0776-0
21. DNMT3A Result Summary | BioGRID. <https://thebiogrid.org/108125/summary/homo-sapiens/dnmt3a.html>. Accessed August 22, 2020.
22. Sandoval JE, Reich NO. The R882H substitution in the human de novo DNA methyltransferase DNMT3A disrupts allosteric regulation by the tumor suppressor p53. *J Biol Chem.* 2019;294(48):18207-18219. doi:10.1074/jbc.RA119.010827
23. Díaz-Eufracio BI, Naveja JJ, Medina-Franco JL. Protein-Protein Interaction Modulators for Epigenetic Therapies. In: *Advances in Protein Chemistry and Structural Biology.* Vol 110. Academic Press Inc.; 2018:65-84. doi:10.1016/bs.apcsb.2017.06.002

24. Ni D, Lu S, Zhang J. Emerging roles of allosteric modulators in the regulation of protein-protein interactions (PPIs): A new paradigm for PPI drug discovery. *Med Res Rev.* 2019;39(6):2314-2342. doi:10.1002/med.21585
25. Russler-Germain DA, Spencer DH, Young MA, et al. Cancer Cell The R882H DNMT3A Mutation Associated with AML Dominantly Inhibits Wild-Type DNMT3A by Blocking Its Ability to Form Active Tetramers. 2014. doi:10.1016/j.ccr.2014.02.010
26. Cheng SS, Yang GJ, Wang W, Leung CH, Ma DL. The design and development of covalent protein-protein interaction inhibitors for cancer treatment. *J Hematol Oncol.* 2020;13(1):26. doi:10.1186/s13045-020-00850-0
27. Wenthur CJ, Gentry PR, Mathews TP, Lindsley CW. Drugs for Allosteric Sites on Receptors. *Annu Rev Pharmacol Toxicol.* 2014;54(1):165-184. doi:10.1146/annurev-pharmtox-010611-134525
28. Dokholyan N V. Controlling Allosteric Networks in Proteins. *Chem Rev.* 2016. doi:10.1021/acs.chemrev.5b00544
29. Peracchi A, Mozzarelli A. Exploring and exploiting allostery: Models, evolution, and drug targeting. *Biochim Biophys Acta - Proteins Proteomics.* 2011;1814(8):922-933. doi:10.1016/j.bbapap.2010.10.008
30. Dahlin JL, Walters MA. The essential roles of chemistry in high-throughput screening triage. *Future Med Chem.* 2014;6(11):1265-1290. doi:10.4155/fmc.14.60
31. Siedlecki P, Boy RG, Musch T, et al. Discovery of two novel, small-molecule inhibitors of DNA methylation. *J Med Chem.* 2006;49(2):678-683. doi:10.1021/jm050844z
32. Valente S, Liu Y, Schnekenburger M, et al. Selective non-nucleoside inhibitors of human DNA methyltransferases active in cancer including in cancer stem cells. *J Med Chem.* 2014;57(3):701-713. doi:10.1021/jm4012627
33. Ceccaldi A, Rajavelu A, Ragozin S, et al. Identification of novel inhibitors of dna methylation by screening of a chemical library. *ACS Chem Biol.* 2013;8(3):543-548. doi:10.1021/cb300565z
34. Blaazer AR, Singh AK, De Heuvel E, et al. Targeting a Subpocket in Trypanosoma brucei Phosphodiesterase B1 (TbrPDEB1) Enables the Structure-Based Discovery of Selective Inhibitors with Trypanocidal Activity. *J Med Chem.* 2018;61(9):3870-3888. doi:10.1021/acs.jmedchem.7b01670
35. Orrling KM, Jansen C, Vu XL, et al. Catechol pyrazolinones as trypanocidals: Fragment-based design, synthesis, and pharmacological evaluation of nanomolar inhibitors of trypanosomal phosphodiesterase B1. *J Med Chem.* 2012;55(20):8745-8756. doi:10.1021/jm301059b
36. Datta J, Ghoshal K, Denny WA, et al. A new class of quinoline-based DNA hypomethylating agents reactivates tumor suppressor genes by blocking DNA methyltransferase 1 activity and inducing its degradation. *Cancer Res.* 2009;69(10):4277-4285. doi:10.1158/0008-5472.CAN-08-3669
37. Segel IH. *Enzyme Kinetics: Behavior and Analysis of Rapid Equilibrium and Steady-State Enzyme Systems.* Wiley; 1975.
38. López-López E, Prieto-Martínez FD, Medina-Franco JL. Activity landscape and molecular modeling to explore the SAR of dual epigenetic inhibitors: A focus on G9a and DNMT1. *Molecules.* 2018;23(12). doi:10.3390/molecules23123282
39. Newton AS, Faver JC, Micevic G, et al. Structure-Guided Identification of DNMT3B Inhibitors. *ACS Med Chem Lett.* 2020.

doi:10.1021/acsmchemlett.0c00011

40. Caulfield T, Medina-Franco JL. Molecular dynamics simulations of human DNA methyltransferase 3B with selective inhibitor nanaomycin A. *J Struct Biol*. 2011;176(2):185-191. doi:10.1016/j.jsb.2011.07.015
41. Shao Z, Xu P, Xu W, et al. Discovery of novel DNA methyltransferase 3A inhibitors via structure-based virtual screening and biological assays. *Bioorganic Med Chem Lett*. 2017;27(2):342-346. doi:10.1016/j.bmcl.2016.11.023
42. Dokholyan N V. Controlling Allosteric Networks in Proteins. *Chem Rev*. 2016;116(11):6463-6487. doi:10.1021/acs.chemrev.5b00544
43. Zhang ZM, Lu R, Wang P, et al. Structural basis for DNMT3A-mediated de novo DNA methylation. *Nature*. 2018;554(7692):387-391. doi:10.1038/nature25477
44. hen T, Ueda Y, Dodge JE, Wang Z, Li E. Establishment and Maintenance of Genomic Methylation Patterns in Mouse Embryonic Stem Cells by Dnmt3a and Dnmt3b. *Mol Cell Biol*. 2003;23(16):5594-5605. doi:10.1128/mcb.23.16.5594-5605.2003
45. Kaneda M, Okano M, Hata K, et al. Essential role for de novo DNA methyltransferase Dnmt3a in paternal and maternal imprinting. *Nature*. 2004;429(6994):900-903. doi:10.1038/nature02633
46. Purdy MM, Holz-Schietinger C, Reich NO. Identification of a second DNA binding site in human DNA methyltransferase 3A by substrate inhibition and domain deletion. *Arch Biochem Biophys*. 2010;498(1):13-22. doi:10.1016/j.abb.2010.03.007

Chapter VII

1. Bird, A. (2007) Perceptions of epigenetics. *Nature*. **447**, 396–398
2. Hanna, C. W., and Kelsey, G. (2021) Features and mechanisms of canonical and noncanonical genomic imprinting. *Genes Dev*. **35**, 821–834
3. Álvarez-Errico, D., Vento-Tormo, R., Sieweke, M., and Ballestar, E. (2015) Epigenetic control of myeloid cell differentiation, identity and function. *Nat Rev Immunol*. **15**, 7–17
4. Kiefer, J. C. (2007) Epigenetics in development. *Developmental Dynamics*. **236**, 1144–1156
5. Biswas, S., and Rao, C. M. (2018) Epigenetic tools (The Writers, The Readers and The Erasers) and their implications in cancer therapy. *European Journal of Pharmacology*. **837**, 8–24
6. Nicholson, T. B., Veland, N., and Chen, T. (2015) Chapter 3 - Writers, Readers, and Erasers of Epigenetic Marks. in *Epigenetic Cancer Therapy* (Gray, S. G. ed), pp. 31–66, Academic Press, Boston, [10.1016/B978-0-12-800206-3.00003-3](https://doi.org/10.1016/B978-0-12-800206-3.00003-3)
7. Ye, F., Huang, J., Wang, H., Luo, C., and Zhao, K. (2019) Targeting epigenetic machinery: Emerging novel allosteric inhibitors. *Pharmacology & Therapeutics*. **204**, 107406
8. Zucconi, B. E., and Cole, P. A. (2017) Allosteric regulation of epigenetic modifying enzymes. *Current Opinion in Chemical Biology*. **39**, 109–115
9. Qi, W., Zhao, K., Gu, J., Huang, Y., Wang, Y., Zhang, H., Zhang, M., Zhang, J., Yu, Z., Li, L., Teng, L., Chuai, S., Zhang, C., Zhao, M., Chan, H., Chen, Z., Fang, D., Fei, Q., Feng, L., Feng, L., Gao, Y., Ge, H., Ge, X., Li, G., Lingel, A., Lin, Y., Liu, Y., Luo, F., Shi, M., Wang, L., Wang, Z., Yu, Y., Zeng, J., Zeng, C., Zhang, L., Zhang, Q., Zhou, S., Oyang, C., Atadja, P., and Li, E. (2017) An allosteric PRC2 inhibitor targeting the H3K27me3 binding pocket of EED. *Nat Chem Biol*. **13**, 381–

10. Siarheyeva, A., Senisterra, G., Allali-Hassani, A., Dong, A., Dobrovetsky, E., Wasney, G. A., Chau, I., Marcellus, R., Hajian, T., Liu, F., Korboukh, I., Smil, D., Bolshan, Y., Min, J., Wu, H., Zeng, H., Loppnau, P., Poda, G., Griffin, C., Aman, A., Brown, P. J., Jin, J., Al-awar, R., Arrowsmith, C. H., Schapira, M., and Vedadi, M. (2012) An Allosteric Inhibitor of Protein Arginine Methyltransferase 3. *Structure*. **20**, 1425–1435
11. Liu, F., Li, F., Ma, A., Dobrovetsky, E., Dong, A., Gao, C., Korboukh, I., Liu, J., Smil, D., Brown, P. J., Frye, S. V., Arrowsmith, C. H., Schapira, M., Vedadi, M., and Jin, J. (2013) Exploiting an Allosteric Binding Site of PRMT3 Yields Potent and Selective Inhibitors. *J. Med. Chem.* **56**, 2110–2124
12. Zhang, Q., Chen, Y., Ni, D., Huang, Z., Wei, J., Feng, L., Su, J.-C., Wei, Y., Ning, S., Yang, X., Zhao, M., Qiu, Y., Song, K., Yu, Z., Xu, J., Li, X., Lin, H., Lu, S., and Zhang, J. (2021) Targeting a cryptic allosteric site of SIRT6 with small-molecule inhibitors that inhibit the migration of pancreatic cancer cells. *Acta Pharmaceutica Sinica B*. [10.1016/j.apsb.2021.06.015](https://doi.org/10.1016/j.apsb.2021.06.015)
13. Yu, J., Xie, T., Wang, Z., Wang, X., Zeng, S., Kang, Y., and Hou, T. (2019) DNA methyltransferases: emerging targets for the discovery of inhibitors as potent anticancer drugs. *Drug Discovery Today*. **24**, 2323–2331
14. Santi, D. V., Norment, A., and Garrett, C. E. (1984) Covalent bond formation between a DNA-cytosine methyltransferase and DNA containing 5-azacytosine. *Proc Natl Acad Sci U S A*. **81**, 6993–6997
15. Stresemann, C., and Lyko, F. (2008) Modes of action of the DNA methyltransferase inhibitors azacytidine and decitabine. *Int J Cancer*. **123**, 8–13
16. Siedlecki, P., Garcia Boy, R., Musch, T., Brueckner, B., Suhai, S., Lyko, F., and Zielenkiewicz, P. (2006) Discovery of two novel, small-molecule inhibitors of DNA methylation. *J Med Chem*. **49**, 678–683
17. Brueckner, B., Garcia Boy, R., Siedlecki, P., Musch, T., Kliem, H. C., Zielenkiewicz, P., Suhai, S., Wiessler, M., and Lyko, F. (2005) Epigenetic reactivation of tumor suppressor genes by a novel small-molecule inhibitor of human DNA methyltransferases. *Cancer Res*. **65**, 6305–6311
18. Halby, L., Champion, C., Sénamaud-Beaufort, C., Ajjan, S., Drujon, T., Rajavelu, A., Ceccaldi, A., Jurkowska, R., Lequin, O., Nelson, W. G., Guy, A., Jeltsch, A., Guianvarc’h, D., Ferroud, C., and Arimondo, P. B. (2012) Rapid synthesis of new DNMT inhibitors derivatives of procainamide. *Chembiochem*. **13**, 157–165
19. Datta, J., Ghoshal, K., Denny, W. A., Gamage, S. A., Brooke, D. G., Phiasivongsa, P., Redkar, S., and Jacob, S. T. (2009) A new class of quinoline-based DNA hypomethylating agents reactivates tumor suppressor genes by blocking DNA methyltransferase 1 activity and inducing its degradation. *Cancer Res*. **69**, 4277–4285
20. Valente, S., Liu, Y., Schnekenburger, M., Zwergel, C., Cosconati, S., Gros, C., Tardugno, M., Labella, D., Florean, C., Minden, S., Hashimoto, H., Chang, Y., Zhang, X., Kirsch, G., Novellino, E., Arimondo, P. B., Miele, E., Ferretti, E., Gulino, A., Diederich, M., Cheng, X., and Mai, A. (2014) Selective non-nucleoside inhibitors of human DNA methyltransferases active in cancer including in cancer stem cells. *J Med Chem*. **57**, 701–713
21. Du, J., Johnson, L. M., Jacobsen, S. E., and Patel, D. J. (2015) DNA methylation pathways and their crosstalk with histone methylation. *Nat Rev Mol Cell Biol*. **16**,

22. aissière, T., Sawan, C., and Herceg, Z. (2008) Epigenetic interplay between histone modifications and DNA methylation in gene silencing. *Mutation Research/Reviews in Mutation Research*. **659**, 40–48
23. Lian, Y., Meng, L., Ding, P., and Sang, M. (2018) Epigenetic regulation of MAGE family in human cancer progression-DNA methylation, histone modification, and non-coding RNAs. *Clin Epigenet*. **10**, 115
24. Viré, E., Brenner, C., Deplus, R., Blanchon, L., Fraga, M., Didelot, C., Morey, L., Van Eynde, A., Bernard, D., Vanderwinden, J.-M., Bollen, M., Esteller, M., Di Croce, L., de Launoit, Y., and Fuks, F. (2006) The Polycomb group protein EZH2 directly controls DNA methylation. *Nature*. **439**, 871–874
25. Mohammad, H. P., Cai, Y., McGarvey, K. M., Easwaran, H., Noste, L. V., Ohm, J. E., O'Hagan, H. M., and Baylin, S. B. (2009) Polycomb CBX7 Promotes Initiation of Heritable Repression of Genes Frequently Silenced with Cancer-Specific DNA Hypermethylation. *Cancer Res*. **69**, 6322–6330
26. Zhao, Q., Rank, G., Tan, Y. T., Li, H., Moritz, R. L., Simpson, R. J., Cerruti, L., Curtis, D. J., Patel, D. J., Allis, C. D., Cunningham, J. M., and Jane, S. M. (2009) PRMT5-mediated methylation of histone H4R3 recruits DNMT3A, coupling histone and DNA methylation in gene silencing. *Nat Struct Mol Biol*. **16**, 304–311
27. ao, R., Wang, L., Wang, H., Xia, L., Erdjument-Bromage, H., Tempst, P., Jones, R. S., and Zhang, Y. (2002) Role of Histone H3 Lysine 27 Methylation in Polycomb-Group Silencing. *Science*. **298**, 1039–1043
28. Kuzmichev, A., Nishioka, K., Erdjument-Bromage, H., Tempst, P., and Reinberg, D. (2002) Histone methyltransferase activity associated with a human multiprotein complex containing the Enhancer of Zeste protein. *Genes Dev*. **16**, 2893–2905
29. Blackledge, N. P., Rose, N. R., and Klose, R. J. (2015) Targeting Polycomb systems to regulate gene expression: modifications to a complex story. *Nat Rev Mol Cell Biol*. **16**, 643–649
30. Shin, W.-H., Kumazawa, K., Imai, K., Hirokawa, T., and Kihara, D. (2020) Current Challenges and Opportunities in Designing Protein–Protein Interaction Targeted Drugs. *Adv Appl Bioinform Chem*. **13**, 11–25
31. Lu, H., Zhou, Q., He, J., Jiang, Z., Peng, C., Tong, R., and Shi, J. (2020) Recent advances in the development of protein–protein interactions modulators: mechanisms and clinical trials. *Sig Transduct Target Ther*. **5**, 1–23
32. Linhares, B. M., Grembecka, J., and Cierpicki, T. (2020) Targeting epigenetic protein–protein interactions with small-molecule inhibitors. *Future Medicinal Chemistry*. **12**, 1305–1326
33. Wang, Y. A., Kamarova, Y., Shen, K. C., Jiang, Z., Hahn, M. J., Wang, Y., and Brooks, S. C. (2005) DNA methyltransferase-3a interacts with p53 and represses p53-mediated gene expression. *Cancer Biology & Therapy*. **4**, 1138–1143
34. Li, Y.-Q., Zhou, P.-Z., Zheng, X.-D., Walsh, C. P., and Xu, G.-L. (2007) Association of Dnmt3a and thymine DNA glycosylase links DNA methylation with base-excision repair. *Nucleic Acids Res*. **35**, 390–400
35. Karetta, M. S., Botello, Z. M., Ennis, J. J., Chou, C., and Chédin, F. (2006) Reconstitution and Mechanism of the Stimulation of de Novo Methylation by Human DNMT3L *. *Journal of Biological Chemistry*. **281**, 25893–25902
36. Ley, T. J., Ding, L., Walter, M. J., McLellan, M. D., Lamprecht, T., Larson, D. E., Kandoth, C., Payton, J. E., Baty, J., Welch, J., Harris, C. C., Lichti, C. F., Townsend,

- R. R., Fulton, R. S., Dooling, D. J., Koboldt, D. C., Schmidt, H., Zhang, Q., Osborne, J. R., Lin, L., O’Laughlin, M., McMichael, J. F., Delehaunty, K. D., McGrath, S. D., Fulton, L. A., Magrini, V. J., Vickery, T. L., Hundal, J., Cook, L. L., Conyers, J. J., Swift, G. W., Reed, J. P., Alldredge, P. A., Wylie, T., Walker, J., Kalicki, J., Watson, M. A., Heath, S., Shannon, W. D., Varghese, N., Nagarajan, R., Westervelt, P., Tomasson, M. H., Link, D. C., Graubert, T. A., DiPersio, J. F., Mardis, E. R., and Wilson, R. K. (2010) DNMT3A Mutations in Acute Myeloid Leukemia. *New England Journal of Medicine*. **363**, 2424–2433
37. Gaidzik, V. I., Schlenk, R. F., Paschka, P., Stölzle, A., Späth, D., Kuendgen, A., von Lilienfeld-Toal, M., Brügger, W., Derigs, H. G., Kremers, S., Greil, R., Raghavachar, A., Ringhoffer, M., Salih, H. R., Wattad, M., Kirchen, H. G., Runde, V., Heil, G., Petzer, A. L., Girschikofsky, M., Heuser, M., Kayser, S., Goehring, G., Teleanu, M.-V., Schlegelberger, B., Ganser, A., Krauter, J., Bullinger, L., Döhner, H., and Döhner, K. (2013) Clinical impact of DNMT3A mutations in younger adult patients with acute myeloid leukemia: results of the AML Study Group (AMLSSG). *Blood*. **121**, 4769–4777
38. Yang, L., Rau, R., and Goodell, M. A. (2015) DNMT3A in haematological malignancies. *Nat Rev Cancer*. **15**, 152–165
39. Huang, S., Stillson, N. J., Sandoval, J. E., Yung, C., and Reich, N. O. (2021) A novel class of selective non-nucleoside inhibitors of human DNA methyltransferase 3A. *Bioorganic & Medicinal Chemistry Letters*. **40**, 127908
40. Li, B.-Z., Huang, Z., Cui, Q.-Y., Song, X.-H., Du, L., Jeltsch, A., Chen, P., Li, G., Li, E., and Xu, G.-L. (2011) Histone tails regulate DNA methylation by allosterically activating de novo methyltransferase. *Cell Res*. **21**, 1172–1181
41. Guo, X., Wang, L., Li, J., Ding, Z., Xiao, J., Yin, X., He, S., Shi, P., Dong, L., Li, G., Tian, C., Wang, J., Cong, Y., and Xu, Y. (2015) Structural insight into autoinhibition and histone H3-induced activation of DNMT3A. *Nature*. **517**, 640–644
42. Sandoval, J. E., and Reich, N. O. (2019) The R882H substitution in the human de novo DNA methyltransferase DNMT3A disrupts allosteric regulation by the tumor suppressor p53. *J Biol Chem*. **294**, 18207–18219
43. Sandoval, J. E., and Reich, N. O. (2021) p53 and TDG are dominant in regulating the activity of the human de novo DNA methyltransferase DNMT3A on nucleosomes. *J Biol Chem*. **296**, 100058
44. Holz-Schietinger, C., Matje, D. M., Harrison, M. F., and Reich, N. O. (2011) Oligomerization of DNMT3A Controls the Mechanism of de Novo DNA Methylation. *J Biol Chem*. **286**, 41479–41488
45. Holz-Schietinger, C., Matje, D. M., and Reich, N. O. (2012) Mutations in DNA Methyltransferase (DNMT3A) Observed in Acute Myeloid Leukemia Patients Disrupt Processive Methylation. *Journal of Biological Chemistry*. **287**, 30941–30951
46. Sandoval, J. E., Huang, Y.-H., Muise, A., Goodell, M. A., and Reich, N. O. (2019) Mutations in the DNMT3A DNA methyltransferase in acute myeloid leukemia patients cause both loss and gain of function and differential regulation by protein partners. *Journal of Biological Chemistry*. **294**, 4898–4910
47. Koya, J., Kataoka, K., Sato, T., Bando, M., Kato, Y., Tsuruta-Kishino, T., Kobayashi, H., Narukawa, K., Miyoshi, H., Shirahige, K., and Kurokawa, M. (2016) DNMT3A R882 mutants interact with polycomb proteins to block haematopoietic stem and leukaemic cell differentiation. *Nat Commun*. **7**, 10924
48. Russler-Germain, D. A., Spencer, D. H., Young, M. A., Lamprecht, T. L., Miller, C.

- A., Fulton, R., Meyer, M. R., Erdmann-Gilmore, P., Townsend, R. R., Wilson, R. K., and Ley, T. J. (2014) The R882H DNMT3A mutation associated with AML dominantly inhibits wild-type DNMT3A by blocking its ability to form active tetramers. *Cancer Cell*. **25**, 442–454
49. Purdy, M. M., Holz-Schietinger, C., and Reich, N. O. (2010) Identification of a second DNA binding site in human DNA methyltransferase 3A by substrate inhibition and domain deletion. *Arch Biochem Biophys*. **498**, 13–22
50. Holz-Schietinger, C., and Reich, N. O. (2010) The inherent processivity of the human de novo methyltransferase 3A (DNMT3A) is enhanced by DNMT3L. *J Biol Chem*. **285**, 29091–29100
- A. Ayed, *et al.*, Latent and active p53 are identical in conformation. *Nat Struct Mol Biol* **8**, 756–760 (2001).
51. Schuermann, D., Scheidegger, S. P., Weber, A. R., Bjørås, M., Leumann, C. J., and Schär, P. (2016) 3CAPS – a structural AP-site analogue as a tool to investigate DNA base excision repair. *Nucleic Acids Research*. **44**, 2187–2198
52. Peterson, S. N., and Reich, N. O. (2006) GATC Flanking Sequences Regulate Dam Activity: Evidence for how Dam Specificity may Influence pap Expression. *Journal of Molecular Biology*. **355**, 459–472
53. Waterhouse, A., Bertoni, M., Bienert, S., Studer, G., Tauriello, G., Gumienny, R., Heer, F. T., de Beer, T. A. P., Rempfer, C., Bordoli, L., Lepore, R., and Schwede, T. (2018) SWISS-MODEL: homology modelling of protein structures and complexes. *Nucleic Acids Research*. **46**, W296–W303
54. orris, G. M., Huey, R., Lindstrom, W., Sanner, M. F., Belew, R. K., Goodsell, D. S., and Olson, A. J. (2009) AutoDock4 and AutoDockTools4: Automated Docking with Selective Receptor Flexibility. *J Comput Chem*. **30**, 2785–2791
55. Ropp, P. J., Spiegel, J. O., Walker, J. L., Green, H., Morales, G. A., Milliken, K. A., Ringe, J. J., and Durrant, J. D. (2019) Gypsum-DL: an open-source program for preparing small-molecule libraries for structure-based virtual screening. *Journal of Cheminformatics*. **11**, 34
56. Van Der Spoel, D., Lindahl, E., Hess, B., Groenhof, G., Mark, A. E., and Berendsen, H. J. C. (2005) GROMACS: fast, flexible, and free. *J Comput Chem*. **26**, 1701–1718
57. Hess, B., Kutzner, C., van der Spoel, D., and Lindahl, E. (2008) GROMACS 4: Algorithms for Highly Efficient, Load-Balanced, and Scalable Molecular Simulation. *J Chem Theory Comput*. **4**, 435–447
58. Pronk, S., Páll, S., Schulz, R., Larsson, P., Bjelkmar, P., Apostolov, R., Shirts, M. R., Smith, J. C., Kasson, P. M., van der Spoel, D., Hess, B., and Lindahl, E. (2013) GROMACS 4.5: a high-throughput and highly parallel open source molecular simulation toolkit. *Bioinformatics*. **29**, 845–854
59. Huang, J., Rauscher, S., Nawrocki, G., Ran, T., Feig, M., de Groot, B. L., Grubmüller, H., and MacKerell, A. D. (2017) CHARMM36m: An Improved Force Field for Folded and Intrinsically Disordered Proteins. *Nat Methods*. **14**, 71–73
60. Vanommeslaeghe, K., Hatcher, E., Acharya, C., Kundu, S., Zhong, S., Shim, J., Darian, E., Guvench, O., Lopes, P., Vorobyov, I., and Mackerell, A. D. (2010) CHARMM general force field: A force field for drug-like molecules compatible with the CHARMM all-atom additive biological force fields. *J Comput Chem*. **31**, 671–690
61. Vanommeslaeghe, K., Raman, E. P., and MacKerell, A. D. (2012) Automation of the CHARMM General Force Field (CGenFF) II: Assignment of Bonded Parameters and Partial Atomic Charges. *J. Chem. Inf. Model*. **52**, 3155–3168

62. Vanommeslaeghe, K., Raman, E. P., and MacKerell, A. D. (2012) Automation of the CHARMM General Force Field (CGenFF) II: Assignment of Bonded Parameters and Partial Atomic Charges. *J. Chem. Inf. Model.* **52**, 3155–3168
63. Miller, B. R., McGee, T. D., Swails, J. M., Homeyer, N., Gohlke, H., and Roitberg, A. E. (2012) MMPBSA.py: An Efficient Program for End-State Free Energy Calculations. *J. Chem. Theory Comput.* **8**, 3314–3321